

Controlling the Activity of Organocatalysts: Modulating Conformation and Acidity

A Thesis Submitted for the Degree of

Doctor of Philosophy

by

Arjun Kumar Chittoory



New Chemistry Unit

Jawaharlal Nehru Centre for Advanced Scientific Research

(A Deemed University)

Jakkur, Bangalore - 560064

India

September-2017

Declaration

I hereby declare that the matter embodied in this thesis entitled “*Controlling the Activity of Organocatalysts: Modulating Conformation and Acidity*” is the result of investigations carried out by me at the New Chemistry Unit, Jawaharlal Nehru Centre for Advanced Scientific Research, Bangalore, India under the supervision of **Prof. Sridhar Rajaram** and that it has not been submitted elsewhere for the award of any degree or diploma.

In keeping with the general practice in reporting the scientific observations, due acknowledgment has been made whenever the work described is based on the findings of other investigators. Any omission that might have occurred due to oversight or error in judgment is regretted.

Mr. Arjun Kumar Chittoory
(Ph.D. Student)

Certificate

I hereby certify that the matter embodied in this thesis entitled “*Controlling the Activity of Organocatalysts: Modulating Conformation and Acidity*” has been carried out by **Mr. Arjun Kumar Chittoory** at the New Chemistry Unit, Jawaharlal Nehru Centre for Advanced Scientific Research, Bangalore, India under my supervision and that it has not been submitted elsewhere for the award of any degree or diploma.

Prof. Sridhar Rajaram
(Research Supervisor)

Dedicated to my Parents, and my Wife

Acknowledgement

It is indeed a great pleasure to express my gratitude to my research supervisor **Prof. Sridhar Rajaram** for giving me an opportunity to work in his research group. I am grateful to him for being not only my doctoral guide providing me the motivation and encouragement during my doctoral studies but also more as my teacher and a well wisher during my stay here.

I am thankful to Prof. Sridhar Rajaram, Prof. Subi Jacob George, Prof. Balasubramanian Sundaram of JNCASR and Prof. Siddhartha P. Sarma of IISc for the chemistry they taught me during course work. I am also thankful to Prof. S. Baskaran of IITM for teaching me organic chemistry in my early research career. I am thankful to my collaborators Prof. Chandrabhas Narayana, Dr. Partha P. Kundu, and Dr. Gayatri Kumari for IR, Raman, and DFT studies. I am thankful to Prof. T. K. Maji, and Dr. Sudip Mohapatra for single crystal XRD studies. I would also like to thank Prof. E. N. Prabhakaran and Prof. K. R. Prasad from IISc for their valuable scientific discussions.

I am grateful to my lab mates Dr. Ramana Reddy, Mr. Sunil Kumar Kandappa, Ms. Debopreeti Mukherjee, Mr. Chaitanya Krishna, Mr. M. S. Ramesh, Ms. Anusha S. Avadhani, Ms. Priyanka Jain, and Dr. M. Pavan Kumar for providing a very friendly and congenial atmosphere in the laboratory. I sincerely thank Dr. M. G. Sankar, Dr. P. Manohar from IITM for mentoring me in my early research career.

I thank Mr. M. S. Ramesh and Dr. Devi Sirisha Janni for proof-reading part of my thesis and I would like to thank Mrs. Vinutha Lakshman for proof-reading and editing my thesis.

I would like to thank Mr. Mahesh, Mr. Shiva and Mr. Vasu for recording NMR, HRMS, and IR spectra for my sample. I gratefully acknowledge Prof. K. R. Prasad for helping me to record HPLC data at IISc. I extend my thanks to Dr. Omkar Revu and Mr. Manoj Uphade Bajirao for helping me in using HPLC instrument at IISc.

I thank all my friends at JNCASR for making my stay pleasant and enjoyable one. I thank academic, administration, and NCU office staff for their constant help. I thank JNCASR library, computer lab, hostel, health centre, and gym for providing and maintaining the various facilities that have helped me immensely.

I would like to thank my gurus Chalapathi rao and Sharma for choosing chemistry as my research career in my life.

I thank CSIR, JNCASR, and SERB for granting fellowship during my Ph.D.

Words cannot express my affection to my adorable friends Mr. Ravi, Mr. Sai Satish, Dr. Satish, Dr. Jagan, Dr. Mallik, Dr. Matte, Dr. Chandan, Dr. Naidu, Mr. Vinod, Mr. Sudheer, Mr. Ratan, Dr. Senthil, Mr. Nagarjuna, and Mrs. Swapna for their great friendship and support.

Finally and most importantly, I am ever indebted to my family members **Rama Satyam Chittoory** (Father), **Satya Ganga Ratnam** (Mother), **Srikanth Chittoory** (Brother), **Harika Grandhi** (Sister), and to my loving wife **Devi Sirisha Chittoory** for their love, care, affection, encouragement and moral support.

Above all, I thank God for giving me the knowledge, vision and ability to proceed and “make it so”.

Arjun Kumar Chittoory

Thesis Synopsis

Controlling the Activity of Organocatalysts: Modulating Conformation and Acidity

Organocatalysts have been proposed as safer alternatives to organometallic catalysts. More importantly, novel reactivity that is not accessible via organometallic catalysts have also been reported. In this thesis, we report on our work on modulating the catalytic activity of organocatalysts.

Non-covalent interactions often play a pivotal role in organocatalysis. In the first chapter the role of these interactions in enhancing selectivity is reviewed. Specifically, the role of cation- π interactions, π - π interactions, anion- π interactions, lone pair- π interactions and hydrogen bonds in stabilizing transition states and catalyst conformation is reviewed. Recent applications of novel catalyst designs that exploit these features are shown.

In the second chapter, our work on controlling the conformation of a hydrogen-bonding catalyst using sodium cation is discussed. Catalyst-Substrate interactions in the transition state governs the maximum selectivity that can be obtained from a reaction. In the case of catalysts that use hydrogen bonds to activate substrates, the acidity of the hydrogen bond donating group is important. This has been demonstrated in studies by the Sigman group and the Cheng group. Keeping this in mind, we synthesized a C_2 symmetric biscamphorsulfonyl urea as potential hydrogen-bonding catalyst. The sulfonyl urea was expected to be highly acidic based on pK_a measurements of similar compounds in literature reports. Additionally, the camphorsulfonyl groups were expected to provide a chiral environment. Using the camphorsulfonyl urea as a catalyst, a Friedel-Crafts reaction between nitrostyrene and pyrrole was performed. The reaction proceeded in good yield albeit with low selectivity. Based on the lack of background reaction, we hypothesized that

the low selectivity in the reaction was due to the locking up of the catalyst in an unfavorable conformation (Scheme 1). It was posited that dipole-dipole repulsion between the carbonyl and sulfonyl oxygens would push the chiral camphorsulfonyl group away from the incipient chiral center. This was supported by single crystal X-ray diffraction studies on our catalyst (Figure 1). Taking a cue from the Crimmins aldol reaction, we hypothesized that the dipole-dipole repulsion can be overcome by using a mild Lewis acid (Scheme 2). Our screen of Lewis acids showed that NaBPh₄ was optimal for this purpose. Addition of NaBPh₄ showed

Scheme 1: Proposed Conformational Equilibrium

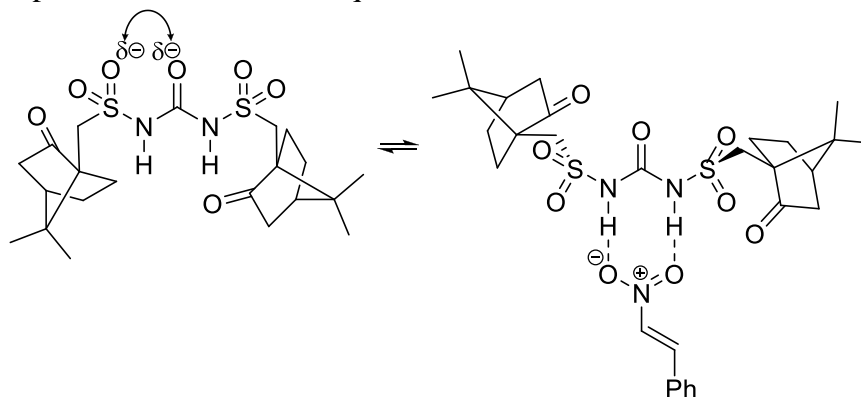
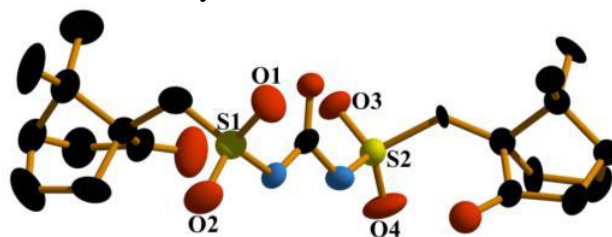
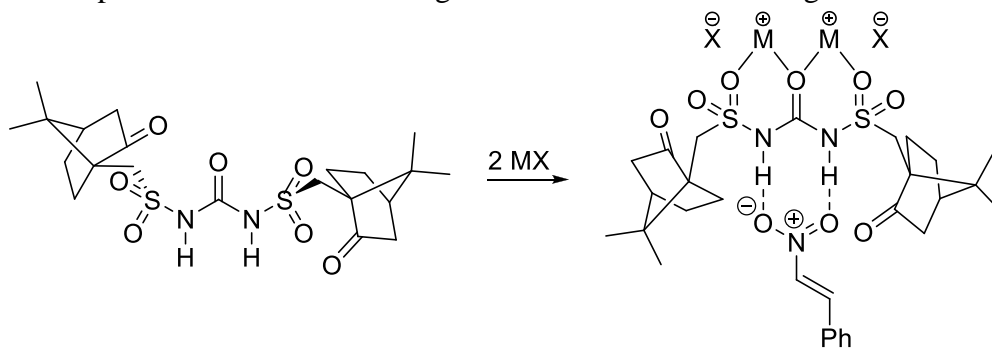


Figure 1: Crystal Structure of Urea Catalyst



Scheme 2: Proposed Conformation Change due to Lewis Acid Binding

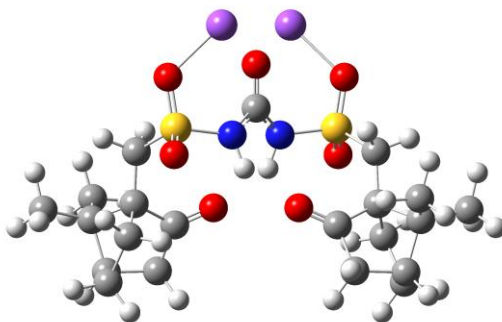


improved selectivity with a reversal in face selection. Importantly, control reactions with NaBPh₄ alone showed that it was not a competent catalyst for the Friedel-Crafts reaction. After further optimization, the products were obtained in moderate to good selectivities. Reaction with various substrates showed that the effect of NaBPh₄ was general. Exploration of the substrate scope showed that the reaction worked well for aromatic nitroalkenes.

The effect of NaBPh₄ on catalyst structure was studied conveniently using vibrational spectroscopy. IR and Raman studies showed that addition of NaBPh₄ led to sodium cations binding the carbonyl and sulfonyl groups as reflected in the changes to the stretching frequencies. Further, DFT calculations were performed on the sodium bound structures and the group frequencies were calculated for this structure (Figure 2). This correlated well with the experimentally obtained values, thereby supporting our hypothesis that NaBPh₄ alters the catalyst conformation.

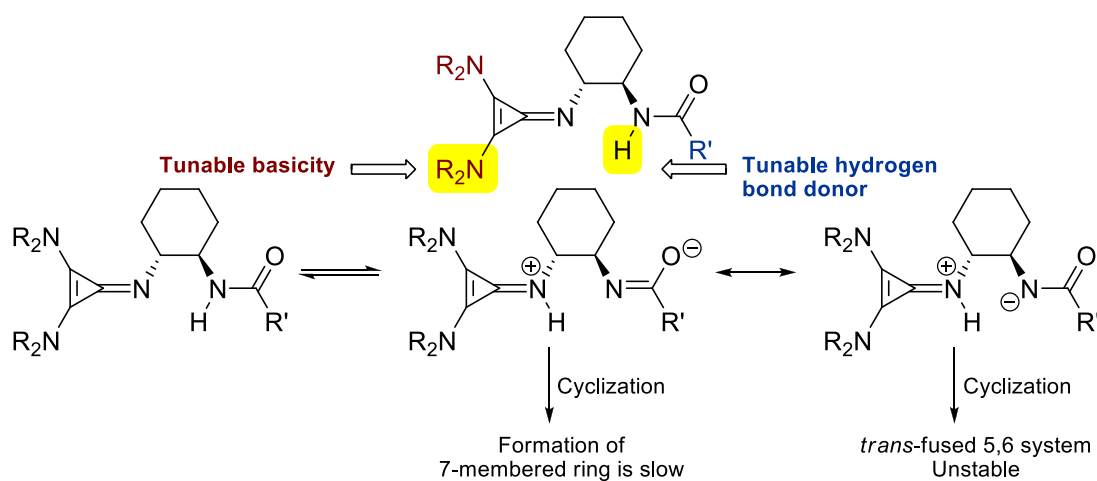
Figure 2: Optimized structures of urea bound by one and two Na cations at B3LYP/6-31G (d,p) level. Color codes: white–H, grey–C, blue – N, red–O, yellow–S, and violet–Na.

Disodium Complex

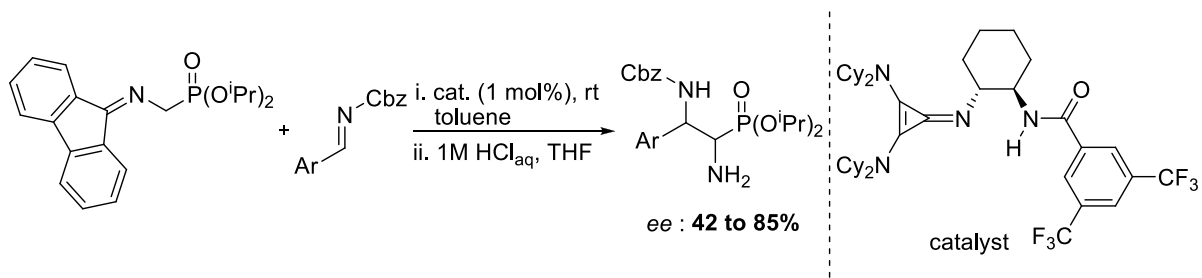


In the third chapter, our work on developing a strongly basic bifunctional organocatalyst is reported. The use of strong-bases can facilitate deprotonation of weaker acids and generate nucleophiles for novel reactions. Pioneering work in this area has been performed by the Najera, Kobayashi, Dixon and Lambert group. One of the strongest bases reported so far is the bifunctional chiral cyclopropeneimine developed by Lambert group. A key problem with this catalyst is the low-stability which precludes its use for reactions that require longer times. In order to address these issues we have designed a cyclopropeneimine with a chiral cyclohexanediamine backbone (Figure 3). One of the amino-groups from cyclohexane diamine is attached to the cyclopropeneimine, while the other group is converted to a carboxamide. The catalysts were synthesized using a simple synthetic protocol and showed enhanced stability. Further the, acidity of the carboxamide could be easily tuned. Using this catalyst, we have developed an enantioselective method for the synthesis of diaminophosphonates(Scheme 3). Chiral diaminophosphonates have been used in the synthesis of peptide isosteres for inhibiting protease enzymes. We have shown that the

Figure 3: Structure of Proposed Catalyst and Explanation for Expected Stability



Scheme 3: Synthesis of Diaminophosphonates



selectivity of the catalyst can be varied by tuning the acidity of the carboxamide group. The substrate scope for this reaction has been evaluated. The application of this catalyst for other reactions is currently under progress.

Table of Contents

Acknowledgement	ix
Thesis Synopsis	xi
List of Abbreviations	xxi
Chapter 1 Importance of Non-Covalent Interactions in Organocatalysis	
1.1 Introduction	1
1.2 π - π Interactions	3
1.2.1 π - π interactions in Povarov reaction	3
1.2.2 π - π interactions in Aldol reaction	6
1.3 Cation- π Interactions	8
1.3.1 Cation- π interactions in ring opening of episulfonium ions with indole derivatives	9
1.3.2 Cation- π interactions in 1,4-addition of N-Me pyrrole to cinnamaldehyde in the reaction catalyzed by MacMillan imidazolidinone catalyst	11
1.4 Anion- π interactions	13
1.4.1 Addition of enamine to nitroolefins on π -acidic surfaces	13
1.4.2 Domino reactions on π -acidic surfaces	15
1.5 Lone pair- π interactions	17
1.5.1 Achiral directing group vs chiral anion in an asymmetric fluorination reaction	17
1.6 Structural optimization	20
1.6.1 Role of conformation of catalyst in atropselective bromination reaction	20
1.7 S \cdots O interactions in controlling the conformation	23
1.7.1 Dual S \cdots O interactions in controlling chemo and enantioselectivity in an annulation reaction	23
1.8 Conclusions	26
1.9 References	27

**Chapter 2 Effect of Sodium Cation on the Enantioselectivity of a Bis-sulfonyl Urea
Catalyzed Friedel-Crafts Reaction**

2.1	Introduction	29
2.2	Background	30
2.3	Results and Discussion	37
2.4	Conclusions	52
2.5	Experimental Section	53
2.5.1	General Information	53
2.5.2	Synthesis of Urea Catalyst (2.33)	54
2.5.3	Sample procedure for the catalytic enantioselective Friedel-Crafts reaction	55
2.5.4	X-ray Crystallography CCDC number - CCDC 943949	66
2.5.4.1	Crystal data and structure refinement parameters for compound 2.33	67
2.5.5	Infrared and Raman Spectroscopy and Quantum Chemical Calculations	68
2.5.5.1	Tentative vibrational band assignment of catalyst 2.33	68
2.6	References	70

**Chapter 3 Bifunctional Strong-Base Catalyst for the Synthesis of Diamino
Phosphonates**

3.1	Introduction	75
3.2	Background	76
3.3	Results and Discussion	85
3.4	Conclusions	96
3.5	Experimental Section	96
3.5.1	General Information	96
3.5.2	Synthesis of fluorenone imine phosphonic acid esters	97
3.5.3	Synthesis of catalyst	101
3.5.3.1	Sample procedure for diaminobenzamide synthesis	101
3.5.3.2	Sample procedure for the catalyst synthesis	104

3.5.3.3 Preparation of Free Base	105
3.5.4 General procedure for the catalytic enantioselective Mannich reaction	119
3.5.5 General procedure for the benzoyl protection of amino phosphonates	129
3.5.6 Acidic hydrolysis of amino phosphonates	138
3.6 References	139
Appendix 1. NMRs	143
Appendix 2. HPLC Traces	249

List of Abbreviations

NMR	:	Nuclear Magnetic Resonance
IR	:	Infrared Spectroscopy
mp	:	Melting Point
THF	:	Tetrahydrofuran
DCM	:	Dichloromethane
DCE	:	1,2 Dichloroethane
DMSO	:	Dimethylsulfoxide
Boc	:	tert-Butyloxycarbonyl
Cbz	:	Carboxybenzyl
Equiv.	:	Equivalent
Aq.	:	Aqueous
DMAP	:	4-Dimethylaminopyridine
rt	:	Room Temperature
Dec.	:	Decomposed
<i>ee</i>	:	Enantiomeric Excess
Cy	:	Cyclohexyl
PTC	:	Phase Transfer Catalysts
BEMP	:	2- <i>tert</i> -Butylimino-2-diethylamino-1,3-dimethylperhydro-1,3,2-diazaphosphorine
DBU	:	1,8-Diazabicyclo(5.4.0)undec-7-ene

Conv.	:	Conversion
MTBE	:	Methyl tert-Butyl Ether
DI Water	:	Deionized Water
OTf	:	Trifluoromethanesulfonate
Cat.	:	Catalyst
Sat.	:	Saturated
TOF	:	Turn Over Frequency
NBS	:	N-Bromosuccinimide
TFA	:	Trifluoroacetic Acid
Conc.	:	Concentration
M.S.	:	Molecular Sieves
Dias.	:	Diastereomer

Chapter 1

IMPORTANCE OF NON-COVALENT INTERACTIONS IN ORGANOCATALYSIS

1.1 Introduction

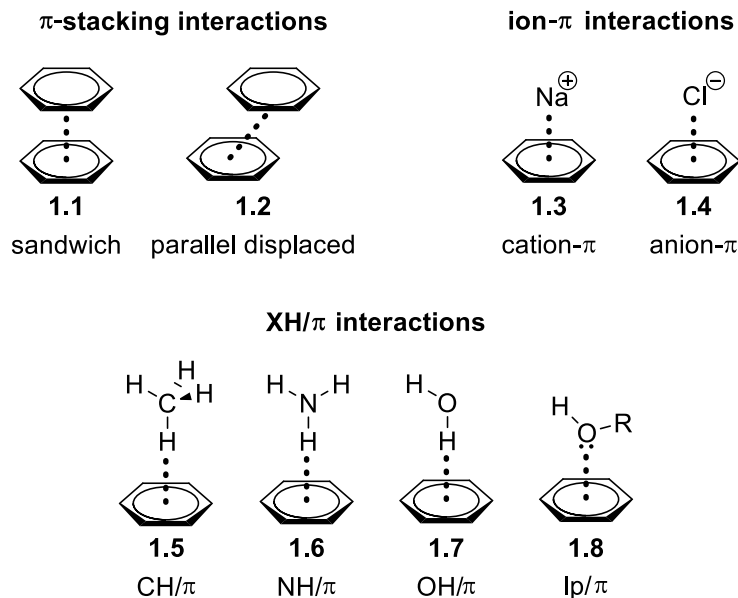
The catalyst-substrate interaction in organocatalysis is weaker than the corresponding interactions in organometallic catalysis. In the case of organocatalysis, non-covalent interactions (NCI) play an important role in enhancing these interactions. Conventionally, restricting the access of reactant to one face of a prochiral substrate is often accomplished by steric factors in an enantioselective process. In general the shape complementarity of the chiral binding pocket to the transition states of the reaction is a prerequisite for a stereoselective process. In the case of organocatalysts, the inherent structural flexibility reduces the energy difference between the transition structures associated with each prochiral face. Therefore additional interactions in the form of NCIs are important in enhancing the

energy difference between these transition structures. NCIs are dispersive in nature and are individually weak but are important collectively. Also these interactions are less directional and less distance dependent¹ in comparison to covalent and dative bonds. A proper balance has to be achieved between steric repulsions and NCIs to make a catalyst suitable for imparting selectivity in a reaction.

In most of the catalytic systems, the existence of favorable NCIs has been established post facto i.e. after the reaction has been optimized for high selectivity. Modern spectroscopic techniques and computational methods have been used to establish the importance of these interactions in the reaction of interest. However, integrating these features *a priori* as design elements has remained a challenging task. This is due to the fact that the optimized reaction proceeds through a transition structure where many competing interactions are finely balanced. In this regard, catalyst modularity plays an important role as this allows for a “guided-empiricism” approach for optimizing a reaction. Additionally, the modular systems can be used to generate structure-function data sets that can be helpful in obtaining reliable insights into NCIs.

Initial reports from the Miller² group showed that short peptides can be used to catalyze kinetic resolutions. Miller used split-pool synthesis to obtain a library of peptides that used hydrogen bonding to activate substrates. Jacobsen has reported on the utility of cation- π interactions as secondary interactions in organizing the cationic transition state via H-bonding or ion-pair catalysis. The Matile group has recently reported on the utility of anion- π interactions in catalyst design.³ This chapter will outline the role of non-covalent interactions like π - π , cation- π , anion- π , lone pair (lp)- π interactions (Figure 1.1) in organocatalysis, as well as the role of modular catalysts in evaluating the role of NCIs.

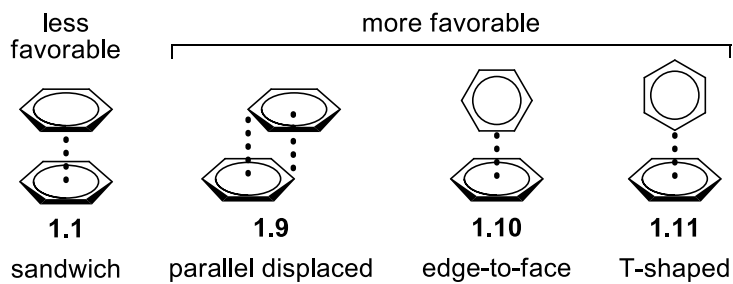
Figure 1.1: A Prototype for Non-Covalent Interactions



1.2 π - π Interactions

The attraction between two neutral aromatic rings is often characterized using the terms π - π interaction or π stacking. The strength of this interaction is dictated by the geometry of stacking. Parallel stacking is less favorable (a difference of 0.9 kcal/mol) compared to parallel displaced⁴ and edge-to-face or T-shaped as shown in Figure 1.2. High level *ab initio* studies reveal that these interactions are stabilized by dispersion forces.⁵ Moreover, recent studies from Wheeler and Houk points out that the strength of the π - π interaction depends on the interactions between the local C-X/H dipoles of substituted aromatic rings.⁶

Figure 1.2: A Prototype for π - π Interactions



1.2.1 π - π Interactions in Povarov Reaction

In a recent report from the Jacobsen group on an enantioselective Povarov reaction, π - π interactions were shown to play an important role in organizing the transition state (2.1 kcal/mol).⁷ Stereocontrol in a [4+2] cycloaddition between imine and a dihydrofuran, was achieved using a chiral urea catalyst (Scheme 1.1). Kinetic and computational studies have shown that in the transition state, a protonated imine is bound by a hydrogen bond to the sulfonyl oxygen and π - π interaction with the bis-trifluoromethyl phenyl group (Figure 1.3). The triflate counterion is bound tightly to the urea and forms a hydrogen bond with the

Scheme 1.1: Brønsted Acid Promoted, Urea Catalyzed Povarov Reaction

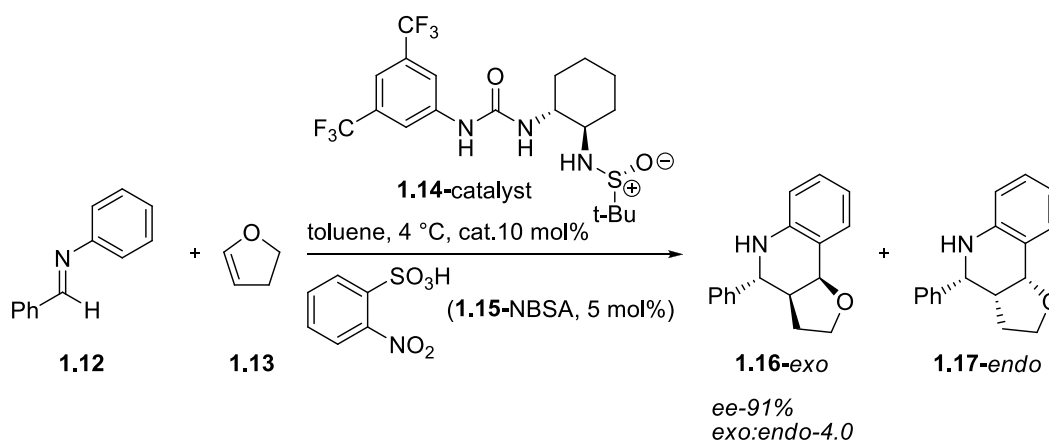
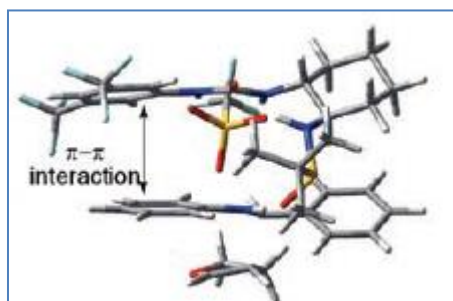
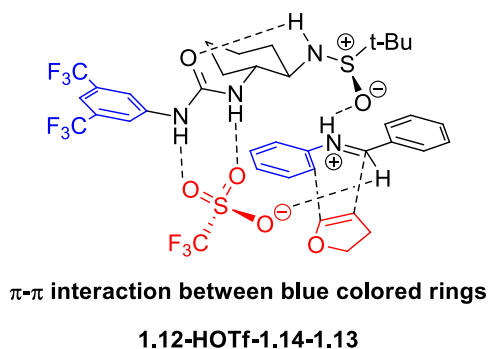
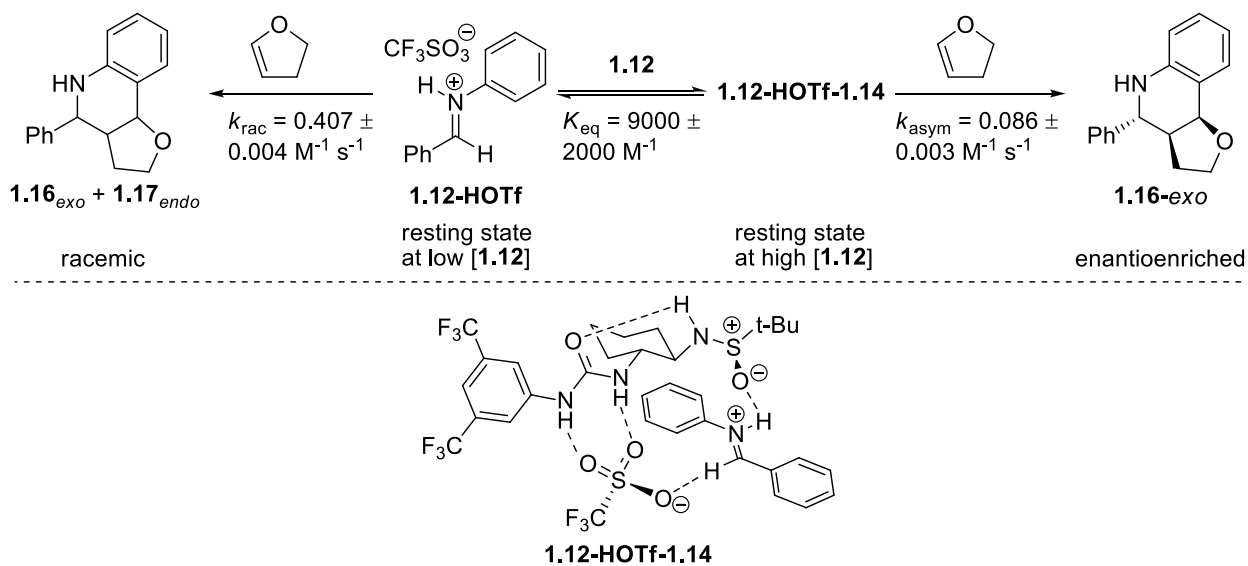


Figure 1.3: Diastereomeric Transition State Stabilized by π - π Interactions. Reprinted with Permission from The American Association for the Advancement of Science. Permission no. 4177660569972



aldimine proton. The protonated imine can react with the dihydrofuran in the absence of the catalyst. Indeed this reaction proceeds at a faster rate than the catalyzed reaction (Scheme 1.2). In the catalyzed reaction, interaction between sulfoxide and the protonated imine lowers the reaction rate. However, the equilibrium constant for binding between the protonated imine and catalyst is $K = 9000 \pm 2000 \text{ M}^{-1}$. This ensures that the protonated imine is always bound by the catalyst. To suppress the background reaction, a sub-catalytic quantity of triflic acid with respect to the urea catalyst, was used. This ensured a very low concentration of the free iminium, which enabled the reaction to proceed in a highly enantioselective pathway. The π - π interaction between the aniline arene group of the substrate and the bis-trifluoromethyl phenyl group of catalyst led to major isomer (*R*) of the product (Figure 1.3). This feature was absent in the competing diastereomeric transition state. This reaction demonstrates the importance of weak NCIs in controlling the reactivity of molecules and to channelize into substrates for enantioselective reactions.

Scheme 1.2: Reaction Equilibrium between Chiral and Racemic Pathway



1.2.2 π - π Interactions in Aldol Reaction

Enantioselective aldol reactions catalyzed by amino acid derived organocatalysts that proceed via enamine intermediates are well known.⁸ Among them proline derived catalysts are an important class of organocatalysts in aldol reactions developed by List et al.⁹ Di and tripeptide proline based catalysts have been used by several research groups as catalysts in asymmetric aldol reactions.¹⁰ In this class of catalysts, interestingly Juaristi et al have shown that NCIs play an important role in catalyzing an intermolecular reaction of ketone with aromatic aldehydes.¹¹ Dipeptide catalysts having pendent aromatic core have been used in aldol reaction to obtain good diastereo and enantioselectivities as shown in Scheme 1.3. Best results were reported by using the catalyst with pendent indole group, derived from tryptophan amino acid residue. Juaristi et al proposed that the observed selectivity could be due to possible π - π interactions between pendent aromatic groups of catalyst and the aromatic core of aldehyde substrates. To validate this postulate a naphthyl-alanine based dipeptide catalyst was screened in an aldol reaction between cyclohexanone and various aromatic aldehydes.¹¹ Good improvements in yields and turn over frequencies were observed. This supported the idea that the transition states were stabilized by π - π interactions. Upon screening various aromatic aldehydes with substituents ranging from electron poor to rich, good enantioselectivities ranging from 78 to 98% *ee* were observed for the *anti* diastereomer (major), albeit with varied TOF. A comparison of reaction between pentafluorobenzaldehyde, benzaldehyde, and 4-MeO benzaldehyde was performed (Scheme 1.3) to clarify the role of π - π interactions between naphthyl aromatic core of catalyst and the aldehyde substrates (Figure 1.4). Aromatic rings with an electron withdrawing group showed a large improvement in yield and *ee* which supported the role of π - π interactions. Further

Scheme 1.3: Screen of Various Aromatic Aldehydes in a Dipeptide Catalyzed Aldol Reaction

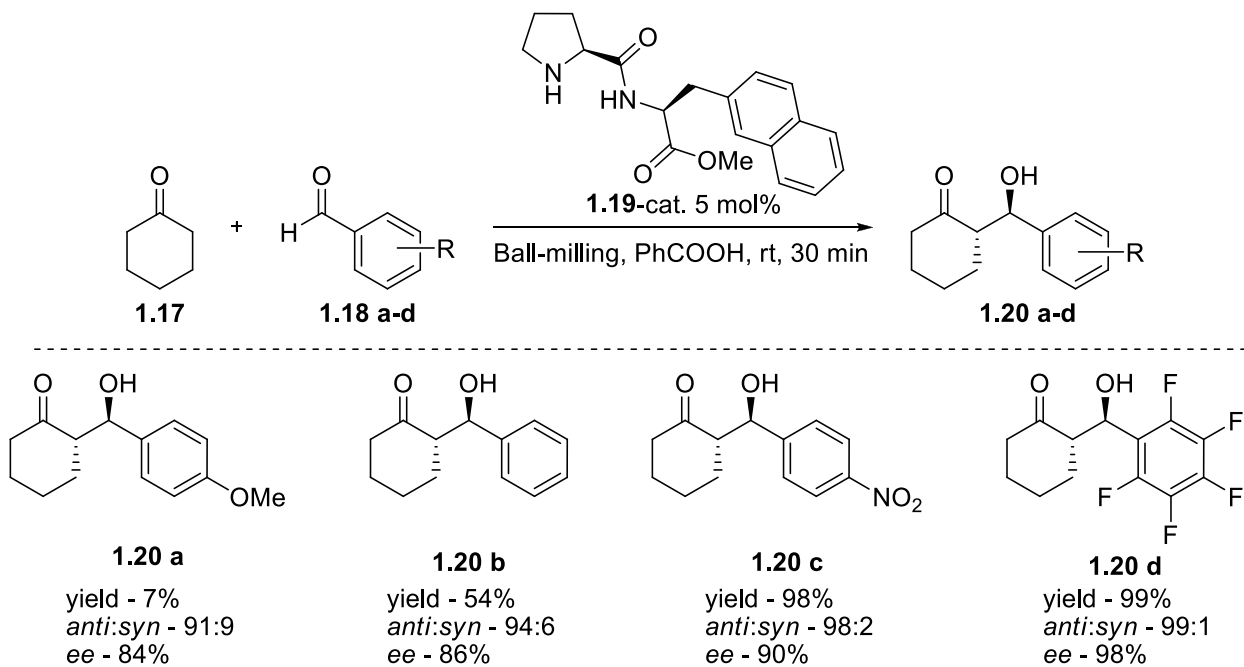
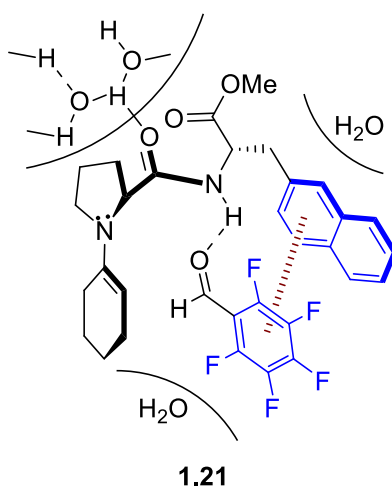


Figure 1.4: Key π - π Interactions for Enhanced Reactivity and Selectivity

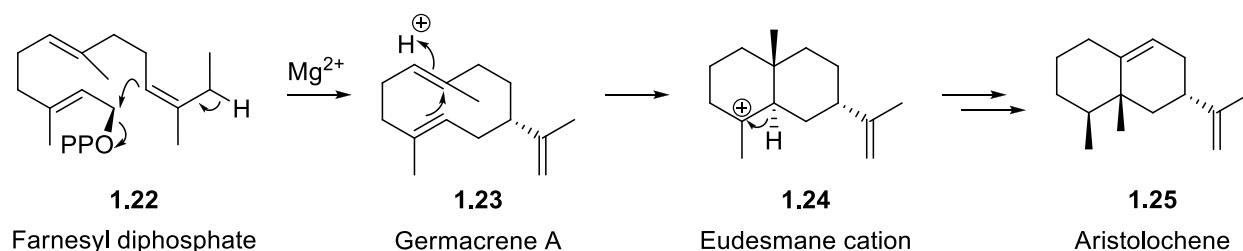


support from the computational studies was not reported by the Juaristi group. This brings another important example wherein π - π interactions are important in rigidifying and organizing the transition state for enhanced selectivities.

1.3 Cation- π Interactions

The stabilization of a cation by the neighboring π -basic aromatic surface is often termed as cation- π interaction. These interactions are well recognized and studied and often play important role in the biosynthesis. A systematic study by Allemann et al¹² to evaluate the role of tryptophan residue in the synthesis of aristolochene synthase, confirmed the occurrence of cation- π catalysis. The eudesmane cationic intermediate (Scheme 1.4) was expected to be stabilized by the indole moiety of the tryptophan. When the tryptophan was replaced by non-proteinogenic amino acids with different π -acidic aromatic residues, accumulation of germacrene A was observed. Eventually a decrease in the yield of aristolochene with increasing π -acidity confirmed the role of cation- π interactions.

Scheme 1.4: Enzymatic Synthesis of (+)-Aristolochene

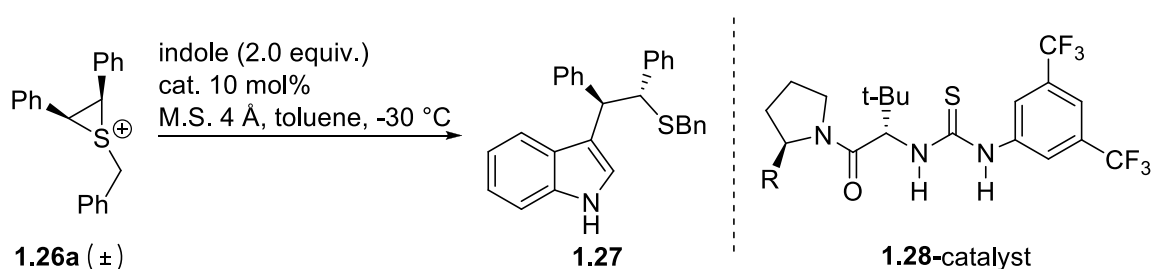


1.3.1 Cation- π Interactions in Ring Opening of Episulfonium Ions with Indole Derivatives

Considering the lessons learned from the precedents it should be possible to come up with new catalyst designs that can stabilize the cationic transition states to explore unusual reaction patterns. To this end, Jacobsen group has used small molecules having extended π -systems as arms in controlling the kinetics of enantioselective reactions.¹³ One among them

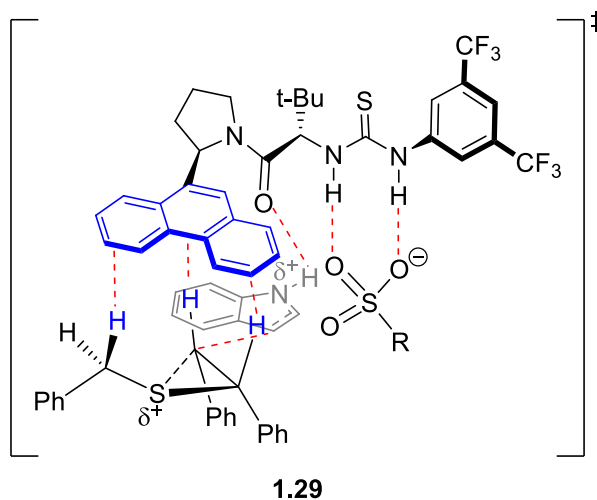
is the selective ring opening of meso-episulfonium ions with indole where cation- π interactions play an important role (Scheme 1.5). Based on NMR and kinetic experiments, dual hydrogen-bond interactions for anion binding were proposed. Also an important hydrogen-bond interaction between amide carbonyl of catalyst and the N-H group of nucleophile led to the opening of the episulfonium ion precisely from one side (Figure 1.5). Calculation of rate constants of major and minor asymmetric pathways pointed to the role of

Scheme 1.5: Ring Opening of Episulfonium Ions with Indole Derivatives



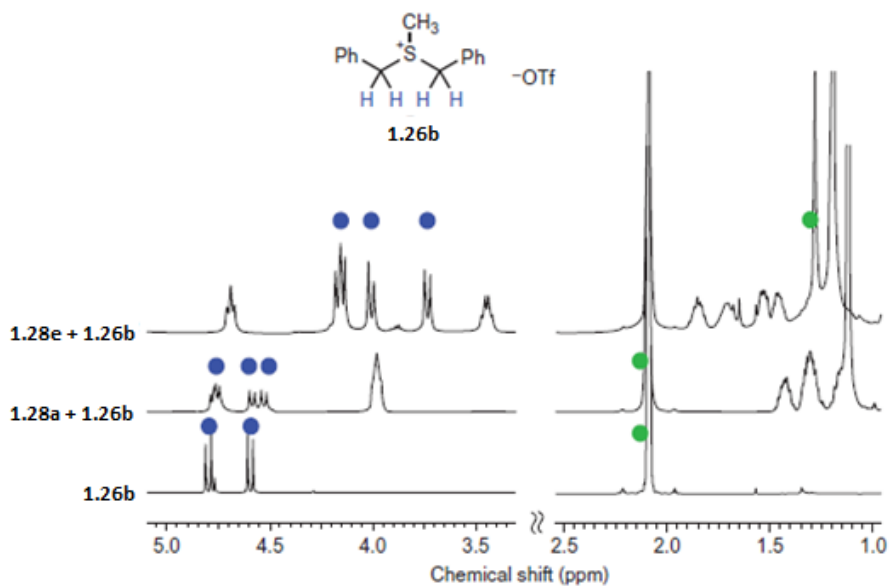
catalyst	R	ee (%)
1.28a	H	12
1.28b	Ph	73
1.28c	1-naphthyl	84
1.28d	2-naphthyl	85
1.28e	9-phenanthryl	93

Figure 1.5: Network of NCIs in the Transition State Model



extended π -systems in stabilizing the transition state through cation- π interactions. Indeed, NMR experiments also supported the cation- π interactions, where a shift of 0.6 - 0.8 ppm was observed in benzylic hydrogens of a model sulfonium salt **1.26b** in the presence of the thiourea catalyst having phenanthrene moiety **1.28e** (Figure 1.6). This was further supported by electron-potential mapping calculations using density functional theory. With all these network of attractive interactions between the catalyst and reacting components in the transition structure assembly as shown in Figure 1.5 good enantioselectivities were achieved. This study rigorously demonstrates the importance of cation- π stabilization in controlling the reactivity of reactants to achieve high enantio-selection.

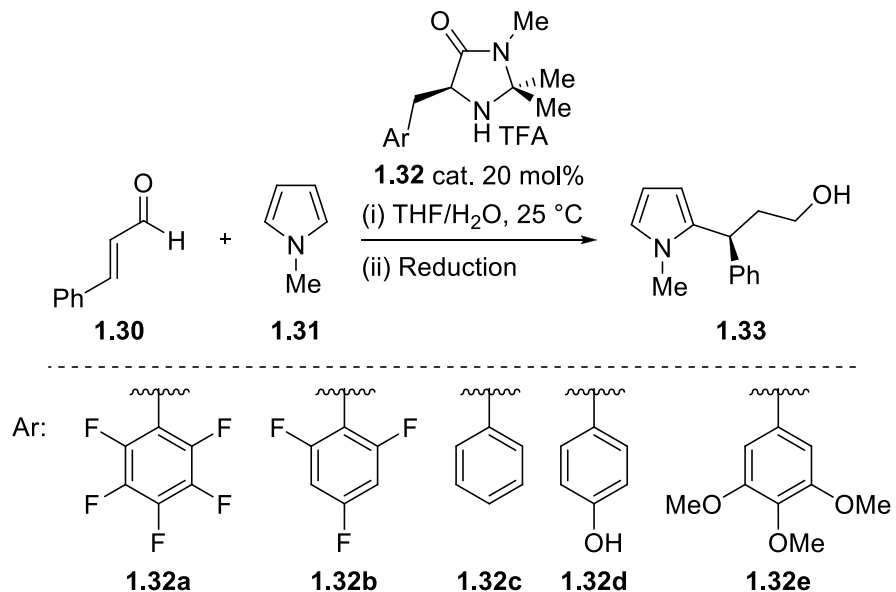
Figure 1.6: ^1H NMR Binding Study of Thiourea **1.28** and the Sulfonium Salt **1.26b** in Toluene- d_8 (benzylic hydrogens – blue, methyl hydrogens – green). Reprinted with Permission from Nature Publishing Group. Permission no. 4177650612517



1.3.2 Cation- π Interactions in 1,4-Addition of N-Me Pyrrole to Cinnamaldehyde in the Reaction Catalyzed by MacMillan Imidazolidinone Catalyst

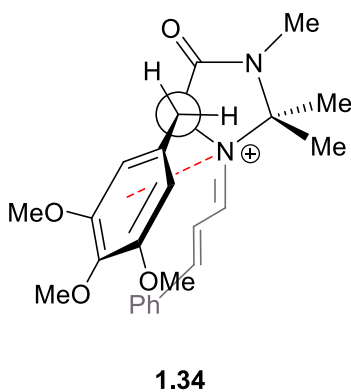
In an attempt to see the role of possible cation- π interactions in a MacMillan first generation imidazolidinone catalyst a systematic study was done in a Friedel-Crafts alkylation.¹⁴ Validation of this intriguing hypothesis was done by electronic modulation of the aromatic core in the catalyst. The traceless quadrupole moment tensor (Q_{zz}) reflects the electronic component of the aryl group, lying orthogonal to the aromatic ring. The magnitude of the tracer varies from negative to positive upon substituting the aromatic ring with electron withdrawing groups as shown in the table of Scheme 1.6. To assess the role of the pendent aryl group in the stabilization of the covalent iminium intermediate, various catalysts were screened in the reaction of enones with N-Me pyrrole. With increasingly negative Q_{zz} value as shown in the table face selection was improved. In the case of tri methoxy derived catalyst a high enantio-selection was seen with 94% *ee*. This can be a consequence of participation of trimethoxy aryl group in stabilizing cation- π interactions in the transition state (Figure 1.7). The enhanced cation- π interactions led to the development of a more efficient catalyst. This catalyzes the reaction at ambient conditions, at a much faster rate (reduction in time from 42h to 3h) without loss in selectivity. Further examination of these catalyst features using computational techniques can lead to formulation of guidelines for catalyst development.

Scheme 1.6: Screen of Imidazolidinone Catalyst for Probing the Cation- π Interactions



entry	catalyst	Q_{zz}	ee %
1	1.32a	+ 3.01	65
2	1.32b	+0.28	70
3	1.32c	-3.46	84
4	1.32d	-3.71	90
5	1.32e	-5.68	94

Figure 1.7: Possible Cation- π Interactions in the Transition State Model

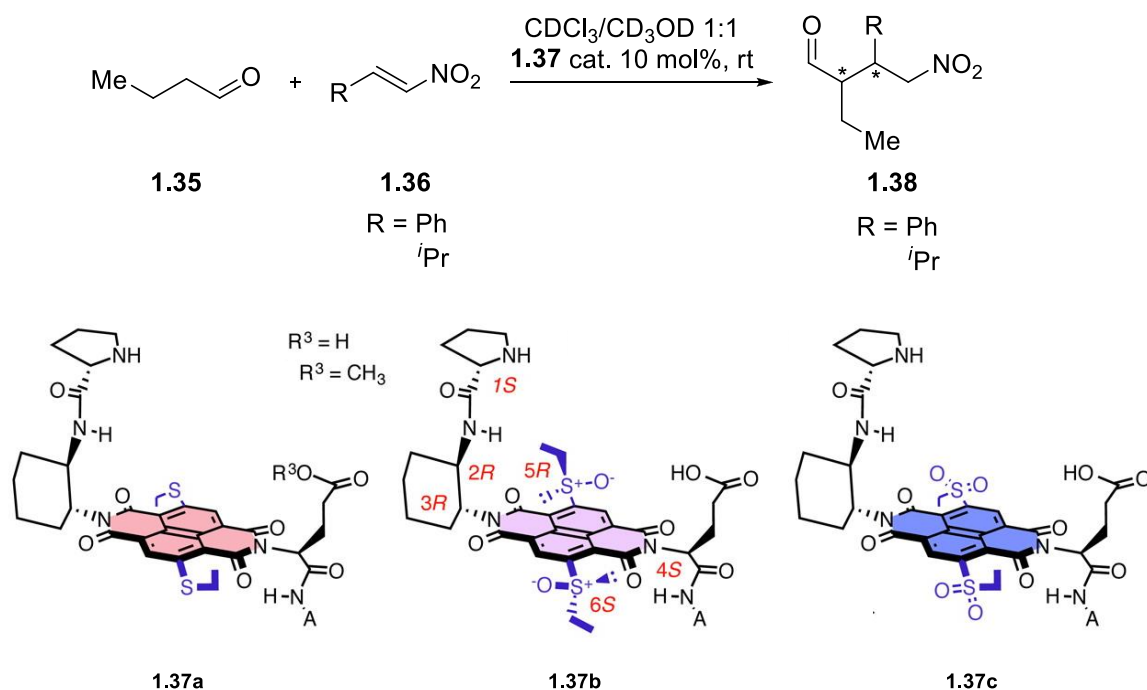


1.4 Anion- π Interactions

1.4.1 Addition of Enamine to Nitroolefins on π -Acidic Surfaces

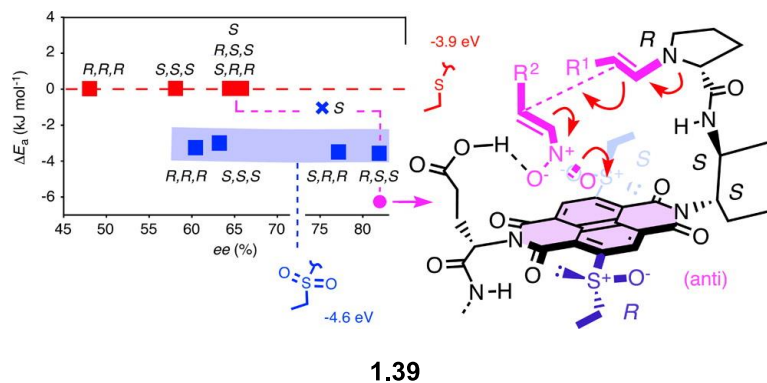
Anion- π interactions are not well known in nature. Recently the Matile group has developed catalytic reaction wherein these interactions play an important role. The interaction between anion and aromatic core with positive quadrupole moment is termed as anion- π interaction and these are in contrast to interactions discussed in the above section. Matile and co-workers have used a naphthalenediimide (NDI) aromatic core having electron withdrawing groups as anion transporter or anionic transition state stabilizer.¹⁵ Initially these type of interactions were shown to play an important role in Kemp elimination reaction promoted by NDIs.^{15a} Besides this, an enantioselective reaction has been reported by the Matile group using enamine chemistry and they were able to achieve up to 83% *ee*.¹⁶ In this work, a reaction between aldehyde and a nitroolefin was sought to be carried out on a π -acidic platform. For this purpose they decided to explore the catalyst having NDI core with proline at one end and carboxylic acid group at the other end (Scheme 1.7). Aldehydes react with the proline group at one end of the NDI to form an enamine. The enamine nucleophile reacts with nitroalkene in a Michael reaction to generate a nitronate anion. This is then protonated by the carboxyl group at the other end of the NDI. The transition state for the Michael addition is negatively charged and is likely to be stabilized by anion- π interactions. If this is indeed the case, then the transition state should be sensitive to the substitution pattern on the NDI core. To explore this, two electron donating sulfide groups were attached to the NDI core **1.37a** as shown in Scheme 1.7. Upon gradual oxidation they were converted to sulfoxides **1.37b** and sulfones **1.37c**. When these catalysts were screened, reaction rates and enantioselectivities increased with an increase in the π -acidity of the NDI core. The

Scheme 1.7: Anion- π Catalysts in the Addition of Enamine to Nitroolefin. Adapted with Permission from American Chemical Society



observed rate enhancements were correlated to decrease in activation energy ΔE_a and plotted with *ee* (Figure 1.8). High match and mismatch scenarios were seen in the case of chiral sulfoxides **1.37b** and a broad range of *ees* (48% to 83%) were obtained. Improvement in reaction rate along with selectivity on π -acidic sulfone catalyst **1.37c** suggests the role of anion- π catalysis. This phenomenon of obtaining better selectivity with enhanced reaction rates were often seen in hydrogen-bonding catalysts when their acidity strengths were tuned. These unprecedented experimental data provides the proof for the existence of anion- π interactions and contributes to the enamine catalysis.

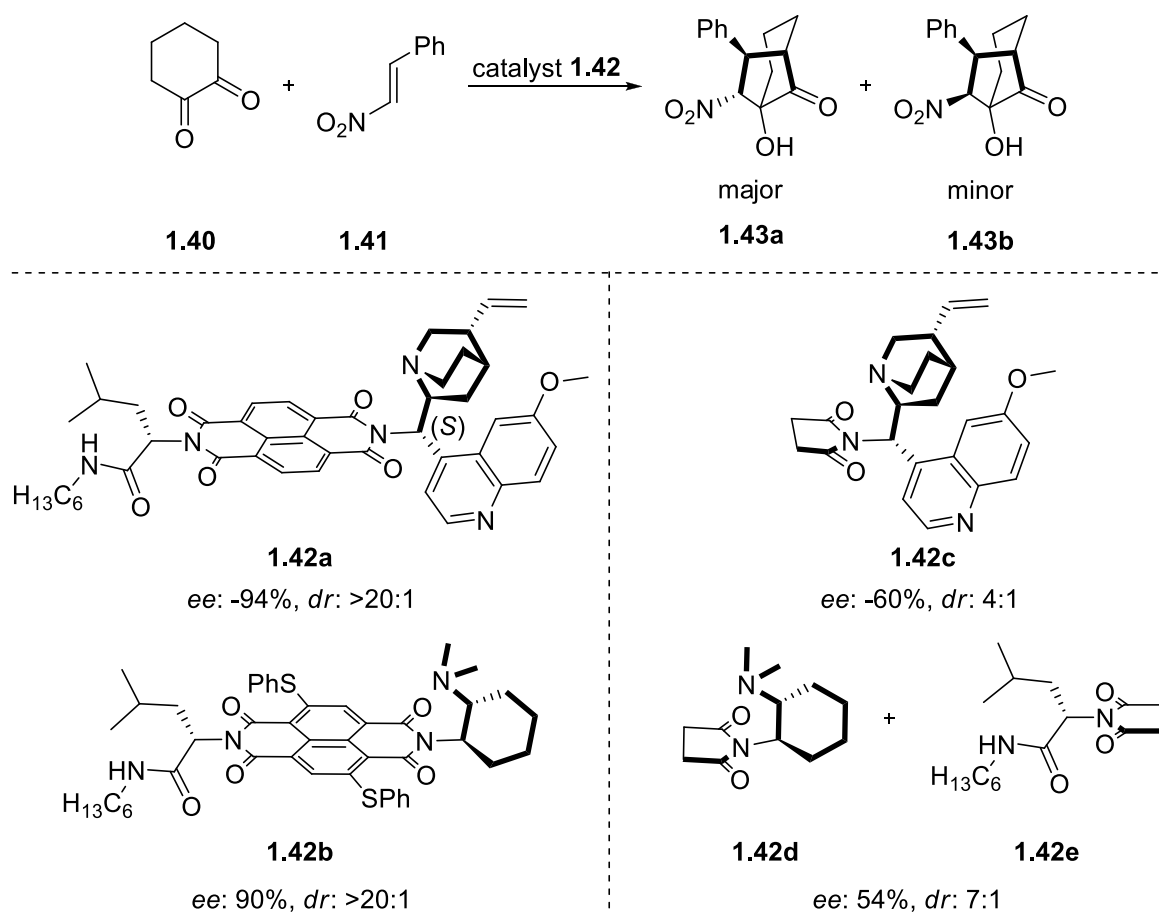
Figure 1.8: Kinetic Chiral Space Covered by Catalysts on the Left and the Stabilization of Anionic Intermediate on π -Surface on the Right. Reprinted with Permission from American Chemical Society



1.4.2 Domino Reactions on π -Acidic Surfaces

In another example, the Matile group has used anion- π interactions to achieve improved selectivities in a domino reaction compared to conventional metal-free organocatalysts.¹⁷ Domino reactions involve long-distance charge displacements. In the domino Michael-Henry reaction between hexanedione and nitroolefin the two C-C bonding steps proceed *via* anion intermediates. When an NDI based catalyst is used for this reaction, the anionic enolate and nitronate intermediates can be potentially stabilized by these π -acidic surfaces. To test this hypothesis, catalyst **1.42a** and **1.42b** were synthesized. Domino reactions carried out using these catalysts, were more diastereoselective than reactions carried out with conventional organocatalysts (Scheme 1.8). Upon using catalysts with π -surface connected to a tertiary amine *via* a fixed Leonard turn enantio-selectivities up to 86% were achieved. While screening the same with π -surface connected to quinine resulted in high enantioselectivity with -94% ee and excellent diastereoselectivity (>20:1).

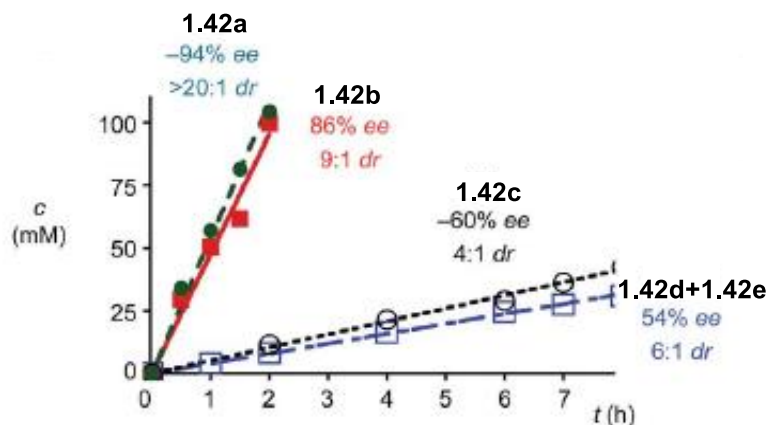
Scheme 1.8: π -Acidic Catalysts in Domino Reaction between Cyclohexanedione and Nitroolefin



In both cases controls with no π -acidic surface resulted in moderate selectivity with a drop in reaction rate (Figure 1.9). Addition of C_6D_6 solvent has positive contribution to the reaction when added in small quantities, whereas upon addition of large quantities of C_6D_6 synergistic anion- π interactions with polarization of π -surface disrupted leading to loss of enantioselection. In addition to this, introduction of anions ($NO_3^- > Br^- > BF_4^- > PF_6^-$) into the reaction inhibited the reaction. All of these results taken together corroborate the fact that anion- π interactions are crucial for the catalysis. This once again shows the importance of NCIs in organocatalysis.

Figure 1.9: Enhancement of Reaction Rates and Selectivities with the π -Acidic Surface.

[DOI: 10.1039/C7SC00525C] Published by The Royal Society of Chemistry



In the presence of catalysts **1.42a**(●), **1.42b**(■), **1.42c**(○), **1.42d+1.42e**(□).

1.5 Lone Pair- π Interactions

1.5.1 Achiral Directing Group vs Chiral Anion in an Asymmetric Fluorination Reaction

The stabilizing interaction between lone pair of electrons and π -electron cloud is described as lone pair (lp)- π interaction. In general aromatic core with positive quadrupole moment (Q_{zz}) are expected to stabilize these weak attractions similar to anion- π interactions. However, both theoretical and experimental studies revealed that these interactions are found to be stable in electron rich aromatic systems. This is thought to be due to the importance of electron correlation or dispersion effects.¹⁸ Although these interactions were rarely cited, Toste¹⁹ and Sigman had invoked the presence of these lp- π attractive forces in an asymmetric fluorination of allylic alcohol based on series of experimental structure-selectivity studies. To render the allylic alcohols more reactive in the fluorination reaction, boronic acids (BAs) were used as traceless directing groups. Both alcohols and BAs condense to form a mixed boronic ester and coordinate via hydrogen-bonding with phosphonate group of the catalyst.

Interesting features were observed in their study between various phosphoric acid (PA) catalysts and BAs in this reaction. Substitution patterns on aromatic rings of BAs have differential role on selectivity ranging from -73% to 90%. The key structural observations were (1) Inversion in selectivity with meta-substituted BAs when compared with other BA substituted patterns, (2) Effect of size of substituents on the phosphoric acid catalyst in the sensitiveness of BAs towards the reaction as shown in Table 1.1.

To probe the effect of 3,5 substituents of boronic acids on selectivity, screening with various meta substituted BAs were done as shown in Table 1.2. This experiment was designed to distinguish steric effects of substituent groups from the possible interaction of methoxy group of BA with the aromatic groups of catalyst. Interestingly, BAs without methoxy groups were observed to give poor selectivity. This intrigued them to validate the possible non-covalent interaction. Inspired by previous results, a key change was made in catalyst to reinforce this interaction (Scheme 1.9).

Table 1.1: Combinations of BAs and PAs in Fluorination of Allylic Alcohols

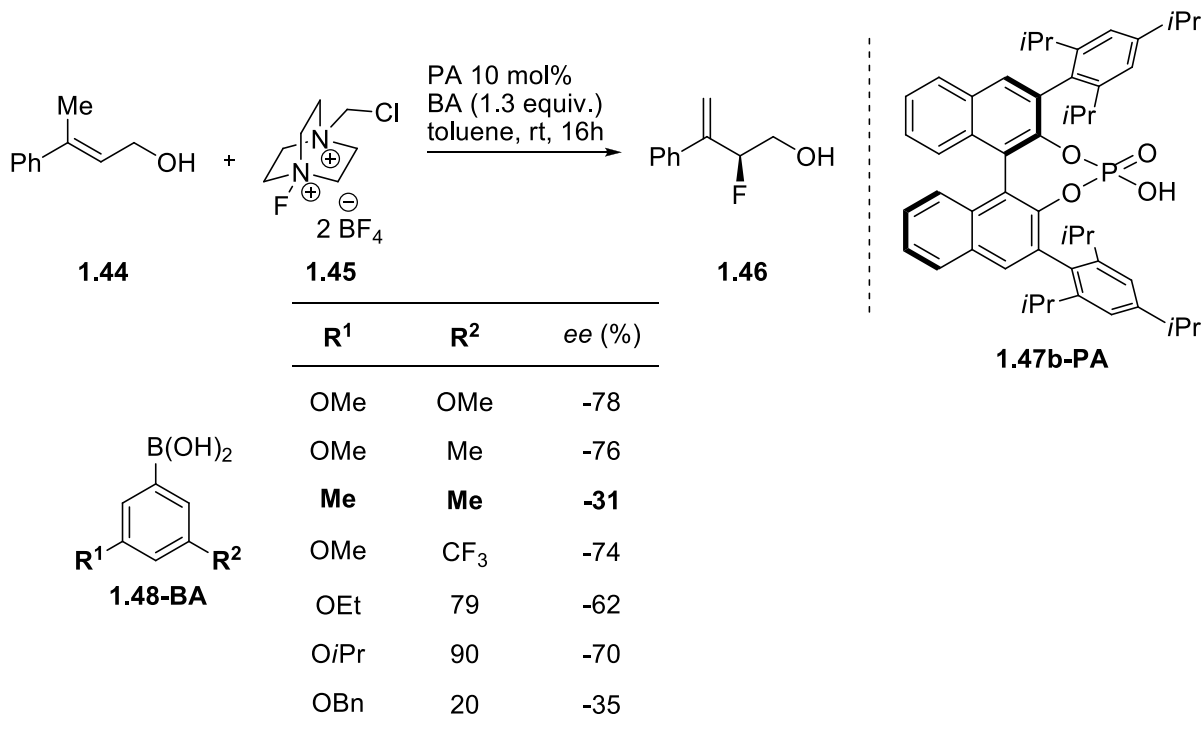
1.44 + **1.45** $\xrightarrow{\text{PA 10 mol% BA (1.3 equiv.) toluene, rt, 16h}}$ **1.46**
-78%(S) to 90%(R) ee

1.47

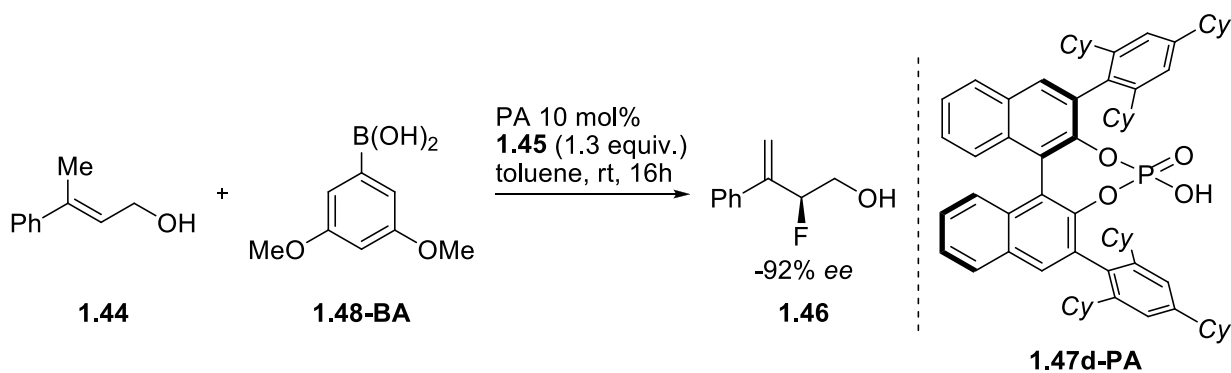
	R¹	1.47a ee (%)	1.47b ee (%)	1.47c ee (%)	
 1.48-BA	H	79	54	-	1.47a , R ² =R ³ =Me
	4-Me	90	66	34	1.47b , R ² =R ³ = <i>i</i> Pr
	3,5-(OMe) ₂	20	-78	-10	
	3,5-(Me) ₂	63	-31	12	1.47c , R ² = <i>i</i> Pr, R ³ =H

1.48-BA

Table 1.2: Screen of Various Boronic Acids with Catalyst **1.47b** in the Reaction



Scheme 1.9: Catalyst Structure Optimization to Enhance Ip- π Interaction



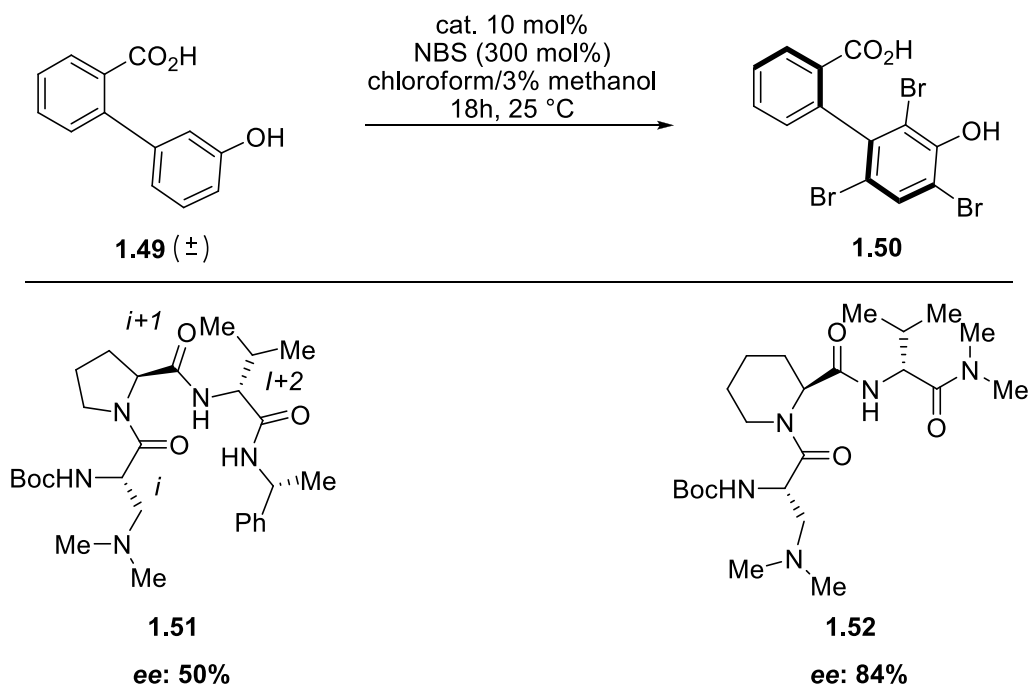
Catalysts with bulkier substituents at 2,4,6 positions were expected to have change in torsional angles with the binaphthyl backbone, which would facilitate the Ip- π interaction. Indeed, on screening catalyst **1.47d**, -92% *ee* was observed in the reaction. Although computational support was not available, the experimental results made them invoke Ip- π interactions essential for the switch in the face selection from 90% to -92% *ee*.

1.6 Structural Optimization

1.6.1 Role of Conformation of Catalyst in Atropselective Bromination Reaction

Increasing the interaction between catalyst and the substrates is the rational way of tuning the catalyst. This is often achieved by aiming for specific interaction as discussed in the above sections and optimizing the structure by incorporating functional groups for stabilizing that particular interaction. In spite of this, catalysts may not be effective for the stipulated process. To overcome this, tuning the conformation can be an option. This inherently requires modularity in the design of catalyst. In this manner, Miller et al used their empirical knowledge to solve the long-standing problem of organo-catalytic dynamic kinetic resolution of biarylatropisomers.²⁰ The choice of a simple tripeptide catalyst with β -turn played a decisive role in the face selection. Replacing the five membered pyrrolidine moiety of proline with six membered piperidine, improved the *ee* from 50% to 80% (Scheme 1.10).

Scheme 1.10: Tuning the Conformation in Optimizing the Selectivity



It is known that N-acylpiperidines minimize allylic strain by positioning substituents at the second position in an axial orientation.²¹ This classical case reveals the role of conformation on reaction selectivity. Further optimization of the catalyst resulted in achieving upwards of 90% *ee* in majority of the substrates tried. Reverse engineering the structure of catalyst revealed the importance of amide group on reactivity, as the reaction was sluggish in the absence of catalyst (Scheme 1.11). Taken together Miller et al postulated the docked structure of substrate inside the chiral pocket of catalyst using non-covalent interactions, as well as conformational restraints (Figure 1.10). This example demonstrates the importance of structural optimization in tuning the conformation of the catalyst.

Scheme 1.11: Probing the Role of Structural Features of Catalyst on Reactivity

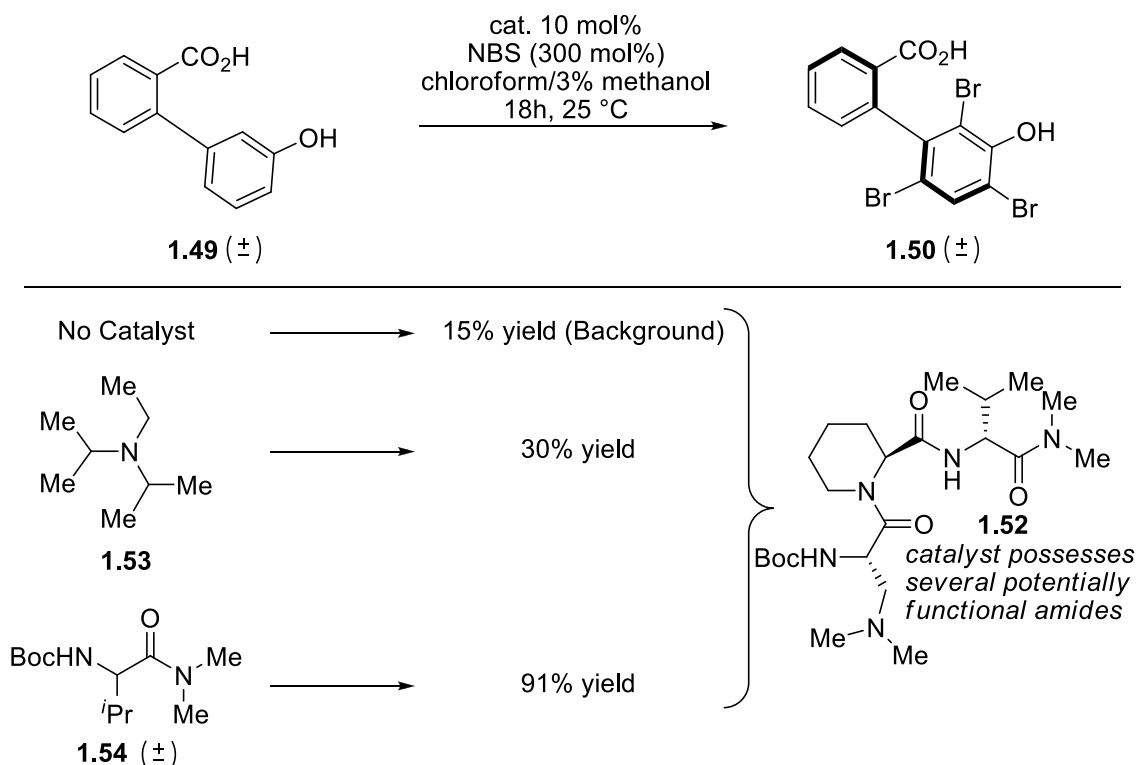
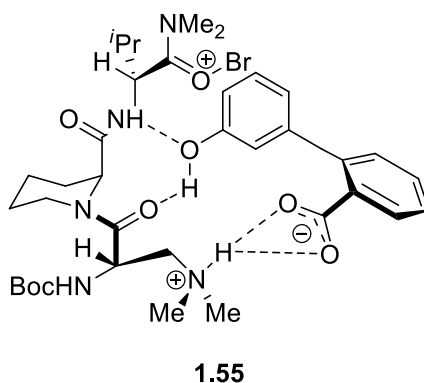


Figure 10: Proposed Docking Model

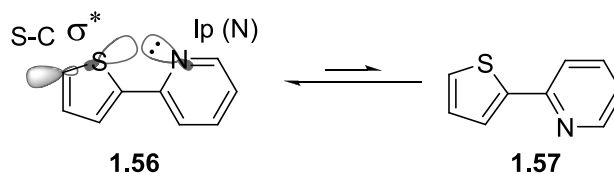


1.7 S \cdots O Interactions in Controlling the Conformation

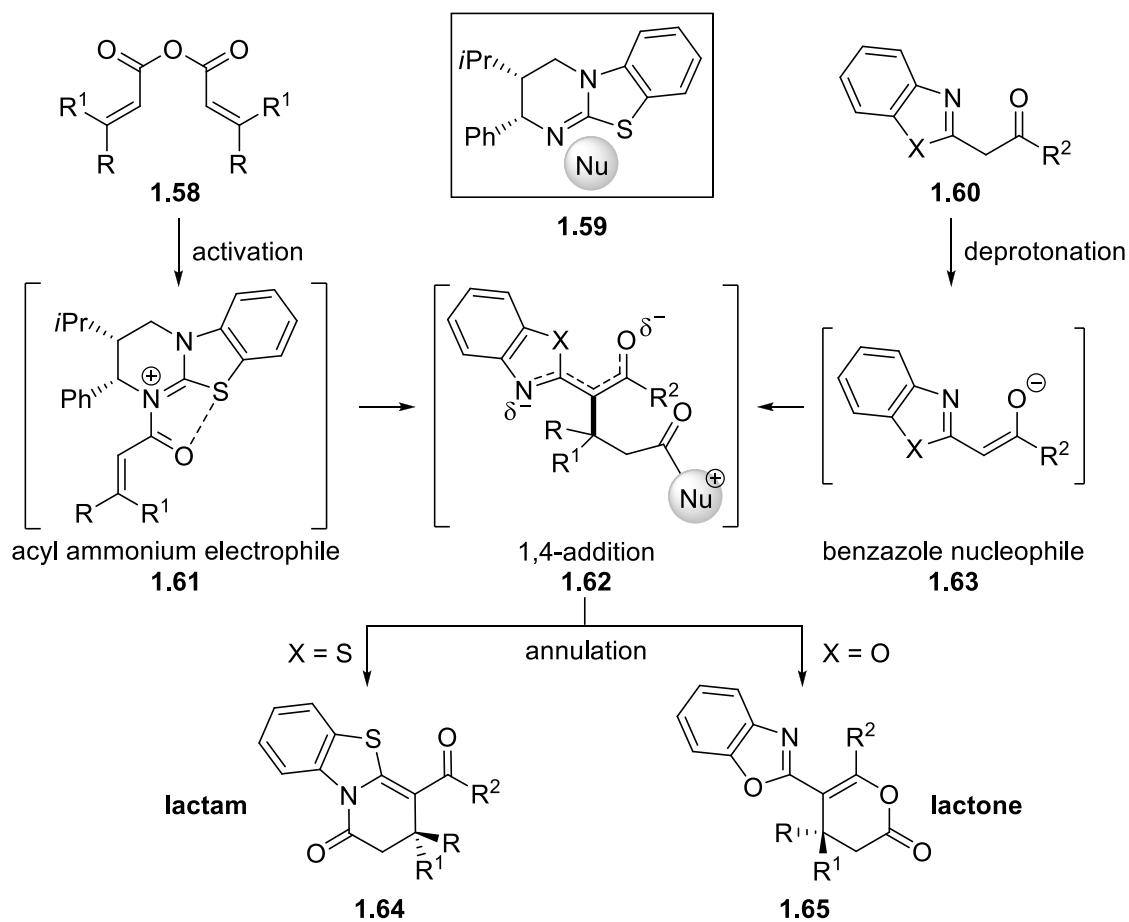
1.7.1 Dual S \cdots O Interactions in Controlling Chemo and Enantioselectivity in an Annulation Reaction

The $\sigma^*_{\text{C-S}}$ orbitals of sulfur in heterocycles, can participate in non-bonding interactions with the vicinal n lone pair of heteroatom as shown in the Figure 1.11 thereby favoring the *syn* conformation (0.7 Kcal/mol).²² These types of interactions are useful in controlling molecular conformation, which eventually turned to be reason for high s -factor up to 355 in a benztetramisole catalyzed kinetic resolution of secondary alcohols.²³ Very recently Smith et al exploited these interactions using the same benztetramisole based catalyst **1.59** to achieve high chemo and enantioselection in isothiurea-catalyzed annulations of benzazoles (Scheme 1.12).²⁴ In the reaction between 2-acyl benzothiazoles and α,β -unsaturated acyl ammonium intermediates dual 1,5-S \cdots O interactions **1.66** played a major role in the formation of lactam **1.64** over lactone **1.65** heterocycles. The seemingly trivial change of substrate to 2-acyl benzoxazole from benzothiazole had a differential effect in the annulation with the formation of lactone (O-cyclization) rather than lactam. The effective 1,5-S \cdots O interactions in the substrate are not available leading to O-cyclization.

Figure 1.11: S...O Interactions Favoring *Syn* Conformation



Scheme 1.12: S...O Interactions Guided Chemo and Enantioselective Lactam and Lactone Formation



high enantioselectivity up to 99%
chemoselectivity up to > 95:5 for lactam and lactone formation

Computational studies reveal that a new C-H \cdots O interaction **1.69** (C-H adjacent to positively charged nitrogen) stabilize the transition state geometry to obtain lactones with up to 98% *ee* (Figure 1.12).

In the presence of base no conversion of lactone **1.65** to lactam **1.64** was observed. This confirms the interplay between S/O and C-H/O interactions were due to kinetic control over annulation. The key 1,5-S \cdots O interactions planarize the electrophilic acylammonium intermediate as well as the nucleophile and allow nucleophile attack through the less hindered face, accounting for high enantioselectivity (Figure 1.13). Also the two key stabilizing interactions shown in Figure 1.12 accounts for the excellent chemoselectivity, once again brings to focus the importance of these interactions for the development of field of catalysis.

Figure 1.12: Model Systems Probing the Relative Stability of Transition States Governed by S/O and C-H/O Interactions

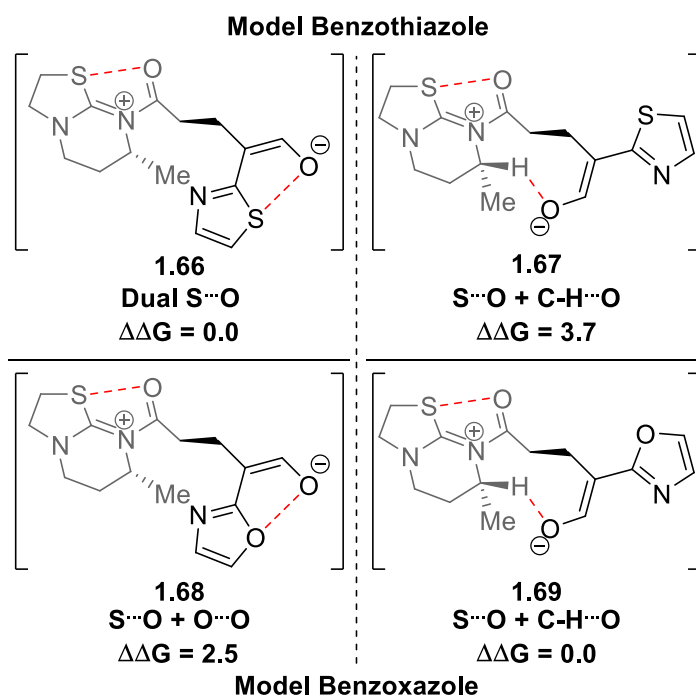
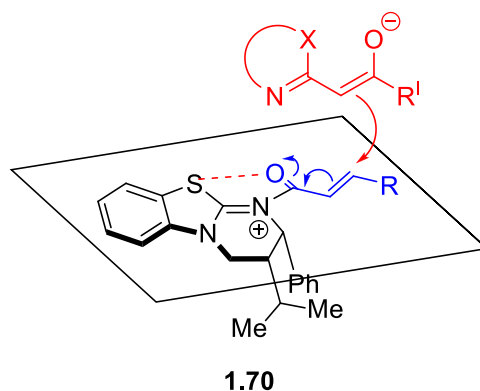


Figure 1.13: Attack of Nucleophile from Less Hindered Top Face of the Stabilized Electrophile



1.8 Conclusions

In all of the above cases, NCIs play an important role in obtaining optimal selectivity. While in most of the cases NCIs were essential in stabilizing favored transition structures, in the case of Miller's peptide-based catalyst, they also help in stabilizing favored conformation. Importantly, in many cases, the role of NCIs has been clarified using structure-function correlations. These guidelines strongly imply the importance of modularity in catalyst design. In a report from Sigman group, role of acidity in selectivity was supported with structure-activity correlations (explained in detail in chapter 2).²⁵ From this perspective enhancement of acidity can be a useful design principle in the design of catalysts. In the case of bifunctional catalysts a careful optimization of the acidity is important. Excessively acidic hydrogen-bond donors can end up protonating the Lewis basic site. The optimal acidity has to be determined empirically and for this purpose a modular catalyst design is helpful. In the third chapter, our design of a bifunctional strong-base catalyst is reported. The modularity of the catalyst design in this case helped us to tune the

acidity of the H-bond arm. Based on this we were able to develop an enantioselective synthesis of α,β -diaminophosphonates.

In the second chapter we detailed our efforts towards a highly-acidic sulfonyl-urea catalyst which is a simple system to synthesize, but not highly modular in design. During the study we understood that the catalyst native conformation is not suitable for obtaining high selectivities. To stabilize the favorable conformation of our catalyst we used a mild Lewis acid and the results were discussed in the second chapter. This demonstrates a new way of gaining access over conformation of catalyst which is much simpler than structure optimization.

1.9 References

1 Knowles, R. R.; Jacobsen, E. N. *Proc. Natl. Acad. Sci. U.S.A.* **2010**, *107*, 20678–20685 and the references cited therein.

2 Copeland, G. T.; Miller, S. J. *J. Am. Chem. Soc.* **2001**, *123*, 6496–6502.

3 a) Zhao, Y.; Beuchat, C.; Mareda, J.; Domoto, Y.; Gajewy, J.; Wilson, A.; Sakai, N.; Matile, S. *J. Am. Chem. Soc.* **2014**, *136*, 2101–2111. b) Dawson, R. E.; Hennig, A.; Weimann, D. P.; Emery, D.; Ravikumar, V.; Montenegro, J.; Takeuchi, T.; Gabutti, S.; Mayor, M.; Mareda, J.; Schalley, C. A.; Matile, S. *Nat. Chem.* **2010**, *2*, 533–538.

4 Neel, A. J.; Hilton, M. J.; Sigman, M. S.; Toste, D. F. *Nature*, **2017**, *543*, 637–646.

5 Wagner, J. P.; Schreiner, P. R. *Angew. Chem., Int. Ed.* **2015**, *54*, 12274–12296.

6 a) Wheeler, S. E. *J. Am. Chem. Soc.* **2011**, *133*, 10262–10274. b) Raju, R. K.; Bloom, J. W. G.; An, Y.; Wheeler, S. E. *ChemPhysChem*, **2011**, *12*, 3116–3130. c) Wheeler, S. E.; Houk, K. N. *Mol. Phys.* **2009**, *107*, 749–760. d) Wheeler, S. E.; Houk, K. N. *J. Am. Chem. Soc.* **2008**, *130*, 10854–10855. e) Sinnokrot, M. O.; Sherrill, C. D. *J. Am. Chem. Soc.* **2004**, *126*, 7690–7697.

7 Xu, H.; Zuend, S. J.; Woll, M. G.; Tao, Y.; Jacobsen, E. N. *Science*, **2010**, *327*, 986–990.

8 Hajos, Z. G.; Parrish, D. R. *J. Org. Chem.* **1974**, *39*, 1615–1621.

9 a) Notz, W.; List, B. *J. Am. Chem. Soc.* **2000**, *122*, 7386–7387. b) List, B.; Lerner, R. A.; Barbas, C. F., III. *J. Am. Chem. Soc.* **2000**, *122*, 2395–2396.

10 a) Yolacan, C.; Mavis, M. E.; Aydogan, F. *Tetrahedron* **2014**, *70*, 3707–3713. b) Bayat, S.; Tejo, B. A.; Salleh, A. B.; Abdmalek, E.; Normi, Y. M.; Rahman, M. B. A. *Chirality* **2013**, *25*, 726–734. c) Kolundzic, F.; Noshi, M. N.; Tjandra, M.; Movassaghi, M.; Miller, S. J. *J. Am. Chem. Soc.* **2011**, *133*, 9104–9111. d) Wennemers, H. *Chem. Commun.* **2011**, 12036–12041.

11 Machuca, E.; Juaristi, E. *Tetrahedron Lett.* **2015**, *56*, 1144–1148.

12 Faraldos, J. A.; Antonczak, A. K.; Gonzalez, V.; Fullerton, R.; Tippmann, E. M.; Allemann, R. K. *J. Am. Chem. Soc.* **2011**, *133*, 13906–13909.

13 a) Lin, S.; Jacobsen, E. N. *Nat. Chem.* **2012**, *4*, 817–824. b) Uyeda, C.; Jacobsen, E. N. *J. Am. Chem. Soc.* **2011**, *133*, 5062–5075. c) Knowles, R. R.; Lin, S.; Jacobsen, E. N. *J. Am. Chem. Soc.* **2010**, *132*, 5030–5032.

14 Holland, M. C.; Paul, S.; Schweizer, W. B.; Bergander, K.; Mück-Lichtenfeld, C.; Lakhdar, S.; Mayr, H.; Gilmour, R. *Angew. Chem., Int. Ed.* **2013**, *52*, 7967–7971.

15 a) Zhao, Y.; Domoto, Y.; Orentas, E.; Beuchat, C.; Emery, D.; Mareda, J.; Sakai, N.; Matile, S. *Angew. Chem., Int. Ed.* **2013**, *52*, 9940–9943. b) Dawson, R. E.; Hennig, A.; Weimann, D. P.; Emery, D.; Ravikumar, V.; Montenegro, J.; Takeuchi, T.; Gabutti, S.; Mayor, M.; Mareda, J.; Schalley, C. A.; Matile, S. *Nat. Chem.* **2010**, *2*, 533–538.

16 Zhao, Y.; Cotellet, Y.; Avestro, A.-J.; Sakai, N.; Matile, S. *J. Am. Chem. Soc.* **2015**, *137*, 11582–11585.

17 Liu, L.; Cotellet, Y.; Klehr, J.; Sakai, N.; Ward, T. R.; Matile, S. *Chem. Sci.* **2017**, *8*, 3770–3774.

18 Gung, B. W.; Zou, Y.; Xu, Z.; Amicangelo, J. C.; Irwin, D. G.; Ma, S.; Zhou, H. -C. *J. Org. Chem.* **2008**, *73*, 689–693.

19 Neel, A. J.; Milo, A.; Sigman, M. S.; Toste, F. D. *J. Am. Chem. Soc.* **2016**, *138*, 3863–3875.

20 Gustafson, J. L.; Lim, D.; Miller, S. J. *Science*. **2010**, *328*, 1251–1255.

21 Johnson, F. *Chem. Rev.* **1968**, *68*, 375–413 and the references cited therein.

22 Gökce, H.; Bahçeli, S. *J. Mol. Struct.* **2011**, *1005*, 100–106.

23 a) Birman, V. B.; Li, X.; Han, Z. *Org. Lett.* **2007**, *9*, 37–40. b) Birman, V. B.; Li, X. *Org. Lett.* **2006**, *8*, 1351–1354.

24 Robinson, E. R. T.; Walden, D. M.; Fallan, C.; Greenhalgh, M. D.; Cheong, P. H.-Y.; Smith, A. D. *Chem. Sci.* **2016**, *7*, 6919–6927.

25 a) Jensen, K. H.; Sigman, M. S. *J. Org. Chem.* **2010**, *75*, 7194–7201. b) Jensen, K. H.; Sigman, M. S. *Angew. Chem., Int. Ed.* **2007**, *46*, 4748–4750.

Chapter 2

EFFECT OF SODIUM CATION ON THE ENANTIOSELECTIVITY OF A BIS-SULFONYL UREA CATALYZED FRIEDEL-CRAFTS REACTION

2.1 Introduction

Hydrogen-bond promoted catalysis has been developed as an alternative to Lewis acid catalysts.¹ In these catalysts, a Lewis basic substrate is activated by hydrogen-bonding with the catalyst. While this mode of activation is well known in enzyme chemistry,² chemists have started taking advantage of this only recently. One of the main advantages of hydrogen-bonding catalysts is their relative insensitivity to moisture and air. This is in contrast to Lewis acid catalysts, which are usually sensitive to moisture and oxygen. The lack of sensitivity enables easy handling and the possibility of catalyst recycling. Additionally, the usage of toxic metals is avoided although the toxicity of the hydrogen-

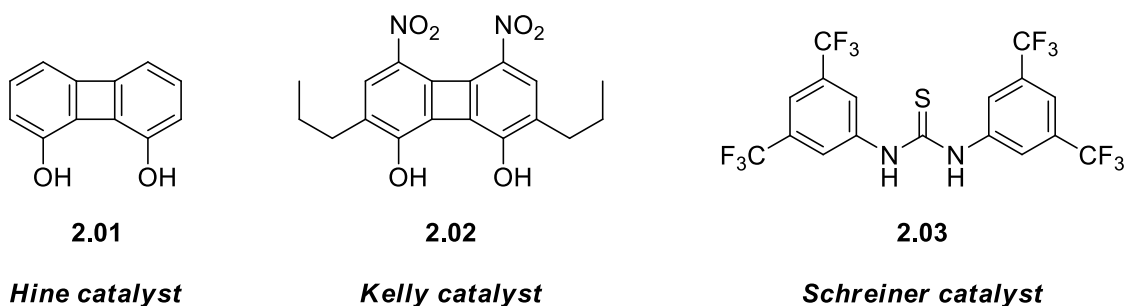
bonding catalysts have not been evaluated. The mode of activation is expected to be similar to the activation of these substrates by Lewis acid catalysts. Typically, a LUMO lowering effect as well as stabilization of transition states has been invoked for the activation.³ The energy of a hydrogen-bond varies significantly depending on the hydrogen-bonding partners. Binding energies ranging from 4-40 Kcal/mol have been measured previously.^{1b} For small molecules that activate their substrate via hydrogen-bonding, the binding energies typically range from 4-14 Kcal/mol. This is significantly lower than the binding energies observed in the case of substrates binding to metal complexes. Therefore, hydrogen-bonding catalysts usually show lower turnover frequencies. In order to overcome this limitation, higher catalyst loadings are used. Additionally, some of these catalysts are very flexible. Therefore, effective control of conformation is necessary for good selectivity.

2.2 Background

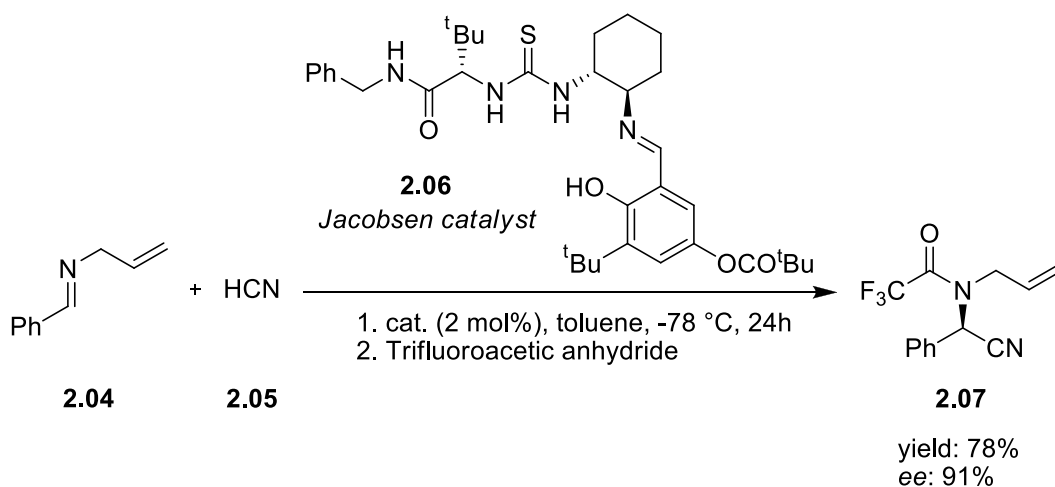
The utility of hydrogen-bond donors in catalysis was initially examined by several groups. The earliest report in this area was from Wasserman in 1942, wherein phenol was shown to catalyze the Diels-Alder reaction of quinone with cyclopentadiene.⁴ After a break of more than four decades, Hine and coworkers showed that a biphenylene-diol could be used to catalyze the ring opening of epoxides (Figure 2.1).⁵ Later, Kelly and coworkers showed that a structurally similar catalyst could catalyze a Diels-Alder reaction (Figure 2.1).⁶ This was further followed by Schreiner's report that the same reaction could be catalyzed by di-aryl thioureas (Figure 2.1).⁷

Prior to this, the Jacobsen group reported on an enantioselective Strecker reaction that was catalyzed by a chiral thiourea (Scheme 2.1).⁸ Here a combinatorial library of various thioureas was screened for the enantioselective Strecker reaction and an optimal catalyst was identified. Subsequently, variations of this catalyst have been used in a wide variety of reactions.^{1b} Takemoto and coworkers developed a chiral bifunctional catalyst that contained both a thiourea and a tertiary amine group (Scheme 2.2).⁹ This catalyst was used in an enantioselective Michael addition of a malonate ester to nitrostyrene.

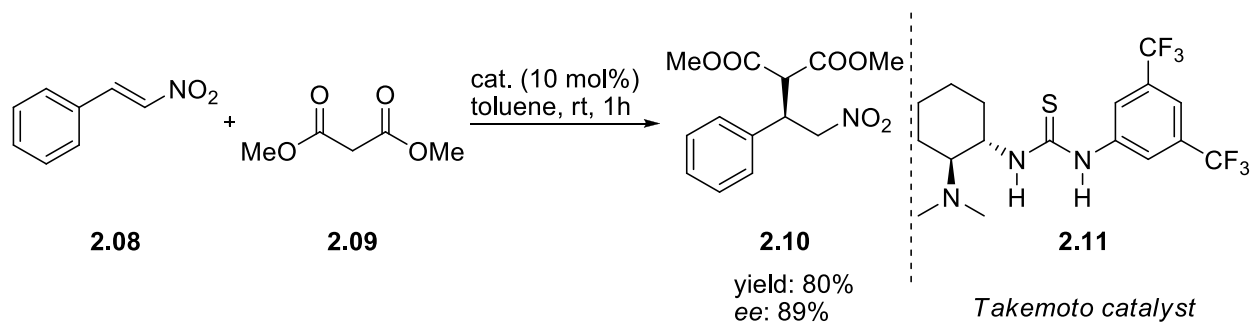
Figure 2.1: Hydrogen-Bond Catalysts for the Diels-Alder Reaction



Scheme 2.1: Thiourea Catalyzed Asymmetric Strecker Reaction

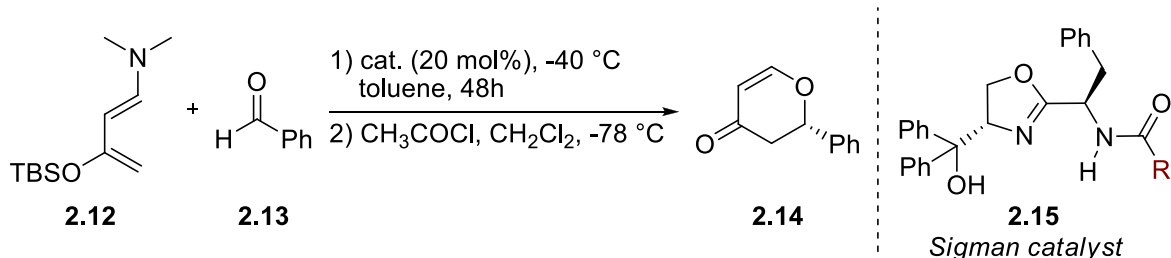


Scheme 2.2: Bifunctional Thiourea Catalyzed Michael Reaction



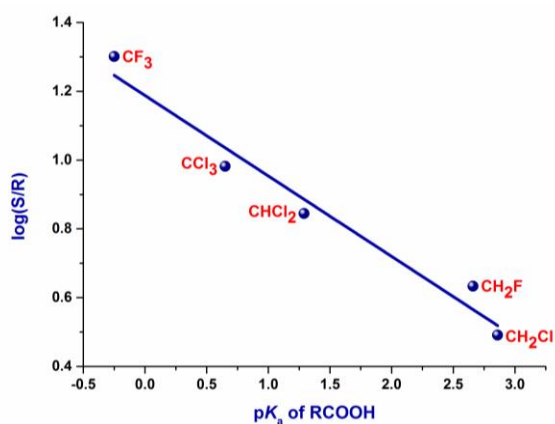
In most of the initial work, the acidity of the catalyst was thought to be important and typically, the thiourea catalysts contained an electron-withdrawing aryl group that enhanced the acidity of the hydrogen-bond donor. However, a systematic study of the effect of acidity was absent. This was addressed by Sigman and coworkers in their study of the effect of catalyst acidity on the reaction rate and selectivity.¹⁰ In earlier work, an oxazoline based hydrogen-bond donor was shown to catalyze an enantioselective hetero-Diels-Alder reaction.^{10c} The acidity of the hydrogen-bond donor could be easily tuned by changing the substituent on the nitrogen atom. A series of halo-acetamide catalysts were synthesized and the rate constant for the hetero-Diels-Alder were measured along with the enantiomeric ratio (Scheme 2.3). A plot of the pK_a of the parent halo-acetic acid vs the log of the rate constant showed a linear relationship. Further, the pK_a of the parent acids also correlated very well with the logarithm of the enantiomeric ratio as shown in Figure 2.2.

Scheme 2.3: Oxazoline Catalyzed Hetero-Diels-Alder Reaction



R	pK _a of RCO ₂ H	yield	ee (%)	ER(S/R)
CF ₃	-0.25	67	91	20
CCl ₃	0.65	61	81	9.6
CHCl ₂	1.29	53	75	7.0
CH ₂ F	2.66	17	62	4.3
CH ₂ Cl	2.86	32	52	3.1

Figure 2.2: Correlations of pK_a Values with Enantioselectivity in the Hetero-Diels-Alder Reaction



This study clearly showed the importance of the acidity of the hydrogen-bond donating groups in these catalysts. Although, excellent correlations were obtained, the pK_a of the catalysts were not measured in this study. To address this issue, the Luo and Cheng groups prepared a series of bifunctional catalysts similar to Takemoto's catalyst.¹¹ The acidity of the NH group on thiourea was varied systematically and the pK_a of the catalysts

were measured in DMSO (Scheme 2.4). These catalysts were then used in an enantioselective reaction of malonates with nitrostyrene. Excellent correlations between catalyst acidity and reactivity were obtained. The acidity also correlated with the reaction selectivity (Figure 2.3). In similar work, Schreiner and coworkers measured the pK_a of various well known thiourea catalysts¹² and showed that the acidity of the catalyst was important for its catalytic activity.

The importance of catalyst acidity led Ellman and coworkers to explore the use of highly acidic sulfinyl ureas in an enantioselective Aza-Henry reaction (Scheme 2.5a).¹³ The attachment of an electron withdrawing group to the nitrogen enhances the acidity of the NH

Scheme 2.4: pK_a Values of Bifunctional Thioureas and the *ee* of Michael Reactions Catalyzed by them

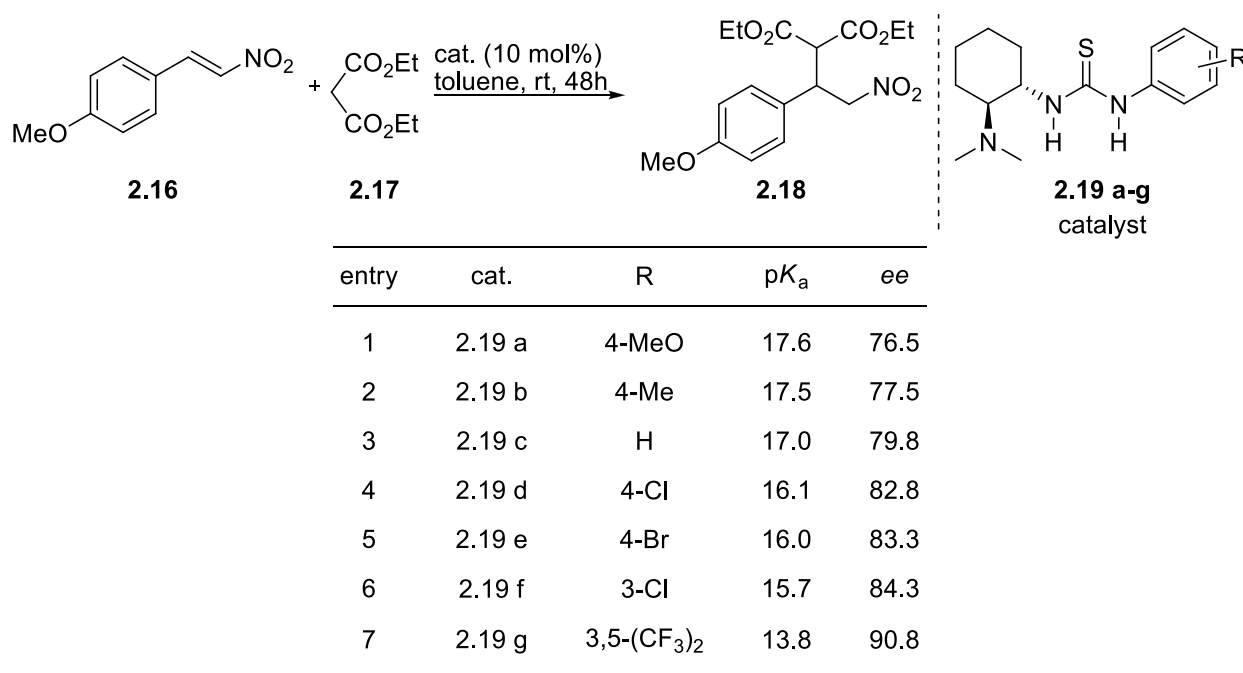
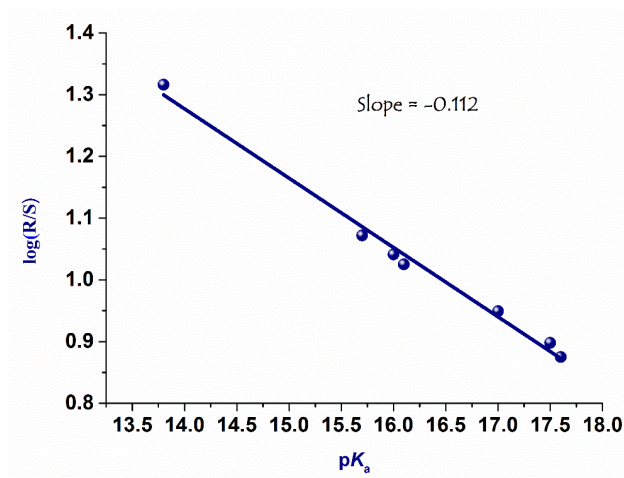
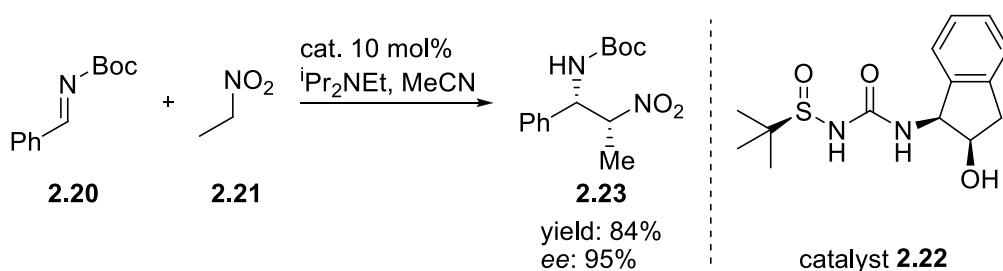


Figure 2.3: Correlations of pK_a Values with Enantioselectivity in the Michael Addition of Diethyl Malonate to Nitrostyrene

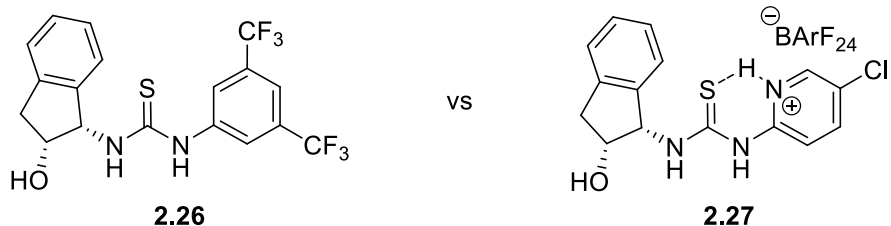
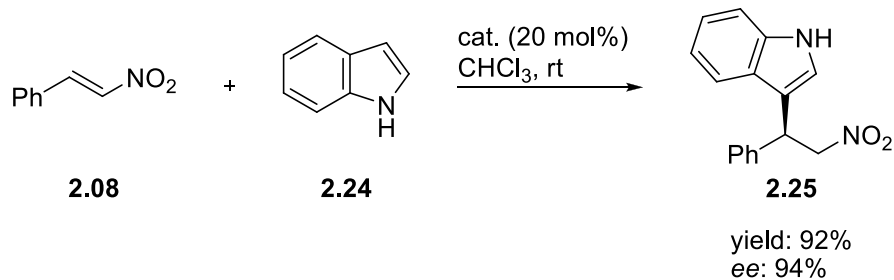


Scheme 2.5a: Sulfinamide Catalyzed Aza-Henry Reaction



bond. While the catalysts gave excellent selectivity, a direct comparison of turn over frequencies with less acidic catalysts was not reported. An alternate possibility for enhancing the acidity of thioureas is the coordination of a Brønsted acid to the sulfur atom. This would enhance the polarization of the NH bond and result in a more active catalyst. Seidel and coworkers explored this possibility using the catalyst system shown in the Scheme 2.5b.¹⁴ The catalysts were used in a Friedel-Crafts reaction of nitroalkene with indole. Compared to a conventional thiourea (**2.26**) catalyst, the reactions with the protonated catalyst (**2.27**) proceeded at a much higher rate.

Scheme 2.5b: Importance of Catalyst Acidity in H-bond Promoted Catalyzed Reactions

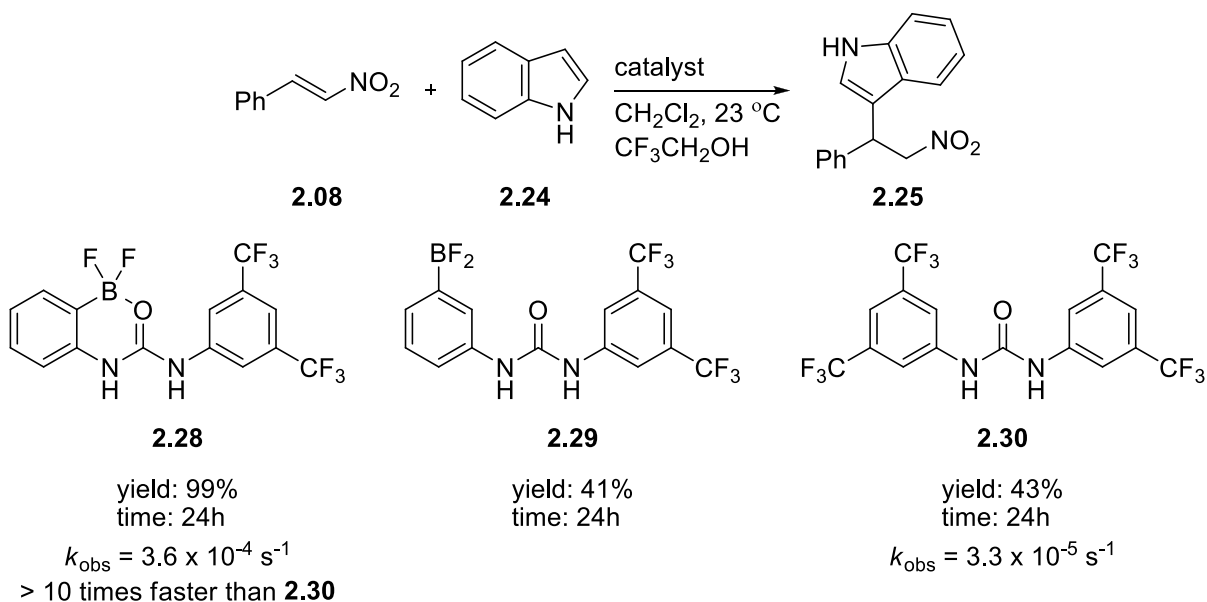


catalyst	conc. (M)	time (h)	% ee
2.26	1	144	35
2.27	0.25	3	60

Prior to this work, Smith and coworkers had shown that intramolecular coordination of a boron Lewis acid could be useful in enhancing the polarization of the NH bond in urea.¹⁵ This was exploited in catalytic reactions by Mattson coworkers (Scheme 2.6).¹⁶ Once again a Friedel-Crafts reaction of nitroalkenes was chosen as the test reaction. A ten-fold acceleration of the reaction rate was observed when catalyst **2.28** was used instead of the conventional urea **2.30**. The catalyst was later applied in an NH insertion reaction.¹⁷

Based on these reports, it is very clear that enhancing the acidity of the urea NH bond can significantly increase the catalyst activity. Therefore, we decided to explore the utility of sulfonyl ureas as highly acidic catalysts. Literature reports show that sulfonyl ureas are as acidic as Brønsted acids.¹⁸ In this chapter, we describe our efforts in the development of a chiral sulfonyl-urea catalyst. Initially, our catalyst showed poor selectivity. We

Scheme 2.6: Comparison of Rates of Friedel-Crafts Reactions Catalyzed by Boron Containing and Conventional Ureas

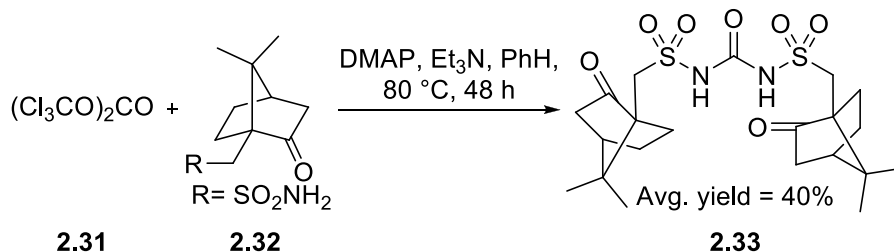


hypothesized that this was due to the catalyst being locked in an unfavorable conformation. To obtain a more favorable conformation we used sodium cations. The binding of the sodium cation resulted in the formation of a conformation that is more conducive to enantioselectivity.

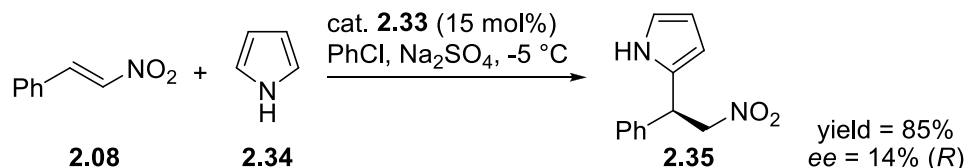
2.3 Results and Discussion

Our studies began with the synthesis of bis-camphorsulfonyl urea (**2.33**) in a single step from camphorsulfonamide and triphosgene (Scheme 2.7). The urea **2.33** was isolated after a simple extractive work up followed by recrystallization and the reactions could be performed on a gram scale. To evaluate our catalyst, we decided to pursue the previously described enantioselective Friedel-Crafts reaction of nitrostyrene with pyrrole.¹⁹ In our initial attempt, we performed the reaction in chlorobenzene as shown in Scheme 2.8 with

Scheme 2.7: Synthesis of Urea Catalyst



Scheme 2.8: Initial Results with Urea Catalyst 2.33



15 mol% of urea **2.33** as the catalyst.²⁰ The reaction was performed at -5°C for 52 h and the product was obtained in 85% yield with an *ee* of 14% favoring the *R* isomer.

A control reaction in the absence of catalyst showed very little background reaction. This clearly showed that the catalyst was responsible for reactivity and the lack of selectivity was due to unfavorable structural features of the catalyst. We hypothesized that the lack of selectivity may be due to an unfavorable conformation in which the chiral elements in the catalyst are away from the incipient chiral center (Scheme 2.9). The oxygen atoms of the carbonyl group and sulfonyl group bear partial negative charges. These groups are likely to be pointing away from each other in order to minimize dipole-dipole repulsion. Consequently, the chiral camphor groups are likely to be pointing away from the hydrogen-bond donating arm as shown in Scheme 2.9. If the dipole-dipole repulsion is strong, the catalyst is expected to be locked into this conformation. When nitrostyrene binds the catalyst in this conformation, the incipient chiral center is likely to be far away from the

camphorsulfonyl group. We hypothesized that this could be reason for low selectivity. To support this hypothesis, we grew single crystals of the catalyst and determined the solid state structure using X-ray diffraction (Figure 2.4).

The crystal structure revealed that one oxygen atom from each of the sulfonyl groups (O2 and O4) was in an anti-periplanar orientation with respect to the carbonyl oxygen (177.5° and 174.3°). The other oxygen (O1 and O3) is in a gauche-like orientation in each case (49.2° and 47.2° respectively). Notably, each of the camphor groups is also in a gauche-like conformation with respect to the urea carbonyl (56.3° and 59.3°). For obtaining maximal selectivity, the camphor groups have to be nearly anti-periplanar to the carbonyl oxygen. If nitrostyrene were to bind the catalyst in this conformation, the camphorsulfonyl

Scheme 2.9: Proposed Conformational Equilibrium

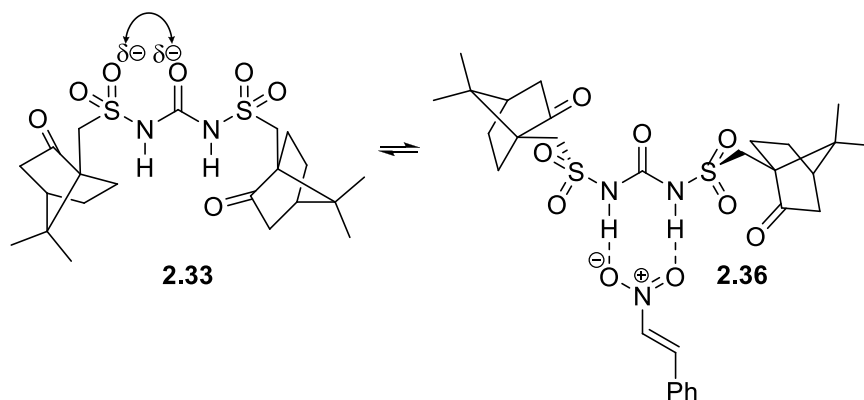
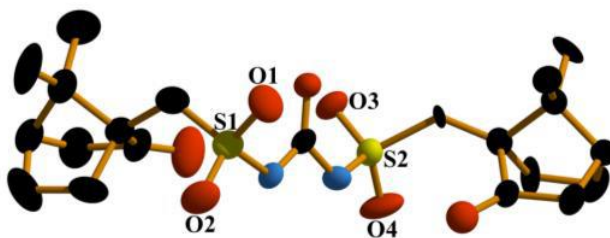


Figure 2.4: Crystal Structure of Urea Catalyst 2.33

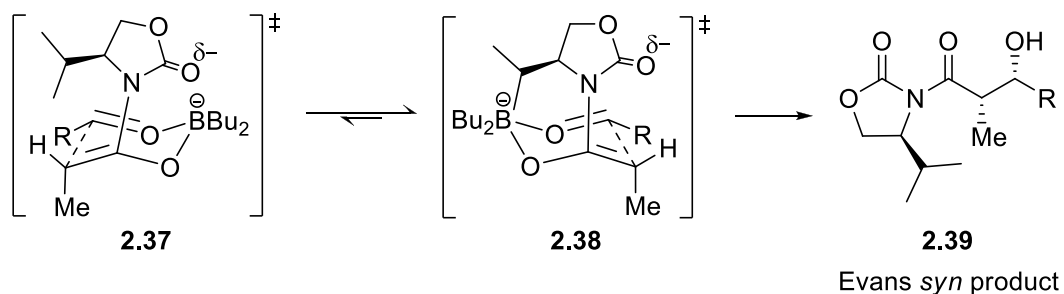


groups will not be close to the incipient chiral center. Therefore, the camphorsulfonyl group is unlikely to bias the approach of pyrrole. This would result in low enantioselectivity for this reaction.

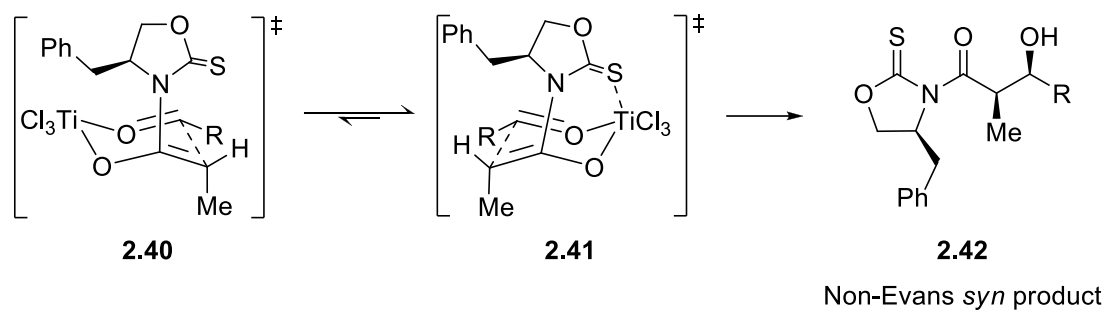
Conformational locking due to dipole-dipole repulsion is a well-known phenomenon in organic chemistry. In the transition state for the Evans aldol reaction, dipole-dipole repulsion forces the oxazolidone carbonyl group to point away from the boron atom (Scheme 2.10, Panel A).²¹ This results in the formation of the favoured *syn*-aldol product. Importantly, the orientation of the dipoles can be reversed using a suitable Lewis acid that can coordinate both of the dipoles. This has been demonstrated by Crimmins and coworkers. Replacement of the boron enolate with a titanium enolate results in the alignment of dipoles due to coordination with titanium, resulting in the switching of face selection (Scheme 2.10, Panel B). Addition of Lewis acids to constrain the conformation is also known in other cases. Canary and coworkers have shown that coordination of copper ions can favorably

Scheme 2.10: Role of Dipole-Dipole Repulsions in the Formation of *Syn*-Aldol Product

Panel A



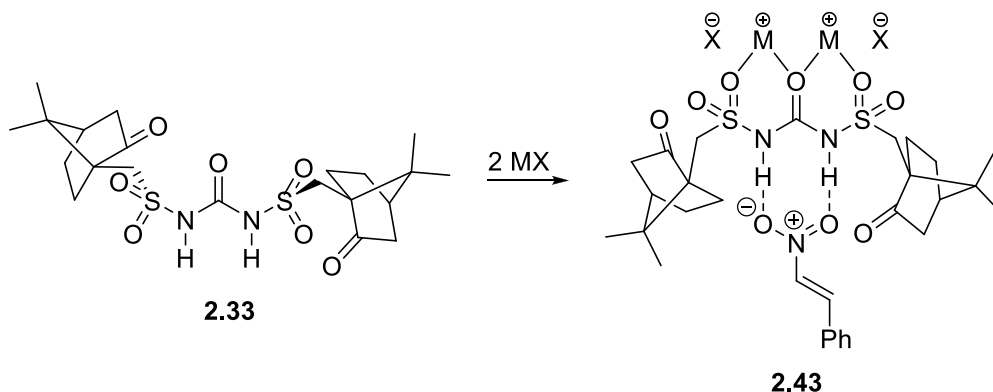
Panel B



orient urea groups for reactivity while Mancheño and coworkers have shown that anions can be used to stabilize conformation.²² Apart from this, De Filippis and coworkers have shown that sodium ions can stabilize the structure of thrombin.²³

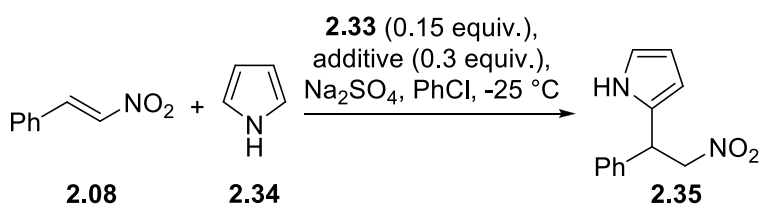
Inspired by the Crimmins aldol reaction, we hypothesized that we could similarly reverse the orientation of dipoles and align them in the same direction by coordinating to mild Lewis acids. The formation of a chelate should in turn push the camphor groups towards the hydrogen bond donors. Binding of nitrostyrene in this conformation would ensure that the bias-inducing camphor groups are closer to the incipient chiral center (Scheme 2.11).

Scheme 2.11: Proposed Conformation Change due to Lewis Acid Binding



To test our hypothesis that a Lewis acid could change the conformation, we performed a Friedel-Crafts reaction with the urea **2.33** as the catalyst and two equivalents of sodium tetraphenyl borate as an additive. Under these conditions, a reversal in face selection was observed along with a slight improvement in the enantioselectivity (Table 2.1). To identify the optimal Lewis acid for this reaction, we tested other alkali metal tetraphenylborates as well as magnesium bromide etherate under similar conditions. The reactions with other alkali metal ions were very slow and the selectivity did not improve. In the case of magnesium bromide, the reactions were completed immediately with little selectivity. Control reactions showed that magnesium bromide etherate catalyzed the rapid reaction of nitrostyrene and pyrrole. On the other hand, there was very little background reaction in the presence of NaBPh₄. This implied that the correct choice of Lewis acid is necessary for avoiding background reaction. Addition of 1 equiv. of NaBPh₄ (with respect to

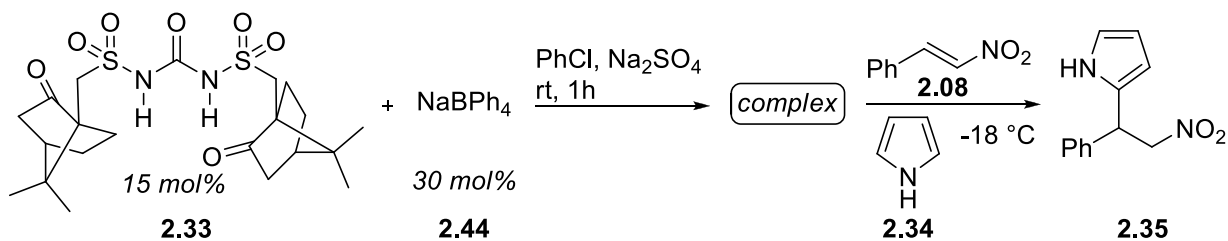
Table 2.1: Screen of Metal Salts in the Friedel-Crafts Reaction



entry	additive	time (h)	% yield	% ee
1	NaBPh ₄	36	69	16 (S)
2	LiBPh ₄	72	60	3 (S)
3	KBPh ₄	90	77	15 (R)
4	RbBPh ₄	102	76	15 (R)
5	CsBPh ₄	102	66	15 (R)
6	MgBr ₂ .Et ₂ O	0.5	62	2 (R)

urea **2.33**), led to isolation of racemic product. This showed that two equivalents of sodium cation are required for enhancing selectivity. Having confirmed that NaBPh₄ was indeed useful in enhancing the selectivity, we proceeded to further optimize the reaction. As NaBPh₄ has low solubility in the reaction solvent (chlorobenzene), we hypothesized that the low *ee* observed in our reaction is possibly due to incomplete complexation. To test this hypothesis, we ran four reactions and worked them up at different times. With increasing reaction times, the *ee* of the product increased (Table 2.2). This clearly suggested that ensuring complete complexation was necessary for good *ee*. For this purpose, the sulfonyl urea was mixed with NaBPh₄ in dichloroethane and the mixture was heated under refluxing conditions. After removal of solvent, the residue was dried under vacuum and used as a catalyst. Friedel-Crafts reactions performed with this catalyst resulted in the formation of the *S* isomer as the major product in 64% *ee*.

Table 2.2: Effect of Extent of Complexation on Selectivity



entry	<i>t</i> (h)	yield (%)	<i>ee</i> %
1	2.5	24	31
2	5	43	41
3	9	83	46
4	20	85	50

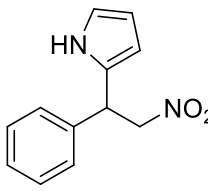
The configuration of major isomer was assigned by comparison with literature reports.²⁴ In the absence of NaBPh₄, the *R* isomer was obtained as the major product in 15% *ee*. This once again demonstrated the beneficial effect of NaBPh₄ on the selectivity of the reaction. To evaluate the generality of NaBPh₄ in enhancing the selectivity, we performed the reaction with various nitrostyrenes using pyrrole and indole²⁵ as the nucleophiles (Table 2.3) and obtained products **2.35**, **2.46-2.49**. In each of these cases, there was a clear enhancement of selectivity in the presence of NaBPh₄ along with a reversal of face selection.

Table 2.3: Comparison of Results Catalyzed by **2.33** with and without NaBPh₄

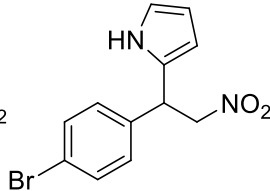
$$\mathbf{2.33} + 2 \text{ NaBPh}_4 \xrightarrow{\text{DCE, 85 }^\circ\text{C, 1h}} \text{Urea-NaBPh}_4 \text{ complex } \mathbf{2.45}$$

$$\text{R-CH=CH-NO}_2 + \text{Nu} \xrightarrow[\text{Na}_2\text{SO}_4, \text{PhCl, -20 }^\circ\text{C}]{\mathbf{2.45} (0.15 \text{ equiv.})} \text{R-CH(Nu)-CH}_2\text{-NO}_2$$

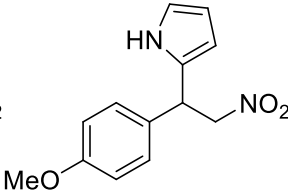
Nu = pyrrole or indole



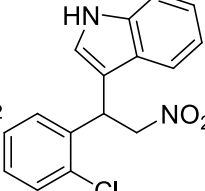
2.35



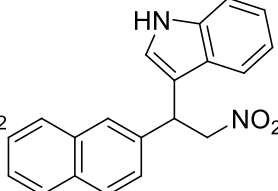
2.46



2.47



2.48



2.49

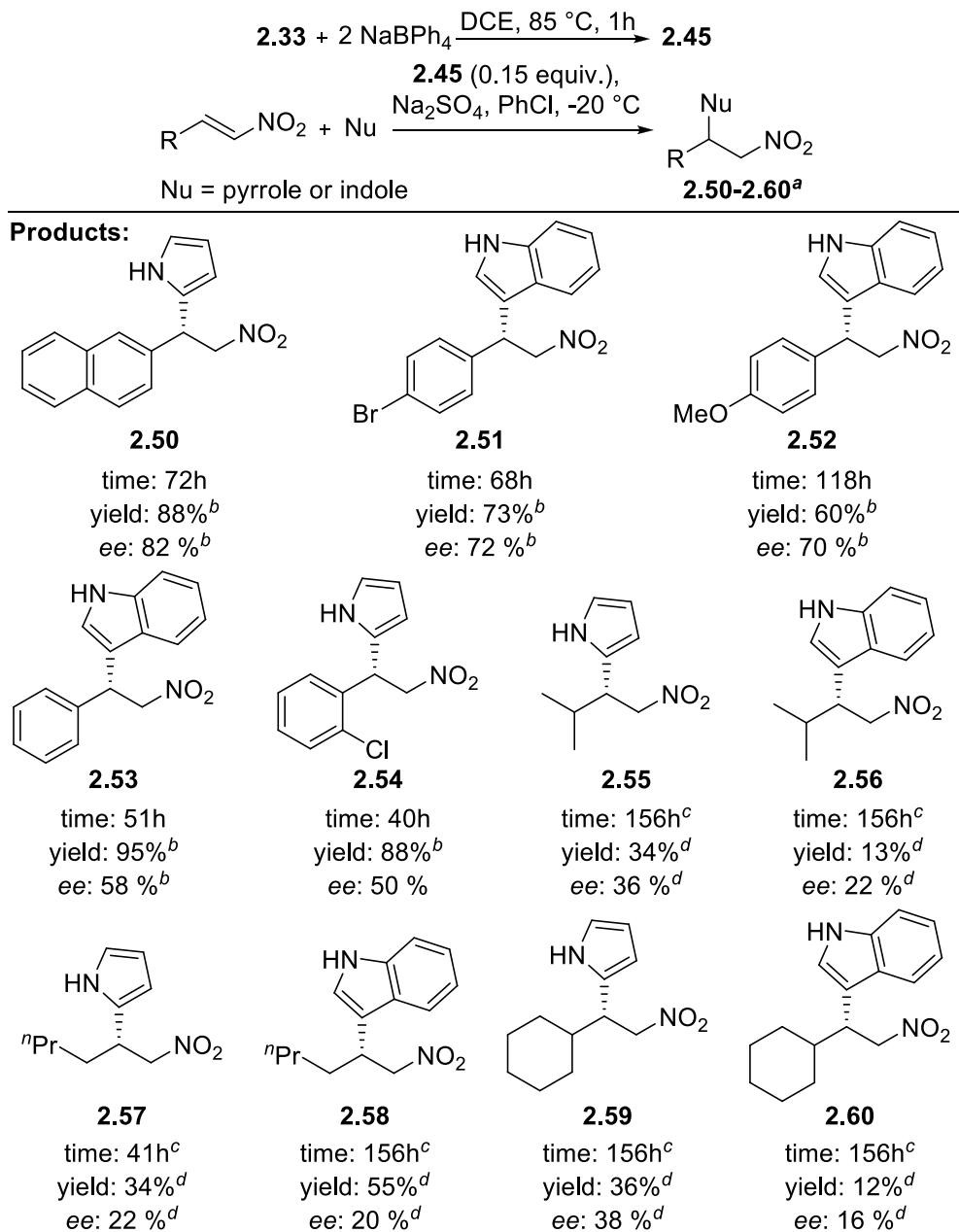
product	time ^a h	% yield ^{a, b}	% <i>ee</i> w/o NaBPh ₄	% <i>ee</i> with NaBPh ₄ ^b
2.35	36 (60)	89 (87)	15 (<i>R</i>)	64 (<i>S</i>)
2.46	78 (96)	86 (78)	10 (<i>R</i>)	72 (<i>S</i>)
2.47	65 (138)	89 (78)	11 (<i>R</i>)	56 (<i>S</i>)
2.48	25 (55)	93 (97)	7 (<i>S</i>)	66 (<i>R</i>)
2.49	58 (114)	60 (93)	4 (<i>S</i>)	66 (<i>R</i>)

Conditions: Pyrrole or indole (3 equiv.), Na₂SO₄ (2.5 equiv.), nitroalkene (0.56 M). See experimental section for details. ^aValues in the parentheses corresponds to results without NaBPh₄. ^bAverage of 3 runs.

We evaluated the substrate scope of this reaction with various nitroalkenes (Table 2.4). Aryl groups with electron donating and electron withdrawing moieties worked well in this reaction. However, nitroalkenes with alkyl substituents performed poorly in the reaction (Table 2.4). Nitroalkenes with alkyl substituents are generally poor substrates for this reaction. A notable exception to this is Seidel's catalyst which gives good yields and selectivity with alkyl substituted nitroalkenes.¹⁴

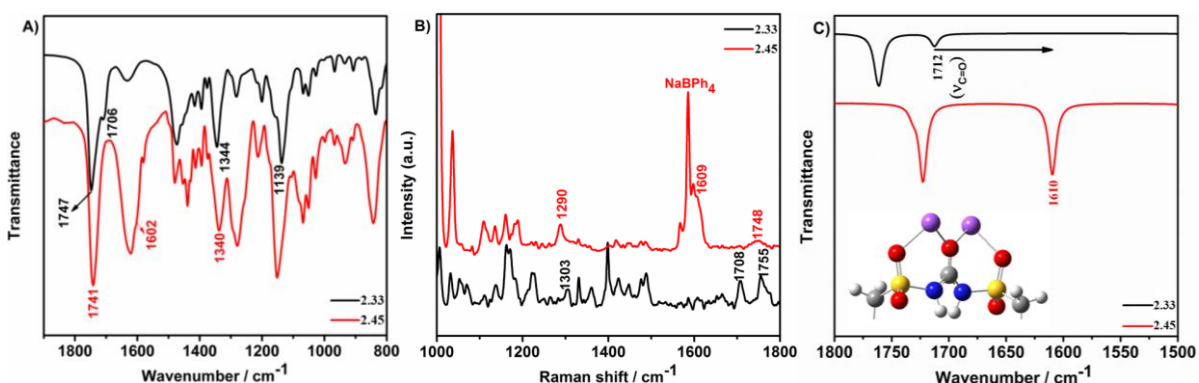
Having clearly demonstrated the impact of NaBPh₄ on enantioselectivity, we sought to understand the structural basis for the selectivity improvement. The poor solubility of the complex precluded the possibility of growing single crystals and our efforts at growing crystals were not successful. Therefore, we decided to study the structural effect of NaBPh₄ addition using vibrational spectroscopy. The vibration group frequencies are highly sensitive to even small structural changes. Subtle changes in the structure, coordination, bond lengths, and bond angles can cause small to large changes in vibrational spectra (IR and Raman spectra). A shift of few wavenumbers in the frequency is detectable and is a significant indicator for structural changes. The complexation of NaBPh₄ with the carbonyl and sulfonyl groups was expected to result in a change of the stretching frequencies of these groups. Since these are the two groups that are expected to show the maximal difference, we restrict our discussion to the stretching frequency of these two groups. A complete list of the peak assignments is given in experimental section **2.5.5.1**. The infrared and Raman spectrum of urea **2.33** is shown in Figure 2.5 (panel A and panel B). We assigned the mode at 1747 cm⁻¹ to the keto carbonyl of camphor and the shoulder at 1706 cm⁻¹ to the urea carbonyl based on literature values for similar compounds.²⁶ To support our assignment we calculated the

Table 2.4: Substrate Scope



Conditions: Pyrrole or indole (3 equiv.), Na₂SO₄ (2.5 equiv.), nitroalkene (0.56 M). See experimental section for details. ^aConfiguration of major isomer was assigned by comparing values from literature.²⁴ ^bAverage of 3 runs. ^cReaction did not go to completion. ^dAverage of 2 runs.

Figure 2.5: A) Infrared spectra of **2.33** and **2.45**. B) Raman spectra of **2.33** and **2.45**. C) Calculated infrared spectra for **2.33** and **2.45** in the C=O stretching region. Inset shows a part of the optimized structure of **2.45**. Color codes: white–H, grey–C, blue–N, red–O, yellow–S, and violet–Na



expected stretching frequency using density functional theory (DFT).²⁷ The calculated value for the keto group was 1760 cm^{-1} and the urea group was 1712 cm^{-1} in alignment with our literature based assignment. When we recorded the IR spectrum of the urea - NaBPh₄ complex (**2.45**), the shoulder at 1706 cm^{-1} disappeared and a new peak around 1620 cm^{-1} was observed along with two shoulders. Curve fitting analysis with Lorentzian functions revealed a peak at 1602 cm^{-1} , which we assigned to the urea carbonyl complexed with sodium. This overlaps with the O-H bending region of water. To confirm our assignment, we used DFT to calculate the IR spectrum of our putative complex.²⁵ In our calculated spectrum, the sodium bound carbonyl mode appears at 1610 cm^{-1} , thereby confirming our assignment of the experimental spectrum. The combination of experimental and theoretical results clearly shows a large shift (104 cm^{-1} and 102 cm^{-1} , respectively) of the urea carbonyl in the presences of NaBPh₄. This clearly supports our hypothesis that the carbonyl oxygen is

coordinated to the sodium cation. Similar results are observed in our Raman spectra of urea **2.35** (Figure 2.5, panel B), where the stretching frequency of the urea carbonyl and the keto carbonyl are seen at 1708 cm^{-1} and 1755 cm^{-1} , respectively. As observed in the IR spectra, the peak at 1708 cm^{-1} disappears upon complexation. However, the strong phenyl ring modes from the tetraphenylborate anion are observed near 1600 cm^{-1} and mask the appearance of the urea carbonyl. In spite of this, the disappearance of the mode at 1708 cm^{-1} along with similar results from IR spectroscopy strongly supports the coordination of sodium cation to the carbonyl oxygen. The sulfonyl stretching modes in the IR spectrum of urea **2.33** are seen at 1344 cm^{-1} (antisymmetric) and 1139 cm^{-1} (symmetric).²⁸ This assignment is supported by DFT calculation wherein the peaks corresponding peaks appear at 1303 cm^{-1} and 1079 cm^{-1} . In the recorded IR spectrum of the complex, a new peak was observed at 1340 cm^{-1} . We assigned this to the antisymmetric stretch of the sodium bound sulfonyl oxygen. The symmetric stretching mode of sulfonyl group in the complex overlaps with tetraphenylborate modes and therefore, we were unable to make a clear assignment. Once again, DFT calculations helped to clarify this. In the calculated spectrum, the symmetric stretch shifts from 1079 cm^{-1} in the free urea to 1069 cm^{-1} in the complex. The correlation between theoretical and experimental results clearly supported the binding of the sulfonyl oxygen.

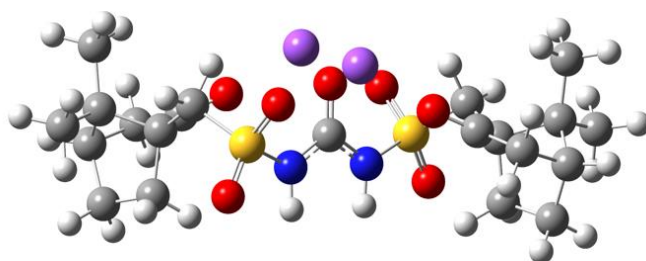
In the Raman spectrum, the sulfonyl antisymmetric stretch of urea **2.33** is seen at 1303 cm^{-1} which shifts to 1290 cm^{-1} upon complexation, whereas calculations show a shift of 5 cm^{-1} . Disagreement between the theory and experimental value could most probably be due to the fact that in the calculation we considered a single molecule in gas phase. This ignores the

intermolecular interactions present in real system. The calculations could be possibly improved by the inclusion of counter anions (tetraphenylborate), whose relative position with the catalyst is not known experimentally. As a control, we have simulated the infrared spectra for other possible conformations (Figure 2.6) using a lower level theory (B3LYP/6-31G(d)) and results are shown in Table 2.5. The simulated and experimental spectra did not match well for these conformations.

Figure 2.6: Optimized structure of two other conformations at B3LYP/6-31G(d) level.

Color codes: white–H, grey–C, blue–N, red–O, yellow–S, and violet–Na

Conformation **2.61**



Conformation **2.62**

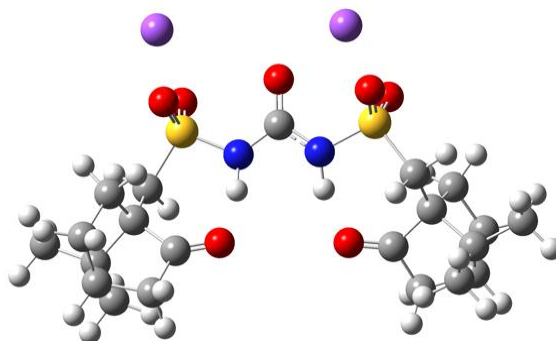


Table 2.5: Comparison of experimental infrared frequency data (cm^{-1}) of complex **2.45** with the potential alternate conformations of complex calculated at B3LYP/6-31G(d) level

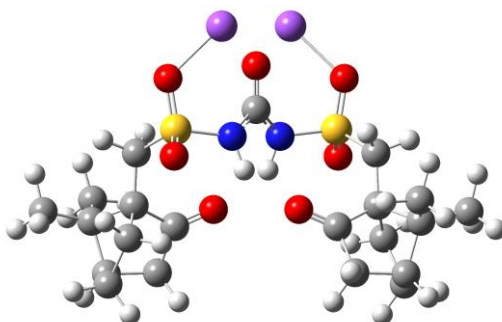
structure	$\nu(\text{C}=\text{O})$ U	$\nu(\text{C}=\text{O})$ Cp	$\nu_{\text{as}}(\text{S}=\text{O})$
urea catalyst 2.33 (Expt.)	1706	1734,1747	1344
urea catalyst 2.33 (Calc.)	1721	1752	1302
complex 2.45 (Expt.)	1602	1730,1741	1340
complex 2.45 (Calc.)	1615	1732	1287
conformation 2.61 (Calc.)	1634	1702	1289
conformation 2.62 (Calc.)	1656	1707	1200

U-urea, Cp-camphor, ν -stretching, as-antisymmetric

We have also simulated the structure of a single sodium complexed to urea **2.64** (Figure 2.7) using B3LYP/6-31G(d,p) program and the results are shown in Table 2.6. Again, a poor correlation was observed with experimentally recorded spectrum. Overall, the best match was seen between the experimental and simulated spectra for the conformation shown in Figure 2.5 (panel C), wherein two sodium cations are bound to the urea carbonyl.²⁹ This substantiates our hypothesis that the sodium cation forms a complex through coordination of the oxygens on the urea carbonyl and sulfonyl groups. As a result, the camphor groups should be closer to the hydrogen bond donors as shown in Scheme 2.11. When nitroalkenes bind the catalyst in this conformation, the incipient stereocenter is closer to the bias-inducing camphorsulfonyl groups, thereby resulting in greater enantioselection.

Figure 2.7: Optimized structures of urea bound by one and two Na cations at B3LYP/6-31G (d,p) level. Color codes: white–H, grey–C, blue – N, red–O, yellow–S, and violet–Na.

Disodium Complex **2.63**



Monosodium Complex **2.64**

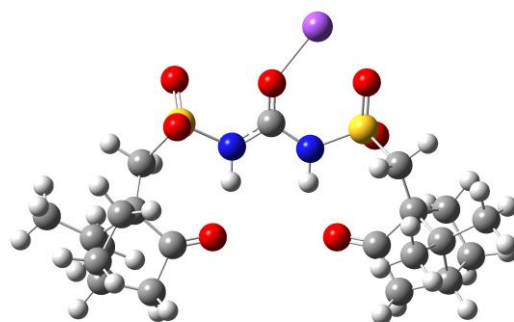


Table 2.6: Comparison of experimental infrared frequency data (cm^{-1}) of complex **2.45** with the simulated mono and disodium complexes calculated at B3LYP/6-31G(d,p) level

structure	$\nu(\text{C}=\text{O})$ U	$\nu_{\text{as}}(\text{S}=\text{O})$
urea catalyst 2.33 (Expt.)	1706	1344
complex 2.45 (Expt.)	1602	1340
disodium complex 2.63 (Calc.)	1610	1294
monosodium complex 2.64 (Calc.)	1681	1302 (unbound) 1272 (bound)

U-urea, ν -stretching, as-antisymmetric

2.4 Conclusions

The design of a novel catalyst class is a challenging area of research. In this chapter, our efforts at the development of a novel class of highly acidic catalysts has been reported. Although sulfinyl ureas have been reported previously, our catalyst is one of the first examples of a sulfonyl-urea catalyst. The single step synthesis with a simple purification protocol makes this an attractive catalyst for further applications. In the native catalyst, conformational locking due to dipole-dipole repulsion pushes the chiral groups away from the hydrogen-bond donating arms resulting in poor enantioselectivity. This is also clearly seen in the single crystal X-ray structure of the catalyst. We have shown that the addition of NaBPh₄ a mild Lewis acid can impact the face selection and enhance the enantioselectivity. The sodium cation is complexed by the sulfonyl and carbonyl oxygens. This results in the bias-inducing camphor sulfonyl groups coming closer to the hydrogen-bonding donating arms. Support for this structural change emerged from vibrational spectroscopy. The recorded spectra were compared with calculated spectra for a disodium ligated urea. A clear correlation was observed between the recorded and calculated spectra which suggested that sodium is bound to the carbonyl and sulfonyl oxygens, thereby changing the relative orientation of the camphor and NH groups. Thus, we have effectively modulated the conformation of a urea catalyst by the addition of an easy-to-handle sodium salt. As mentioned earlier, a similar effect has been observed in the conformation of the protein thrombin. This suggests that the addition of weak Lewis acids could be a general strategy for controlling the conformation in flexible systems. This could have wide ranging applications in organo-catalysis as well as other fields like medicinal chemistry.

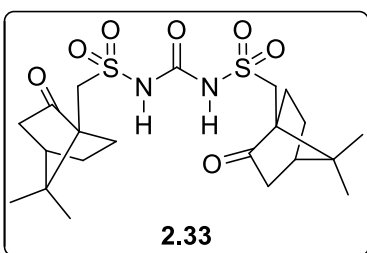
2.5 Experimental Section

2.5.1 General Information

All glassware was dried overnight in an oven prior to use. Reactions were carried out under argon atmosphere using standard Schlenk techniques. Reactions were monitored by thin layer chromatography (TLC) using TLC silica gel plates. Flash chromatography was performed using silica gel 230-400 mesh. Unless otherwise noted all reagents were used as received from commercial suppliers without further purification. Anhydrous dichloroethane and chlorobenzene were purchased and used directly for reactions. DMAP was recrystallized from toluene. Triethylamine and benzene were distilled from CaH₂ prior to use. Analytical grade Na₂SO₄ was crushed and dried at 600 °C for 6-7 h under inert atmosphere and used in the reactions. Analytical grade cyclohexane, dichloromethane and toluene were used for recrystallization. Grease free solvents were obtained by distillation and used for chromatography. Infrared spectra were recorded using a FTIR spectrometer. Sample pellets for IR spectroscopic studies were prepared by mixing a few milligrams of compound with dry KBr. ¹H and ¹³C NMRs were recorded on a 400 MHz Fourier transform NMR spectrometer. Chemical shifts are reported in parts per million (ppm) with respect to the residual undeuterated solvent in CDCl₃ (δ = 7.27 ppm) at room temperature. ¹³C NMRs were recorded at 100 MHz using proton decoupling. Chemical shifts are reported with respect to the deuterated solvent in CDCl₃ (δ = 77.16 ppm) or (CD₃)₂CO (δ = 29.84 ppm) at room temperature. HRMS was recorded using Q-TOF spectrometer. MALDI was recorded using TOF spectrometer using α-Cyano-4-hydroxy-Cinnamic Acid (CCA) as the matrix. Melting points were recorded using an electrothermal capillary melting point apparatus and are

uncorrected. Camphor sulfonamide³⁰ and nitro olefins³¹ were synthesized using previously reported procedures. Compounds **2.35**,³² **2.46–2.47**,³² **2.48–2.49**,^{24a} **2.50**,³² **2.51–2.53**,³³ **2.54–2.55**,³² **2.56**³³, **2.57**³², **2.58**^{24a}, **2.59**³², **2.60**^{24a} have been reported previously in the literature. Crystallographic data for the structure of **2.33** have been deposited with the Cambridge Crystallographic Data Centre (CCDC 943949).

2.5.2 Synthesis of urea catalyst (**2.33**)

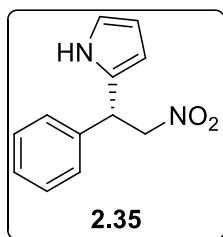


Camphor sulfonamide (2.35 g, 10.2 mmol) and DMAP (1.24 g, 10.2 mmol) were weighed into a 100 mL 2-neck flask and the flask was flushed with argon. To this, benzene (25 mL) and triethylamine (1.42 mL, 10.2 mmol) were added. In a separate flask, triphosgene (502 mg, 1.7 mmol) was dissolved in benzene (25 mL) under argon and cannulated dropwise in to the flask containing camphor sulfonamide at 0 °C. After completion of addition, the reaction mixture was slowly warmed to 40 °C and stirred for 2 h (reaction mixture was a milky white suspension). The temperature was then raised to 80 °C and the contents were stirred for 48 h (precipitation of a white solid was observed as the reaction progressed). It was then cooled to 0 °C and quenched by dropwise addition of 4 M HCl in dioxane (7 mL) followed by stirring for 12 h. The contents were then diluted with ethyl acetate (~75 mL) and washed with 1 M HCl (3 × 75 mL). The organic layer was extracted with saturated NaHCO₃ until all of the catalyst was extracted in to the aqueous layer (checked by TLC). The aqueous layer was separated and washed with ethyl acetate. After acidification with 1 M HCl, it was extracted with dichloromethane (3 × 100 mL). The organic layers were combined, dried over Na₂SO₄ and concentrated. The residue (1.58 g)

was dissolved in a mixture of toluene (17.8 mL) and dichloromethane (5.4 mL). After transferring to a Schlenk tube, the solution was layered with cyclohexane (30 mL) and crystals of **2.33** (1.08 g) were collected by filtration after 10 days (Yield: 44%, Average yield: 40% over three runs). mp 149–152 °C (dec.); R_f: 0.5 in 10% MeOH/CH₂Cl₂. [α]_D²⁴ = +42.0° (c 1, CH₂Cl₂). Crystallographic data for the structure of **2.31** have been deposited with the Cambridge Crystallographic Data Centre (CCDC 943949). ¹H NMR (400 MHz, CDCl₃) δ 9.13 (brs, 2H, NH), 3.97 (d, *J* = 15.1 Hz, 2H, CH_aH_bSO₂), 3.39 (d, *J* = 15.1 Hz, 2H, CH_aH_bSO₂), 2.43 (ddd, *J* = 18.7 Hz, 4.4 Hz, 3.3 Hz, 2H, CH₂exoCO), 2.29 (ddd, *J* = 14.7 Hz, 11.7 Hz, 3.7 Hz, 2H, CH₂CH₂exoCH), 2.15 (dd, *J* = 4.4 Hz, 4.4 Hz, 2H, CH), 2.11–2.02 (m, 2H, CH₂exoC_{quaternary}), 1.97 (d, *J* = 18.7 Hz, 2H, CH₂endoCO), 1.89 (ddd, *J* = 14.0 Hz, 9.3 Hz, 4.6 Hz, 2H, CH₂CH₂endoCH), 1.49 (ddd, *J* = 12.8 Hz, 9.3 Hz, 3.8 Hz, 2H, CH₂endoC_{quaternary}), 1.07 (s, 6H, Me₂C), 0.94 (s, 6H, Me₂C); ¹³C NMR {¹H} (100 MHz CDCl₃) δ 216.3, 148.1, 59.2, 52.3, 49.0, 43.1, 42.9, 27.1, 26.3, 20.0, 19.6; ν_{max} (KBr) 1747, 1734, 1706, 1482, 1470, 1344, 1162, 1139, 1131 cm⁻¹; HRMS (ESI-TOF) m/z: [M + H]⁺ Calcd. for C₂₁H₃₃N₂O₇S₂ 489.1724; Found 489.1726.

2.5.3 Sample procedure for the catalytic enantioselective Friedel-Crafts reaction

2-(2-nitro-1-phenylethyl)-1H-pyrrole (**2.35**)³²



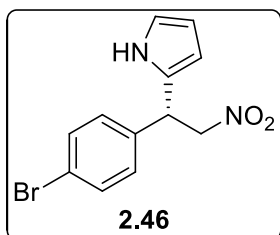
Sodium tetraphenylborate (253 mg) was weighed in to a 10 mL flask and dried at 80 °C for 1 h under high vacuum. To this, catalyst **2.33** (180 mg) was added under argon atmosphere followed by 1,2-dichloroethane (8.8 mL). The flask was fitted with a condenser and the

contents were refluxed for 1 h at 85 °C with vigorous stirring. It was then cooled to 45 °C

and the solvent was removed by sparging with argon. The residue was dried under high vacuum for an hour (The solvent can also be removed using a rotary evaporator. In this case the vacuum is released using argon). The obtained complex **2.45** was used immediately to setup 3 reactions with different nitro olefins.

A dried Schlenk tube was charged with 118 mg of complex **2.45** (0.1 mmol), 100 mg of (*E*)-1-(2-nitrovinyl)benzene (0.67 mmol) and 245 mg of Na₂SO₄. The tube was flushed with argon and 820 μ L of chlorobenzene was added. The contents were stirred at room temperature for 45 min (NOTE: A slow stir rate was used to avoid deposition of solids above the solvent level). The tube was cooled to -20 °C, stirred for 45 min, and a solution of pyrrole in chlorobenzene (4.03 M, 500 μ L, 2 mmol) was added. After completion of reaction, (by TLC) the product was purified by column chromatography on silica gel to yield 127 mg of **2.35** as a pale yellow solid (Yield: 88%, Average yield: 89% over three runs). R_f: 0.50 in 20% EtOAc/hexanes. Enantiomeric excess (*ee*) = 65% (Average *ee* = 64% over three runs). $[\alpha]_D^{25} = -36.8^\circ$ (*c* 0.1, CH₂Cl₂). ¹H NMR (400 MHz, CDCl₃) δ 7.84 (brs, 1H, NH), 7.39–7.30 (m, 3H, H_{arom}), 7.26–7.24 (m, 2H, H_{arom}), 6.70 (ddd, *J* = 2.7 Hz, 2.7 Hz, 1.5 Hz, 1H, H_{pyrrole}), 6.19–6.17 (m, 1H, H_{pyrrole}), 6.11–6.09 (m, 1H, H_{pyrrole}), 5.00 (dd, *J* = 12.0 Hz, 7.3 Hz, 1H, O₂NCH_aH_bCH), 4.91 (dd, *J* = 7.4 Hz, 7.4 Hz, 1H, CHCH_aH_bNO₂), 4.82 (dd, *J* = 12.0 Hz, 7.6 Hz, 1H, O₂NCH_aH_bCH); ¹³C NMR {¹H} (100 MHz CDCl₃) δ 138.1, 129.4, 129.1, 128.3, 128.1, 118.3, 108.8, 106.0, 79.4, 43.1; ν_{\max} (liquid film) 3426, 1550, 1430, 1378, 704 cm⁻¹; HRMS (ESI-TOF) *m/z*: [M + H]⁺ Calcd. for C₁₂H₁₃N₂O₂ 217.0972; Found 217.0973.

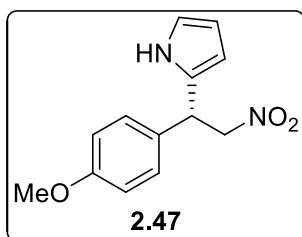
2-(1-(4-bromophenyl)-2-nitroethyl)-1H-pyrrole (**2.46**)³²



Prepared according to sample procedure using (*E*)-1-bromo-4-(2-nitrovinyl)benzene (153 mg, 0.67 mmol) and 4.03 M pyrrole solution (500 μ L, 2 mmol) to yield 174 mg of **2.46** as a white solid (Yield: 88%, Average yield: 86% over three runs). R_f : 0.40 in 20%

EtOAc/hexanes. Enantiomeric excess = 76% (Average *ee* = 72% over three runs). $[\alpha]_D^{25} = -44.7^\circ$ (*c* 0.1, CH_2Cl_2). ^1H NMR (400 MHz, CDCl_3) δ 7.84 (brs, 1H, NH), 7.49 (dt, $J = 8.9$ Hz, 2.2 Hz, 2H, H_{arom}), 7.12 (dt, $J = 8.8$ Hz, 2.1 Hz, 2H, H_{arom}), 6.72 (ddd, $J = 2.6$ Hz, 2.6 Hz, 1.5 Hz, 1H, $\text{H}_{\text{pyrrole}}$), 6.19–6.17 (m, 1H, $\text{H}_{\text{pyrrole}}$), 6.09–6.07 (m, 1H, $\text{H}_{\text{pyrrole}}$), 4.98 (dd, $J = 12.2$ Hz, 7.0 Hz, 1H, $\text{O}_2\text{NCH}_a\text{H}_b\text{CH}$), 4.88 (dd, $J = 7.5$ Hz, 7.5 Hz, 1H, $\text{CHCH}_a\text{H}_b\text{NO}_2$), 4.79 (dd, $J = 12.2$ Hz, 8.0 Hz, 1H, $\text{O}_2\text{NCH}_a\text{H}_b\text{CH}$); ^{13}C NMR $\{^1\text{H}\}$ (100 MHz CDCl_3) δ 137.2, 132.4, 129.7, 128.4, 122.3, 118.6, 108.9, 106.1, 79.0, 42.5; ν_{max} (liquid film) 3433, 1550, 1488, 1378, 727 cm^{-1} ; HRMS (ESI-TOF) m/z : $[\text{M} + \text{H}]^+$ Calcd. for $\text{C}_{12}\text{H}_{12}\text{BrN}_2\text{O}_2$ 295.0077; Found 295.0073.

2-(1-(4-methoxyphenyl)-2-nitroethyl)-1H-pyrrole (**2.47**)³²

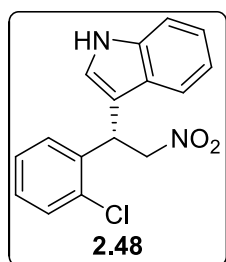


Prepared according to sample procedure using (*E*)-1-methoxy-4-(2-nitrovinyl)benzene (120 mg, 0.67 mmol) and 4.03 M pyrrole solution (500 μ L, 2 mmol) to yield 151 mg of **2.47** as a yellow oil (Yield: 92%, Average yield: 89% over three runs). R_f : 0.36 in

20% EtOAc/hexanes. Enantiomeric excess = 61% (Average *ee* = 56% over three runs). $[\alpha]_D^{25} = -54.0^\circ$ (*c* 0.1, CH_2Cl_2). ^1H NMR (400 MHz, CDCl_3) δ 7.84 (brs, 1H, NH), 7.16 (dt, $J = 8.7$ Hz, 2.6 Hz, 2H, H_{arom}), 6.89 (dt, $J = 8.8$ Hz, 2.6 Hz, 2H, H_{arom}), 6.70 (ddd, $J = 2.7$ Hz,

2.7 Hz, 1.6 Hz, 1H, H_{pyrrole}), 6.19–6.16 (m, 1H, H_{pyrrole}), 6.08–6.06 (m, 1H, H_{pyrrole}), 4.98 (dd, $J = 11.9$ Hz, 7.0 Hz, 1H, $\text{O}_2\text{NCH}_a\text{H}_b\text{CH}$), 4.86 (dd, $J = 7.5$ Hz, 7.5 Hz, 1H, $\text{CHCH}_a\text{H}_b\text{NO}_2$), 4.78 (dd, $J = 12.0$ Hz, 8.1 Hz, 1H, $\text{O}_2\text{NCH}_a\text{H}_b\text{CH}$), 3.80 (s, 3H, OMe); ^{13}C NMR $\{^1\text{H}\}$ (100 MHz CDCl_3) δ 159.5, 130.0, 129.4, 129.2, 118.2, 114.7, 108.8, 105.7, 79.6, 55.5, 42.4; ν_{max} (liquid film) 3418, 2919, 1550, 1511, 1249, 1030, 722 cm^{-1} ; HRMS (ESI-TOF) m/z : $[\text{M} + \text{H}]^+$ Calcd. for $\text{C}_{13}\text{H}_{15}\text{N}_2\text{O}_3$ 247.1077; Found 247.1068.

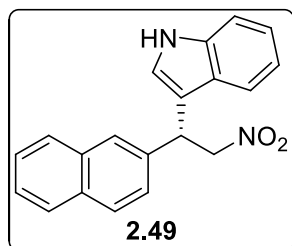
3-[1-(2-chlorophenyl)-2-nitroethyl]-1H-indole (2.48)^{24a}



Prepared according to sample procedure using (*E*)-1-chloro-2-(2-nitrovinyl)benzene (123 mg, 0.67 mmol) and indole (235 mg, 2 mmol) to yield 186 mg of **2.48** as a white viscous oil (Yield: 92%, Average yield: 93% over three runs). R_f : 0.27 in 20% EtOAc/hexanes. Enantiomeric

excess = 67% (Average $ee = 66\%$ over three runs). $[\alpha]_{\text{D}}^{25} = -22.9^\circ$ (c 0.1, CH_2Cl_2). ^1H NMR (400 MHz, CDCl_3) δ 8.13 (brs, 1H, NH), 7.46–7.44 (m, 2H, H_{arom}), 7.39–7.37 (m, 1H, H_{arom}), 7.25–7.16 (m, 4H, H_{arom}), 7.15–7.14 (m, 1H, H_{arom}), 7.09 (ddd, $J = 8.0$ Hz, 7.1 Hz, 1.0 Hz, 1H, H_{arom}), 5.76 (dd, $J = 7.8$ Hz, 7.8 Hz, 1H, $\text{CHCH}_a\text{H}_b\text{NO}_2$), 5.03 (dd, $J = 12.9$ Hz, 8.6 Hz, 1H, $\text{O}_2\text{NCH}_a\text{H}_b\text{CH}$), 4.98 (dd, $J = 12.8$ Hz, 7.1 Hz, 1H, $\text{O}_2\text{NCH}_a\text{H}_b\text{CH}$); ^{13}C NMR $\{^1\text{H}\}$ (100 MHz CDCl_3) δ 136.6, 136.5, 133.9, 130.2, 129.1, 128.9, 127.4, 126.3, 122.8, 122.1, 120.1, 119.0, 113.2, 111.5, 77.8, 38.0; ν_{max} (liquid film) 3420, 3060, 1551, 1378, 744 cm^{-1} ; HRMS (ESI-TOF) m/z : $[\text{M} + \text{H}]^+$ Calcd. for $\text{C}_{16}\text{H}_{14}\text{ClN}_2\text{O}_2$ 301.0738; Found 301.0731.

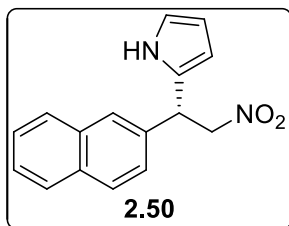
3-[1-naphth-2-yl-2-nitroethyl]-1H-indole (2.49)^{24a}



Prepared according to sample procedure using (*E*)-2-(2-nitrovinyl)naphthalene (134 mg, 0.67 mmol) and indole (235 mg, 2

mmol) to yield 132 mg of **2.49** as a grey solid (Yield: 62%, Average yield: 60% over three runs). R_f : 0.23 in 20% EtOAc/hexanes. Enantiomeric excess = 68% (Average ee = 66% over three runs). $[\alpha]_D^{25} = -3.3^\circ$ (c 0.1, CH_2Cl_2). ^1H NMR (400 MHz, CDCl_3) δ 8.12 (brs, 1H, NH), 7.82–7.80 (m, 4H, H_{arom}), 7.51–7.43 (m, 4H, H_{arom}), 7.39–7.37 (m, 1H, H_{arom}), 7.21 (ddd, $J = 8.1$ Hz, 7.1 Hz, 1.0 Hz, 1H, H_{arom}), 7.09–7.05 (m, 2H, H_{arom}), 5.38 (dd, $J = 8.0$ Hz, 8.0 Hz, 1H, $\text{CHCH}_a\text{H}_b\text{NO}_2$), 5.17 (dd, $J = 12.6$ Hz, 7.5 Hz, 1H, $\text{O}_2\text{NCH}_a\text{H}_b\text{CH}$), 5.07 (dd, $J = 12.6$ Hz, 8.5 Hz, 1H, $\text{O}_2\text{NCH}_a\text{H}_b\text{CH}$); ^{13}C NMR $\{^1\text{H}\}$ (100 MHz CDCl_3) δ 136.8, 136.7, 133.6, 132.9, 128.9, 128.0, 127.8, 126.54, 126.48, 126.3, 126.2, 125.9, 122.9, 121.9, 120.2, 119.1, 114.5, 111.5, 79.5, 41.8; ν_{max} (liquid film) 3426, 3055, 1550, 1378, 744 cm^{-1} ; HRMS (ESI-TOF) m/z : $[\text{M} + \text{H}]^+$ Calcd. for $\text{C}_{20}\text{H}_{17}\text{N}_2\text{O}_2$ 317.1285; Found 317.1286.

*2-(1-(naphthalen-2-yl)-2-nitroethyl)-1H-pyrrole (2.50)*³²

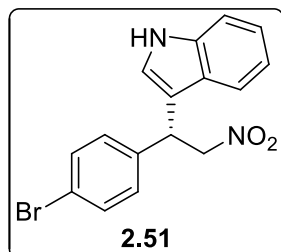


Prepared according to sample procedure using (*E*)-2-(2-nitrovinyl)naphthalene (134 mg, 0.67 mmol) and 4.03 M pyrrole solution (500 μL , 2 mmol) to yield 155 mg of **2.50** as a grey solid (Yield: 87%, Average yield: 88% over three runs). R_f : 0.40 in 20%

EtOAc/hexanes. Enantiomeric excess 83% (Average ee = 82% over three runs). $[\alpha]_D^{25} = -85.3^\circ$ (c 0.1, CH_2Cl_2). ^1H NMR (400 MHz, CDCl_3) δ 7.86–7.81 (m, 4H, H_{arom}), 7.72 (brs, 1H, NH), 7.55–7.49 (m, 2H, H_{arom}), 7.33 (dd, $J = 8.5$ Hz, 1.8 Hz, 1H, H_{arom}), 6.71–6.69 (m, 1H, $\text{H}_{\text{pyrrole}}$), 6.22–6.19 (m, 1H, $\text{H}_{\text{pyrrole}}$), 6.15 (m, 1H, $\text{H}_{\text{pyrrole}}$), 5.12–5.06 (m, 2H, $\text{O}_2\text{NCH}_a\text{H}_b\text{CH}$, $\text{CHCH}_a\text{H}_b\text{NO}_2$), 4.94 (dd, $J = 15.2$ Hz, 10.8 Hz, 1H, $\text{O}_2\text{NCH}_a\text{H}_b\text{CH}$); ^{13}C NMR $\{^1\text{H}\}$ (100 MHz CDCl_3) δ 135.4, 133.5, 133.1, 129.4, 129.0, 128.0, 127.9, 127.1, 126.8, 126.6, 125.5, 118.5, 108.9, 106.0, 79.2, 43.2; ν_{max} (liquid film) 3430, 1550, 1377,

749, 726 cm^{-1} ; HRMS (ESI-TOF) m/z : $[M + H]^+$ Calcd. for $\text{C}_{16}\text{H}_{15}\text{N}_2\text{O}_2$ 267.1128; Found 267.1124.

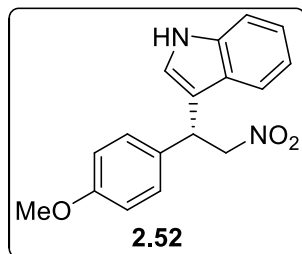
*3-[1-(4-bromophenyl)-2-nitroethyl]-1H-indole (2.51)*³³



Prepared according to sample procedure using (*E*)-1-bromo-4-(2-nitrovinyl)benzene (153 mg, 0.67 mmol) and indole (235 mg, 2 mmol) to yield 132 mg of **2.51** as a white solid (Yield: 75%, Average yield: 73% over three runs). R_f : 0.27 in 20%

EtOAc/hexanes. Enantiomeric excess = 76% (Average ee = 72% over three runs). $[\alpha]_D^{25} = -1.3^\circ$ (c 0.1, CH_2Cl_2). ^1H NMR (400 MHz, CDCl_3) δ 8.13 (brs, 1H, NH), 7.46 (dt, J = 8.9 Hz, 2.2 Hz, 2H, H_{arom}), 7.42–7.37 (m, 2H, H_{arom}), 7.24–7.20 (m, 3H, H_{arom}), 7.10 (ddd, J = 8.0 Hz, 7.1 Hz, 1.0 Hz, 1H, H_{arom}), 7.04 (dd, J = 2.5 Hz, 0.6 Hz, 1H, H_{arom}), 5.17 (dd, J = 7.9 Hz, 7.9 Hz, 1H, $\text{CHCH}_a\text{H}_b\text{NO}_2$), 5.07 (dd, J = 12.5 Hz, 7.3 Hz, 1H, $\text{O}_2\text{NCH}_a\text{H}_b\text{CH}$), 4.92 (dd, J = 12.5 Hz, 8.6 Hz, 1H, $\text{O}_2\text{NCH}_a\text{H}_b\text{CH}$); ^{13}C NMR $\{^1\text{H}\}$ (100 MHz CDCl_3) δ 138.4, 136.7, 132.2, 129.6, 128.5, 126.0, 123.0, 121.7, 120.3, 118.9, 114.1, 111.6, 79.3, 41.2; ν_{max} (liquid film) 3423, 1550, 1488, 1378, 1011, 744 cm^{-1} ; HRMS (ESI-TOF) m/z : $[M + H]^+$ Calcd. for $\text{C}_{16}\text{H}_{14}\text{BrN}_2\text{O}_2$ 345.0233; Found 345.0231.

*3-[1-(4-methoxyphenyl)-2-nitroethyl]-1H-indole (2.52)*³³

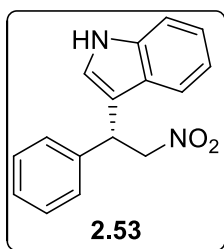


Prepared according to sample procedure using (*E*)-1-methoxy-4-(2-nitrovinyl)benzene (120 mg, 0.67 mmol) and indole (235 mg, 2 mmol) to yield 126 mg of **2.52** as a white solid (Yield: 63%, Average yield: 60% over three runs). R_f : 0.23 in 20%

EtOAc/hexanes. Enantiomeric excess = 73% (Average ee = 70% over three runs). $[\alpha]_D^{24} =$

-24.8° (*c* 0.1, CH₂Cl₂). ¹H NMR (400 MHz, CDCl₃) δ 8.08 (brs, 1H, NH), 7.46–7.44 (m, 1H, H_{arom}), 7.37 (dt, *J* = 8.1 Hz, 0.8 Hz, 1H, H_{arom}), 7.26 (dt, *J* = 9.5 Hz, 2.5 Hz, 2H, H_{arom}), 7.21 (ddd, *J* = 8.2 Hz, 7.1 Hz, 1.1 Hz, 1H, H_{arom}), 7.09 (ddd, *J* = 8.0 Hz, 7.1 Hz, 1.0 Hz, 1H, H_{arom}), 7.04 (dd, *J* = 2.5 Hz, 0.7 Hz, 1H, H_{arom}), 6.86 (dt, *J* = 9.4 Hz, 2.6 Hz, 2H, H_{arom}), 5.15 (dd, *J* = 8.0 Hz, 8.0 Hz, 1H, CHCH_aH_bNO₂), 5.06 (dd, *J* = 12.3 Hz, 7.5 Hz, 1H, O₂NCH_aH_bCH), 4.91 (dd, *J* = 12.3 Hz, 8.4 Hz, 1H, O₂NCH_aH_bCH), 3.79 (s, 3H, OMe); ¹³C NMR {¹H} (100 MHz CDCl₃) δ 159.0, 136.6, 131.3, 128.9, 126.2, 122.8, 121.6, 120.0, 119.1, 114.9, 114.4, 111.5, 79.9, 55.4, 41.0; ν_{max} (liquid film) 3414, 1550, 1512, 1249, 746 cm⁻¹; HRMS (ESI-TOF) *m/z*: [M + H]⁺ Calcd. for C₁₇H₁₇N₂O₃ 297.1234; Found 297.1230.

*3-(2-nitro-1-phenylethyl)-1H-indole (2.53)*³³

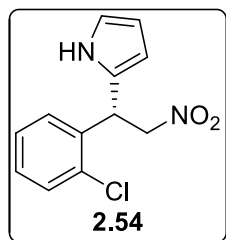


Prepared according to sample procedure using (*E*)-1-(2-nitrovinyl)benzene (100 mg, 0.67 mmol) and indole (235 mg, 2 mmol) to yield 172 mg of **2.53** as a light yellow oil (Yield: 96%, Average yield: 95% over three runs). R_f: 0.27 in 20% EtOAc/hexanes. Enantiomeric excess = 60% (Average *ee* = 58% over three runs). [α]_D²⁴ = -18.9° (*c* 0.1, CH₂Cl₂).

¹H NMR (400 MHz, CDCl₃) δ 8.09 (brs, 1H, NH), 7.46 (dd, *J* = 8.0 Hz, 0.8 Hz, 1H, H_{arom}), 7.39–7.31 (m, 5H, H_{arom}), 7.30–7.25 (m, 1H), 7.21 (ddd, *J* = 8.2 Hz, 7.2 Hz, 1.1 Hz, 1H, H_{arom}), 7.08 (ddd, *J* = 8.0 Hz, 7.1 Hz, 1.0 Hz, 1H, H_{arom}), 7.06 (dd, *J* = 2.5 Hz, 0.6 Hz, 1H, H_{arom}), 5.21 (dd, *J* = 8.0 Hz, 8.0 Hz, 1H, CHCH_aH_bNO₂), 5.09 (dd, *J* = 12.5 Hz, 7.6 Hz, 1H, O₂NCH_aH_bCH), 4.96 (dd, *J* = 12.5 Hz, 8.4 Hz, 1H, O₂NCH_aH_bCH); ¹³C NMR {¹H} (100 MHz CDCl₃) δ 139.3, 136.6, 129.0, 127.9, 127.7, 126.2, 122.8, 121.7, 120.1, 119.1, 114.6,

111.5, 79.7, 41.7; ν_{\max} (liquid film) 3423, 1550, 1456, 1379, 744, 703 cm^{-1} ; HRMS (ESI-TOF) m/z : $[M + H]^+$ Calcd. for $\text{C}_{16}\text{H}_{15}\text{N}_2\text{O}_2$ 267.1128; Found 267.1129.

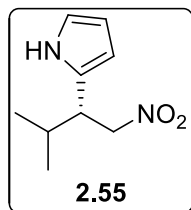
*2-(1-(2-chlorophenyl)-2-nitroethyl)-1H-pyrrole (2.54)*³²



Prepared according to sample procedure using (*E*)-1-chloro-2-(2-nitrovinyl)benzene (123 mg, 0.67 mmol) and 4.03 M pyrrole solution (500 μL , 2 mmol) to yield 152 mg of **2.54** as a white solid (Yield: 91%, Average yield: 88% over three runs). R_f : 0.30 in 10% EtOAc/hexanes.

Enantiomeric excess = 52% (Average ee = 50% over three runs). $[\alpha]_D^{24} = -51.4^\circ$ (c 0.1, CH_2Cl_2). ^1H NMR (400 MHz, CDCl_3) δ 8.00 (brs, 1H, NH), 7.46–7.41 (m, 1H, H_{arom}), 7.26–7.23 (m, 2H, H_{arom}), 7.17–7.12 (m, 1H, H_{arom}), 6.73 (ddd, $J = 2.7$ Hz, 2.7 Hz, 1.5 Hz, 1H, $\text{H}_{\text{pyrrole}}$), 6.20–6.18 (m, 1H, $\text{H}_{\text{pyrrole}}$), 6.15–6.13 (m, 1H, $\text{H}_{\text{pyrrole}}$), 5.47 (dd, $J = 8.8$ Hz, 6.7 Hz, 1H, $\text{CHCH}_a\text{H}_b\text{NO}_2$), 4.95 (dd, $J = 13.3$ Hz, 8.9 Hz, 1H, $\text{O}_2\text{NCH}_a\text{H}_b\text{CH}$), 4.88 (dd, $J = 13.3$ Hz, 6.6 Hz, 1H, $\text{O}_2\text{NCH}_a\text{H}_b\text{CH}$); ^{13}C NMR $\{^1\text{H}\}$ (100 MHz $(\text{CD}_3)_2\text{CO}$) δ 137.7, 134.2, 130.7, 130.1, 129.8, 128.7, 128.4, 119.1, 108.7, 107.2, 78.0, 40.2; ν_{\max} (liquid film) 3433, 1552, 1377, 1036, 758, 731 cm^{-1} ; HRMS (ESI-TOF) m/z : $[M + H]^+$ Calcd. for $\text{C}_{12}\text{H}_{12}\text{ClN}_2\text{O}_2$ 251.0582; Found 251.0582.

*2-(3-methyl-1-nitrobutan-2-yl)-1H-pyrrole (2.55)*³²

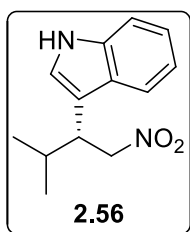


Prepared according to sample procedure using (*E*)-3-methyl-1-nitrobut-1-ene (77 mg, 0.67 mmol) and 4.03 M pyrrole solution (500 μL , 2 mmol) to yield 51 mg of **2.55** as a colorless oil (Yield: 42%, Average yield: 34% over two runs). R_f : 0.50 in 20% EtOAc/hexanes. Enantiomeric excess = 44%

(Average ee = 36% over two runs). $[\alpha]_D^{25} = +10.6^\circ$ (c 0.1, CH_2Cl_2). ^1H NMR (400 MHz,

CDCl₃) δ 8.06 (brs, 1H, NH), 6.69 (ddd, $J = 2.7$ Hz, 2.7 Hz, 1.5 Hz, 1H, H_{pyrrole}), 6.18–6.15 (m, 1H, H_{pyrrole}), 6.00–5.98 (m, 1H, H_{pyrrole}), 4.68 (dd, $J = 12.6$ Hz, 6.1 Hz, 1H, O₂NCH_aH_bCH), 4.59 (dd, $J = 12.6$ Hz, 9.0 Hz, 1H, O₂NCH_aH_bCH), 3.36 (ddd, $J = 9.0$ Hz, 6.3 Hz, 6.3 Hz, 1H, CHCH_aH_bNO₂), 2.03–1.91 (m, 1H, CHMe₂), 0.98 (d, $J = 6.8$ Hz, 3H, Me₂CH), 0.91 (d, $J = 6.7$ Hz, 3H, Me₂CH); ¹³C NMR {¹H} (100 MHz CDCl₃) δ 128.7, 117.2, 108.8, 106.2, 78.4, 44.3, 30.9, 20.8, 19.6; ν_{max} (liquid film) 3422, 2964, 1551, 1381, 721 cm⁻¹; HRMS (ESI-TOF) m/z: [M + H]⁺ Calcd. for C₉H₁₅N₂O₂ 183.1128; Found 183.1122.

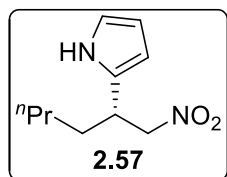
*3-(3-methyl-1-nitrobutan-2-yl)-1H-indole (2.56)*³³



Prepared according to sample procedure using (*E*)-3-methyl-1-nitrobut-1-ene (77 mg, 0.67 mmol) and indole (235 mg, 2 mmol) to yield 20 mg of **2.56** as a light yellow oil (Yield: 13%, Average yield: 13% over two runs).

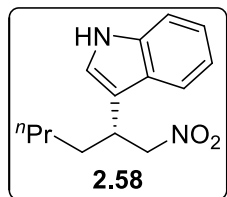
R_f: 0.30 in 20% EtOAc/hexanes. Enantiomeric excess = 24% (Average *ee* = 22% over two runs). [α]_D²⁵ = +11.5° (*c* 0.1, CH₂Cl₂). ¹H NMR (400 MHz, CDCl₃) δ 8.08 (brs, 1H, NH), 7.63–7.61 (m, 1H, H_{indole}), 7.39–7.36 (m, 1H, H_{indole}), 7.21 (ddd, $J = 8.1$ Hz, 7.1 Hz, 1.1 Hz, 1H, H_{indole}), 7.14 (ddd, $J = 8.0$ Hz, 7.2 Hz, 1.1 Hz, 1H, H_{indole}), 7.03 (d, $J = 2.4$ Hz, 1H, H_{indole}), 4.81 (dd, $J = 12.0$ Hz, 6.3 Hz, 1H, O₂NCH_aH_bCH), 4.73 (dd, $J = 12.0$ Hz, 9.1 Hz, 1H, O₂NCH_aH_bCH), 3.69 (ddd, $J = 9.1$ Hz, 6.7 Hz, 6.7 Hz, 1H, CHCH_aH_bNO₂), 2.25–2.13 (m, 1H, CHMe₂), 1.02 (d, $J = 6.8$ Hz, 3H, Me₂CH), 0.94 (d, $J = 6.7$ Hz, 3H, Me₂CH); ¹³C NMR {¹H} (100 MHz CDCl₃) δ 136.4, 127.0, 122.4, 122.2, 119.8, 119.2, 113.4, 111.5, 78.8, 42.7, 30.8, 20.8, 20.2; ν_{max} (liquid film) 3420, 2962, 1550, 1383, 743 cm⁻¹; HRMS (ESI-TOF) m/z: [M + H]⁺ Calcd. for C₁₃H₁₇N₂O₂ 233.1285; Found 233.1284.

2-(1-nitrohexan-2-yl)-1H-pyrrole (**2.57**)³²



Prepared according to sample procedure using (*E*)-1-nitrohex-1-ene (87 mg, 0.67 mmol) and 4.03 M pyrrole solution (500 μ L, 2 mmol) to yield 41 mg of **2.57** as a colorless oil (Yield: 31%, Average yield: 34% over two runs). R_f : 0.43 in 75% CH_2Cl_2 /hexanes. Enantiomeric excess = 26% (Average ee = 22% over two runs). $[\alpha]_D^{25} = +37.4^\circ$ (c 0.1, CH_2Cl_2). ^1H NMR (400 MHz, CDCl_3) δ 8.08 (brs, 1H), 6.71 (ddd, $J = 2.7$ Hz, 2.7 Hz, 1.5 Hz, 1H), 6.18–6.16 (m, 1H), 6.02–6.00 (m, 1H), 4.55 (dd, $J = 12.5$ Hz, 6.8 Hz, 1H), 4.50 (dd, $J = 12.5$ Hz, 7.8 Hz, 1H), 3.51 (dddd, $J = 7.5$ Hz, 7.5 Hz, 7.5 Hz, 7.5 Hz, 1H), 1.73–1.64 (m, 2H), 1.36–1.26 (m, 4H), 0.88 (t, $J = 7.0$ Hz, 3H); ^{13}C NMR $\{^1\text{H}\}$ (100 MHz CDCl_3) δ 130.2, 117.5, 108.9, 105.6, 80.6, 37.6, 32.2, 29.3, 22.6, 14.0; HRMS (ESI-TOF) m/z : $[\text{M} + \text{H}]^+$ Calcd. for $\text{C}_{10}\text{H}_{17}\text{N}_2\text{O}_2$ 197.1285; Found 197.1299.

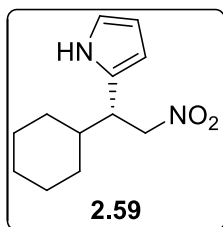
3-[1-nitrohexan-2-yl]-1H-indole (**2.58**)^{24a}



Prepared according to sample procedure using (*E*)-1-nitrohex-1-ene (87 mg, 0.67 mmol) and indole (235 mg, 2 mmol) to yield 89 mg of **2.58** as a yellow oil (Yield: 54%, Average yield: 55% over two runs). R_f : 0.50 in 20% EtOAc/hexanes. Enantiomeric excess 22% (Average ee = 20% over two runs). $[\alpha]_D^{24} = +18.2^\circ$ (c 0.1, CH_2Cl_2). ^1H NMR (400 MHz, CDCl_3) δ 8.07 (brs, 1H), 7.65–7.63 (m, 1H), 7.39 (ddd, $J = 8.1$ Hz, 0.9 Hz, 0.9 Hz, 1H), 7.23 (ddd, $J = 8.1$ Hz, 7.1 Hz, 1.1 Hz, 1H), 7.16 (ddd, $J = 8.0$ Hz, 7.0 Hz, 1.1 Hz, 1H), 7.06 (d, $J = 2.4$ Hz, 1H), 4.69 (dd, $J = 11.9$ Hz, 7.3 Hz, 1H), 4.64 (dd, $J = 11.9$ Hz, 7.8 Hz, 1H), 3.81 (dddd, $J = 9.5$ Hz, 7.5 Hz, 7.5 Hz, 5.2 Hz, 1H), 1.94–1.76 (m, 2H), 1.37–1.25 (m, 4H), 0.85 (t, $J = 7.0$ Hz, 3H); ^{13}C NMR $\{^1\text{H}\}$ (100 MHz

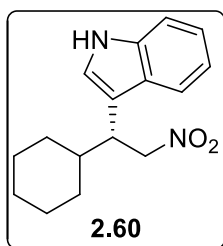
CDCl₃) δ 136.6, 126.3, 122.6, 122.0, 119.9, 118.9, 114.3, 111.7, 80.7, 36.5, 32.3, 29.4, 22.6, 14.0; HRMS (ESI-TOF) m/z : [M + H]⁺ Calcd. for C₁₄H₁₉N₂O₂ 247.1441; Found 247.1468.

*2-(1-cyclohexyl-2-nitroethyl)-1H-pyrrole (2.59)*³²



Prepared according to sample procedure using (*E*)-(2-nitrovinyl)cyclohexane (104 mg, 0.67 mmol) and 4.03 M pyrrole solution (500 μ L, 2 mmol) to yield 47 mg of **2.59** as a colorless oil (Yield: 32%, Average yield: 36% over two runs). R_f : 0.43 in 20% EtOAc/hexanes. Enantiomeric excess 40% (Average ee = 38% over two runs). $[\alpha]_D^{25} = +11.6^\circ$ (c 0.1, CH₂Cl₂). ¹H NMR (400 MHz, CDCl₃) δ 8.02 (brs, 1H), 6.69 (ddd, J = 2.7 Hz, 2.7 Hz, 1.5 Hz, 1H), 6.17–6.15 (m, 1H), 5.98–5.96 (m, 1H), 4.70 (dd, J = 12.7 Hz, 5.9 Hz, 1H), 4.59 (dd, J = 12.6 Hz, 9.2 Hz, 1H), 3.35 (ddd, J = 9.1 Hz, 6.3 Hz, 6.3 Hz, 1H), 1.77–1.56 (m, 6H), 1.31–0.91 (m, 5H); ¹³C NMR {¹H} (100 MHz CDCl₃) δ 129.1, 117.2, 108.8, 106.2, 78.3, 43.7, 40.8, 31.3, 30.2, 26.3, 26.2; MALDI-TOF (CCA matrix, positive mode) m/z : [M + H]⁺ Calcd. for C₁₂H₁₉N₂O₂ 223.1441; Found 223.007.

3-(1-Cyclohexyl-2-nitroethyl)-1H-indole (2.60)^{24a}



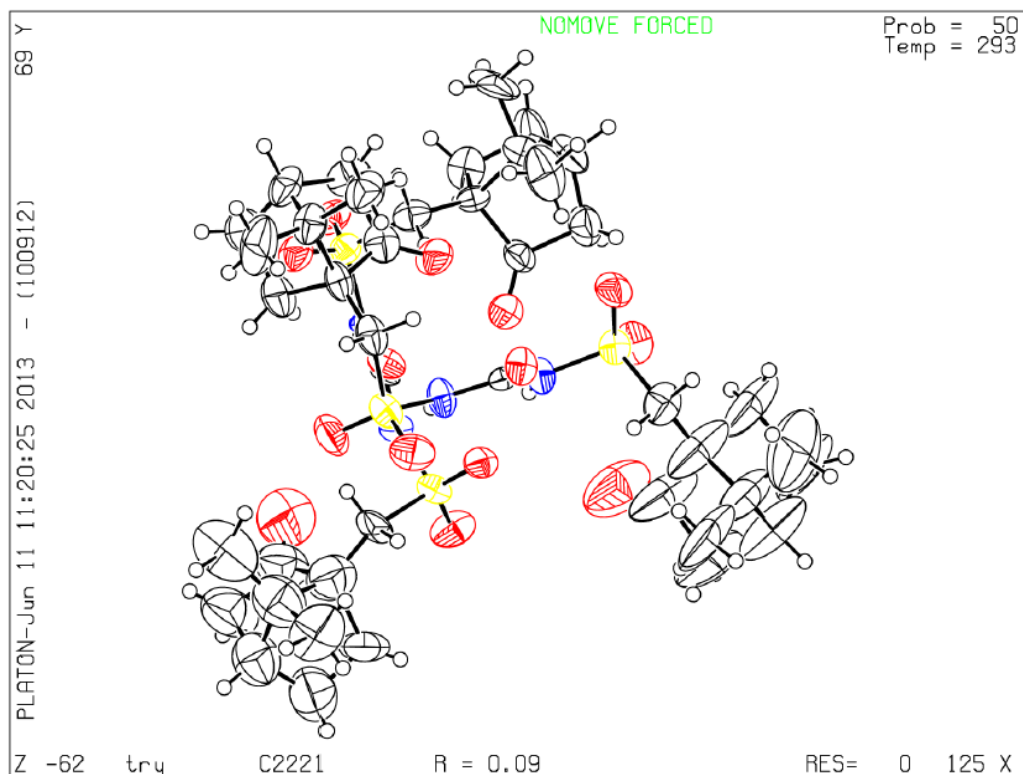
Prepared according to sample procedure using (*E*)-(2-nitrovinyl)cyclohexane (104 mg, 0.67 mmol) and indole (235 mg, 2 mmol) to yield 21 mg of **2.60** as a pale yellow oil (Yield: 12%, Average yield: 12% over two runs). R_f : 0.50 in 20% EtOAc/hexanes. Enantiomeric excess 18% (Average ee = 16% over two runs). $[\alpha]_D^{25} = +6.5^\circ$ (c 0.1, CH₂Cl₂). ¹H NMR (400 MHz, CDCl₃) δ 8.07 (brs, 1H), 7.63–7.61 (m, 1H), 7.38–7.36 (m, 1H), 7.22 (ddd, J = 8.1 Hz, 7.1 Hz, 1.1 Hz, 1H), 7.15 (ddd, J = 7.9 Hz, 7.1 Hz, 1.0 Hz, 1H), 7.00 (d, J =

2.4 Hz, 1H), 4.84 (dd, $J = 12.0$ Hz, 6.2 Hz, 1H), 4.73 (dd, $J = 12.0$ Hz, 9.4 Hz, 1H), 3.70 (ddd, $J = 9.3$ Hz, 6.7 Hz, 6.7 Hz, 2H), 1.88–1.61 (m, 6H), 1.36–0.95 (m, 5H); ^{13}C NMR (^1H) (100 MHz CDCl_3) δ 136.4, 127.0, 122.4, 122.3, 119.8, 119.2, 113.4, 111.5, 78.6, 42.0, 40.6, 31.3, 30.6, 26.4, 26.32, 26.30; MALDI-TOF (CCA matrix, positive mode) m/z : $[\text{M} + \text{H}]^+$ Calcd. for $\text{C}_{16}\text{H}_{21}\text{N}_2\text{O}_2$ 273.1598; Found 273.093.

2.5.4 X-ray Crystallography CCDC number - CCDC 943949

ORTEP X-Ray crystal structure display of 2.33; ellipsoids drawn at 50% probability level.

CCDC number: CCDC 943949



Crystallographic data were collected on a Bruker Smart-CCD diffractometer equipped with a normal focus, 2.4 kW sealed tube X-ray source with graphite monochromated Mo- $K\alpha$ radiation ($\lambda = 0.71073$ Å) operating at 50 kV and 30 mA. The

program SAINT³⁴ was used for integration of diffraction profiles and absorption correction was made with SADABS³⁵ program. The structure was solved by SIR 92³⁶ and refined by full matrix least square method using SHELXL-97.³⁷ All the non-hydrogen atoms were refined anisotropically and all the hydrogen atoms were fixed by HFIX and placed in ideal positions. All calculations were carried out using SHELXL- 97, PLATON³⁸ and WinGX system, Ver 1.70.01.³⁹

2.5.4.1 Crystal data and structure refinement parameters for compound 2.33

Parameter	2.33
Formula	C ₂₁ H ₃₂ N ₂ O ₇ S ₂
<i>M</i>	488.63
crystal system	Orthorhombic
space group	C222 ₁
<i>a</i> [Å]	16.6760 (6)
<i>b</i> [Å]	23.3517 (8)
<i>c</i> [Å]	27.7936 (10)
α [°]	90
β [°]	90
γ [°]	90
<i>V</i> [Å ³]	10823.2 (7)
<i>Z</i>	16
<i>T</i> [K]	293
μ [mm ⁻¹]	0.235
ρ_c [g/cm ³]	1.199
<i>F</i> (000)	4160
reflections [<i>I</i> > 2 σ (<i>I</i>)]	5897
Unique reflections	9276
measured reflections	44952
GOF	1.31
Flack <i>x</i>	0.02 (13)
<i>R</i> _{int}	0.075

$R_1[I > 2\sigma(I)]^{[a]}$	0.0934
$R_w[I > 2\sigma(I)]^{[b]}$	0.2489
$\Delta\rho$ max/min [$e \text{ \AA}^{-3}$]	0.97/-0.51

a, b: $R_1 = \sum ||F_o| - |F_c|| / \sum F_o$; $R_w = [\sum \{w(F_o^2 - F_c^2)^2\} / \sum \{w(F_o^2)^2\}]^{1/2}$

2.5.5 Infrared and Raman Spectroscopy and Quantum Chemical Calculations

Raman studies were done using a custom-built Raman spectrometer.⁴⁰ The wavelength of laser source used was 632.8 nm (HeNe red laser) and the power at the sample was about 8 mW. The spectra were smoothed using 5 point FFT filter and baseline corrected to remove the background. Peak positions were determined by fitting Lorentzian line profiles. All the quantum chemical calculations have been performed based on density functional theory (DFT) as implemented in Gaussian 09 (G09) suite of program.⁴¹ For catalyst in its free form, initial geometry was taken from the crystal structure and subsequently geometry optimization was performed using Becke three-parameter hybrid-exchange functional⁴² and Lee, Yang and Parr (B3LYP) gradient corrected correlation functional.⁴³ Basis set employed for such calculation is 6-31G (d,p). Harmonic vibrational frequencies were calculated on the optimized geometry using the same level of theory. The absence of any negative frequency confirms that the geometries correspond to the local minima at the potential energy surface. Same level of theory was employed to optimize the catalyst in its bound form with Na^+ and vibrational frequency calculation. A dual scaling factor was used for the calculated vibrational frequencies, where frequencies below 1000 cm^{-1} were not scaled, whereas that above 1000 cm^{-1} were scaled with 0.961.⁴⁴

2.5.5.1 Tentative vibrational band assignment of catalyst 2.33⁴⁵

Raman modes cm ⁻¹	IR modes cm ⁻¹	Band assignments
190		Γ ring
199		Γ ring
274		Γ ring
288		C-S-N bend, Γ CCC
324		σ SO ₂
399		CCC def,
431	427	δ ring (CCC def, Γ CC)
474	468	δ ring (CCC def, Γ CC)
484	479	ν _s SO ₂ , skeletal ring,
517	512	C-C-C def
525	524	C-C-C def
560	559	O-S-O def, symmetric skeletal vibration of urea, δ C-
590	566	O-S-O def, δ N-C-N
689	681	asymmetric skeletal vibration of urea
711	730	in-phase ρ CH ₂ , ν C-S
768	740	β C-C-C
778	767	ν _{as} C-S-N, π CO
792	777	ν _{as} C-S-N, π skeletal urea
825	814	ρ CH ₂
	836	β N-C-O
855	853	ρ CH ₂ , ω NH ₂
881	880	ν S-N
906, 914	906	ρ CH ₃
943	931	ν C-C
	938	ν C-C
971	967	ν C-N
1006		ρ C-H
1032		τ C-H
1069	1051	τ C-H
1075	1068	τ C-H
1137		τ C-H
1162	1131, 1139	ν _s SO ₂
1171	1162	ν C-C, CH ₃ rock, ν _s SO ₂
1184		ω CH ₂ , ν C-C
1206	1200	δ NH ₂ , ω or τ CH ₂
1225	1218	δ NH ₂ , ω or τ CH ₂
	1282	ω CH ₂ , τ CH ₂
1303		ν _{as} SO ₂

1307		ω CH ₂
	1344	ν_{as} SO ₂
1359		ω CH ₂
1398	1394	δ_{s} CH ₃
1423	1417	σ C-H (CH ₂ , CH ₃)
1447	1445	def C-H (CH ₂ , CH ₃)
	1455	def C-H (CH ₂ , CH ₃)
1476	1470	ν_{as} C-N, δ CH ₃ , σ CH ₂
1488	1482	ν_{as} C-N, σ CH ₂
	1633	β O-H (water)
1708	1706	ν C=O (urea)
1755		ν C=O (of camphor ring)
	1734, 1747	Fermi resonance (ω CH ₂ and β C=O) of ring
	2886	ν_{s} C-H
2926	2922	ν_{as} C-H
2931	2926	ν_{as} C-H
2969		ν_{as} C-H
2990	2985	ν_{as} C-H
	3268 br	ν N-H

β : bending, δ_{s} : in plane deformation, ω : wagging, τ : twist, ρ : rocking, σ : scissor, ν : stretching, π : out of plane deformation, s : symmetric, as : antisymmetric, def : deformation, Γ : torsion and br : broad, ring: camphor ring.

2.6 References

1 a) Doyle, A. G.; Jacobsen, E. N. *Chem. Rev.* **2007**, *107*, 5713–5743. b) Taylor, M. S.; Jacobsen, E. N. *Angew. Chem., Int. Ed.* **2006**, *45*, 1520–1543. c) Connon, S. J. *Chem. –Eur. J.* **2006**, *12*, 5418–5427. d) Pihko, P. M. *Angew. Chem., Int. Ed.* **2004**, *43*, 2062–2064. e) Schreiner, P. R. *Chem. Soc. Rev.* **2003**, *32*, 289–296. f) Schreiner, P. R.; Wittkopp, A. *Org. Lett.* **2002**, *4*, 217–220.

2 Hedstrom, L. *Chem. Rev.* **2002**, *102*, 4501–4523.

3 a) Blake, J. F.; Jorgensen, W. L. *J. Am. Chem. Soc.* **1991**, *113*, 7430–7432. b) Bryan, P.; Pantoliano, M. W.; Quill, S. G.; Hsiao, H.-Y.; Poulos, T. *Proc. Natl. Acad. Sci. U.S.A.* **1986**, *83*, 3743–3745.

-
- 4 Wassermann, A. *J. Chem. Soc.* **1942**, 618–621.
- 5 a) Hine, J.; Ahn, K.; Gallucci, J. C.; Linden, S. *J. Am. Chem. Soc.* **1984**, *106*, 7980–7981.
b) Hine, J.; Linden, S.; Kanagasabapathy, V. M. *J. Am. Chem. Soc.* **1985**, *107*, 1082–1083.
c) Hine, J.; Linden, S.; Kanagasabapathy, V. M. *J. Org. Chem.* **1985**, *50*, 5096–5099.
- 6 Kelly, T. R.; Meghani, B.; Ekkundi, V. S. *Tetrahedron Lett.* **1990**, *31*, 3381–3384.
- 7 Wittkopp, A.; Schreiner, P. R. *Chem. –Eur. J.* **2003**, *9*, 407–414.
- 8 Sigman, M. S.; Jacobsen, E. N. *J. Am. Chem. Soc.* **1998**, *120*, 4901–4902.
- 9 Okino, T.; Hoashi, Y.; Furukawa, T.; Xu, X. N.; Takemoto, Y. *J. Am. Chem. Soc.* **2005**, *127*, 119–125.
- 10 a) Jensen, K. H.; Sigman, M. S. *J. Org. Chem.* **2010**, *75*, 7194–7201. b) Jensen, K. H.; Sigman, M. S. *Angew. Chem., Int. Ed.* **2007**, *46*, 4748–4750. c) Rajaram, S.; Sigman, M. S. *Org. Lett.* **2005**, *7*, 5473–5475.
- 11 Li, X.; Deng, H.; Zhang, B.; Li, J.; Zhang, L.; Luo, S.; Cheng, J.–P. *Chem. –Eur. J.* **2010**, *16*, 450–455.
- 12 Jakab, G.; Tancon, C.; Zhang, Z.; Lippert, K. M.; Schreiner, P. R. *Org. Lett.* **2012**, *14*, 1724–1727.
- 13 a) Kimmel, K. L.; Weaver, J. D.; Lee, M.; Ellman, J. A. *J. Am. Chem. Soc.* **2012**, *134*, 9058–9061. b) Kimmel, K. L.; Robak, M. T.; Thomas, S.; Lee, M.; Ellman, J. A. *Tetrahedron* **2012**, *68*, 2704–2712. c) Robak, M. T.; Herbage, M. A.; Ellman, J. A. *Tetrahedron* **2011**, *67*, 4412–4416. d) Kimmel, K. L.; Robak, M. T.; Ellman, J. A. *J. Am. Chem. Soc.* **2009**, *131*, 8754–8755. e) Robak, M. T.; Trincado, M.; Ellman, J. A. *J. Am. Chem. Soc.* **2007**, *129*, 15110–15111.
- 14 Ganesh, M.; Seidel, D. *J. Am. Chem. Soc.* **2008**, *130*, 16464–16465.
- 15 a) Hughes, M. P.; Smith, B. D. *J. Org. Chem.* **1997**, *62*, 4492–4499. b) Hughes, M. P.; Shang, M. Y.; Smith, B. D. *J. Org. Chem.* **1996**, *61*, 4510–4511.
- 16 a) Nickerson, D. M.; Angeles, V. V.; Auvil, T. J.; So, S. S.; Mattson, A. E. *Chem. Commun.* **2013**, 4289–4291. b) Nickerson, D. M.; Mattson, A. E. *Chem.–Eur. J.* **2012**, *18*, 8310–8314. c) So, S. S.; Auvil, T. J.; Garza, V. J.; Mattson, A. E. *Org. Lett.* **2012**, *14*, 444–447. d) So, S. S.; Burkett, J. A.; Mattson, A. E. *Org. Lett.* **2011**, *13*, 716–719.

-
- 17 So, S. S.; Mattson, A. E. *J. Am. Chem. Soc.* **2012**, *134*, 8798–8801.
- 18 a) Yates, M. H.; Kallman, N. J.; Ley, C. P.; Wei, J. N. *Org. Process Res. Dev.* **2009**, *13*, 255–262. b) Lobb, K. L.; Hipskind, P. A.; Aikins, J. A.; Alvarez, E.; Cheung, Y. -Y.; Considine, E. L.; De Dios, A.; Durst, G. L.; Ferrito, R.; Grossman, C. S.; Giera, D. D.; Hollister, B. A.; Huang, Z.; Iversen, P. W.; Law, K. L.; Li, T.; Lin, H.-S.; Lopez, B.; Lopez, J. E.; Cabrejas, L. M. M.; McCann, D. J.; Molero, V.; Reilly, J. E.; Richett, M. E.; Shih, C.; Tiecher, B.; Wikel, J. H.; White, W. T.; Mader, M. M. *J. Med. Chem.* **2004**, *47*, 5367–5380. c) Wright, J. B.; Willitte, R. E. *J. Med. Chem.* **1962**, *5*, 815–822.
- 19 a) Sheng, Y.-F.; Gu, Q.; Zhang, A.-J.; You, S.-L. *J. Org. Chem.* **2009**, *74*, 6899–6901. b) Liu, H.; Lu, S.-F.; Xu, J.; Du, D.-M. *Chem. –Asian J.* **2008**, *3*, 1111–1121.
- 20 Chittoory, A. K.; Kumari, G.; Mohapatra, S.; Kundu, P. P.; Maji, T. K.; Narayana C.; Rajaram, S. *Tetrahedron* **2014**, *70*, 3459–3465.
- 21 a) Evans, D. A.; Bartroli, J.; Shih, T. L. *J. Am. Chem. Soc.* **1981**, *103*, 2127–2129. b) Crimmins, M. T.; King, B. W.; Tabet, E. A.; Chaudhary, K. *J. Org. Chem.* **2001**, *66*, 894–902. For other examples of dipole–dipole repulsion in selective reaction see Refs. 20c–20d. c) Clayden, J.; McCarthy, C.; Westlund, N.; Frampton, C. S. *J. Chem. Soc., Perkin Trans. I* **2000**, 1363–1378. d) Giese, B.; Damm, W.; Wetterich, F.; Zeitz, H.-G. *Tetrahedron Lett.* **1993**, *34*, 5885–5888.
- 22 a) Mortezaei, S.; Catarineu, N. R.; Canary, J. W. *J. Am. Chem. Soc.* **2012**, *134*, 8054–8057. b) Zurro, M.; Asmus, S.; Beckendorf, S.; Mück-Lichtenfeld, C.; García Mancheño, O. *J. Am. Chem. Soc.* **2014**, *136*, 13999–14002.
- 23 De Filippis, V.; De Dea, E.; Lucatello, F.; Frasson, R. *Biochem. J.* **2005**, *390*, 485–492.
- 24 a) Lu, S. -F.; Du, D. -M.; Xu, J. *Org. Lett.* **2006**, *8*, 2115–2118. b) Trost, B. M.; Müller, C. *J. Am. Chem. Soc.* **2008**, *130*, 2438–2439.
- 25 a) Schafer, A. G.; Wieting, J. M.; Mattson, A. E. *Org. Lett.* **2011**, *13*, 5228–5231. b) Itoh, J.; Fuchibe, K.; Akiyama, T. *Angew. Chem., Int. Ed.* **2008**, *47*, 4016–4018. c) Fleming, E. M.; McCabe, T.; Connon, S. J. *Tetrahedron Lett.* **2006**, *47*, 7037–7042. d) Herrera, R. P.; Sgarzani, V.; Bernardi, L.; Ricci, A. *Angew. Chem., Int. Ed.* **2005**, *44*, 6576–6579. e) Zhuang, W.; Hazell, R. G.; Jørgensen, K. A. *Org. Biomol. Chem.* **2005**, *3*, 2566–2571.
- 26 Meganathan, C.; Sebastian, S.; Sivanesan, I.; Lee, K. W.; Jeong, B. R.; Oturak, H.; Sudha, S.; Sundaraganesan, N. *Spectrochim. Acta, Part A* **2012**, *95*, 331–340.

-
- 27 Kundu, P. P. Experimental and Quantum Calculation Studies of Molecular Systems of Biological and Chemical Importance by Raman, Infrared, and SERS. Ph.D. Thesis, *Jawaharlal Nehru Centre for Advanced Scientific Research*, **2014**.
- 28 a) Chandran, A.; Mary, Y. S.; Varghese, H. T.; Panicker, C. Y.; Pazdera, P.; Rajendran, G.; Babu, N. *J. Mol. Struct.* **2011**, *992*, 77–83. b) Chohan, Z. H.; Youssoufi, M. H.; Jarrahpour, A.; Hadda, T. B. *Eur. J. Med. Chem.* **2010**, *45*, 1189–1199.
- 29 For an example of a urea carbonyl bound to two sodium cations see: a) Armentano, D.; De Munno, G.; Rossi, R. *New J. Chem.* **2006**, *30*, 13–17. b) Al-Harbi, A.; Sattler, W.; Sattler, A.; Parkin, G. *Chem. Commun.* **2011**, 3123–3125. c) Geier, J.; Harmer, J.; Grützmacher, H. *Angew. Chem., Int. Ed.* **2004**, *43*, 4093–4097. d) Gilroy, J. B.; Lemaire, M. T.; Patrick, B. O.; Hicks, R. G. *CrystEngComm* **2009**, *11*, 2180–2184.
- 30 Davis, F. A.; Jenkins, R. H.; Awad, S. B.; Stringer, O. D.; Watson, W. H.; Galloy, J. J. *Am. Chem. Soc.* **1982**, *104*, 5412–5418.
- 31 Kumaran, G.; Kulkarni, G. H. *Tetrahedron Lett.* **1994**, *35*, 9099–9100.
- 32 Guo, F.; Chang, D.; Lai, G.; Zhu, T.; Xiong, S.; Wang, S.; Wang, Z. *Chem. –Eur. J.* **2011**, *17*, 11127–11130.
- 33 Lin, S. –Z.; You, T. –P. *Tetrahedron* **2009**, *65*, 1010–1016.
- 34 SMART (V 5.628), SAINT (V 6.45a), XPREP, SHELXTL; Bruker AXS Inc. Madison, Wisconsin, USA, **2004**.
- 35 Sheldrick, G. M. *Siemens Area Detector Absorption Correction Program*; University of Göttingen, Göttingen, Germany, **1994**.
- 36 Altomare, A.; Cascarano, G.; Giacovazzo, C.; Guagliaradi, A. *J. Appl. Cryst.* **1993**, *26*, 343–350.
- 37 Sheldrick, G. M. SHELXL97, *Program for Crystal Structure Solution and Refinement*; University of Göttingen, Göttingen, Germany, **1997**.
- 38 Spek, A. L. *J. Appl. Cryst.* **2003**, *36*, 7–13.
- 39 Farrugia, L. J. *J. Appl. Cryst.* **1999**, *32*, 837–838.
- 40 Kumar, G. V. P.; Narayana, C. *Curr. Sci.* **2007**, *93*, 778–781.

41 Frisch, M. J.; Trucks, G. W.; Schlegel, H. B.; Scuseria, G. E.; Robb, M. A.; Cheeseman, J. R.; Scalmani, G.; Barone, V.; Mennucci, B.; Petersson, G. A.; Nakatsuji, H.; Caricato, M.; Li, X.; Hratchian, H. P.; Izmaylov, A. F.; Bloino, J.; Zheng, G.; Sonnenberg, J. L.; Hada, M.; Ehara, M.; Toyota, K.; Fukuda, R.; Hasegawa, J.; Ishida, M.; Nakajima, T.; Honda, Y.; Kitao, O.; Nakai, H.; Vreven, T.; Montgomery, J. A.; Peralta, J. E.; Ogliaro, F.; Bearpark, M.; Heyd, J. J.; Brothers, E.; Kudin, K. N.; Staroverov, V. N.; Kobayashi, R.; Normand, J.; Raghavachari, K.; Rendell, A.; Burant, J. C.; Iyengar, S. S.; Tomasi, J.; Cossi, M.; Rega, N.; Millam, J. M.; Klene, M.; Knox, J. E.; Cross, J. B.; Bakken, V.; Adamo, C.; Jaramillo, J.; Gomperts, R.; Stratmann, R. E.; Yazyev, O.; Austin, A. J.; Cammi, R.; Pomelli, C.; Ochterski, J. W.; Martin, R. L.; Morokuma, K.; Zakrzewski, V. G.; Voth, G. A.; Salvador, P.; Dannenberg, J. J.; Dapprich, S.; Daniels, A. D.; Farkas, Ö.; Foresman, J. B.; Ortiz, J. V.; Cioslowski, J.; Fox, D. J. *Gaussian09, Revision B. 01*, **2009**.

42 Becke, A. D. *J. Chem. Phys.* **1993**, *98*, 5648–5652.

43 Lee, C.; Yang, W.; Parr, R. G. *Phys. Rev. B* **1988**, *37*, 785–789.

44 NIST Computational Chemistry Comparison and Benchmark Database (CCCBDB), NIST Standard Reference Database Number 101, Release 16a, August **2013**, Editor: Johnson III, Russell D.; <http://cccbdb.nist.gov/> .

45 a) Morita, H. E.; Kodama, T. S.; Tanaka, T. *Chirality* **2006**, *18*, 783–789. b) Hagemann, H.; Dulak, M.; Wesolowski, T. A.; Chapuis, C.; Jurczak, J. *Helv. Chim. Acta* **2004**, *87*, 1748–1766. c) Mayo, D. W.; Miller, F. A.; Hannah, R. W. *Course Notes on the Interpretation of Infrared and Raman Spectra*, Wiley-Interscience, New Jersey, **2004**. d) Otero, J. C.; Lopez-Cantarero, E.; Chacon, A.; Marcos, J. I. *Vib Spectrosc.* **1991**, *1*, 395–400. e) Stewart, J. E. *J. Chem. Phys.* **1957**, *26*, 248–254.

Chapter 3

BIFUNCTIONAL STRONG-BASE CATALYST FOR THE SYNTHESIS OF DIAMINO PHOSPHONATES

3.1 Introduction

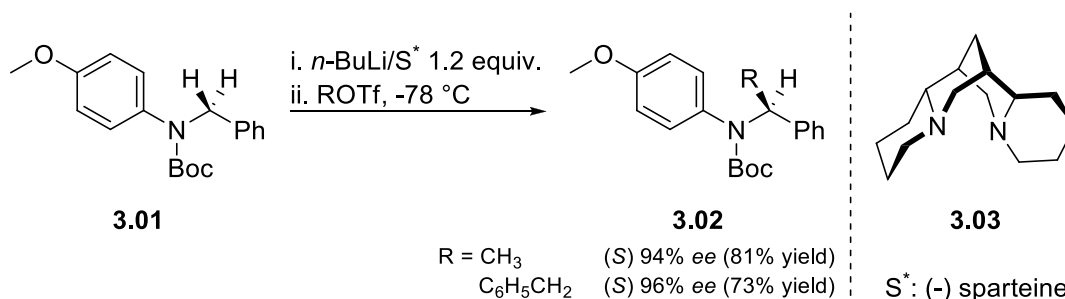
The use of chiral bases can provide access to novel bond formation processes that are not possible by other means. In earlier work, strong anionic bases with stoichiometric amounts of a chiral ligand for the counter cation were used. The deprotonation in these cases were irreversible as the difference in pK_a between the substrate and the conjugate acid of the base is substantial. Chiral induction was achieved via interaction between the conjugate base of the substrate and the chiral cationic species. A major limitation of this was the need for stoichiometric amounts of the chirality inducing agent. In more recent work, weaker neutral bases have been used in catalytic enantioselective transformations. Although the reactions are catalytic in nature, the range of substrates that can be deprotonated by these catalysts is

limited by the low basicity of the catalysts. Therefore, there is a need for highly basic chiral catalysts. In this chapter, we discuss our work on the development of a chiral strong-base catalyst based on a cyclopropeneimine scaffold. We have applied this catalyst in an enantioselective reaction between an iminophosphonate and an N-carbamoyl imine. The diaminophosphonate products were obtained in good selectivities and have potential applications in the synthesis of peptidomimetics.

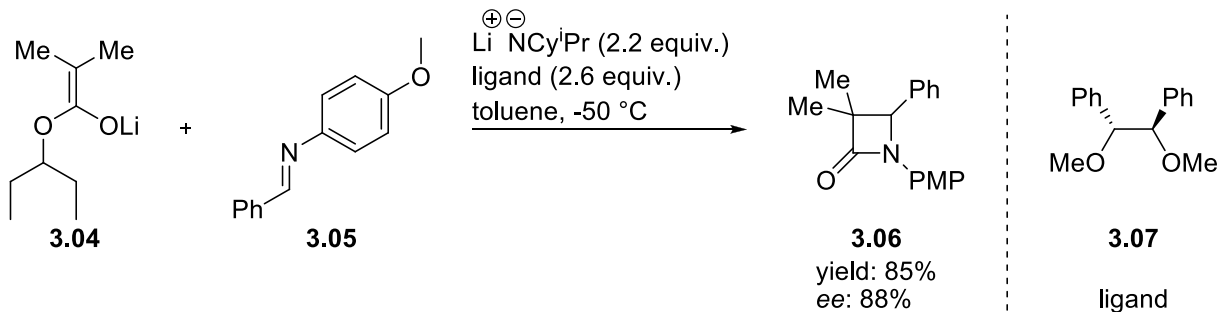
3.2 Background

Beak and coworkers pioneered the use of chiral lithium bases in enantioselective reactions.¹ In their reported reactions, a BOC protected secondary amine was deprotonated with a chiral BuLi-sparteine complex (Scheme 3.1). Reaction of electrophiles with this anion, resulted in the formation of products with good *ees*. Tomioka and coworkers used a similar approach in their synthesis of β -lactams via a Gilman-Speeter reaction (Scheme 3.2).² In this case, an ester was deprotonated by lithium diisopropylamide complexed with a chiral diether. The early work from the Beak and Tomioka groups used a stoichiometric amount of the chiral ligand. Subsequently, the Tomioka group has shown that sub-stoichiometric quantities of the ligand (20 mol%) can be used to obtain products in excellent selectivity.^{2a} However, further application of this system has been limited.

Scheme 3.1: Asymmetric Alkylation Mediated by (-) Sparteine



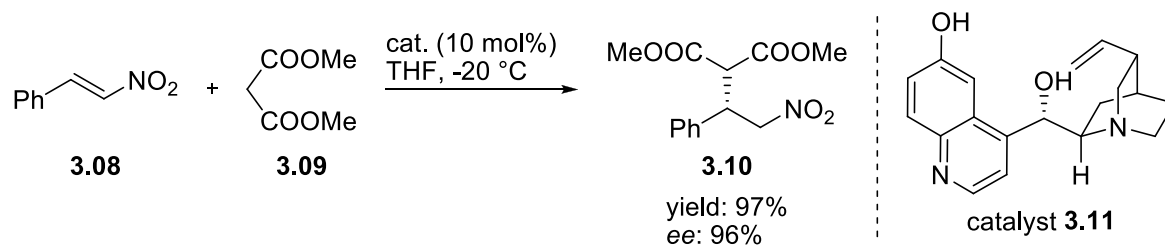
Scheme 3.2: Strong-Base Mediated β -Lactam Synthesis Using Chiral Ligand



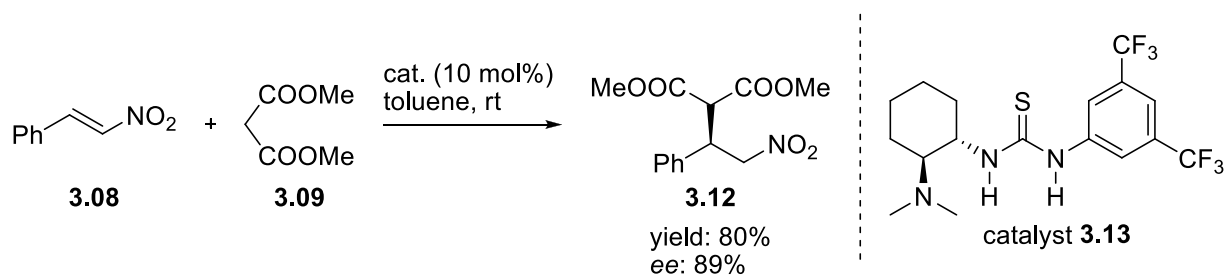
The development of chiral bases that can be used catalytically has focused on weaker non-ionic bases. One of the earliest reports in this area was from the Deng group wherein a modified quinine catalyst was used in the Michael reaction of malonates with nitrostyrene (Scheme 3.3).³ In this catalyst, the methoxy ether on the quinolone ring was converted to a hydroxyl group. This was crucial for obtaining good enantioselectivity. Subsequently, this catalyst has been used in another Michael addition wherein a chiral quaternary center was generated.⁴ Another early report in this area was by Takemoto and coworkers, wherein a bifunctional catalyst based on a cyclohexanediamine scaffold was used.⁵ One of the amino groups was derivatized as a thiourea moiety while the other was converted to a tertiary amine as shown in Scheme 3.4. The pK_a of the protonated tertiary amine is expected to be around 9. This catalyst was used in the Michael addition of 1,3-dicarbonyl compounds to nitroalkenes. The products were obtained in excellent selectivities (Scheme 3.4). It was proposed that the amine group deprotonates the enol form of the 1,3-dicarbonyl compounds, which then react with the thiourea-bound nitroalkene. Later, this catalyst has been used in other reactions as well.⁶

Around the same time, Soós and coworkers reported on a bifunctional catalyst based on cinchona alkaloids (Scheme 3.5).⁷ Here, the quinuclidine nitrogen, acts as a base and deprotonates nitromethane. Addition of the nitronate anion to chalcones proceeded in

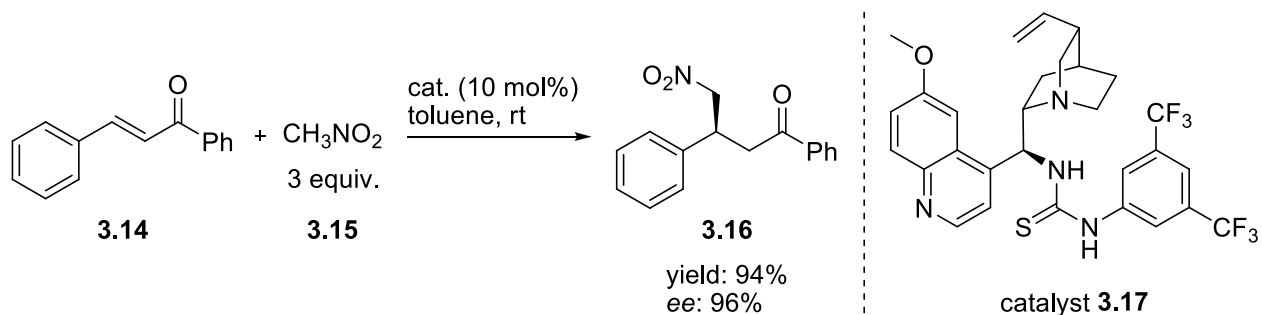
Scheme 3.3: Demethylated Quinine Catalyzed Michael Reaction



Scheme 3.4: Bifunctional Thiourea Catalyzed Michael Reaction



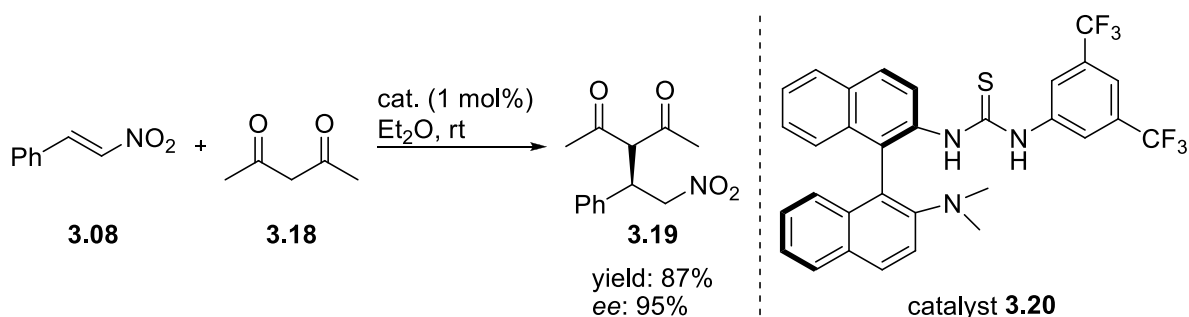
Scheme 3.5: Michael Reaction Catalyzed by a Cinchona Alkaloid Based Bifunctional Thiourea



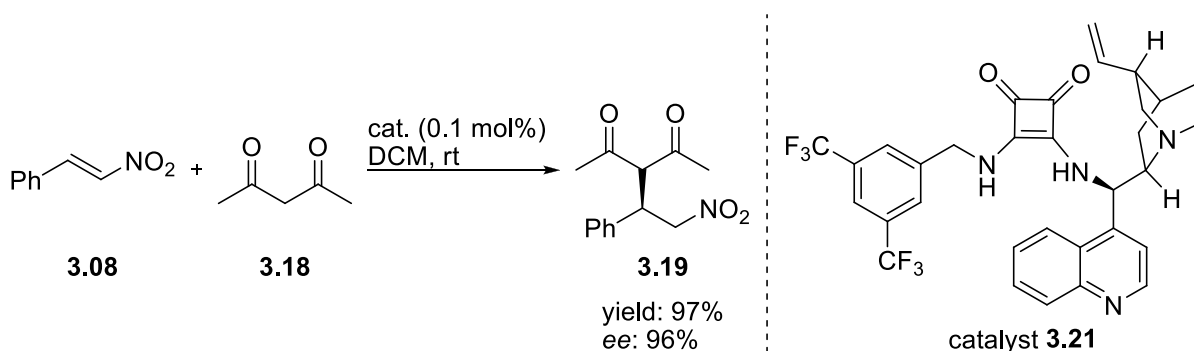
excellent selectivity. Previous work from the Sera group had shown that the cinchona alkaloid by itself catalyzed the reaction under high pressures with modest enantioselectivity.⁸ Inclusion of thiourea moiety in the catalyst enhances selectivity and permits the reaction to be carried out under ambient pressure. However, no attempt was made to compare the efficiency of this catalyst with Takemoto's catalyst. Subsequently, this has become a highly utilized system for other reactions.⁹ Interestingly, during the development of a biaryl based

bifunctional catalyst, Wang and coworkers have compared the Takemoto catalyst with the cinchona alkaloid catalyst in a Michael addition between 2,4-pentanedione and nitrostyrene.¹⁰ Here, the Takemoto catalyst (**3.13**) outperformed the cinchona alkaloid system in turn over frequency (TOF), while selectivity was better with the cinchona alkaloid system (Scheme 3.6). More importantly, the biaryl catalyst outperformed both the cinchona alkaloid and Takemoto's catalyst in TOF as well as selectivity. The Rawal group has shown that by moving to a chiral squaramide (Scheme 3.7), the Michael reaction can be performed with very low catalyst loadings.¹¹

Scheme 3.6: Michael Reaction Catalyzed by a Biaryl Based Bifunctional Thiourea

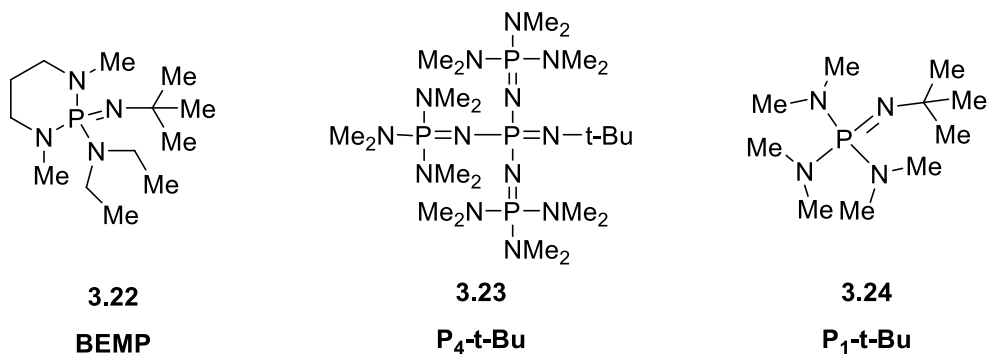


Scheme 3.7: Chiral Squaramide Catalyzed Addition of 2,4 Pentanedione to Nitrostyrene



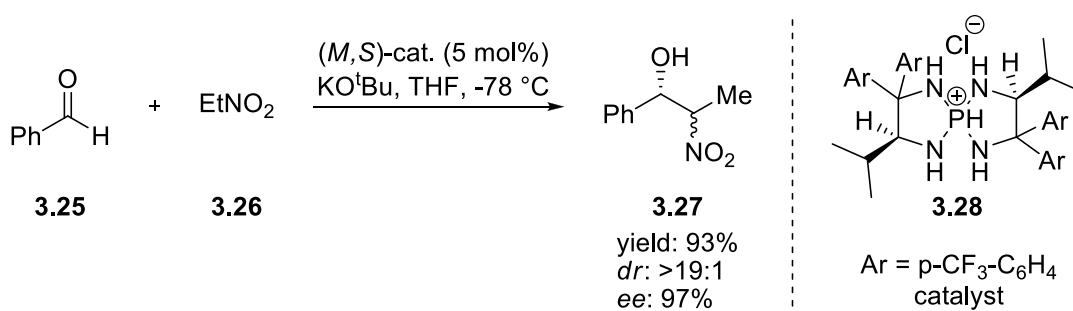
In all of the above cases, the conjugate acid of the basic component has a pK_a in the range of 9-11. These are often sufficient for deprotonating pro-nucleophiles that are somewhat acidic. Deprotonation of less acidic pro-nucleophiles would require stronger bases. This has been partly accomplished using phase transfer catalysts (PTC) that can transfer a hydroxide ion from aqueous to organic phase. However, the use of aqueous basic conditions can limit the substrate scope as well as the range of temperatures that can be used in a reaction. A more direct approach is the use of a strong base that is soluble in organic solvents. In this regard, two classes of strong organic bases have found widespread applications viz., phosphazenes and guanidines. Phosphazenes were developed by Schwesinger and are typically characterized by phosphorus nitrogen double bonds. The most commonly used phosphazenes are BEMP and P_4 -t-Bu (Figure 3.1).¹² A large number of polymerization reactions have been performed with these bases. Hedrick and coworkers have used BEMP and P_1 -t-Bu in ring opening polymerizations (ROP) of lactides and esters (Figure 3.1).¹³ The catalysts were found to be slower than guanidine bases for this system. Kakuchi and coworkers have utilized P_4 -t-Bu in a group transfer polymerization of methylmethacrylate¹⁴ and in an ROP of styrene oxide.¹⁵ In all these cases, the phosphazene base deprotonates an alcohol initiator and sustains an alkoxide propagating species.

Figure 3.1: Phosphazene Catalysts

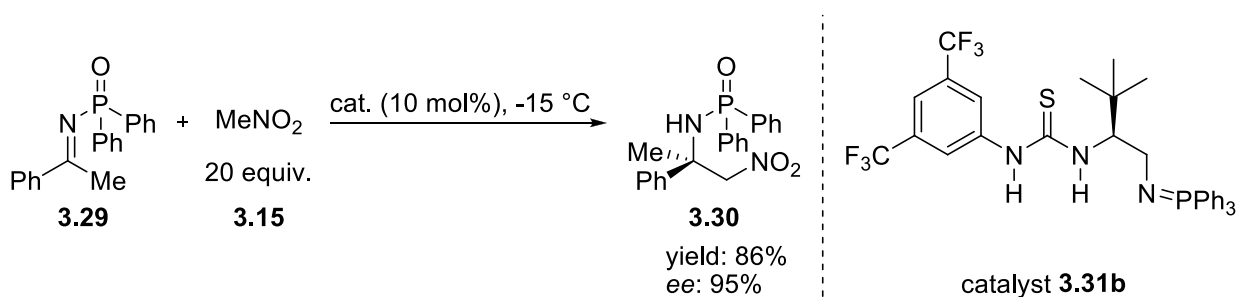


In the realm of asymmetric catalysis, Ooi and coworkers have developed a spirophosphazene using a valine derived diamine.¹⁶ This has been used in a catalytic Henry reaction with very high enantio and diastereoselectivity (Scheme 3.8). Subsequently, this has been applied in 1,4-additions, 1,6-additions, and 1,8-additions.¹⁷ Dixon and coworkers have explored the possibility of bifunctional catalysis using phosphazene bases.¹⁸ In their catalyst, a phosphazene base is connected to a highly acidic thiourea group, which acts as a hydrogen-bond donor. In their initial work, they have utilized their catalyst in a nitro-Mannich reaction with ketimines (Scheme 3.9). The reaction proceeds with good enantioselectivity. Importantly, the reaction does not proceed with a less basic catalyst derived from a cinchona alkaloid. The phosphazene catalyst has been subsequently used in a Pudovik reaction¹⁹ and a Michael reaction.²⁰ In general, a strong base catalyst is likely to deprotonate any strong hydrogen-bond donor and the conjugate base of the hydrogen-bond donor is likely to be the

Scheme 3.8: Spirophosphazene Catalyzed Henry Reaction

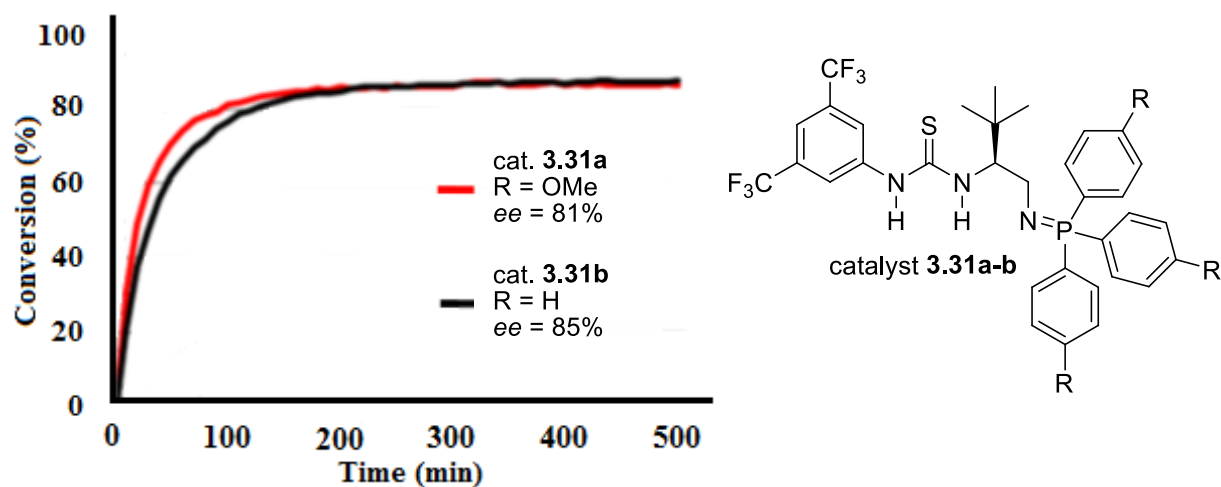


Scheme 3.9: Bifunctional Phosphazene Catalyzed Nitro-Mannich Reaction



basic species. Dixon and coworkers have measured the basicity of a structurally similar phosphazene base without the thiourea and found that it is more basic than DBU. Studies from the Schreiner group on the pK_a of thioureas has demonstrated that DBU is likely to deprotonate 3,5-bistrifluoromethyl phenyl substituted thioureas.²¹ From these two studies, it would appear that the deprotonated thiourea is the basic species in this system. In their initial study, Dixon et al have reported that changing the phosphorous substituent from phenyl to *p*-methoxy phenyl does not impact the rate of the reaction (Figure 3.2). The *p*-methoxy substituent is expected to increase the basicity and hence enhance the rate of reaction. This suggests that enhancing the basicity beyond a point would simply result in the deprotonation of the hydrogen-bond donating arm. This is a key design principle that has to be kept in mind while designing bifunctional catalysts with strong bases.

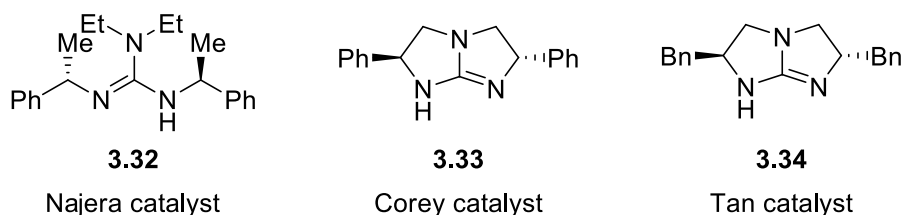
Figure 3.2: Study of Catalyst Basicity in the Nitro-Mannich Reaction. Adapted with permission from American Chemical Society



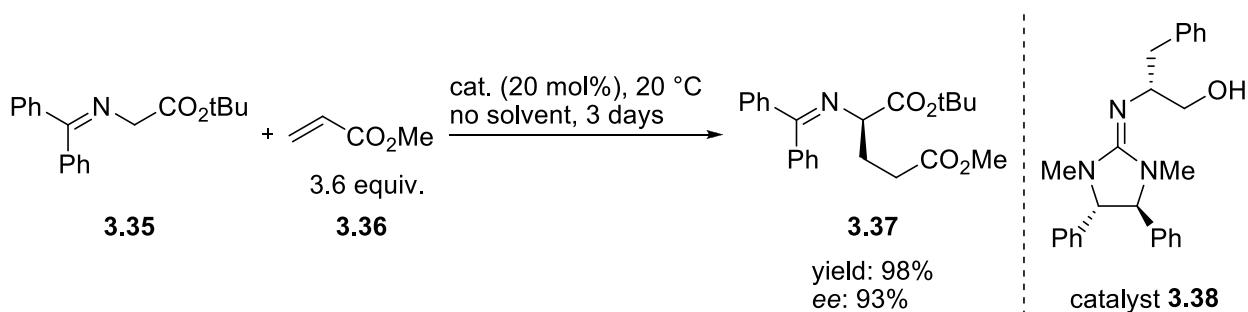
One of the earliest reports on a chiral strong-base catalyst was from the Najera group, wherein, a C_2 -symmetric guanidine was used in a nitro-aldol reaction.²² The products were obtained in modest enantioselectivity. Following this, the Corey and Tan groups have reported the use of bicyclic guanidines (Figure 3.3) in a number of enantioselective reactions.²³ In most of these cases the nucleophiles used are fairly acidic.

Ishikawa and coworkers have showed that the chiral guanidine in Scheme 3.10 can be used to deprotonate the benzophenone imine of glycine *tert*-butyl ester.²⁴ The pK_a of the corresponding ethyl ester has been shown to be 18.7 by O'Donnell and coworkers.²⁵ Using this catalyst, a Michael reaction with acrylates as the acceptor was reported to proceed with good selectivity. Importantly, the reaction required 20 mol% of the catalyst and took 3 days to reach completion. This appears to suggest that the deprotonation equilibrium is not favorable. A breakthrough in this area was achieved when Lambert and coworkers reported the use of cyclopropenimine as strong-base catalyst.²⁶ The enhanced basicity of this catalyst

Figure 3.3: Chiral Guanidine Bases

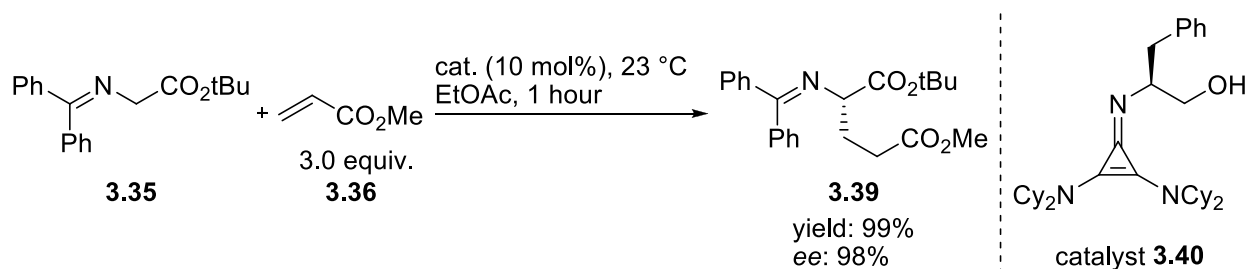


Scheme 3.10: Michael Reaction Catalyzed by a Chiral Guanidine

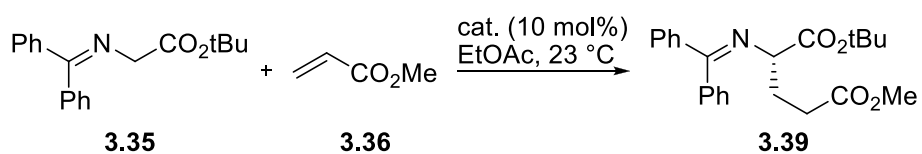


was attributed to the formation of an aromatic cyclopropenyl cation upon protonation. Using this catalyst, the Michael reaction described in the previous reaction was performed in 1 hour at a catalyst loading of 10 mol% (Scheme 3.11). This clearly suggests that the deprotonation equilibrium lies much more to the right in this case. The hydroxyl group in the catalyst acts as a hydrogen bond donor. Removal of this group results in substantially reduced catalyst activity (Scheme 3.12).^{26b} Subsequently, this catalyst has been used in the synthesis of diamino acids. A disadvantage of this catalyst is the low stability as seen in its half-life of 7 hours. The stability of the catalyst was substantially enhanced by replacing the phenyl alaninol group with an amino-indanol.²⁷

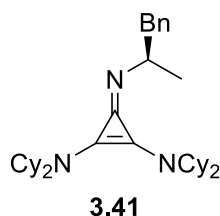
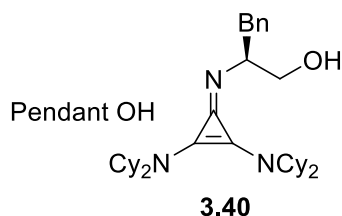
Scheme 3.11: Cyclopropenimine Catalyzed Michael Addition



Scheme 3.12: Role of Pendant OH on Imparting Selectivity in the Michael Reaction



catalyst	time (h)	conv. (%)	ee (%)
3.40	1	>95	98
3.41	24	11	0



The excellent basicity along with low stability prompted us to design a catalyst system that would be more stable than the Lambert catalyst. Along with this, we sought a more modular system that would allow us to vary the acidity of the hydrogen-bond donor. In Lambert's work this aspect of the catalyst has not been explored beyond showing the necessity of the hydrogen-bond donor.

3.3 Results and Discussion

The low half-life of the Lambert catalyst makes it unsuitable for reactions that require longer times to go to completion.^{26b} Decomposition of the catalyst is initiated by a deprotonation of the alcohol by the basic nitrogen. The alkoxide then attacks the positively charged carbon atom followed by ring opening of the cyclopropene ring (Scheme 3.13). In our proposed design, the cyclopropeneimine scaffold with the cyclohexyl groups is retained while the chirality is provided by the readily available trans-diaminocyclohexane moiety (Figure 3.4). One of the nitrogens is part of the cyclopropeneimine group while the other is derivatized as an amide. The acidity of the NH group can be readily tuned by changing the electronics around the aryl ring. Deprotonation of the NH group would result in an amide anion. The amide anion is less nucleophilic than an alkoxide due to delocalization of the

Scheme 3.13: Decomposition Pathway of Lambert Catalyst

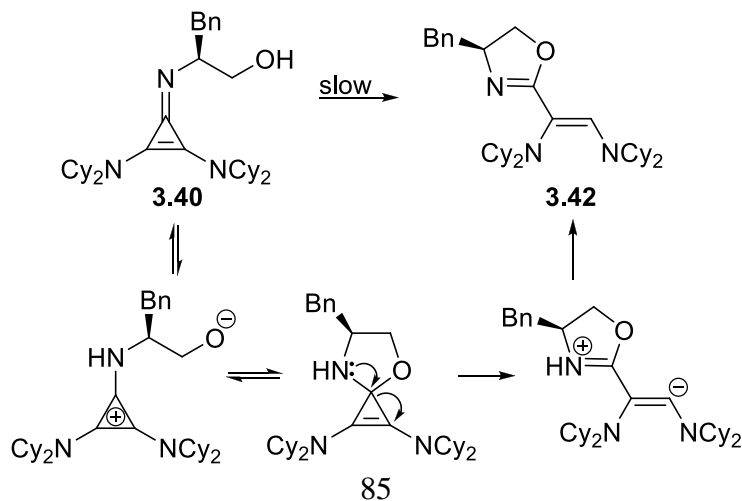
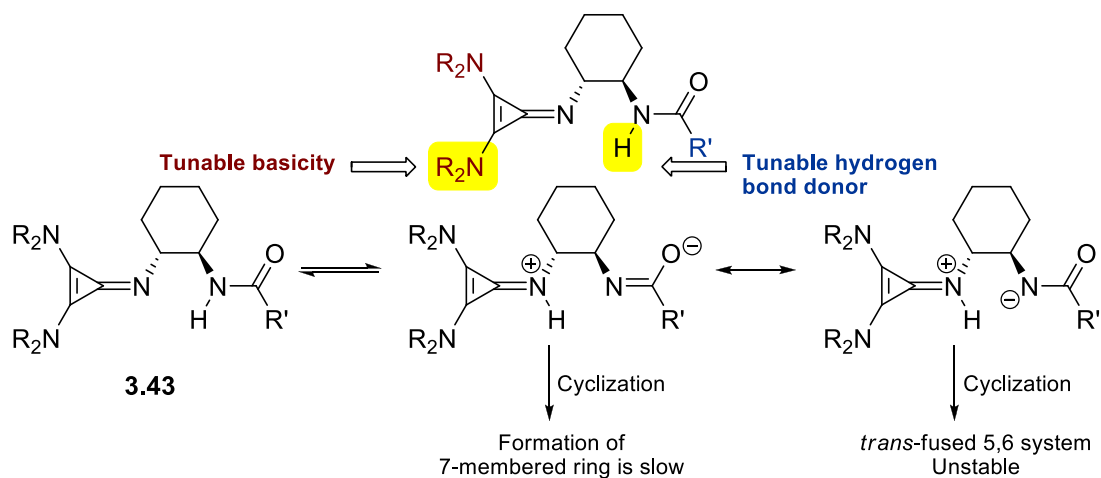


Figure 3.4: Structure of Proposed Catalyst and Explanation for Expected Stability

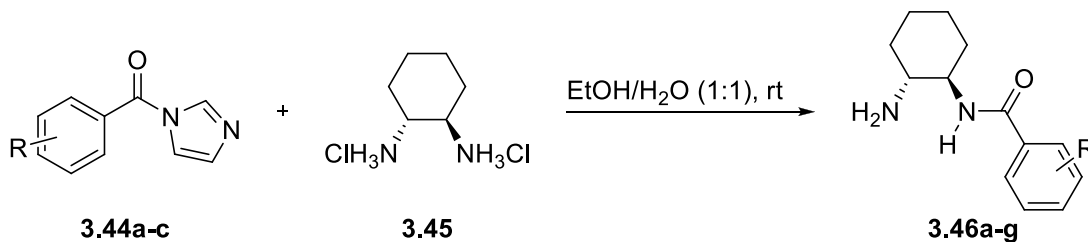


negative charge. Attack through the oxygen atom is likely to be slow as this would lead to a 7-membered ring (Figure 3.4). On the other hand, attack through nitrogen atom would lead to a strained trans-fused 5,6 ring system. Due to these reasons, we hypothesized that our catalyst would have greater stability than the Lambert catalyst.

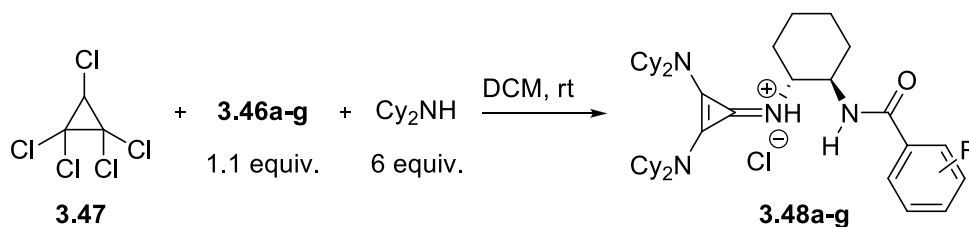
We began our studies by synthesizing the mono functionalized diamine shown in Scheme 3.14. This was made from the corresponding acyl imidazole as shown in panel A.²⁸ The catalyst synthesis began with the reaction of pentachlorocyclopropane **3.47** with 6 equiv. of dicyclohexylamine (Panel B). The mono functionalized diamine was added to the reaction after 48 hours. After stirring for a further 12 hours, the reaction mixture was worked up and the product was isolated by chromatography. In order to examine the utility of our cyclopropeneimine, we decided to use it as a catalyst in the synthesis of diaminophosphonates. The aminophosphonate moiety has been used in medicinal chemistry as an isostere of amino acids.²⁹ The tetrahedral structure of the phosphonate mimics the tetrahedral intermediate observed in the hydrolysis of peptides. Therefore, this has been used in the synthesis of protease inhibitors. Aminophosphonates have also found application as

Scheme 3.14: Synthetic Route to Proposed Catalyst

Panel A



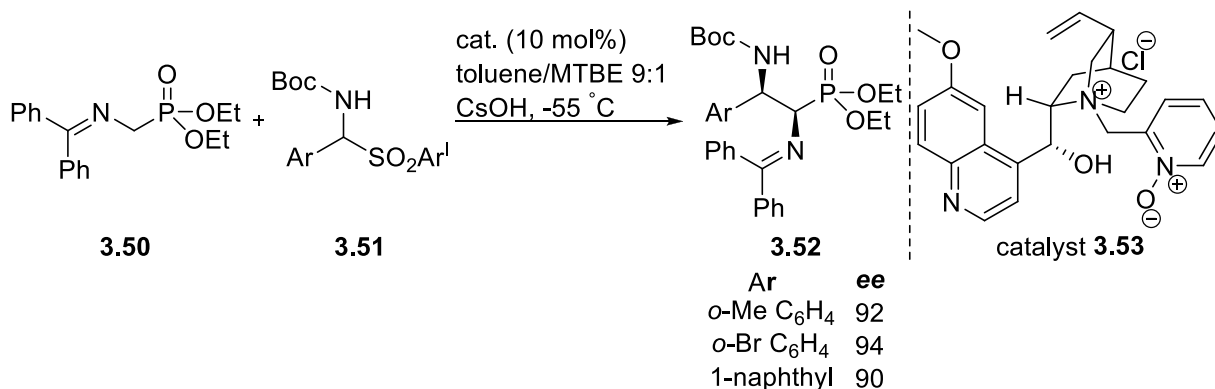
Panel B



HIV inhibitors.³⁰ Based on the well-known utility of these systems, we decided to pursue a synthesis of diaminophosphonates.

In earlier work, Ricci and coworkers had shown that benzophenone imine **3.50** can be deprotonated under phase transfer conditions and treated with imines to yield diaminophosphonates (Scheme 3.15).³¹ The corresponding diaminophosphonates were obtained in high *ees* in the case of the three imines shown below. In all other cases, the *ees* were low. Kobayashi and coworkers have shown that fluorenone imine can be used instead

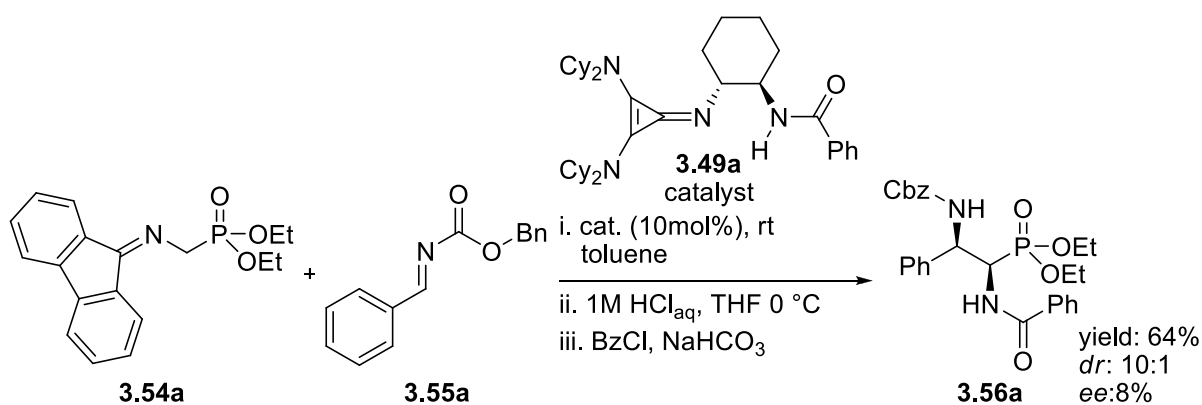
Scheme 3.15: Synthesis of Diamino Phosphonates under Phase Transfer Conditions



of **3.50** in the synthesis of diaminophosphonates.³² Fluorenone imines are more acidic than the corresponding benzophenone imines. Deprotonation of the fluorenone imine phosphonates were performed with either lithium p-methoxyphenoxide or potassium t-butoxide as the base in catalytic quantities. Upon reaction with N-carbonyl imines, the corresponding diaminophosphonates were obtained in excellent diastereoselectivity. Significantly, weaker bases like Et₃N were found to be ineffective for this reaction. We expected our catalyst to be a stronger base than phenoxide and therefore sought to use them in the synthesis of diaminophosphonates.

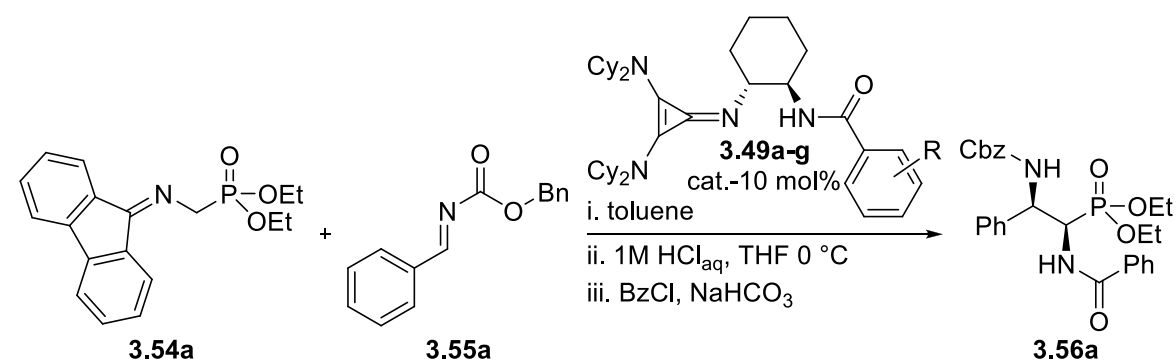
In our initial reaction, we used 10 mol% of **3.49a** as the catalyst with toluene as solvent (Scheme 3.16). The product was hydrolyzed to remove the fluorenone group and derivatized as the benzamide to measure the enantioselectivity. Using this protocol, we measured the *ee* of the product to be 8%. As the reactions were completed rapidly at room temperature, we hypothesized that performing the reaction at lower temperatures might improve the selectivity.

Scheme 3.16: Initial Results



However, when the reaction was performed at $-40\text{ }^{\circ}\text{C}$, we obtained the product with the same *ee* albeit with an increase in the diastereomer ratio (Table 3.1). At this juncture, we decided to utilize the modularity of the catalyst to improve the selectivity. Using the method described above, we systematically, increased the acidity of the NH group. The corresponding mono-substituted diamines were synthesized either from the acyl imidazoles or directly from the acid chlorides. With 10 mol% of these catalysts, reactions between

Table 3.1: Catalyst Screen for the Synthesis of Diaminophosphonate



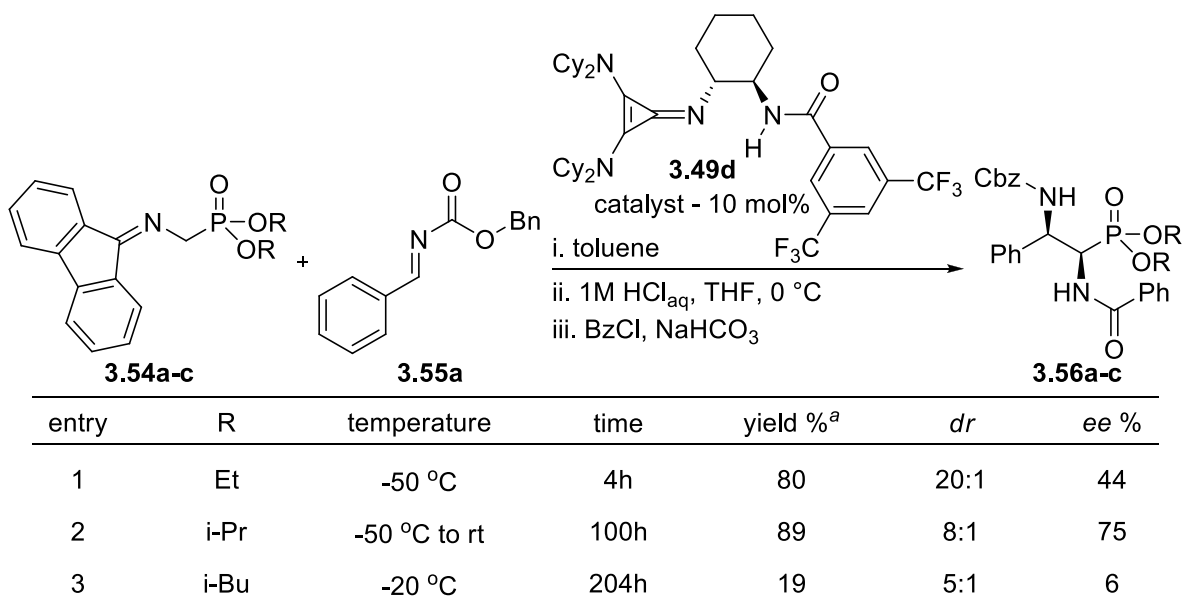
entry	catalyst	catalyst-R	temperature	time	yield % ^a	<i>dr</i>	<i>ee</i> %
1	3.49a	H	RT	0.5h	64	10:1	8
2	3.49a	H	$-40\text{ }^{\circ}\text{C}$	12h	26	>20:1	8
3	3.49b	4-Br	$-40\text{ }^{\circ}\text{C}$	12h	39	>20:1	28
4	3.49c	4-NO ₂	$-40\text{ }^{\circ}\text{C}$	12h	72	>20:1	32
5	3.49d	3,5-Bis CF ₃	$-40\text{ }^{\circ}\text{C}$	12h	75	>20:1	19
6	3.49b	4-Br	$-50\text{ }^{\circ}\text{C}$	26h	99	>20:1	33
7	3.49c	4-NO ₂	$-50\text{ }^{\circ}\text{C}$	NR ^b	NA	NA	NA
8	3.49d	3,5-Bis CF ₃	$-50\text{ }^{\circ}\text{C}$	4h	80	>20:1	44
9	3.49e	3-Cl	$-50\text{ }^{\circ}\text{C}$	26h	86	>20:1	27
10	3.49f	2-Cl	$-60\text{ }^{\circ}\text{C}$	18h	59	>20:1	14
11	3.49g	3,4,5-tri Fluoro	$-50\text{ }^{\circ}\text{C}$	03h	88	>20:1	29
12	3.49d	3,5-Bis CF ₃	$-80\text{ }^{\circ}\text{C}$	54h	69	>20:1	13

^acrude yield of amine after work up of hydrolysis. ^bcatalyst is insoluble at lower temperatures.

imine phosphonates and the N-Cbz imine were performed at -40 °C. While all catalysts gave excellent diastereoselectivity, the catalyst derived from p-nitrobenzamide gave the highest *ee* under these conditions (Table 3.1, entry 4). To further enhance the *ee*, we attempted reactions, at -50 °C. At this temperature, the 3,5-bis trifluoromethylbenzoic acid derived catalyst gave an *ee* of 44%. Other catalysts did not give good *ees* under similar conditions (Table 3.1, entries 9 to 11). Surprisingly, a further decrease in temperature to -80 °C resulted in a lowering of the selectivity (Table 3.1, entry 12).

In an effort to further enhance the *ee*, we decided to use the diisopropyl phosphonate **3.54b** as the substrate. With this substrate, we initially attempted the reaction at -50 °C. However, the reaction did not appear to be proceeding at this temperature. Therefore, the reaction mixture was allowed to warm to room temperature. Under these conditions, the product was obtained in 75% *ee* (Table 3.2, entry 2). In order to further enhance the *ee*, we

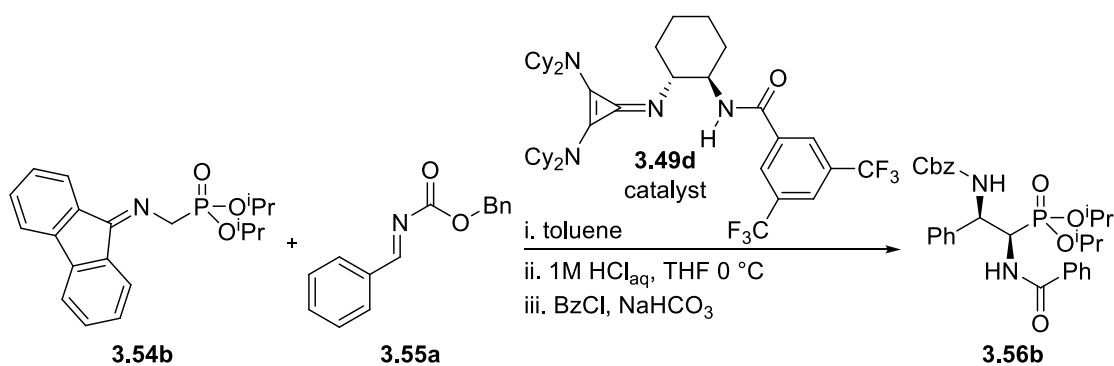
Table 3.2: Variation of Phosphonate Structure for Optimizing the Selectivity



^acrude yield of amine after workup of hydrolysis

attempted to use the diisobutyl phosphonate **3.54c** as the substrate. However, the reaction was very slow with this substrate and the product was obtained in 6% *ee* (Table 3.2, entry 3). We then tried to optimize the *ee* for the diisopropyl substrate **3.54b**. Surprisingly, when the reaction was performed at lower temperatures, lower selectivities were observed. When 10 mol% of the catalyst was used and the reaction was performed at room temperature, an *ee* of 66% was obtained. Carrying out the same reaction at 0 °C and -20 °C gave the product in 46% *ee* and 23% *ee*, respectively (Table 3.3, entries 6 and 3). This seemed to indicate

Table 3.3: Study of Aggregation Effects in the Reaction

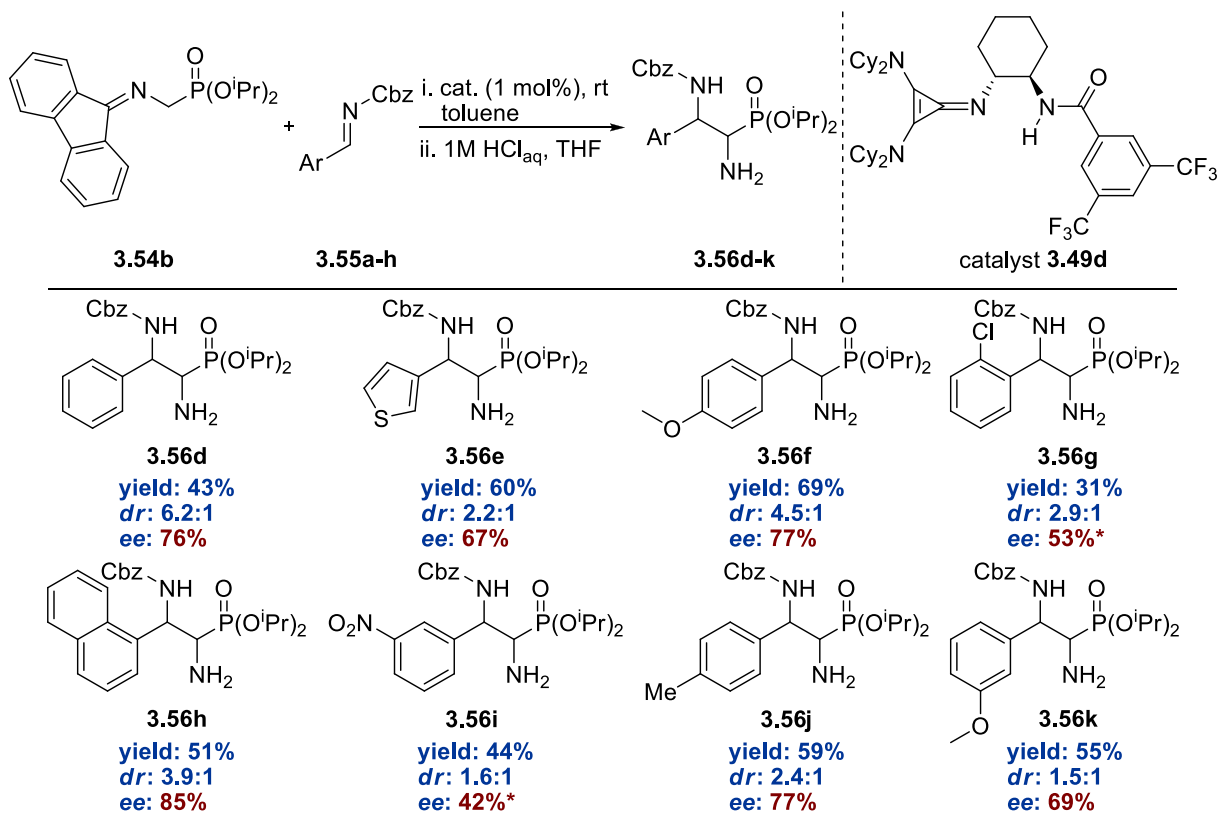


entry	temperature	time	yield % ^a	cat. mol%	<i>ee</i> %
1	-20 °C	NR	NR	1	NR
2	-20 °C	30min	84	5	24
3	-20 °C	20min	82	10	23
4	0 °C	4d	40	1	72
5	0 °C	30min	79	5	51
6	0 °C	30min	67	10	46
7	0 °C	30min	69	15	43
8	rt	<30min	60	1	69.2
9	rt	<30min	82	5	69
10	rt	<30min	80	10	66

^acrude yield of amine after work up of hydrolysis

aggregation of catalyst at lower temperatures. The aggregate structures probably catalyze the reaction with lower selectivity. If this hypothesis were correct, we expected that we could get better selectivities with lower catalyst loading. Indeed, when the reaction was performed at room temperature with 1 mol% of catalyst, we obtained the product in 69% *ee*. When the temperature was lowered to 0 °C, the *ee* remained at similar levels which is in contrast to the reactions performed with 10 mol% catalyst. In order to support the aggregation hypothesis, we performed reactions in a mixture of toluene and ether with 5 mol% catalyst. Ether is a Lewis basic solvent and is likely to disaggregate the catalyst. Indeed, in these solvent mixtures, the selectivity improved when temperatures were lowered. Overall, the best selectivities for the test reaction (76%) were conveniently obtained by running the reaction at room temperature with a catalyst loading of 1 mol%.

Using these conditions, we examined the substrate scope of the reaction. With electron rich aromatic rings, the products were obtained in similar *ee* to the test reaction. Substrates derived from 4-methoxybenzaldehyde, 3-thiophenyl aldehyde, and 4-methyl benzaldehyde gave the corresponding products in 77%, 67%, and 77% *ee* respectively. The highest *ee* of 85% was obtained with the 1-naphthaldehyde derived substituent. Generally, we obtained better selectivities when the reactions were carried out with electron-rich aromatic imines (Table 3.4). This is in contrast to the report by Ricci and coworkers where the best selectivities were obtained for electron deficient systems. In our system, with the p-methoxyphenyl imine **3.55c** we obtained the product in 77% *ee*, whereas this product was obtained in 50% *ee* using the Ricci protocol. The p-tolyl imine **3.55g** gave slightly better *ee* under our conditions. In the case of electron-deficient aromatic imines, the Ricci protocol gave much better *ees* than our conditions. Thus, our reaction conditions are complementary

Table 3.4: Substrate Scope

* ee of the minor diastereomer. ees were measured for the corresponding benzoylated derivative

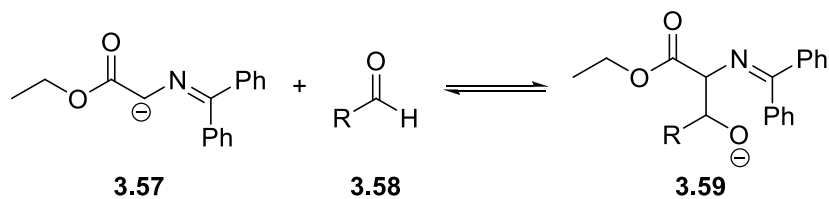
to the conditions reported by Ricci and coworkers and gives access to products that cannot be obtained in good selectivity using the Ricci protocol.

To determine the identity of the major diastereomer, we hydrolyzed **3.56d** and compared the NMR of this compound with previously reported material.³¹ This showed that the *syn*-isomer was the major diastereomer (see experimental section). To test the durability of our catalyst, we stored the catalyst under ambient atmosphere in a flask at room temperature for more than three months. Reactions performed with this catalyst gave the same yield and selectivity as freshly prepared batch of catalyst. Thus, our catalyst system appears to be stable under ambient conditions and does not require special storage conditions. The Lambert catalyst is stable for 20 days when stored in the solid state at -20 °C. The

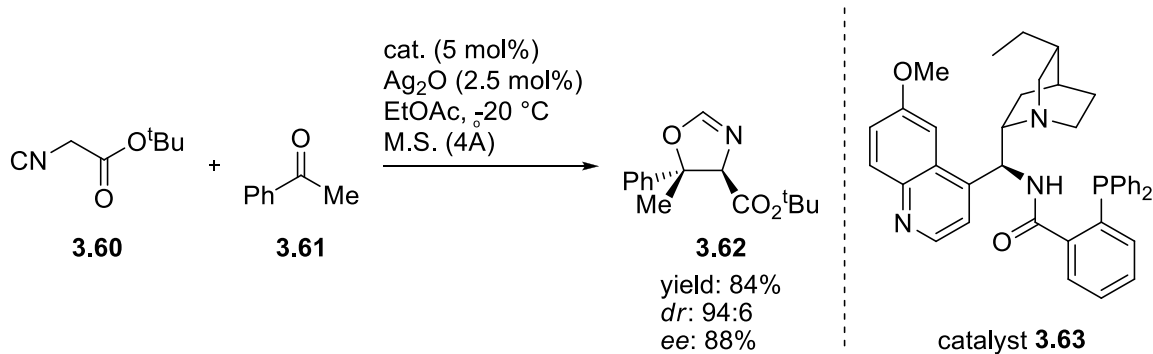
stability of our catalyst **3.49d** in solutions were measured using NMR spectroscopy in C₆D₆. Over a period of ten days we did not observe any changes in the NMR.

The modular and strongly basic nature of the cyclopropeneimine can also be used in other enantioselective reactions. In our laboratory, we are currently working on developing a synthesis of β -hydroxy- α -amino acids using these catalysts. The simple aldol reaction of glycine imine esters with aldehydes is plagued by reversibility and low selectivity (Figure 3.5). To overcome these issues, elaborate procedures with catalysts that require long synthetic sequences have been reported.³³ Even under these conditions, the reactions with aromatic aldehydes do not proceed with good selectivity and *ee*. The reversibility of the aldol reaction has been addressed by using isocyanoacetate esters as reactants. In these cases, the reaction leads to the irreversible formation of oxazolines which are readily hydrolyzed to β -hydroxy- α -amino acids. In comparison to benzophenone imine of glycine esters, isocyanoacetate esters are less acidic. Therefore, deprotonation of these esters would require a strong base. The Dixon group has solved this problem using a soft enolization approach which uses a silver catalyst (Scheme 3.17).³⁴ Other than this, isocyanoacetates with an α -aromatic substituent have been used as substrates with weaker bases in enantioselective reactions. Here, the presence of a phenyl ring decreases the pK_a and enables easy deprotonation with weak tertiary amine bases (Scheme 3.18).³⁵ A similar approach has also

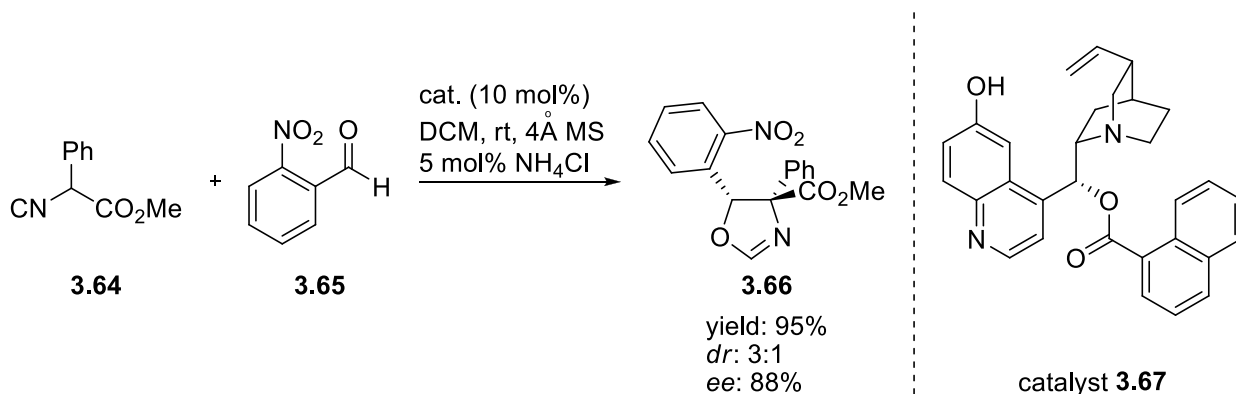
Figure 3.5: Reactivity of Aldehydes with Anion of Imine Esters



Scheme 3.17: Silver Based Catalyst for the Preparation of Oxazolines



Scheme 3.18: Cinchona Based Catalyst for the Synthesis of Oxazolines

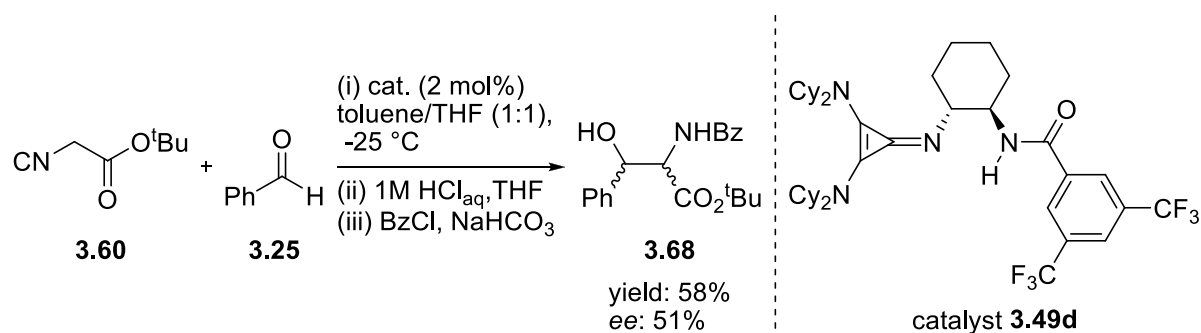


been used with isothiocyanatoacetate where thiazolidinones were obtained as the product.

The hydrolysis of these species are not as straight-forward as the hydrolysis of oxazolines.

We hypothesized that our catalytic system provides an alternative approach to this problem and we used it in a reaction between *tert*-butyl isocyanoacetate and benzaldehyde. In an initial reaction, we obtained the product β -hydroxy- α -amino acid in 51% *ee* after hydrolysis of the oxazolines (Scheme 3.19). Currently, we are working on optimizing this reaction by tuning the catalyst along with the reaction conditions.

Scheme 3.19: Initial Attempt at the Synthesis of β -hydroxy- α -amino esters



3.4 Conclusions

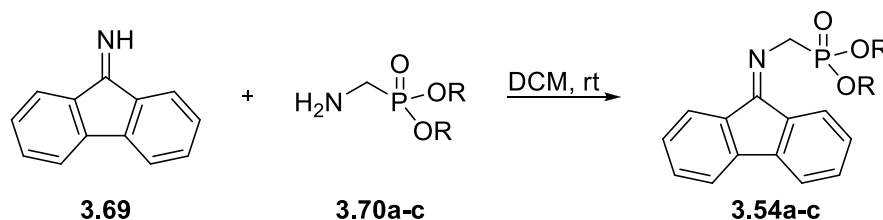
We have developed a modular bifunctional strong-base catalyst using the cyclopropenimine scaffold. In contrast to the earlier work from the Lambert group, the hydrogen-bond donating group can be easily tuned. Using this catalyst, we have developed an enantioselective synthesis of α,β diamino phosphonates. Although the exact pK_a of our fluorenone imine phosphonate is not known, earlier work suggests that weak bases like triethylamine are not efficient for deprotonating this substrate. Therefore, the strongly basic nature of our catalyst is important for this reaction. The tunability of our catalyst system proved to be critical for optimizing the selectivity. The *ee* was sensitive to the acidity of the NH bond as well as the steric crowding around it. Currently, we are working on a more systematic study of the effect of NH acidity on the selectivity of these reactions. In contrast to earlier work from the Ricci group, aromatic imines with electron-donating substituents perform better than imines with electron-withdrawing substituents. Further research will focus on applying these catalysts to other enantioselective reactions.

3.5 Experimental Section

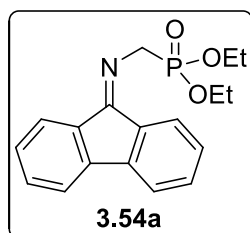
3.5.1 General Information

All glassware was dried overnight in an oven prior to use. Reactions were carried out under argon atmosphere using standard Schlenk techniques. Reactions were monitored by thin layer chromatography using TLC silica gel plates. Flash chromatography was performed using silica gel 230-400 mesh. Unless otherwise noted all reagents were used as received from commercial suppliers without further purification. Toluene was distilled from CaH₂ prior to use. Grease free solvents were obtained by distillation and used for chromatography. Infrared spectra were recorded using an FTIR spectrometer. ¹H and ¹³C NMRs were recorded on a 400 MHz Fourier transform NMR spectrometer and for the compound **3.48g**, ¹³C NMR (150 MHz) was recorded on a 600 MHz Fourier transform NMR spectrometer. Chemical shifts are reported in ppm with respect to the residual undeuterated solvent in CDCl₃ (δ = 7.27 ppm) or D₂O (δ = 4.79 ppm) at room temperature. ¹³C NMRs were recorded at 100 MHz using proton decoupling. Chemical shifts are reported with respect to the deuterated solvent in CDCl₃ (δ = 77.16 ppm) at room temperature. HRMS was recorded using Q-TOF spectrometer. Melting points were recorded using an electro-thermal capillary melting point apparatus and are uncorrected.

3.5.2 Synthesis of fluorenone imine phosphonic acid esters



Diethyl (fluoren-9-ylideneamino)methylphosphonate (3.54a)



In a clean 2-neck 50 mL flask amine phosphonate **3.70a** (2.05 g, 12.30 mmol) was weighed and the flask was flushed with argon. To the flask, 22 mL DCM was added at rt followed by fluorenone imine **3.69** (2.0 g, 11.20 mmol). The reaction was stopped after 2 days. The

residue obtained after the removal of DCM was directly loaded on to column for purification.

NOTE: Compound decomposes on silica on prolonged exposure. Therefore, elution was done rapidly to purify the material.

Column Chromatography:

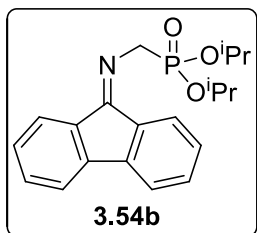
Approximately 80 mL of silica was packed into a column using 25% EtOAc in hexanes as the solvent. The material obtained from work-up was loaded on the column after dissolution in a minimum amount of DCM. Approximately 600 mL of 25% EtOAc in hexanes was eluted followed by elution with 500 mL of 40% EtOAc in hexanes and with 1.1 L of 60% EtOAc in hexanes. The eluted solvent was collected in 25 mL fractions. Fractions 33 – 80 contained product. These fractions were concentrated and dried under high vacuum to give 2.95 g of product **3.54a** (yield: 80%).

Characterization:

R_f: 0.2 in 75% EtOAc/Hexanes. ¹H NMR (400 MHz, CDCl₃) δ 7.90 (d, *J* = 7.7 Hz, 1H), 7.77 (d, *J* = 7.5 Hz, 1H), 7.64 (d, *J* = 7.5 Hz, 1H), 7.55 (d, *J* = 7.5 Hz, 1H), 7.45 – 7.37 (m, 2H), 7.29 – 7.24 (m, 2H), 4.70 (d, *J* = 16.6 Hz, 2H), 4.29 – 4.21 (m, 4H), 1.33 (t, *J* = 7.1 Hz, 6H); ¹³C NMR {¹H} (100 MHz CDCl₃) δ 166.2 (d, *J* = 20.8 Hz), 144.0, 141.1, 138.4 (d, *J* = 2.3 Hz), 131.8, 131.3, 128.5, 128.1, 127.6, 123.0, 120.6, 119.5, 62.9 (d, *J* = 6.7 Hz), 50.9 (d, *J* = 163.4 Hz), 16.6 (d, *J* = 5.7 Hz); ν_{max} (liquid film) 2981, 1644, 1600, 1450, 1241,

1024, 963, 731 cm^{-1} ; HRMS (ESI-TOF) m/z : $[\text{M} + \text{H}]^+$ Calcd. for $\text{C}_{18}\text{H}_{21}\text{NO}_3\text{P}$ 330.1254; Found 330.1254.

Diisopropyl (fluoren-9-ylideneamino)methylphosphonate (3.54b)



In a clean 2-neck 50 mL flask amine phosphonate **3.70b** (1.70 g, 8.71 mmol) was weighed and the flask was flushed with argon. To the flask, 16 mL DCM was added at rt followed by fluorenone imine **3.69** (1.419 g, 7.92 mmol). The reaction was stopped after 65 h. The

residue obtained after the removal of DCM was directly loaded on to column for purification.

NOTE: Compound decomposes on silica on prolonged exposure. Therefore, elution was done rapidly to purify the material.

Column Chromatography:

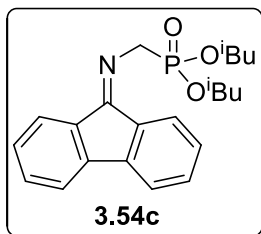
Approximately 80 mL of silica was packed into a column using 30% EtOAc in hexanes as the solvent. The material obtained from work-up was loaded on the column after dissolution in a minimum amount of DCM. Approximately 700 mL of 30% EtOAc in hexanes was eluted followed by elution with 1.1 L of 50% EtOAc in hexanes. The eluted solvent was collected in 25 mL fractions. Fractions 20 – 70 contained product. These fractions were concentrated and dried under high vacuum to give 2.38 g of product **3.54b** (yield: 84%).

Characterization:

R_f : 0.27 in 50% EtOAc/Hexanes. ^1H NMR (400 MHz, CDCl_3) δ 7.91 (d, $J = 7.7$ Hz, 1H), 7.78 (d, $J = 7.4$ Hz, 1H), 7.63 (d, $J = 7.5$ Hz, 1H), 7.55 (d, $J = 7.5$ Hz, 1H), 7.44 – 7.37 (m, 2H), 7.27 (t, $J = 7.5$ Hz, 2H), 4.93 – 4.82 (m, 2H), 4.65 (d, $J = 16.6$ Hz, 2H), 1.35 (d, $J = 6.2$ Hz, 6H), 1.34 (d, $J = 6.3$ Hz, 6H); ^{13}C NMR $\{^1\text{H}\}$ (100 MHz CDCl_3) δ 165.9 (d, $J = 21.1$

Hz), 144.0, 141.1, 138.5 (d, $J = 2.4$ Hz), 131.9 (d, $J = 2.4$ Hz), 131.8, 131.2, 128.5, 128.1, 127.6 (d, $J = 1.3$ Hz), 123.0, 120.5, 119.4, 71.4 (d, $J = 6.8$ Hz), 51.5 (d, $J = 164.8$ Hz), 24.3 (d, $J = 3.7$ Hz), 24.2 (d, $J = 5.0$ Hz); ν_{max} (liquid film) 2978, 1645, 1601, 1450, 1244, 1105, 981, 732 cm^{-1} ; HRMS (ESI-TOF) m/z : $[\text{M} + \text{H}]^+$ Calcd. for $\text{C}_{20}\text{H}_{25}\text{NO}_3\text{P}$ 358.1567; Found 358.1572.

Diisobutyl (fluoren-9-ylideneamino)methylphosphonate (3.54c)



In a clean 2-neck 10 mL flask amine phosphonate **3.70c** (196 mg, 0.88 mmol) was weighed and the flask was flushed with argon. To the flask 1.5 mL DCM was added at rt followed by fluorenone imine **3.69** (143 mg, 0.80 mmol). The reaction was stopped after 26 h. The

residue obtained after the removal of DCM was directly loaded on to column for purification.

NOTE: Compound decomposes on silica on prolonged exposure. Therefore, elution was done rapidly to purify the material.

Column Chromatography:

Approximately 45 mL of silica was packed into a column using 15% EtOAc in hexanes as the solvent. The material obtained from work-up was loaded on the column after dissolution in a minimum amount of DCM. Approximately 300 mL of 15% EtOAc in hexanes was eluted followed by elution with 400 mL of 25% EtOAc in hexanes, 300 mL of 40% EtOAc in hexanes and finally with 300 mL of 50% EtOAc in hexanes. The eluted solvent was collected in 25 mL fractions. Fractions 20 – 41 contained product. These fractions were concentrated and dried under high vacuum to give 304 mg of product **3.54c** (yield: 99%).

Characterization:

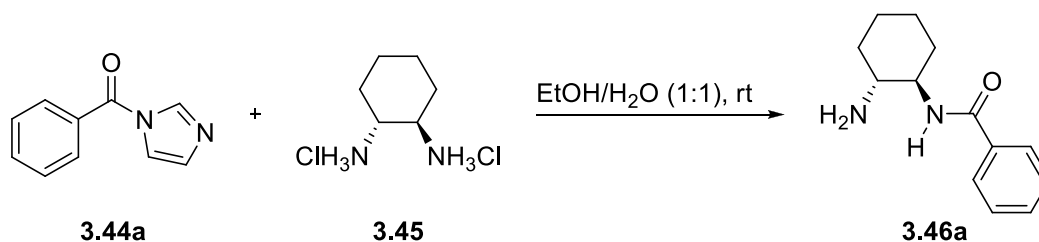
R_f: 0.27 in 40% EtOAc/Hexanes. ¹H NMR (400 MHz, CDCl₃) δ 7.91 (d, *J* = 7.7 Hz, 1H), 7.76 (d, *J* = 7.4 Hz, 1H), 7.62 (d, *J* = 7.5 Hz, 1H), 7.54 (d, *J* = 7.5 Hz, 1H), 7.42 (t, *J* = 7.5 Hz, 1H), 7.39 (t, *J* = 6.9 Hz, 1H), 7.27 (t, *J* = 7.5 Hz, 2H), 4.73 (d, *J* = 16.7 Hz, 2H), 3.98 – 3.94 (m, 4H), 1.95 (sep, *J* = 6.7 Hz, 2H), 0.92 (d, *J* = 6.8 Hz, 12H); ¹³C NMR {¹H} (100 MHz CDCl₃) δ 166.0 (d, *J* = 20.5 Hz), 143.9, 141.1, 138.4 (d, *J* = 2.7 Hz), 131.8, 131.3, 128.4, 128.1, 127.5, 122.9, 120.5, 119.4, 72.7 (d, *J* = 7.1 Hz), 50.6 (d, *J* = 162.8 Hz), 29.3 (d, *J* = 6.0 Hz), 18.7; ν_{max} (liquid film) 2960, 1716, 1645, 1601, 1471, 1450, 1236, 1003, 732, 652 cm⁻¹; HRMS (ESI-TOF) *m/z*: [M + H]⁺ Calcd. for C₂₂H₂₉NO₃P 386.1880; Found 386.1885.

3.5.3 Synthesis of catalyst

3.5.3.1 Sample procedure for diaminobenzamide synthesis

Procedure A:

N-((1*R*,2*R*)-2-aminocyclohexyl)benzamide (**3.46a**)



A 50 mL flask was charged with benzoyl imidazole³⁶ **3.44a** (1051 mg, 6.10 mmol) and 15 mL of ethanol. In a separate flask, dihydrochloride salt **3.45** (1.485 g, 7.93 mmol) was dissolved in 15 mL of DI water. The aqueous salt solution was added to the flask containing benzoyl imidazole dropwise at rt and stirred overnight.

Workup procedure A:

The reaction mixture was concentrated to a fourth of its original volume at reduced pressure using a rotary evaporator. The aqueous layer was washed with 4 X 20 mL of CHCl₃ to remove diacylated product. The aqueous layer was basified with 10 mL of saturated solution of NaOH and washed with 4 X 20 mL of CH₂Cl₂. The organic layers were combined, washed with 2 X 10 mL of DI water, dried over Na₂SO₄, and concentrated.

Column Chromatography:

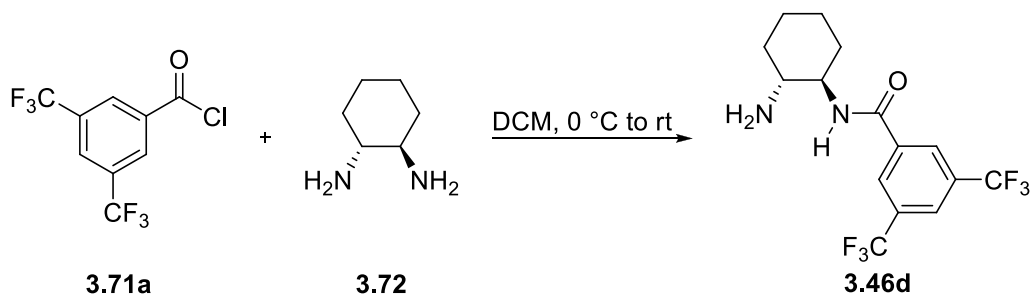
Approximately 33 mL of silica was packed into a column using 3.3% MeOH in CHCl₃ as the solvent. The material obtained from work-up was loaded on the column after dissolution in a minimum amount of CHCl₃. Approximately 300 mL of 3.3% MeOH in CHCl₃ was eluted followed by elution with 400 mL of 4% MeOH in CHCl₃ and finally with 500 mL of 5% MeOH in CHCl₃. The eluted solvent was collected in 25 mL fractions. Fractions 9 – 46 contained product. These fractions were concentrated and dried under high vacuum to give 604 mg of product **3.46a** (yield: 45%).

Characterization:

R_f: 0.37 in 15% MeOH/CHCl₃. $[\alpha]_D^{26} = -166.4^\circ$ (*c* 0.1, CH₂Cl₂), mp 166–168 °C. ¹H NMR (400 MHz, CDCl₃) δ 7.80 – 7.78 (m, 2H), 7.53 – 7.49 (m, 1H), 7.46 – 7.42 (m, 2H), 6.11 (d, *J* = 6.0 Hz, 1H), 3.77 – 3.69 (m, 1H), 2.51 (ddd, *J* = 10.5 Hz, 10.5 Hz, 4.0 Hz, 1H), 2.18 – 2.12 (m, 1H), 2.04 – 2.01 (m, 1H), 1.80 – 1.74 (m, 2H), 1.46 – 1.19 (m, 4H); ¹³C NMR {¹H} (100 MHz CDCl₃) δ 168.0, 134.9, 131.6, 128.7, 127.1, 56.7, 55.7, 35.8, 32.7, 25.3, 25.2; ν_{max} (liquid film) 3291, 2923, 2853, 1632, 1531, 1329, 958, 694 cm⁻¹; HRMS (ESI-TOF) *m/z*: [M + H]⁺ Calcd. for C₁₃H₁₉N₂O 219.1492; Found 219.1494.

*Procedure B:*³⁷

N-((1*R*,2*R*)-2-aminocyclohexyl)-3,5-bis(trifluoromethyl)benzamide (**3.46d**)



A 25 mL two neck flask was charged with diaminocyclohexane **3.72** (600 mg, 5.25 mmol, 3 equiv.) and 5 mL of DCM under argon atmosphere. The flask was cooled to 0 °C using ice bath under argon atmosphere. In a separate flask, bis trifluoromethyl benzoyl chloride **3.71a** (320 μ L, 1.76 mmol, 1 equiv.) was added using syringe followed by 5 mL of DCM under argon atmosphere at rt. The acid chloride solution was added dropwise (for 30 min) to the flask containing diaminocyclohexane at 0 °C. After the completion of addition the reaction was slowly warmed to room temperature and stirred overnight.

Workup procedure B:

The reaction mixture was partitioned between 10% MeOH in CHCl₃ and 0.25 M HCl. The layers were separated and the aqueous layer was washed with 4 X 50 mL of 10% MeOH in CHCl₃ to remove diacylated product. The aqueous layer was basified with 5% NaOH and extracted with 3 X 30 mL of CH₂Cl₂. The organic layers were combined, washed with brine, dried over Na₂SO₄, and concentrated.

Column Chromatography:

Approximately 25 mL of silica was packed into a column using 3.3% MeOH in DCM as the solvent. The material obtained from work-up was loaded on the column after dissolution in a minimum amount of DCM. Approximately 1 L of 3.3% MeOH in DCM was

eluted. The eluted solvent was collected in 25 mL fractions. Fractions 6 – 36 contained product. These fractions were concentrated and dried under high vacuum to give 137 mg of product **3.46d** (yield: 22%).

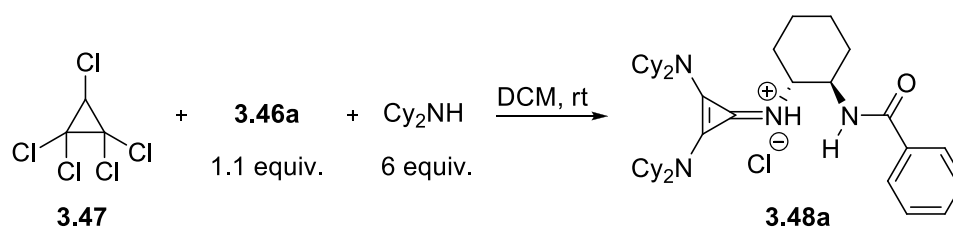
Characterization:

R_f: 0.13 in 10% MeOH/DCM. $[\alpha]_{\text{D}}^{26} = -48.0^{\circ}$ (*c* 0.1, CH₂Cl₂), mp 158–160 °C. ¹H NMR (400 MHz, CDCl₃) δ 8.26 (s, 2H), 8.00 (s, 1H), 6.59 (d, *J* = 6.5 Hz, 1H), 3.76 – 3.68 (m, 1H), 2.63 (ddd, *J* = 10.2 Hz, 10.2 Hz, 4.0 Hz, 1H), 2.26 – 2.20 (m, 1H), 2.05 – 2.00 (m, 1H), 1.81 – 1.78 (m, 2H), 1.46 – 1.23 (m, 4H); ¹³C NMR {¹H} (100 MHz CDCl₃) δ 165.0, 137.0, 132.2 (q, *J* = 33.9 Hz), 127.5, 125.0 (sep, *J* = 3.7 Hz), 123.1 (q, *J* = 272.9 Hz), 57.2, 55.4, 36.6, 32.5, 25.2, 25.0; ν_{max} (liquid film) 3285, 2934, 2861, 1640, 1541, 1276, 1168, 1119, 1108, 905, 697, 680 cm⁻¹; HRMS (ESI-TOF) *m/z*: [M + H]⁺ Calcd. for C₁₅H₁₇F₆N₂O 355.1240; Found 355.1246.

3.5.3.2 *Sample procedure for the catalyst synthesis*

(1R,2R)-N-(2,3-bis(dicyclohexylamino)cycloallyl)-2-benzamidocyclohexanaminiumchloride

(3.48a)



A 50 mL two neck flask was charged with pentachlorocyclopropane **3.47** (285 μL, 2.00 mmol, 90% pure-technical grade from Sigma Aldrich, 1.0 equiv.) and 20 mL of CH₂Cl₂ under argon atmosphere. Dicyclohexylamine (2.39 mL, 12.00 mmol, 6 equiv.) was added drop wise to this flask at room temperature. A white precipitate formed and the reaction mixture was stirred for a further 48 h at room temperature. Following this, aminocyclohexyl

benzamide **3.46a** (480 mg, 2.20 mmol, 1.1 equiv.) was added in one portion and stirred for an additional 12 h. The crude reaction mixture was filtered through a celite plug, washed with 1.0 M HCl (3 x 20 mL), dried over Na₂SO₄, and concentrated to yield crude cyclopropenimine hydrochloride salt.

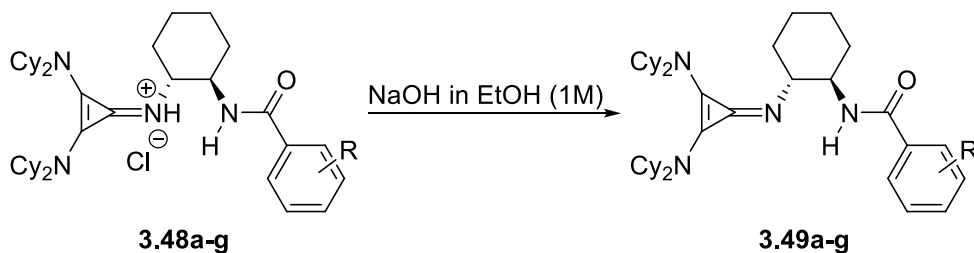
Purification of catalyst:

The material obtained after workup was triturated with *n*-pentane. The obtained solid was dissolved in ~ 20 mL of toluene under refluxing conditions and cooled to rt slowly. After storing overnight, the product precipitated from solution. The mixture was filtered and 717 mg of product **3.48a** (yield: 55%) was obtained.

Characterization:

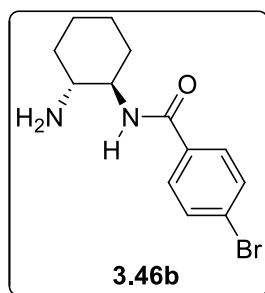
R_f: 0.5 in 10% MeOH/DCM. [α]_D²⁶ = +19° (c 0.1, CH₂Cl₂), mp 248–250 °C. ¹H NMR (400 MHz, CDCl₃) δ 9.89 (d, *J* = 7.9 Hz, 1H), 8.29 – 8.27 (m, 2H), 7.42 – 7.40 (m, 3H), 6.91 (d, *J* = 5.7 Hz, 1H), 4.21 – 4.01 (m, 2H), 3.35 (brs, 4H), 2.60 – 2.50 (m, 1H), 2.03 – 1.73 (m, 24H), 1.58 – 1.35 (m, 23H); ¹³C NMR {¹H} (100 MHz CDCl₃) δ 169.3, 133.4, 131.3, 128.4, 128.2, 115.0, 113.8, 61.9, 59.4, 53.3, 35.3, 32.7, 32.2, 30.7, 25.8, 25.7, 25.2, 24.7, 24.4; ν_{max} (liquid film) 3291, 2923, 2853, 1632, 1531, 1329, 958, 694 cm⁻¹; HRMS (ESI-TOF) m/z: [M-Cl]⁺ Calcd. for C₄₀H₆₁N₄O 613.4840; Found 613.4856.

3.5.3.3 Preparation of Free Base



Pure cyclopropenimine hydrochloride salt was taken in a 10 mL single neck flask (0.10 mmol) and dissolved in 0.5 mL of EtOH. To this flask, 1 M NaOH in ethanol (1.5 mL, 1.50 mmol) was added. A fine precipitate was seen immediately after addition of base. The reaction was stirred for 15 to 20 min. It was then partitioned between diethyl ether and DI water. The layers were separated and the aqueous layer was extracted with 4 x 20 mL of diethyl ether. The organic layers were combined and washed thoroughly with 4 x 15 mL DI water. The ether layer was dried over Na₂SO₄ and concentrated.

N-((1R,2R)-2-aminocyclohexyl)-4-bromobenzamide (3.46b)



The sample procedure A was employed with the following quantities: 4-Br benzoyl imidazole **3.44b** (1255 mg, 5.00 mmol), and cyclohexyldiamine dihydrochloride salt **3.45** (1207 mg, 6.50 mmol).

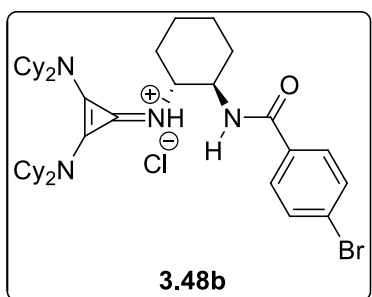
Column Chromatography:

Approximately 25 mL of silica was packed into a column using 3.3% MeOH in CHCl₃ as the solvent. The material obtained from work-up was loaded on the column after dissolution in a minimum amount of CHCl₃. Approximately 300 mL of 3.3% MeOH in CHCl₃ was eluted followed by elution with 200 mL of 6.6% MeOH in CHCl₃ and finally with 300 mL of 8% MeOH in CHCl₃. The eluted solvent was collected in 25 mL fractions. Fractions 9 – 28 contained product. These fractions were concentrated and dried under high vacuum to give 340 mg of product **3.46b** (yield: 23%).

Characterization:

R_f: 0.30 in 20% MeOH/CHCl₃. [α]_D²⁷ = -108.4° (c 0.1, CH₂Cl₂), mp 169–171 °C. ¹H NMR (400 MHz, CDCl₃) δ 7.66 (ddd, *J* = 8.8 Hz, 2.2 Hz, 2.2 Hz, 1H), 7.57 (ddd, *J* = 8.9 Hz, 2.1 Hz, 2.1 Hz, 1H), 6.16 (d, *J* = 7.0 Hz, 1H), 3.73 – 3.64 (m, 1H), 2.51 (ddd, *J* = 10.4 Hz, 10.4 Hz, 4.0 Hz, 1H), 2.20 – 2.13 (m, 1H), 2.04 – 1.98 (m, 1H), 1.80 – 1.74 (m, 2H), 1.46 – 1.18 (m, 4H); ¹³C NMR {¹H} (100 MHz CDCl₃) δ 167.0, 133.8, 131.9, 128.7, 126.2, 56.9, 55.8, 36.2, 32.7, 25.3, 25.2; ν_{max} (liquid film) 3296, 2923, 1631, 1539, 1483, 1330, 1071, 1012, 841, 661 cm⁻¹; HRMS (ESI-TOF) *m/z*: [M + H]⁺ Calcd. for C₁₃H₁₈⁷⁹BrN₂O 297.0597; Found 297.0605, for the other isotope C₁₃H₁₈⁸¹BrN₂O Calcd. 299.0578; Found 299.0589.

(1*R*,2*R*)-*N*-(2,3-bis(dicyclohexylamino)cycloallyl)-2-(4-bromobenzamido)
cyclohexanaminium chloride (**3.48b**)



The sample procedure was employed with the following quantities: pentachlorocyclopropane **3.47** (135 μL, 0.95 mmol, 90% pure), aminocyclohexyl 4-Br benzamide **3.46b** (309 mg, 1.04 mmol), and dicyclohexylamine (1.13 mL, 5.67 mmol).

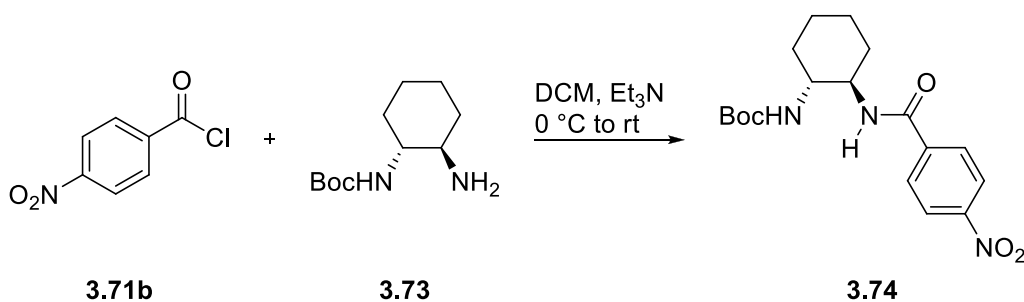
Column Chromatography:

Approximately 50 mL of silica was packed into a column using 2% MeOH in DCM as the solvent. The material obtained from work-up was loaded on the column after dissolution in a minimum amount of DCM. Approximately 300 mL of 2% MeOH in DCM was eluted followed by elution with 1 L of 3% MeOH in DCM. The eluted solvent was collected in 25 mL fractions. Fractions 15 – 52 contained product. These fractions were concentrated and dried under high vacuum to give 191 mg of product **3.48b** (yield: 29%).

Characterization:

R_f: 0.67 in 20% MeOH/CHCl₃. [α]_D²⁷ = -102.6° (c 0.1, CH₂Cl₂), mp 263–265 °C. ¹H NMR (400 MHz, CDCl₃) δ 10.11 (d, *J* = 8.1 Hz, 1H), 8.21 (ddd, *J* = 9.3 Hz, 2.5 Hz, 2.5 Hz, 2H), 7.54 (ddd, *J* = 9.2 Hz, 2.3 Hz, 2.3 Hz, 2H), 6.71 (d, *J* = 5.7 Hz, 1H), 4.18 – 3.99 (m, 2H), 3.36 (brs, 4H), 2.56 – 2.45 (m, 1H), 2.01 – 1.74 (m, 26H), 1.53 – 1.35 (m, 21H); ¹³C NMR {¹H} (100 MHz CDCl₃) δ 168.4, 132.4, 131.5, 126.2, 130.3, 115.0, 113.8, 61.9, 59.4, 53.3, 35.4, 32.7, 32.3, 30.7, 25.9, 25.8, 25.2, 24.7, 24.4; ν_{max} (liquid film) 2930, 2856, 1631, 1500, 1448, 1371, 1179, 1010, 894, 728, 485 cm⁻¹; HRMS (ESI-TOF) *m/z*: [M + H]⁺ Calcd. for C₄₀H₆₀⁷⁹BrN₄O 691.3945; Found 691.3947, for the other isotope C₄₀H₆₀⁸¹BrN₄O Calcd. 693.3933; Found 693.3936.

N-((1R,2R)-2-aminocyclohexyl)-4-Nitrobenzamide (3.46c)



A 25 mL two neck flask was charged with *N*-Boc-1,2-diaminocyclohexane **3.73** (300 mg, 1.40 mmol). To this 10 mL of DCM was added followed by triethylamine (390 μL, 2.80 mmol) under argon atmosphere. The flask was cooled to 0 °C using ice bath under argon atmosphere. In a separate flask, 4-nitro benzoyl chloride **3.71b** (260 mg, 1.40 mmol) was taken, followed by 5 mL of DCM under argon atmosphere at rt. The acid chloride solution was added drop-wise (for 10 min) to the flask containing *N*-Boc-1,2-cyclohexanediamine at 0 °C. After the completion of addition the reaction was slowly warmed to room temperature and stirred for 1 h.

Workup procedure :

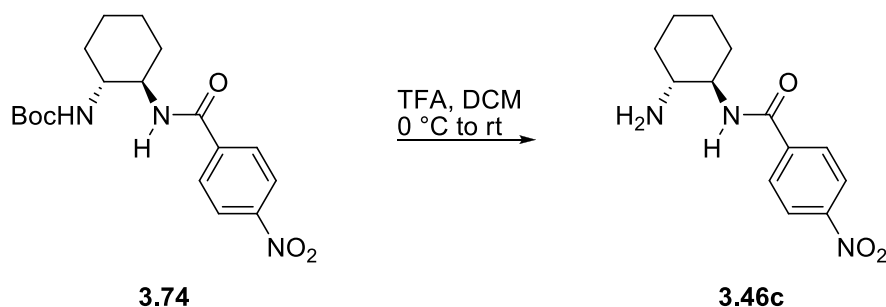
The reaction mixture was diluted with DCM (25 mL), organic layer was washed successively with DI water, 5% NaOH, 1 M HCl, saturated NaHCO₃, and brine (20 mL each). The organic layer was dried over Na₂SO₄, and concentrated.

Column Chromatography:

Approximately 50 mL of silica was packed into a column using 17% EtOAc in hexanes as the solvent. The material obtained from work-up was loaded on the column after dissolution in a minimum amount of DCM. Approximately 700 mL of 17% EtOAc in hexanes was eluted followed by elution with 300 mL of 20% EtOAc in hexanes and 500 mL of 50% EtOAc in hexanes. The eluted solvent was collected in 25 mL fractions. Fractions 16 – 45 contained product. These fractions were concentrated and dried under high vacuum to give 456 mg of product **3.74** (yield: 90%).

Characterization:

R_f: 0.33 in 30% EtOAc/Hexanes. $[\alpha]_D^{24} = -46.8^\circ$ (*c* 0.1, CH₂Cl₂), mp 225–227 °C (dec.). ¹H NMR (400 MHz, CDCl₃) δ 8.25 (d, *J* = 8.8 Hz, 2H), 8.02 (d, *J* = 8.8 Hz, 2H), 7.55 (d, *J* = 6.6 Hz, 1H), 4.68 (d, *J* = 8.2 Hz, 1H), 3.72 (dddd, *J* = 17.8 Hz, 10.9 Hz, 6.9 Hz, 4.0 Hz, 1H), 3.59 – 3.50 (m, 1H), 2.35 – 2.31 (m, 1H), 1.85 – 1.76 (m, 2H), 1.43 – 1.18 (m, 13H); ¹³C NMR {¹H} (100 MHz CDCl₃) δ 165.0, 157.7, 149.7, 140.0, 128.5, 123.7, 80.4, 57.7, 53.3, 32.4, 32.3, 28.4, 25.3, 24.4; ν_{max} (liquid film) 3342, 2935, 2858, 1682, 1520, 1347, 1293, 1161, 836, 622 cm⁻¹;

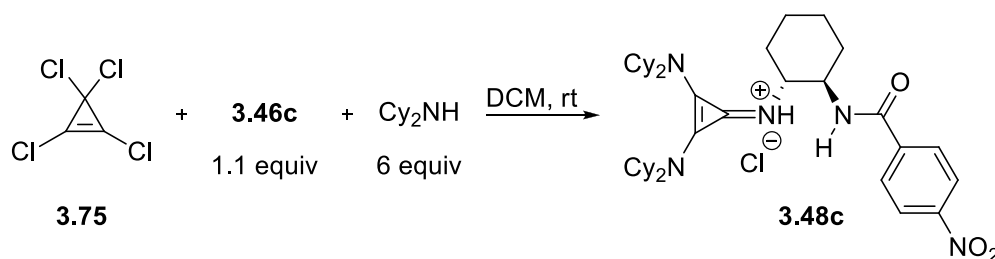


A 25 mL single neck flask was charged with **3.74** (365 mg, 1.00 mmol). To this 2 mL of DCM was added followed by trifluoroacetic acid (1 mL) at 0 °C. After the completion of addition the reaction was slowly warmed to room temperature and stirred for 1 h. After that DCM and trifluoroacetic acid were removed by distillation. The residue left in the flask was diluted with DCM (20 mL) and washed with saturated NaHCO₃ (4 X 25 mL). Organic layer was dried over Na₂SO₄, and concentrated to yield 172 mg of pure product **3.46c** (yield: 65%).

Characterization:

R_f: 0.1 in 10% MeOH/DCM. $[\alpha]_{\text{D}}^{24} = -29.0^{\circ}$ (*c* 0.1, CH₂Cl₂), mp 183–185 °C. ¹H NMR (400 MHz, CDCl₃) δ 8.28 (d, *J* = 8.8 Hz, 2H), 7.96 (d, *J* = 8.8 Hz, 2H), 6.36 (d, *J* = 6.2 Hz, 1H), 3.68 (dddd, *J* = 18.5 Hz, 11.4 Hz, 7.7 Hz, 4.1 Hz, 1H), 2.55 (ddd, *J* = 14.2 Hz, 10.4 Hz, 4.0 Hz, 1H), 2.26 – 2.22 (m, 1H), 2.03 – 2.00 (m, 1H), 1.79 – 1.76 (m, 2H), 1.44 – 1.20 (m, 4H); ¹³C NMR {¹H} (100 MHz CDCl₃) δ 165.9, 149.7, 140.6, 128.3, 123.9, 57.1, 55.5, 36.5, 32.5, 25.2, 25.0; ν_{max} (liquid film) 3296, 2921, 1634, 1538, 1520, 1318, 1332, 845, 827, 706, 690 cm⁻¹; HRMS (ESI-TOF) *m/z*: [M + H]⁺ Calcd. for C₁₃H₁₈N₃O₃ 264.1343; Found 264.1336.

(1R,2R)-N-(2,3-bis(dicyclohexylamino)cycloallyl)-2-(4-nitrobenzamido)cyclohexanaminium chloride (3.48c)



A 25 mL two neck flask was charged with tetrachlorocyclopropane **3.75** (55 μL , 0.45 mmol, 1.0 equiv.) and 5 mL of CH_2Cl_2 under argon atmosphere. Dicyclohexylamine (535 μL , 2.69 mmol, 6 equiv.) was added drop wise to this flask at room temperature. A white precipitate formed and the reaction mixture was stirred for a further 4 h at room temperature. Following this, aminocyclohexyl benzamide **3.46c** (130 mg, 0.49 mmol, 1.1 equiv.) was added in one portion and stirred for an additional 12 h. The crude reaction mixture was filtered through a celite plug, washed with 1.0 M HCl (3 x 20 mL), dried over Na_2SO_4 , and concentrated to yield crude cyclopropenimine hydrochloride salt.

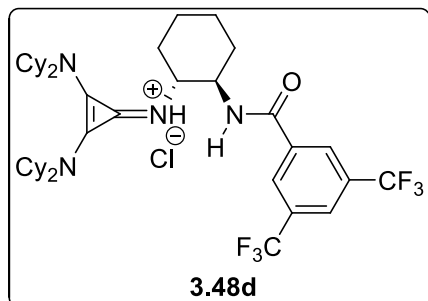
Column Chromatography:

Approximately 30 mL of silica was packed into a column using 1.5% MeOH in DCM as the solvent. The material obtained from work-up was loaded on the column after dissolution in a minimum amount of DCM. Approximately 300 mL of 1.5% MeOH in DCM was eluted followed by elution with 100 mL of 2.5% MeOH in DCM and 150 mL of 10 % MeOH in DCM. The eluted solvent was collected in 25 mL fractions. Fractions 15 – 20 contained product. These fractions were concentrated and dried under high vacuum to give 294 mg of product **3.48c** (yield: 95%). NOTE: The material obtained after column purification was triturated with methyl tert-butyl ether to obtain off white powder.

Characterization:

R_f: 0.4 in 10% MeOH/DCM. $[\alpha]_D^{24} = +43.2^\circ$ (*c* 0.1, CH₂Cl₂), mp 267–269 °C. ¹H NMR (400 MHz, CDCl₃) δ 10.49 (d, *J* = 7.9 Hz, 1H), 8.53 (d, *J* = 8.8 Hz, 2H), 8.23 (d, *J* = 8.8 Hz, 2H), 6.49 (d, *J* = 5.9 Hz, 1H), 4.19 – 4.10 (m, 1H), 4.05 – 3.99 (m, 1H), 3.34 (brm, 4H), 2.54 – 2.43 (m, 1H), 2.03 – 1.73 (m, 23H), 1.53 – 1.32 (m, 24H); ¹³C NMR {¹H} (100 MHz CDCl₃) δ 167.2, 149.6, 139.1, 129.9, 123.5, 114.8, 114.0, 61.8, 59.4, 53.6, 35.5, 32.7, 32.3, 30.7, 25.9, 25.8, 25.1, 24.7, 24.4; ν_{max} (liquid film) 2929, 2854, 1650, 1519, 1496, 1344, 833, 720 cm⁻¹; HRMS (ESI-TOF) *m/z*: [M-Cl]⁺ Calcd. for C₄₀H₆₀N₅O₃ 658.4691; Found 658.4680.

(1R,2R)-N-(2,3-bis(dicyclohexylamino)cycloallyl)-2-(3,5-bis(trifluoromethyl)benzamido)cyclohexanaminium chloride (3.48d)



The sample procedure was employed with the following quantities: pentachlorocyclopropane **3.47** (49 μL, 0.38 mmol, 90% pure), aminocyclohexyl 3,5 bis CF₃ benzamide **3.46d** (133 mg, 0.38 mmol), and dicyclohexylamine (407 μL, 2.05 mmol).

Column Chromatography:

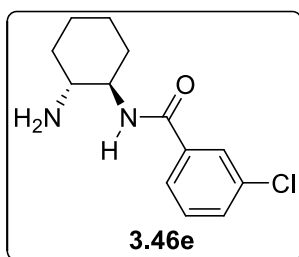
Approximately 40 mL of silica was packed into a column using 2% MeOH in DCM as the solvent. The material obtained from work-up was loaded on the column after dissolution in a minimum amount of DCM. Approximately 200 mL of 2% MeOH in DCM was eluted followed by elution with 200 mL of 2.5% MeOH in DCM, 600 mL of 3% MeOH in DCM and finally with 100 mL of 5% MeOH in DCM. The eluted solvent was collected in

25 mL fractions. Fractions 13 – 37 contained product. These fractions were concentrated and dried under high vacuum to give 221 mg of product **3.48d** (yield: 82%).

Characterization:

R_f: 0.50 in 10% MeOH/DCM. $[\alpha]_D^{26} = -65.2^\circ$ (*c* 0.1, CH₂Cl₂), mp 163–165 °C. ¹H NMR (400 MHz, CDCl₃) δ 10.72 (brs, 1H), 8.81 (s, 2H), 7.91 (s, 1H), 6.69 (s, 1H), 4.15 – 4.13 (brs, 2H), 3.36 (brs, 4H), 2.50 – 2.48 (m, 1H), 2.05 – 1.75 (m, 22H), 1.51 – 1.36 (m, 25H); ¹³C NMR {¹H} (100 MHz CDCl₃) δ 166.5, 135.9, 131.5 (q, *J* = 33.7 Hz), 129.2 (m), 124.7, 123.3 (q, *J* = 272.8 Hz), 114.8, 114.1, 61.7, 59.5, 53.7, 35.5, 32.7, 32.3, 30.6, 25.8, 25.7, 25.1, 24.7, 24.3; ν_{max} (liquid film) 2932, 2859, 1648, 1505, 1278, 1180, 1134, 681 cm⁻¹; HRMS (ESI-TOF) *m/z*: [M + H]⁺ Calcd. for C₄₂H₅₉F₆N₄O 749.4588; Found 749.4598.

N-((1R,2R)-2-aminocyclohexyl)-3-chlorobenzamide (3.46e)



The sample procedure B was employed with the following quantities: 3-Cl benzoyl chloride **3.71c** (250 μL, 1.95 mmol), and diaminocyclohexane **3.72** (669 mg, 5.86 mmol).

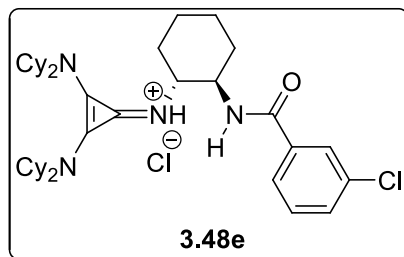
Column Chromatography:

Approximately 20 mL of silica was packed into a column using 4% MeOH in DCM as the solvent. The material obtained from work-up was loaded on the column after dissolution in a minimum amount of DCM. Approximately 1300 mL of 4% MeOH in DCM was eluted. The eluted solvent was collected in 25 mL fractions. Fractions 18 – 50 contained product. These fractions were concentrated and dried under high vacuum to give 72 mg of product **3.46e** (yield: 15%).

Characterization:

R_f: 0.17 in 10% MeOH/CH₂Cl₂. [α]_D²⁶ = -65.2° (*c* 0.1, CH₂Cl₂), mp 150–152 °C. ¹H NMR (400 MHz, CDCl₃) δ 7.77 (dd, *J* = 1.8 Hz, 1.8 Hz, 1H), 7.66 (ddd, *J* = 7.7 Hz, 1.3 Hz, 1.3 Hz, 1H), 7.47 (ddd, *J* = 8.0 Hz, 2.0 Hz, 1.0 Hz, 1H), 7.37 (dd, *J* = 7.8 Hz, 7.8 Hz, 1H), 6.22 (d, *J* = 7.0 Hz, 1H), 3.68 (dddd, *J* = 18.3 Hz, 11.7 Hz, 8.2 Hz, 4.0 Hz, 1H), 2.51 (ddd, *J* = 10.5 Hz, 10.5 Hz, 4.0 Hz, 1H), 2.18 – 2.12 (m, 1H), 2.02 – 1.98 (m, 1H), 1.78 – 1.74 (m, 2H), 1.44 – 1.18 (m, 4H); ¹³C NMR {¹H} (100 MHz CDCl₃) δ 166.6, 136.7, 134.8, 131.5, 129.9, 127.4, 125.2, 56.9, 55.5, 36.0, 32.5, 25.2, 25.1; ν_{\max} (liquid film) 3278, 2937, 2852, 1634, 1535, 1329, 1265, 851, 728, 703 cm⁻¹; HRMS (ESI-TOF) *m/z*: [M + H]⁺ Calcd. for C₁₃H₁₈³⁵ClN₂O 253.1102; Found 253.1104, for the other isotope C₁₃H₁₈³⁷ClN₂O Calcd. 255.1078; Found 255.1077.

(1*R*,2*R*)-*N*-(2,3-bis(dicyclohexylamino)cycloallyl)-2-(3-chlorobenzamido)cyclohexanaminium chloride (**3.48e**)



The sample procedure was employed with the following quantities: pentachlorocyclopropane **3.47** (38 μ L, 0.27 mmol, 90% pure), aminocyclohexyl 3-Cl benzamide **3.46e** (67 mg, 0.27 mmol), and dicyclohexylamine (350 μ L, 1.77

mmol).

Column Chromatography:

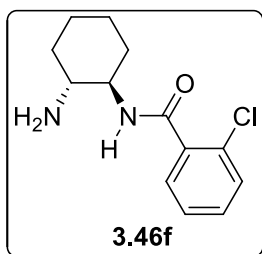
Approximately 40 mL of silica was packed into a column using 2% MeOH in DCM as the solvent. The material obtained from work-up was loaded on the column after dissolution in a minimum amount of DCM. Approximately 250 mL of 2% MeOH in DCM was eluted followed by elution with 300 mL of 3.3% MeOH in DCM and finally with 500

mL of 4% MeOH in DCM. The eluted solvent was collected in 25 mL fractions. Fractions 18 – 37 contained product. These fractions were concentrated and dried under high vacuum to give 84 mg of product **3.48e** (yield: 46%).

Characterization:

R_f: 0.27 in 10% MeOH/CH₂Cl₂. [α]_D²⁶ = +42.2° (*c* 0.1, CH₂Cl₂), mp 229–231 °C. ¹H NMR (400 MHz, CDCl₃) δ 10.05 (d, *J* = 8.0 Hz, 1H), 8.39 – 8.38 (m, 1H), 8.06 (s, 1H), 7.35 – 7.32 (m, 2H), 6.73 (d, *J* = 5.9 Hz, 1H), 4.15 – 4.07 (m, 1H), 3.98 – 3.90 (m, 1H), 3.32 (brs, 4H), 2.53 – 2.43 (m, 1H), 2.27 – 1.71 (m, 26H), 1.54 – 1.32 (m, 21H); ¹³C NMR {¹H} (100 MHz CDCl₃) δ 167.9, 135.2, 134.0, 131.2, 129.9, 128.6, 126.8, 114.9, 113.8, 61.9, 59.4, 53.4, 35.3, 32.7, 32.3, 30.6, 25.8, 25.7, 25.1, 24.6, 24.3; ν_{\max} (liquid film) 2931, 2857, 1630, 1501, 1448, 1328, 1265, 1179, 1078, 894, 728, 697 cm⁻¹; HRMS (ESI-TOF) *m/z*: [M + H]⁺ Calcd. for C₄₀H₆₀³⁵ClN₄O 647.4450; Found 647.4456, for the other isotope C₄₀H₆₀³⁷ClN₄O Calcd. 649.4443; Found 649.4448.

N-((1R,2R)-2-aminocyclohexyl)-2-chlorobenzamide (3.46f)



The sample procedure A was employed with the following quantities: 2-Cl benzoyl imidazole **3.44c** (310 mg, 1.50 mmol), and diaminocyclohexyl dihydrochloride salt **3.45** (365 mg, 1.95 mmol).

Column Chromatography:

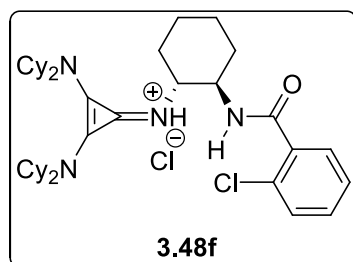
Approximately 25 mL of silica was packed into a column using 1% MeOH in DCM as the solvent. The material obtained from work-up was loaded on the column after dissolution in a minimum amount of DCM. Approximately 200 mL of 1% MeOH in DCM was eluted followed by elution with 200 mL of 2% MeOH in DCM, 200 mL of 3% MeOH in

DCM and finally with 800 mL of 4% MeOH in DCM. The eluted solvent was collected in 25 mL fractions. Fractions 31 – 56 contained product. These fractions were concentrated and dried under high vacuum to give 49 mg of product **3.46f** (yield: 13%).

Characterization:

R_f: 0.17 in 10% MeOH/CH₂Cl₂. [α]_D²⁶ = -51.4° (c 0.1, CH₂Cl₂), mp 144–146 °C. ¹H NMR (400 MHz, CDCl₃) δ 7.62 (dd, *J* = 7.2 Hz, 2.0 Hz, 1H), 7.39 (ddd, *J* = 7.5 Hz, 7.5 Hz, 1.8 Hz, 1H), 7.36 – 7.30 (m, 2H), 6.11 (brs, 1H), 3.79 – 3.71 (m, 1H), 2.47 (ddd, *J* = 10.3 Hz, 10.3 Hz, 3.8 Hz, 1H), 2.16 – 2.10 (m, 1H), 2.03 – 1.98 (m, 1H), 1.78 – 1.75 (m, 2H), 1.44 – 1.18 (m, 4H); ¹³C NMR {¹H} (100 MHz CDCl₃) δ 167.0, 135.8, 131.3, 130.5, 130.2, 130.1, 127.2, 57.2, 55.7, 35.3, 32.4, 25.19, 25.17; ν_{\max} (liquid film) 3254, 2939, 2853, 1635, 1539, 1331, 1039, 735, 700 cm⁻¹; HRMS (ESI-TOF) *m/z*: [M + H]⁺ Calcd. for C₁₃H₁₈³⁵ClN₂O 253.1102; Found 253.1100, for the other isotope C₁₃H₁₈³⁷ClN₂O Calcd. 255.1078; Found 255.1074.

(1*R*,2*R*)-*N*-(2,3-bis(dicyclohexylamino)cycloallyl)-2-(2-chlorobenzamido)cyclohexanaminium chloride (**3.48f**)



The sample procedure was employed with the following quantities: pentachlorocyclopropane **3.47** (26 μ L, 0.19 mmol, 90% pure), aminocyclohexyl 2-Cl benzamide **3.46f** (47 mg, 0.19 mmol), and dicyclohexylamine (250 μ L, 1.12 mmol).

Column Chromatography:

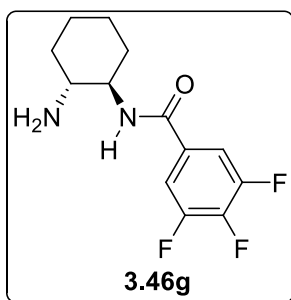
Approximately 30 mL of silica was packed into a column using 1.5% MeOH in DCM as the solvent. The material obtained from work-up was loaded on the column after dissolution in a minimum amount of DCM. Approximately 200 mL of 1.5% MeOH in DCM

was eluted followed by elution with 400 mL of 2% MeOH in DCM and finally with 600 mL of 4% MeOH in DCM. The eluted solvent was collected in 25 mL fractions. Fractions 21 – 44 contained product. These fractions were concentrated and dried under high vacuum to give 59 mg of product **3.48f** (yield: 46%).

Characterization:

R_f: 0.27 in 10% MeOH/CH₂Cl₂. [α]_D²⁶ = -24.8° (c 0.1, CH₂Cl₂), mp 173–175 °C. ¹H NMR (400 MHz, CDCl₃) δ 8.74 (d, *J* = 5.7 Hz, 1H), 7.64 – 7.62 (m, 1H), 7.35 – 7.25 (m, 4H), 4.18 – 4.10 (m, 2H), 3.40 – 3.35 (m, 4H), 2.42 – 2.34 (m, 1H), 2.13 – 1.36 (m, 47H); ¹³C NMR {¹H} (100 MHz CDCl₃) δ 168.8, 135.7, 131.3, 130.7, 130.1, 129.7, 127.0, 116.0, 114.4, 60.3, 59.6, 54.2, 35.2, 32.7, 32.4, 30.4, 27.1, 25.8, 25.1, 24.7, 24.6; ν_{max} (liquid film) 2930, 2857, 1654, 1500, 1448, 1371, 1324, 1265, 894, 729, 697 cm⁻¹; HRMS (ESI-TOF) *m/z*: [M + H]⁺ Calcd. for C₄₀H₆₀³⁵ClN₄O 647.4450; Found 647.4456, for the other isotope C₄₀H₆₀³⁷ClN₄O Calcd. 649.4443; Found 649.4452.

N-((1R,2R)-2-aminocyclohexyl)-3,4,5-trifluorobenzamide (3.46g)



The sample procedure B was employed with the following quantities: 3,4,5 tri fluoro benzoyl chloride **3.71d** (400 μL, 3.05 mmol), and diaminocyclohexane **3.72** (870 mg, 7.63 mmol).

Column Chromatography:

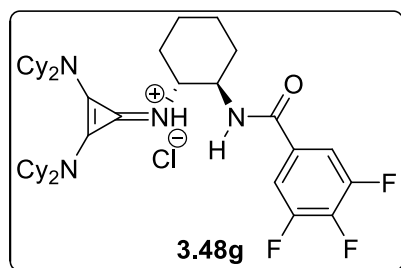
Approximately 40 mL of silica was packed into a column using 2% MeOH in DCM as the solvent. The material obtained from work-up was loaded on the column after dissolution in a minimum amount of DCM. Approximately 600 mL of 2% MeOH in DCM

was eluted followed by elution with 400 mL of 4% MeOH in CHCl₃ and finally with 300 mL of 5% MeOH in CHCl₃. The eluted solvent was collected in 25 mL fractions. Fractions 23 – 47 contained product. These fractions were concentrated and dried under high vacuum to give 105 mg of product **3.46g** (yield: 13%).

Characterization:

R_f: 0.10 in 10% MeOH/DCM. [α]_D²⁶ = -25.8° (c 0.1, CH₂Cl₂), mp 161–163 °C. ¹H NMR (400 MHz, CDCl₃) δ 7.49 – 7.42 (m, 2H), 6.17 (d, *J* = 5.6 Hz, 1H), 3.62 (dddd, *J* = 17.9 Hz, 14.3 Hz, 7.6 Hz, 4.0 Hz, 1H), 2.52 (ddd, *J* = 10.4 Hz, 10.4 Hz, 4.0 Hz, 1H), 2.24 – 2.18 (m, 1H), 2.02 – 1.98 (m, 1H), 1.79 – 1.76 (m, 2H), 1.45 – 1.17 (m, 4H); ¹³C NMR {¹H} (100 MHz CDCl₃) δ 164.8, 152.4 (dd, *J* = 10.3 Hz, 3.5 Hz), 149.9 (dd, *J* = 10.2 Hz, 3.6 Hz), 143.2 (dd, *J* = 15.0, 15.0 Hz), 140.7 (dd, *J* = 15.3, 15.3 Hz), 131.0 – 130.8 (m), 112.0 – 111.7 (m), 57.1, 55.4, 36.4, 32.5, 25.2, 25.0; ν_{max} (liquid film) 3286, 2936, 2860, 1641, 1618, 1519, 1369, 1232, 1043, 732 cm⁻¹; HRMS (ESI-TOF) *m/z*: [M + H]⁺ Calcd. for C₁₃H₁₆F₃N₂O 273.1209; Found 273.1215.

(1R,2R)-N-(2,3-bis(dicyclohexylamino)cycloallyl)-2-(3,4,5-trifluorobenzamido) cyclohexanaminium chloride (3.48g)



The sample procedure was employed with the following quantities: pentachlorocyclopropane **3.47** (48 μL, 0.37 mmol, 90% pure), aminocyclohexyl 3,4,5 trifluoro benzamide **3.46g** (100 mg, 0.37 mmol), and

dicyclohexylamine (400 μL, 2.01 mmol).

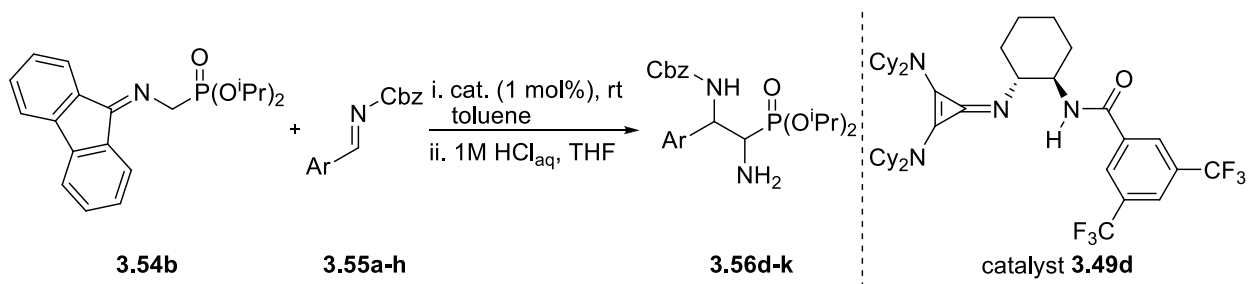
Column Chromatography:

Approximately 60 mL of silica was packed into a column using 3 % MeOH in CHCl₃ as the solvent. The material obtained from work-up was loaded on the column after dissolution in a minimum amount of CHCl₃. Approximately 300 mL of 3% MeOH in CHCl₃ was eluted followed by elution with 300 mL of 4% MeOH in CHCl₃ and finally with 200 mL of 10% MeOH in DCM. The eluted solvent was collected in 25 mL fractions. Fractions 10 – 14 contained product. These fractions were concentrated and dried under high vacuum to give 159 mg of product **3.48g** (yield: 69%).

Characterization:

R_f: 0.30 in 10% MeOH/DCM. [α]_D²⁷ = -61.8° (*c* 0.1, CH₂Cl₂), mp 230–232 °C. ¹H NMR (400 MHz, CDCl₃) δ 10.40 (brs, 1H), 8.13 (brs, 2H), 6.55 (brs, 1H), 4.09 – 4.02 (m, 2H), 3.36 (brs, 4H), 2.54 – 2.45 (m, 1H), 2.01 – 1.75 (m, 24H), 1.49 – 1.36 (m, 23H); ¹³C NMR {¹H} (150 MHz CDCl₃) δ 166.0, 150.7 (dd, *J* = 250.5 Hz, 9.7 Hz), 141.8 (dt, *J* = 255.5 Hz, 15.4 Hz), 129.6, 114.6, 113.9, 113.3 (d, *J* = 3.2 Hz), 113.1, 62.0, 59.4, 53.4, 35.4, 32.6, 32.2, 30.5, 25.8, 25.6, 25.0, 24.6, 24.2; ν_{\max} (liquid film) 2930, 2858, 1647, 1616, 1503, 1448, 1351, 1042, 731 cm⁻¹; HRMS (ESI-TOF) *m/z*: [M + H]⁺ Calcd. for C₄₀H₅₈F₃N₄O 667.4557; Found 667.4572.

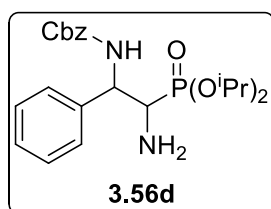
3.5.4 General procedure for the catalytic enantioselective Mannich reaction



Part 1: A dried Schlenk tube was charged with 300 mg of 3 Å molecular sieves. The sieves were activated under high vacuum using a hot-air gun. After activation, the sieves were cooled to room temperature under argon atmosphere. The tube was then charged with 100 mg of diisopropyl phosphonate **3.54b** (0.28 mmol) and *N*-Cbz imine **3.55** (0.56 mmol). The reactants were dissolved in 850 µL of toluene at rt to obtain a clear solution. In a separate flask, 2.1 mg of catalyst **3.49d** was weighed and dissolved in 650 µL of toluene at rt. It was then transferred to the tube containing the starting materials using a syringe. After completion of reaction (by TLC), the reaction was quenched with 1 mL of 1 M acetic acid in DCM and reaction mixture was filtered through cotton plug. The filtrate was concentrated at room temperature to obtain an oily liquid.

Part 2: Hydrolysis of the product was carried out by dissolving the residue from the previous step (part 1) in 8 mL of THF followed by addition of 0.4 mL of 1 M HCl at room temperature. The imine was hydrolyzed in 1 to 2 h. After completion, THF was removed under reduced pressure at rt. The residue was partitioned between diethyl ether (20 mL) and 0.25 M HCl (20 mL) in a separatory funnel. After separation of layers, the aqueous layer was washed with diethyl ether (3 X 20 mL). The organic layers were combined and back extracted with 20 mL of DI water. The aqueous layers were combined and basified with saturated NaHCO₃ solution. It was then extracted with DCM (4 X 20 mL). The DCM layers were combined, dried over Na₂SO₄, and concentrated. The crude mixture was purified by column chromatography on silica gel to yield product **3.56**.

Benzyl 2-amino-2-(diisopropoxyphosphoryl)-1-phenylethylcarbamate (3.56d)



The general procedure was employed with the following quantities: diisopropyl phosphonate **3.54b** (100 mg, 0.28 mmol), phenyl *N*-Cbz

imine **3.55a** (134 mg, 0.56 mmol), catalyst **3.49d** (2.1 mg, 0.0028 mmol – 1 mol %). Reaction was completed in 24 h.

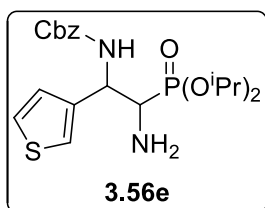
Column Chromatography:

Approximately 40 mL of silica was packed into a column using 50% EtOAc in hexanes as the solvent. The material obtained from work-up was loaded on the column after dissolution in a minimum amount of DCM. Approximately 300 mL of 50% EtOAc in hexanes was eluted followed by elution with 300 mL of 2% MeOH in DCM. The eluted solvent was collected in 15 mL fractions. Fractions 32 – 46 contained product. These fractions were concentrated and dried under high vacuum to give 53 mg of product **3.56d** (yield: 43%).

Characterization:

R_f: 0.17 in 75% EtOAc/hexanes. $[\alpha]_D^{24} = +52.0^\circ$ (*c* 0.1, CH₂Cl₂). ¹H NMR (400 MHz, CDCl₃) δ 7.39 – 7.25 (m, 10H), 6.39 (brs, 1H), 5.14 – 5.02 (m, 3H), 4.79 – 4.54 (m, 2H), 3.34 (dd, *J* = 15.5 Hz, 2.7 Hz, 1H), 1.33 – 1.18 (m, 12H); ¹³C NMR {¹H} (100 MHz CDCl₃) δ 155.8, 136.8, 128.7, 128.5, 128.4, 128.2, 128.1, 127.8, 127.7, 126.7, 71.5 (d, *J* = 7.3 Hz), 71.4 (d, *J* = 8.8 Hz), 66.8, 55.3, 53.9 (d, *J* = 152.6 Hz), 24.24 (d, *J* = 3.6 Hz), 24.17 (d, *J* = 3.6 Hz), 24.1 (d, *J* = 5.5 Hz), 24.0 (d, *J* = 5.7 Hz); ν_{max} (liquid film) 3289, 2978, 1718, 1497, 1223, 982, 698 cm⁻¹; HRMS (ESI-TOF) *m/z*: [M + H]⁺ Calcd. for C₂₂H₃₂N₂O₅P 435.2043; Found 435.2043.

Benzyl 2-amino-2-(diisopropoxyphosphoryl)-1-(thiophen-3-yl)ethylcarbamate (3.56e)



The general procedure was employed with the following quantities: diisopropyl phosphonate **3.54b** (100 mg, 0.28 mmol), 3-thiophenyl N-Cbz imine **3.55b** (137 mg, 0.56 mmol), catalyst **3.49d** (2.1 mg,

0.0028 mmol – 1 mol %). Reaction was completed in 48 h.

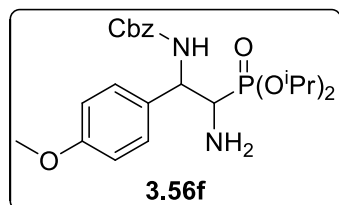
Column Chromatography:

Approximately 30 mL of silica was packed into a column using 50% EtOAc in hexanes as the solvent. The material obtained from work-up was loaded on the column after dissolution in a minimum amount of DCM. Approximately 350 mL of 50% EtOAc in hexanes was eluted followed by elution with 750 mL of 70% EtOAc in hexanes. The eluted solvent was collected in 15 mL fractions. Fractions 24 – 70 contained product. These fractions were concentrated and dried under high vacuum to give 76 mg of product **3.56e** (yield: 61%).

Characterization:

R_f: 0.13 in 75% EtOAc/hexanes. $[\alpha]_D^{24} = -3.2^\circ$ (*c* 0.1, CH₂Cl₂). ¹H NMR (400 MHz, CDCl₃) δ 7.34 – 7.25 (m, 6H), 7.23 – 7.19 (m, 1H), 7.08 – 7.06 (m, 1H), 6.32 (brs, 1H), 5.22 (ddd, *J* = 15.2 Hz, 8.4 Hz, 3.0 Hz, 1H), 5.14 – 5.07 (m, 2H), 4.77 – 4.53 (m, 2H), 3.36 (dd, *J* = 15.3 Hz, 3.0 Hz, 1H), 1.32 – 1.13 (m, 12H); ¹³C NMR {¹H} (100 MHz CDCl₃) δ 155.8, 136.7, 128.6, 128.24, 128.19, 128.1, 126.4, 126.3, 121.8, 71.4 (d, *J* = 7.1 Hz), 71.3 (d, *J* = 7.7 Hz), 66.8, 53.4 (d, *J* = 152 Hz), 52.4, 24.24 (d, *J* = 3.6 Hz), 24.16 (d, *J* = 3.2 Hz), 24.0 (d, *J* = 5.0 Hz), 23.9 (d, *J* = 5.3 Hz); ν_{\max} (liquid film) 3295, 2978, 1720, 1532, 1239, 987, 698 cm⁻¹; HRMS (ESI-TOF) *m/z*: [M + H]⁺ Calcd. for C₂₀H₃₀N₂O₅PS 441.1608; Found 441.1611.

Benzyl 2-amino-2-(diisopropoxyphosphoryl)-1-(4-methoxyphenyl)ethylcarbamate (3.56f)



The general procedure was employed with the following quantities: diisopropyl phosphonate **3.54b** (100 mg, 0.28 mmol), *p*-Meo phenyl N-Cbz imine **3.55c** (151 mg, 0.56 mmol), catalyst

3.49d (2.1 mg, 0.0028 mmol – 1 mol %). Reaction was completed in 48 h.

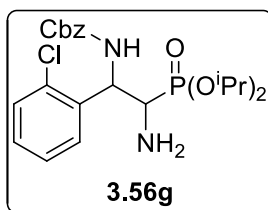
Column Chromatography:

Approximately 30 mL of silica was packed into a column using 50% EtOAc in hexanes as the solvent. The material obtained from work-up was loaded on the column after dissolution in a minimum amount of DCM. Approximately 200 mL of 50% EtOAc in hexanes was eluted followed by elution with 750 mL of 70% EtOAc in hexanes. The eluted solvent was collected in 15 mL fractions. Fractions 15 – 60 contained product. These fractions were concentrated and dried under high vacuum to give 61 mg of product **3.56f** (yield: 47%).

Characterization:

R_f: 0.13 in 75% EtOAc/hexanes. $[\alpha]_D^{23} = -4.6^\circ$ (*c* 0.1, CH₂Cl₂). ¹H NMR (400 MHz, CDCl₃) δ 7.33 – 7.22 (m, 7H), 6.90 – 6.81 (m, 2H), 6.32 (brs, 1H), 5.13 – 4.96 (m, 3H), 4.79 – 4.55 (m, 2H), 3.81 – 3.79 (brs, 3H), 3.30 (dd, *J* = 15.3 Hz, 3.1 Hz, 1H), 1.38 – 1.14 (m, 12H); ¹³C NMR {¹H} (100 MHz CDCl₃) δ 159.2, 159.1, 155.8, 155.7, 136.7, 136.6, 128.7, 128.5, 128.14, 128.06, 127.99, 127.8, 127.7, 127.4, 114.0, 113.9, 113.8, 71.4 (d, *J* = 7.5 Hz), 71.3 (d, *J* = 7.8 Hz), 70.9 (d, *J* = 7.3 Hz), 66.72, 66.67, 55.4, 55.3, 54.8, 53.9 (d, *J* = 152 Hz), 53.8 (d, *J* = 149 Hz), 24.2 (d, *J* = 3.6 Hz), 24.1 (d, *J* = 3.5 Hz), 23.95 (d, *J* = 4.7 Hz), 23.90 (d, *J* = 5.1 Hz); ν_{\max} (liquid film) 3290, 2979, 1721, 1513, 1243, 987, 698 cm⁻¹; HRMS (ESI-TOF) *m/z*: [M + H]⁺ Calcd. for C₂₃H₃₃N₂O₆P 465.2149; Found 465.2149.

Benzyl 2-amino-1-(2-chlorophenyl)-2-(diisopropoxyphosphoryl)ethylcarbamate (**3.56g**)



The general procedure part 1 was employed with the following quantities: diisopropyl phosphonate **3.54b** (100 mg, 0.28 mmol), 2-chloro phenyl N-Cbz imine **3.55d** (153 mg, 0.56 mmol), catalyst

3.49d (2.1 mg, 0.0028 mmol – 1 mol %). Reaction was completed in 120 h. In this case the product was separated using column chromatography before carrying out hydrolysis.

Column Chromatography for the isolation of imine:

Approximately 35 mL of silica was packed into a column using 25% EtOAc in hexanes as the solvent. The material obtained from work-up was loaded on the column after dissolution in a minimum amount of DCM. Approximately 200 mL of 25% EtOAc in hexanes was eluted followed by elution with 300 mL of 33% EtOAc in hexanes and finally with 300 mL of 45% EtOAc in hexanes. The eluted solvent was collected in 25 mL fractions. Fractions 7 – 16 contained product. These fractions were concentrated and dried under high vacuum to give 88 mg of product. The obtained imine was hydrolyzed same as in part 2 of general procedure.

Column Chromatography for the isolation of amine:

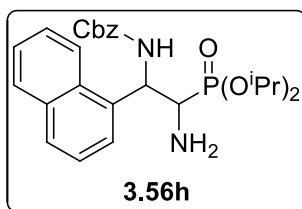
Approximately 30 mL of silica was packed into a column using 33% EtOAc in hexanes as the solvent. The material obtained from work-up was loaded on the column after dissolution in a minimum amount of DCM. Approximately 300 mL of 33% EtOAc in hexanes was eluted followed by elution with 150 mL of 50% EtOAc in hexanes and finally with 500 mL of 75% EtOAc in hexanes. The eluted solvent was collected in 25 mL fractions. Fractions 18 – 31 contained product. These fractions were concentrated and dried under high vacuum to give 40 mg of product **3.56g** (yield: 31%).

Characterization:

R_f: 0.15 in 60% EtOAc/hexanes. $[\alpha]_D^{24} = -11.4^\circ$ (*c* 0.1, CH₂Cl₂). ¹H NMR (400 MHz, CDCl₃) δ 7.47 – 7.19 (m, 9H), 6.81 (major dias., brs, 0.53H), 6.27 (minor dias., brs, 0.27H), [5.55 – 5.52 (minor dias., m), 5.37 (major dias., ddd, *J* = 25.8 Hz, 8.4 Hz, 5.7 Hz),

1H], 5.13 – 5.05 (m, 2H), [4.75 (major dias., sep, $J = 6.3$ Hz), 4.49 – 4.45 (minor dias., m), 2H], 3.59 – 3.46 (m, 1H), 1.34 – 1.02 (m, 12H); ^{13}C NMR $\{^1\text{H}\}$ (100 MHz CDCl_3) δ 156.1, 155.7, 136.6, 133.3, 130.1, 129.7, 128.9, 128.8, 128.5, 128.4, 128.1, 127.0, 126.9, 72.1 (d, $J = 7.5$ Hz), 71.7 (d, $J = 7.3$ Hz), 71.6 (d, $J = 7.2$ Hz), 71.1 (d, $J = 7.5$ Hz), 66.9, 66.8, 56.1, 52.4, 51.6 (d, $J = 150.8$ Hz), 50.8 (d, $J = 154.3$ Hz), 24.4 (d, $J = 3.4$ Hz), 24.3 (d, $J = 3.4$ Hz), 24.2 (d, $J = 3.7$ Hz), 24.1 (d, $J = 5.1$ Hz), 24.0 (d, $J = 5.1$ Hz), 23.9 (d, $J = 5.0$ Hz); ν_{max} (liquid film) 3310, 2978, 1720, 1512, 1237, 1104, 982, 753, 697 cm^{-1} ; HRMS (ESI-TOF) m/z : $[\text{M} + \text{H}]^+$ Calcd. for $\text{C}_{22}\text{H}_{31}\text{ClN}_2\text{O}_5\text{P}$ 469.1654; Found 469.1656.

Benzyl 2-amino-2-(diisopropoxyphosphoryl)-1-(naphthalen-1-yl)ethylcarbamate (3.56h)



The general procedure was employed with the following quantities: diisopropyl phosphonate **3.54b** (100 mg, 0.28 mmol), 1-Naphthyl N-Cbz imine **3.55e** (162 mg, 0.56 mmol), catalyst **3.49d** (2.1 mg, 0.0028 mmol – 1 mol %). Reaction was completed in 120 h.

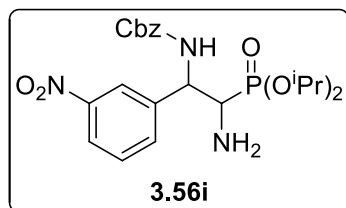
Column Chromatography:

Approximately 40 mL of silica was packed into a column using 50% EtOAc in hexanes as the solvent. The material obtained from work-up was loaded on the column after dissolution in a minimum amount of DCM. Approximately 180 mL of 50% EtOAc in hexanes was eluted followed by elution with 150 mL of 66% EtOAc in hexanes and finally with 300 mL of 2% MeOH in DCM. The eluted solvent was collected in 15 mL fractions. Fractions 17 – 40 contained product. These fractions were concentrated and dried under high vacuum to give 70 mg of product **3.56h** (yield: 51%).

Characterization:

R_f: 0.1 in 50% EtOAc/hexanes. $[\alpha]_D^{24} = -34.6^\circ$ (*c* 0.1, CH₂Cl₂). ¹H NMR (400 MHz, CDCl₃) δ [8.18 (minor dias., d, *J* = 8.6 Hz), 8.14 (major dias., d, *J* = 8.4 Hz), 1H], 7.90 – 7.85 (m, 1H), 7.80 – 7.78 (m, 1H), 7.62 – 7.32 (m, 8H), [6.84 (minor dias., s), 6.70 (major dias., s), 1H], 6.39 (brs, 1H), [6.07 – 6.03 (m), 5.89 (ddd, *J* = 22.8 Hz, 8.4 Hz, 5.3 Hz), 1H], 5.11 – 5.08 (m, 2H), 4.85 – 4.39 (m, 2H), [3.59 (minor dias., d, *J* = 10.1 Hz), 3.50 (major dias., d, *J* = 15.2 Hz), 1H], 1.38 – 0.91 (m, 12H); ¹³C NMR {¹H} (100 MHz CDCl₃) δ 155.8, 136.8, 134.3, 130.3, 129.2, 129.0, 128.6, 128.5, 128.4, 128.1, 126.6, 126.5, 125.9, 125.7, 125.4, 125.3, 123.4, 123.2, 122.8, 71.7 (d, *J* = 7.2 Hz), 71.6 (d, *J* = 7.4 Hz), 66.93, 66.87, 52.2 (d, *J* = 154.3 Hz), 50.6, 24.33 (d, *J* = 3.6 Hz), 24.29 (d, *J* = 3.5 Hz), 24.18 (d, *J* = 5.1 Hz), 24.08 (d, *J* = 4.8 Hz); ν_{\max} (liquid film) 3296, 2978, 1720, 1498, 1235, 984, 794, 698 cm⁻¹; HRMS (ESI-TOF) *m/z*: [M + H]⁺ Calcd. for C₂₆H₃₃N₂O₅P 485.2200; Found 485.2212.

Benzyl 2-amino-2-(diisopropoxyphosphoryl)-1-(3-nitrophenyl)ethylcarbamate (3.56i)



The general procedure was employed with the following quantities: diisopropyl phosphonate **3.54b** (100 mg, 0.28 mmol), 3-Nitro phenyl N-Cbz imine **3.55f** (159 mg, 0.56 mmol), catalyst **3.49d** (2.1 mg, 0.0028 mmol – 1 mol %). Reaction was completed in 144 h.

Column Chromatography:

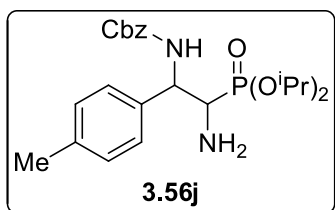
Approximately 60 mL of silica was packed into a column using 1% MeOH in DCM as the solvent. The material obtained from work-up was loaded on the column after dissolution in a minimum amount of DCM. Approximately 300 mL of 1% MeOH in DCM was eluted followed by elution with 500 mL of 1.5% MeOH in DCM. The eluted solvent

was collected in 25 mL fractions. Fractions 33 – 42 contained product. These fractions were concentrated and dried under high vacuum to give 59 mg of product **3.56i** (yield: 44%).

Characterization:

R_f: 0.17 in 75% EtOAc/hexanes. $[\alpha]_D^{24} = +10.6^\circ$ (*c* 0.1, CH₂Cl₂). ¹H NMR (400 MHz, CDCl₃) δ 8.26 (brs, 1H), 8.15 (d, *J* = 8.1 Hz, 1H), 7.72 (dd, *J* = 11.2 Hz, 7.9 Hz, 1H), 7.51 (dd, *J* = 16.4 Hz, 8.2 Hz, 1H), 7.35 (brs, 5H), 6.61 (major dias., brs, 0.53H), 6.50 (minor dias., brs, 0.47H), 5.17 – 5.02 (m, 3H), 4.82 – 4.54 (m, 2H), 3.31 (ddd, *J* = 15.2 Hz, 7.2 Hz, 3.4 Hz, 1H), 1.34 – 1.10 (m, 12H); ¹³C NMR {¹H} (100 MHz CDCl₃) δ 155.9, 148.6, 148.4, 136.4, 134.0, 133.3, 129.5, 129.2, 128.65, 128.62, 128.32, 128.27, 122.8, 122.1, 71.9 (d, *J* = 7.1 Hz), 71.8 (d, *J* = 7.4 Hz), 71.4 (d, *J* = 7.5 Hz), 67.2, 67.1, 56.15, 56.09, 53.4 (d, *J* = 151.5 Hz), 53.3 (d, *J* = 148.8 Hz), 24.22 (d, *J* = 3.6 Hz), 24.16 (d, *J* = 2.2 Hz), 24.09 (d, *J* = 4.7 Hz), 24.0 (d, *J* = 3.4 Hz), 23.9; ν_{max} (liquid film) 3272, 2980, 1717, 1528, 1348, 1219, 984, 698 cm⁻¹; HRMS (ESI-TOF) *m/z*: [M + H]⁺ Calcd. for C₂₂H₃₁N₃O₇P 480.1894; Found 480.1906.

Benzyl 2-amino-2-(diisopropoxyphosphoryl)-1-p-tolyethylcarbamate (3.56j)



The general procedure was employed with the following quantities: diisopropyl phosphonate **3.54b** (100 mg, 0.28 mmol), 4-Methyl phenyl N-Cbz imine **3.55g** (142 mg, 0.56 mmol), catalyst **3.49d** (2.1 mg, 0.0028 mmol – 1 mol %). Reaction was completed in 48 h.

Column Chromatography:

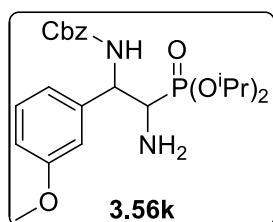
Approximately 35 mL of silica was packed into a column using 40% EtOAc in hexanes as the solvent. The material obtained from work-up was loaded on the column after dissolution in a minimum amount of DCM. Approximately 400 mL of 40% EtOAc in

hexanes was eluted followed by elution with 300 mL of 60% EtOAc in hexanes, 250 mL of 70% EtOAc in hexanes and finally with 200 mL of 100% EtOAc. The eluted solvent was collected in 25 mL fractions. Fractions 18 – 40 contained product. These fractions were concentrated and dried under high vacuum to give 71 mg of product **3.56j** (yield: 56%).

Characterization:

R_f: 0.13 in 75% EtOAc/hexanes. $[\alpha]_D^{24} = -16.0^\circ$ (*c* 0.1, CH₂Cl₂). ¹H NMR (400 MHz, CDCl₃) δ 7.33 (brm, 5H), 7.25 – 7.21 (m, 2H), 7.16 – 7.12 (m, 2H), 6.31 (brs, 1H), 5.12 – 4.93 (m, 3H), 4.77 – 4.54 (m, 2H), 3.31 (dd, *J* = 15.4 Hz, 3.0 Hz, 1H), [2.334 (major dias., s), 2.327 (minor dias., s), 3H], 1.33 – 1.12 (m, 12H); ¹³C NMR {¹H} (100 MHz CDCl₃) δ 155.8, 137.4, 137.3, 136.8, 129.3, 129.1, 128.5, 128.2, 127.5, 126.6, 71.4 (d, *J* = 7.3 Hz), 71.3 (d, *J* = 7.6 Hz), 71.0 (d, *J* = 7.4 Hz), 66.8, 66.7, 55.1, 54.0 (d, *J* = 152.3 Hz), 24.23 (d, *J* = 3.7 Hz), 24.17 (d, *J* = 3.3 Hz), 24.0 (d, *J* = 5.0 Hz), 23.9 (d, *J* = 6.1 Hz), 21.18, 21.15; ν_{\max} (liquid film) 3287, 2978, 1714, 1540, 1254, 1218, 994, 696, 555 cm⁻¹; HRMS (ESI-TOF) *m/z*: [M + H]⁺ Calcd. for C₂₃H₃₃N₂O₅P 449.2200; Found 449.2207.

Benzyl 2-amino-2-(diisopropoxyphosphoryl)-1-(3-methoxyphenyl)ethylcarbamate (3.56k)



The general procedure was employed with the following quantities: diisopropyl phosphonate **3.54b** (100 mg, 0.28 mmol), 3-Methoxy phenyl N-Cbz imine **3.55h** (151 mg, 0.56 mmol), catalyst **3.49d** (2.1 mg, 0.0028 mmol – 1 mol %). Reaction was completed in 18 h.

Column Chromatography:

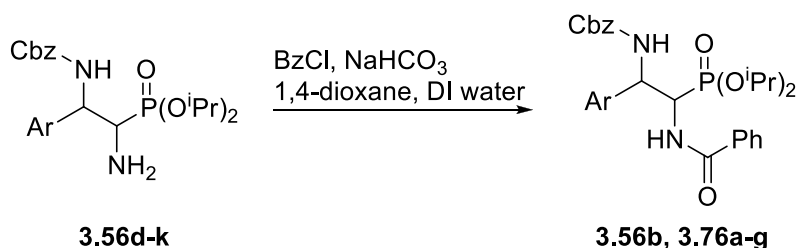
Approximately 30 mL of silica was packed into a column using 50% EtOAc in hexanes as the solvent. The material obtained from work-up was loaded on the column after dissolution in a minimum amount of DCM. Approximately 300 mL of 50% EtOAc in

hexanes was eluted followed by elution with 100 mL of 2% MeOH in DCM and finally with 100 mL of 4% MeOH in DCM. The eluted solvent was collected in 15 mL fractions. Fractions 25 – 28 contained product. These fractions were concentrated and dried under high vacuum to give 71 mg of product **3.56k** (yield: 55%).

Characterization:

R_f: 0.13 in 75% EtOAc/hexanes. [α]_D²⁴ = -4.4° (*c* 0.1, CH₂Cl₂). ¹H NMR (400 MHz, CDCl₃) δ 7.34 – 7.28 (brm, 4H), 7.26 – 7.22 (m, 1H), 6.97 – 6.88 (m, 2H), 6.81 (dd, *J* = 8.2 Hz, 2.3 Hz, 1H), 6.44 – 6.33 (brm, 1H), 5.13 – 4.93 (m, 3H), 4.78 – 4.54 (m, 2H), 3.79 (s, 3H), 3.40 – 3.28 (m, 1H), 1.33 – 1.11 (m, 12H); ¹³C NMR {¹H} (100 MHz CDCl₃) δ 159.9, 159.7, 155.8, 136.8, 136.6, 129.7, 129.4, 128.5, 128.2, 128.1, 119.9, 118.9, 113.3, 113.0, 112.9, 112.4, 71.43 (d, *J* = 7.3 Hz), 71.35 (d, *J* = 7.6 Hz), 71.0 (d, *J* = 7.3 Hz), 66.8, 66.7, 55.31, 55.25, 55.17, 53.9 (d, *J* = 153.0 Hz), 24.2 (d, *J* = 3.6 Hz), 24.1 (d, *J* = 4.0 Hz), 24.0 (d, *J* = 4.7 Hz), 23.9 (d, *J* = 4.7 Hz); ν_{max} (liquid film) 3294, 2978, 1719, 1491, 1238, 987, 697 cm⁻¹; HRMS (ESI-TOF) *m/z*: [M + H]⁺ Calcd. for C₂₃H₃₄N₂O₆P 465.2149; Found 465.2150.

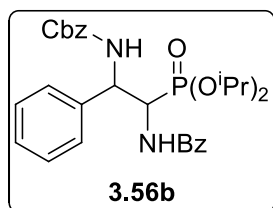
3.5.5 General procedure for the benzoyl protection of amino phosphonates



Amine phosphonate **3.56d-k** (0.07 mmol) was taken in a 10 mL single neck flask to which dioxane:water (450 μL:50 μL) were added. To this solution, NaHCO₃ (18 mg, 0.21 mmol) was added followed by benzoyl chloride (20 μL, 0.18 mmol) and the reaction mixture was stirred at room temperature for 40 min. It was then diluted with saturated NaHCO₃ (20

mL) solution and the compound was extracted with DCM (3×15 mL). The combined organic layers were dried over Na₂SO₄, concentrated, and purified by column chromatography.

Benzyl 2-benzamido-2-(diisopropoxyphosphoryl)-1-phenylethylcarbamate (3.56b)



The general procedure was employed with the amine phosphonate **3.56d** (30 mg, 0.07 mmol).

Column Chromatography:

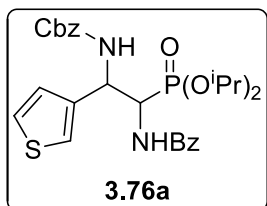
Approximately 35 mL of silica was packed into a column using 40% EtOAc in hexanes as the solvent. The material obtained from work-up was loaded on the column after dissolution in a minimum amount of DCM. Approximately 200 mL of 40% EtOAc in hexanes was eluted followed by elution with 100 mL of 1.8% MeOH in DCM and finally with 2% MeOH in DCM. The eluted solvent was collected in 15 mL fractions. Fractions 18 – 23 contained product. These fractions were concentrated and dried under high vacuum to give 35 mg of product **3.56b** (yield: 95%).

Characterization:

R_f: 0.25 in 50% EtOAc/hexanes. Enantiomeric excess (*ee*) = 76%. Diastereomer ratio 6.2:1. [α]_D²⁴ = +4.0° (*c* 0.1, CH₂Cl₂). ¹H NMR (400 MHz, CDCl₃) δ 7.77 – 7.70 (m, 2H), 7.54 – 7.51 (m, 1H), 7.47 – 7.41 (m, 4H), 7.35 – 7.28 (m, 4H), 7.26 – 7.21 (m, 4H), 6.90 – 6.69 (brm, 1H), 6.63 – 6.33 (brm, 1H), 5.37 – 4.95 (m, 4H), 4.65 – 4.49 (m, 2H), 1.27 – 1.05 (m, 12H); ¹³C NMR {¹H} (100 MHz CDCl₃) δ 167.2 (d, *J* = 6.0 Hz), 156.4, 136.5, 131.8, 128.8, 128.7, 128.6, 128.4, 128.0, 127.4, 127.3, 127.2, 72.1 (m), 66.9, 55.8 (d, *J* = 3.8 Hz), 51.0 (d, *J* = 155.7 Hz), 24.1 (d, *J* = 3.3 Hz), 23.8 (d, *J* = 5.1 Hz), 23.7 (d, *J* = 5.2 Hz);

ν_{max} (liquid film) 3300, 2978, 1721, 1665, 1521, 1231, 990, 735, 696 cm^{-1} ; HRMS (ESI-TOF) m/z : $[M + H]^+$ Calcd. for $\text{C}_{29}\text{H}_{36}\text{N}_2\text{O}_6\text{P}$ 539.2306; Found 539.2319.

Benzyl 2-benzamido-2-(diisopropoxyphosphoryl)-1-(thiophen-3-yl)ethylcarbamate (3.76a)



The general procedure was employed with the amine phosphonate **3.56e** (31 mg, 0.07 mmol).

Column Chromatography:

Approximately 40 mL of silica was packed into a column using 1% MeOH in DCM as the solvent. The material obtained from work-up was loaded on the column after dissolution in a minimum amount of DCM. Approximately 200 mL of 1% MeOH in DCM was eluted followed by elution with 400 mL of 1.25% MeOH in DCM. The eluted solvent was collected in 15 mL fractions. Fractions 29 – 37 contained product. These fractions were concentrated and dried under high vacuum to give 28 mg of product **3.76a** (yield: 75%).

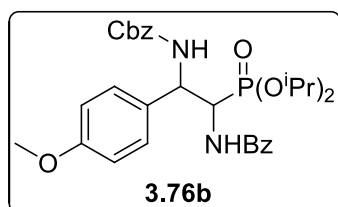
Characterization:

R_f : 0.53 in 75% EtOAc/hexanes. Enantiomeric excess (ee) = 67%. Diastereomer ratio 4.5:1. $[\alpha]_D^{24} = +29.2^\circ$ (c 0.1, CH_2Cl_2). ^1H NMR (400 MHz, CDCl_3) δ 8.10 (dd, $J = 8.3$ Hz, 1.1 Hz, 1H), 7.80 – 7.74 (m, 2H), 7.63 – 7.40 (m, 5H), 7.32 (brm, 1H), 7.25 – 7.22 (m, 4H), 7.16 – 7.12 (m, 1H), 6.85 – 6.40 (m, 1H), 5.46 – 5.36 (m, 1H), 5.17 – 5.03 (m, 3H), 4.75 – 4.56 (m, 2H), 1.32 – 1.12 (m, 12H); ^{13}C NMR $\{^1\text{H}\}$ (100 MHz CDCl_3) δ 167.2 (d, $J = 5.8$ Hz), 156.3, 136.5, 133.8, 133.4, 132.0, 130.3, 128.9, 128.8, 128.5, 128.1, 128.0, 127.3, 126.8, 126.2, 122.7, 72.43 (d, $J = 6.1$ Hz), 72.36 (d, $J = 6.8$ Hz), 67.1, 67.0, 51.9, 50.8 (d, $J = 155.6$ Hz), 24.23 (d, $J = 2.9$ Hz), 24.20 (d, $J = 3.1$ Hz), 23.9 (d, $J = 5.2$ Hz), 23.7 (d, $J = 5.4$ Hz);

ν_{\max} (liquid film) 3301, 2980, 1714, 1655, 1520, 1231, 990, 735, 696, 541 cm^{-1} ; HRMS (ESI-TOF) m/z : $[M + H]^+$ Calcd. for $\text{C}_{27}\text{H}_{34}\text{N}_2\text{O}_6\text{PS}$ 545.1870; Found 545.1856.

Benzyl 2-benzamido-2-(diisopropoxyphosphoryl)-1-(4-methoxyphenyl) ethylcarbamate

(3.76b)



The general procedure was employed with the amine phosphonate **3.56f** (33 mg, 0.07 mmol).

Column Chromatography:

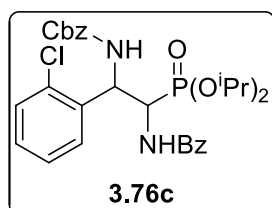
Approximately 40 mL of silica was packed into a column using 40% EtOAc in hexanes as the solvent. The material obtained from work-up was loaded on the column after dissolution in a minimum amount of DCM. Approximately 200 mL of 40% EtOAc in hexanes was eluted followed by elution with 500 mL of 46.5% EtOAc in hexanes. The eluted solvent was collected in 15 mL fractions. Fractions 28 – 50 contained product. These fractions were concentrated and dried under high vacuum to give 31 mg of product **3.76b** (yield: 77%).

Characterization:

R_f : 0.5 in 75% EtOAc/hexanes. Enantiomeric excess (ee) = 77%. Diastereomer ratio 2.2:1. $[\alpha]_D^{24} = +16.4^\circ$ (c 0.1, CH_2Cl_2). ^1H NMR (400 MHz, CDCl_3) δ 7.77 – 7.70 (m, 2H), 7.56 – 7.50 (m, 1H), 7.47 – 7.42 (m, 2H), 7.35 – 7.33 (m, 3H), 7.26 – 7.20 (m, 3H), 6.87 – 6.85 (m, 3H), 6.58 – 6.56 (brm, 1H), 6.28– 6.24 (brs, 1H), 5.32 – 4.94 (m, 4H), 4.66 – 4.54 (m, 2H), 3.79 (s, 3H), 1.26 – 1.09 (m, 12H); ^{13}C NMR $\{^1\text{H}\}$ (100 MHz CDCl_3) δ 167.5 (d, $J = 6.4$ Hz), 167.2 (d, $J = 6.2$ Hz), 159.5, 159.4, 156.3, 156.0, 136.6, 136.5, 133.9, 133.7, 132.2, 131.9, 130.8, 128.9, 128.8, 128.6, 128.5, 128.1, 127.23, 127.19, 114.1, 113.9, 72.5 (d,

$J = 7.4$ Hz), 72.14 (d, $J = 3.3$ Hz), 72.06 (d, $J = 3.5$ Hz), 71.97, 67.0, 66.9, 55.45, 55.42, 51.5 (d, $J = 154.8$ Hz), 51.2 (d, $J = 154.2$ Hz), 24.3 (d, $J = 3.3$ Hz), 24.2, 24.1, 24.0 (d, $J = 3.6$ Hz), 23.83 (d, $J = 5.1$ Hz), 23.81 (d, $J = 5.1$ Hz), 23.7 (d, $J = 5.5$ Hz); ν_{\max} (liquid film) 3300, 2979, 1719, 1652, 1513, 1230, 985, 696, 531 cm^{-1} ; HRMS (ESI-TOF) m/z : $[M + H]^+$ Calcd. for $\text{C}_{30}\text{H}_{38}\text{N}_2\text{O}_7\text{P}$ 569.2411; Found 569.2415.

Benzyl 2-benzamido-1-(2-chlorophenyl)-2-(diisopropoxyphosphoryl)ethylcarbamate (3.76c)



The general procedure was employed with the amine phosphonate **3.56g** (33 mg, 0.07 mmol).

Column Chromatography:

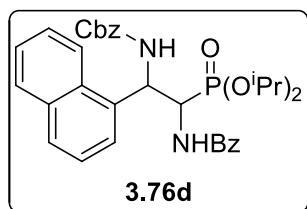
Approximately 25 mL of silica was packed into a column using 20% EtOAc in hexanes as the solvent. The material obtained from work-up was loaded on the column after dissolution in a minimum amount of DCM. Approximately 200 mL of 20% EtOAc in hexanes was eluted followed by elution with 200 mL of 30% EtOAc in hexanes, then with 200 mL of 35% EtOAc in hexanes and finally with 300 mL of 40% EtOAc in hexanes. The eluted solvent was collected in 15 mL fractions. Fractions 37 – 50 contained product. These fractions were concentrated and dried under high vacuum to give 26 mg of product **3.76c** (yield: 64%).

Characterization:

R_f : 0.33 in 50% EtOAc/hexanes. Enantiomeric excess (ee) = 53% (minor diastereomer), Major diastereomer is almost racemic. Diastereomer ratio 2.9:1. $[\alpha]_D^{24} = +11.4^\circ$ (c 0.1, CH_2Cl_2). $^1\text{H NMR}$ (400 MHz, CDCl_3) δ 7.75 – 7.69 (m, 2H), 7.54 – 7.32 (m, 8H), 7.28 – 7.16 (m, 4H), 6.99 (brs, 1H), 6.66 (d, $J = 9.5$ Hz, 1H), [5.72 (minor dias., brm),

5.54 (major dias., ddd, $J = 24.3$ Hz, 8.4 Hz, 6.2 Hz), 1H], 5.31 – 4.86 (m, 3H), 4.74 – 4.44 (m, 2H), 1.29 – 1.02 (m, 12H); ^{13}C NMR $\{^1\text{H}\}$ (100 MHz CDCl_3) δ 166.5(d, $J = 4.6$ Hz), 156.3, 156.1, 136.5, 136.4, 133.8, 133.5, 132.0, 131.9, 130.0, 129.7, 129.2, 128.9, 128.7, 128.6, 128.5, 128.2, 128.1, 127.3, 127.16, 127.14, 126.9, 72.9 (d, $J = 7.6$ Hz), 72.4 (d, $J = 7.4$ Hz), 72.2 (d, $J = 7.6$ Hz), 67.2, 67.0, 54.6, 48.9 (d, $J = 156.7$ Hz), 24.5 (d, $J = 2.9$ Hz), 24.21 (d, $J = 4.6$ Hz), 24.17 (d, $J = 4.1$ Hz), 23.8 – 23.7 (m); ν_{max} (liquid film) 3301, 2980, 1721, 1664, 1523, 1233, 991, 754, 696 cm^{-1} ; HRMS (ESI-TOF) m/z : $[\text{M} + \text{H}]^+$ Calcd. for $\text{C}_{29}\text{H}_{35}\text{ClN}_2\text{O}_6\text{P}$ 573.1916; Found 573.1911.

Benzyl 2-benzamido-2-(diisopropoxyphosphoryl)-1-(naphthalen-1-yl)ethylcarbamate (3.76d)



The general procedure was employed with the amine phosphonate **3.56h** (34 mg, 0.07 mmol).

Column Chromatography:

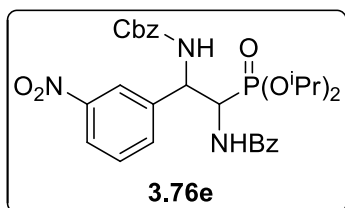
Approximately 30 mL of silica was packed into a column using 25% EtOAc in hexanes as the solvent. The material obtained from work-up was loaded on the column after dissolution in a minimum amount of DCM. Approximately 150 mL of 25% EtOAc in hexanes was eluted followed by elution with 150 mL of 30% EtOAc in hexanes and finally with 150 mL of 40% EtOAc in hexanes. The eluted solvent was collected in 25 mL fractions. Fractions 21 – 36 contained product. These fractions were concentrated and dried under high vacuum to give 41 mg of product **3.76d** (yield: 46%).

Characterization:

R_f : 0.23 in 50% EtOAc/hexanes. Enantiomeric excess (ee) = 85%. Diastereomer ratio 3.9:1. $[\alpha]_{\text{D}}^{24} = +8.6^\circ$ (c 0.1, CH_2Cl_2). ^1H NMR (400 MHz, CDCl_3) δ [8.42 (minor dias.,

d, $J = 7.6$ Hz), 8.24 (major dias., d, $J = 7.8$ Hz), 1H], 7.87 (d, $J = 7.9$ Hz, 1H), 7.80 (d, $J = 8.1$ Hz, 1H), 7.75 – 7.64 (m, 3H), 7.56 – 7.32 (m, 7H), 7.22 – 6.87 (m, 5H), 6.14 – 6.02 (m, 2H), 5.33 (brs, 1H), 5.17 – 4.83 (m, 2H), 4.64 – 4.23 (m, 2H), 1.27 – 0.80 (m, 12H); ^{13}C NMR $\{^1\text{H}\}$ (100 MHz CDCl_3) δ 167.7 (d, $J = 6.5$ Hz), 156.6, 136.3, 134.1, 134.0, 133.8, 132.1, 131.9, 131.2, 131.1, 129.1, 129.0, 128.9, 128.7, 128.6, 128.4, 128.3, 128.04, 127.95, 127.34, 127.26, 127.1, 126.9, 125.9, 125.3, 125.2, 123.2, 72.7 (d, $J = 7.8$ Hz), 72.3 (d, $J = 7.3$ Hz), 72.1 (d, $J = 7.7$ Hz), 71.9 (d, $J = 7.3$ Hz), 67.0, 51.5, 50.2 (d, $J = 156.2$ Hz), 24.3, 24.2 (d, $J = 3.3$ Hz), 23.9, 23.7, 23.61, 23.56; ν_{max} (liquid film) 3311, 2980, 1720, 1671, 1515, 1236, 987, 733, 695 cm^{-1} ; HRMS (ESI-TOF) m/z : $[\text{M} + \text{H}]^+$ Calcd. for $\text{C}_{33}\text{H}_{38}\text{N}_2\text{O}_6\text{P}$ 589.2471; Found 589.2462.

Benzyl 2-benzamido-2-(diisopropoxyphosphoryl)-1-(3-nitrophenyl)ethylcarbamate (3.76e)



The general procedure was employed with the amine phosphonate **3.56i** (33 mg, 0.07 mmol).

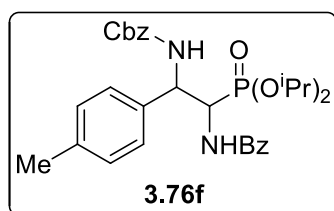
Column Chromatography:

Approximately 30 mL of silica was packed into a column using 45% EtOAc in hexanes as the solvent. The material obtained from work-up was loaded on the column after dissolution in a minimum amount of DCM. Approximately 200 mL of 45% EtOAc in hexanes was eluted followed by elution with 200 mL of 52% EtOAc in hexanes. The eluted solvent was collected in 15 mL fractions. Fractions 13 – 22 contained product. These fractions were concentrated and dried under high vacuum to give 26 mg of product **3.76e** (yield: 79%).

Characterization:

R_f: 0.15 in 50% EtOAc/hexanes. Enantiomeric excess (*ee*) = 42% (minor diastereomer), Major diastereomer is almost racemic. Diastereomer ratio 1.6:1. [α]_D²⁴ = +20.6° (*c* 0.1, CH₂Cl₂). ¹H NMR (400 MHz, CDCl₃) δ 8.32 (s, 1H), 8.14 – 8.09 (m, 1H), 7.82 – 7.69 (m, 3H), 7.56 – 7.35 (m, 7H), 7.25 – 7.13 (brm, 3H), 6.98 – 6.80 (m, 1H), 5.43 – 5.36 (m, 1H), 5.12 – 4.95 (m, 3H), 4.78 – 4.59 (m, 2H), 1.36 – 1.07 (m, 12H); ¹³C NMR {¹H} (100 MHz CDCl₃) δ 168.0 (d, *J* = 7.3 Hz), 167.5 (d, *J* = 5.4 Hz), 156.2, 155.9, 148.4, 136.3, 133.7, 133.5, 133.2, 132.5, 132.1, 129.5, 129.4, 129.0, 128.8, 128.64, 128.58, 128.3, 128.2, 128.0, 127.2, 123.0, 122.9, 122.6, 122.4, 73.2, 73.14, 73.10, 73.06, 72.9, 72.83, 72.75, 72.66, 72.58, 67.3, 67.2, 56.9, 55.7, 51.0 (d, *J* = 153.7 Hz), 50.4 (d, *J* = 156.5 Hz), 24.3, 24.20, 24.15, 24.11, 24.0, 23.92, 23.88, 23.7 (d, *J* = 5.2 Hz); ν_{\max} (liquid film) 3313, 2982, 1714, 1652, 1527, 1348, 1218, 991, 735, 693, 544 cm⁻¹; HRMS (ESI-TOF) *m/z*: [M + H]⁺ Calcd. for C₂₉H₃₅N₃O₈P 584.2186; Found 584.2161.

Benzyl 2-benzamido-2-(diisopropoxyphosphoryl)-1-p-tolyylethylcarbamate (3.76f)



The general procedure was employed with the amine phosphonate **3.56j** (31 mg, 0.07 mmol).

Column Chromatography:

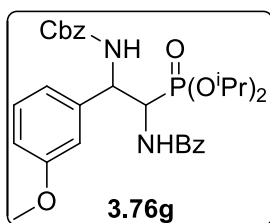
Approximately 25 mL of silica was packed into a column using 20% EtOAc in hexanes as the solvent. The material obtained from work-up was loaded on the column after dissolution in a minimum amount of DCM. Approximately 200 mL of 20% EtOAc in hexanes was eluted followed by elution with 200 mL of 40% EtOAc in hexanes, and finally with 150 mL of 50% EtOAc. The eluted solvent was collected in 15 mL fractions. Fractions

25 – 32 contained product. These fractions were concentrated and dried under high vacuum to give 25 mg of product **3.76f** (yield: 65%).

Characterization:

R_f: 0.33 in 50% EtOAc/hexanes. Enantiomeric excess (*ee*) = 77%. Diastereomer ratio 2.4:1. [α]_D²³ = -4.0° (*c* 0.1, CH₂Cl₂). ¹H NMR (400 MHz, CDCl₃) δ [7.77 (major dias., d, *J* = 7.5 Hz), 7.72 (minor dias., d, *J* = 7.3 Hz), 2H], 7.56 – 7.42 (m, 3H), 7.36 – 7.29 (m, 3H), 7.26 – 7.13 (m, 5H), 7.01 – 6.84 (m, 1H), 6.60 (brs, 1H), 6.21 (brs, 1H), 5.34 – 4.96 (m, 4H), 4.62 – 4.52 (m, 2H), [2.37 (minor dias., s), 2.33 (major dias., s), 3H], 1.27 – 1.07 (m, 12H); ¹³C NMR {¹H} (100 MHz CDCl₃) δ 167.5 (d, *J* = 7.0 Hz), 167.2 (d, *J* = 6.0 Hz), 156.3, 137.7, 137.6, 136.6, 136.5, 133.9, 133.7, 133.3, 132.1, 131.9, 129.3, 129.2, 128.9, 128.7, 128.6, 128.5, 128.0, 127.4, 127.3, 127.2, 72.5 (d, *J* = 7.3 Hz), 72.3 (d, *J* = 7.5 Hz), 72.2 (d, *J* = 7.0 Hz), 72.1 (d, *J* = 7.2 Hz), 67.0, 66.9, 55.63, 55.59, 51.1 (d, *J* = 155.4 Hz), 24.3 (d, *J* = 3.0 Hz), 24.19 (d, *J* = 3.3 Hz), 24.16 (d, *J* = 3.5 Hz), 24.0 (d, *J* = 3.6 Hz), 23.8 (d, *J* = 5.3 Hz), 23.6 (d, *J* = 5.5 Hz), 21.22, 21.17; ν_{\max} (liquid film) 3301, 2979, 1720, 1653, 1517, 1317, 1231, 989, 670, 578 cm⁻¹; HRMS (ESI-TOF) *m/z*: [M + H]⁺ Calcd. for C₃₀H₃₈N₂O₆P 553.2462; Found 553.2464.

Benzyl 2-benzamido-2-(diisopropoxyphosphoryl)-1-(3-methoxyphenyl)ethylcarbamate (3.76g)



The general procedure was employed with the amine phosphonate **3.56k** (33 mg, 0.07 mmol).

Column Chromatography:

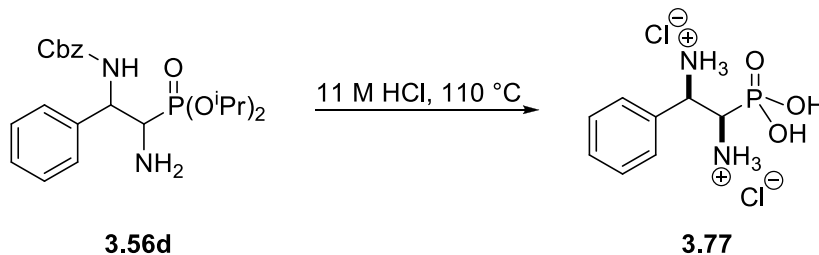
Approximately 30 mL of silica was packed into a column using 30% EtOAc in hexanes as the solvent. The material obtained from work-up was loaded on the column after dissolution in a minimum amount of DCM. Approximately 200 mL of 30% EtOAc in hexanes was eluted followed by elution with 200 mL of 1.5% MeOH in DCM and finally with 200 mL of 1.75% MeOH in DCM. The eluted solvent was collected in 15 mL fractions. Fractions 27 – 29 contained product. These fractions were concentrated and dried under high vacuum to give 29 mg of product **3.76g** (yield: 72%).

Characterization:

R_f: 0.17 in 50% EtOAc/hexanes. Enantiomeric excess (*ee*) = 69%. Diastereomer ratio 1.5:1. $[\alpha]_D^{24} = -3.2^\circ$ (*c* 0.1, CH₂Cl₂). ¹H NMR (400 MHz, CDCl₃) δ 7.75 (d, *J* = 7.5 Hz, 1H), 7.72 – 7.65 (m, 1H), 7.56 – 7.51 (m, 1H), 7.47 – 7.43 (m, 2H), 7.37 – 7.32 (m, 2H), 7.26 – 7.22 (m, 4H), 7.02 – 6.95 (m, 2H), 6.84 – 6.80 (m, 1H), 6.73 – 6.68 (brm, 1H), 6.56 – 6.33 (brm, 1H), 5.34 – 4.96 (m, 4H), 4.68 – 4.38 (m, 2H), [3.76 (minor dias., s), 3.75 (major dias., s), 3H], 1.30 – 1.05 (m, 12H); ¹³C NMR {¹H} (100 MHz CDCl₃) δ 167.5 (d, *J* = 5.6 Hz), 167.2 (d, *J* = 6.2 Hz), 159.8, 156.3, 140.3, 136.5, 133.9, 133.6, 132.2, 131.9, 129.6, 129.5, 128.9, 128.7, 128.5, 128.0, 127.3, 127.2, 119.8, 119.6, 113.9, 113.8, 113.0, 112.8, 72.6 (d, *J* = 7.5 Hz), 72.4, 72.3, 72.2, 72.12, 72.07, 67.0, 66.9, 57.2, 55.9, 55.8, 55.4, 55.3, 51.2 (d, *J* = 157.7 Hz), 50.9 (d, *J* = 155.6 Hz), 24.3 (d, *J* = 2.6 Hz), 24.2 (d, *J* = 2.6 Hz), 24.0 (d, *J* = 3.6 Hz), 23.8 (d, *J* = 5.1 Hz), 23.78 (d, *J* = 5.2 Hz), 23.7 (d, *J* = 5.2 Hz), 23.6 (d, *J* = 5.3 Hz); ν_{max} (liquid film) 3302, 2980, 1723, 1645, 1527, 1235, 995, 698 cm⁻¹; HRMS (ESI-TOF) *m/z*: [M + H]⁺ Calcd. for C₃₀H₃₈N₂O₇P 569.2411; Found 569.2414.

3.5.6 Acidic hydrolysis of amino phosphonates

1-Phenyl-2-phosphonoethane-1,2-diaminium chloride (3.77)



Procedure:

Compound **3.56d** (14 mg, 0.04 mmol) was weighed in a 10 mL single neck flask. To the flask conc. HCl (1.0 mL, 11 M) was added, the flask was sealed and the mixture heated at 110 °C with stirring for 22 h. After cooling to rt., the aqueous phase was diluted with 5 mL DI water and washed with Et₂O (4 X 10 mL), dried over Na₂SO₄ and concentrated. The obtained material was dried under high vacuum to obtain 11.6 mg of white solid.

Characterization:

¹H NMR (400 MHz, D₂O) δ 7.56 (s, major dias., 5H), 4.97 (dd, *J* = 16.8 Hz, 5.5 Hz, 1H), 3.98 (dd, *J* = 14.7 Hz, 5.5 Hz, 1H).

3.6 References

1 Park, Y. S.; Boys, M. L.; Beak, P. *J. Am. Chem. Soc.* **1996**, *118*, 3757–3758.

2 a) Tomioka, K.; Fujieda, H.; Hayashi, S.; Hussein, M. A.; Kambara, T.; Nomura, Y.; Kanai, M.; Koga, K. *Chem. Commun.* **1999**, 715–716. b) Fujieda, H.; Kanai, M.; Kambara, T.; Iida, A.; Tomioka, K. *J. Am. Chem. Soc.* **1997**, *119*, 2060–2061.

3 Li, H.; Wang, Y.; Tang, L.; Deng, L. *J. Am. Chem. Soc.* **2004**, *126*, 9906–9907.

4 Li, H.; Wang, Y.; Tang, L.; Wu, F.; Liu, X.; Guo, C.; Foxman, B. M.; Deng L. *Angew. Chem., Int. Ed.* **2005**, *44*, 105–108.

-
- 5 Okino, T.; Hoashi, Y.; Furukawa, T.; Xu, X. N.; Takemoto, Y. *J. Am. Chem. Soc.* **2005**, *127*, 119–125.
- 6 a) Hoashi, Y.; Okino, T.; Takemoto, Y. *Angew. Chem., Int. Ed.* **2005**, *44*, 4032–4035. b) Takemoto, Y. *Org. Biomol. Chem.* **2005**, *3*, 4299–4036.
- 7 Vakulya, B.; Varga, S.; Csámpai, A.; Soós, T. *Org. Lett.* **2005**, *7*, 1967–1969.
- 8 Sera, A.; Takagi, K.; Katayama, H.; Yamada, H. *J. Org. Chem.* **1988**, *53*, 1157–1161.
- 9 a) Manna, M. S.; Kumar, V.; Mukherjee, S. *Chem. Commun.* **2012**, 5193–5195. b) Rho, H. S.; Oh, S. H.; Lee, J. W.; Lee, J. Y.; Chin, J.; Song, C. E. *Chem. Commun.* **2008**, 1208–1210. c) Dinér, P.; Nielsen, M.; Bertelsen, S.; Niess, B.; Jørgensen, K. A. *Chem. Commun.* **2007**, 3646–3648.
- 10 Wang, J.; Li, H.; Duan, W.; Zu, L.; Wang, W. *Org. Lett.* **2005**, *7*, 4713–4716.
- 11 Malerich, J. P.; Hagihara, K.; Rawal, V. H. *J. Am. Chem. Soc.* **2008**, *130*, 14416–14417.
- 12 a) Schwesinger, R.; Willaredt, J.; Schlemper, H.; Keller, M.; Schmitt, D.; Fritz, H. *Chem. Ber.* **1994**, *127*, 2435–2454. b) Schwesinger, R.; Schlemper, H. *Angew. Chem., Int. Ed.* **1987**, *26*, 1167–1169. c) Schwesinger, R. *Chimia* **1985**, *39*, 269–272.
- 13 Zhang, L.; Nederberg, F.; Pratt, R. C.; Waymouth, R. M.; Hedrick, J. L.; Wade, C. G. *Macromolecules* **2007**, *40*, 4154–4158.
- 14 Kakuchi, T.; Chen, Y.; Kitakado, J.; Mori, K.; Fuchise, K.; Satoh, T. *Macromolecules* **2011**, *44*, 4641–4647.
- 15 Misaka, H.; Sakai, R.; Satoh, T.; Kakuchi, T. *Macromolecules* **2011**, *44*, 9099–9107.
- 16 Uraguchi, D.; Sakaki, S.; Ooi, T. *J. Am. Chem. Soc.* **2007**, *129*, 12392–12393.
- 17 a) Uraguchi, D.; Nakamura, S.; Sasaki, H.; Konakade, Y.; Ooi, T. *Chem. Commun.* **2014**, 3491–3493. b) Uraguchi, D.; Yoshioka, K.; Ueki, Y.; Ooi, T. *J. Am. Chem. Soc.* **2012**, *134*, 19370–19373.
- 18 Núñez, M. G.; Farley, A. J. M.; Dixon, D. J. *J. Am. Chem. Soc.* **2013**, *135*, 16348–16351. <http://pubs.acs.org/doi/abs/10.1021/ja409121s>, further permissions related to the material excerpted should be directed to the ACS.
- 19 Robertson, G. P.; Farley, A. J. M.; Dixon, D. J. *Synlett* **2016**, 21–24.

-
- 20 Yang, J.; Farley, A. J. M.; Dixon, D. J. *Chem. Sci.* **2017**, *8*, 606–610.
- 21 Jakab, G.; Tancon, C.; Zhang, Z.; Lippert, K. M.; Schreiner, P. R. *Org. Lett.* **2012**, *14*, 1724–1727.
- 22 Chinchilla, R.; Nájera, C.; Sánchez -Agulló, P. *Tetrahedron Asymmetry* **1994**, *5*, 1393–1402.
- 23 a) Corey, E. J.; Grogan, M. J. *Org. Lett.* **1999**, *1*, 157–160. b) Shen, J.; Nguyen, T. T.; Goh, Y.-P.; Ye, W.; Fu, X.; Xu, J.; Tan, C.-H. *J. Am. Chem. Soc.* **2006**, *128*, 13692–13693.
- 24 Ishikawa, T.; Araki, Y.; Kumamoto, T.; Seki, H.; Fukudac, K.; Isobeac, T. *Chem. Commun.* **2001**, 245–246.
- 25 O'Donnell, M. J.; Bennett, W. D.; Bruder, W. A.; Jacobsen, W. N.; Knuth, K.; LeClef, B.; Polt, R. L.; Bordwell, F. G.; Mrozack, S. R.; Cripe, T. A. *J. Am. Chem. Soc.* **1988**, *110*, 8520–8525.
- 26 a) Bandar, J. S.; Lambert, T. H. *J. Am. Chem. Soc.* **2013**, *135*, 11799–11802. b) Bandar, J. S.; Lambert, T. H. *J. Am. Chem. Soc.* **2012**, *134*, 5552–5555.
- 27 Bandar, J. S.; Barthelm, A.; Mazori, A. Y.; Lambert, T. H. *Chem. Sci.* **2015**, *6*, 1537–1547.
- 28 We have developed a more efficient synthesis of this compound starting from mono-*N*-Boc protected diamino cyclohexane. See: Experimental section compound **3.74**.
- 29 a) Mucha, A.; Kafarski, P.; Berlicki, Ł. *J. Med. Chem.* **2011**, *54*, 5955–5980. b) Viso, A.; Fernández de la Pradilla, R.; García, A.; Flores, A. *Chem. Rev.* **2005**, *105*, 3167–3196. c) Lejczak, B.; Kafarski, P.; Zygmunt, J. *Biochemistry* **1989**, *28*, 3549–3555.
- 30 a) Alonso, E.; Alonso, E.; Solis, A.; del Pozo, C. *Synlett* **2000**, 698–700. b) Camp, N. P.; Hawkins, P. C. D.; Hitchcock, P. B.; Gani, D. *Bioorg. Med. Chem. Lett.* **1992**, *2*, 1047–1052.
- 31 Momo, R. D.; Fini, F.; Bernardi, L.; A. Ricci. *Adv. Synth. Catal.* **2009**, *351*, 2283–2287.
- 32 Kobayashi, S.; Yazaki, R.; Seki, K.; Yamashita, Y. *Angew. Chem., Int. Ed.* **2008**, *47*, 5613–5615.
- 33 a) Ooi, T.; Kameda, M.; Taniguchi, M.; Maruoka, K. *J. Am. Chem. Soc.* **2004**, *126*, 9685–9694. b) Trost, B. M.; Miede, F. *J. Am. Chem. Soc.* **2014**, *136*, 3016–3019.

34 Campa, R.; Irene Ortín, I.; Dixon, D. J. *Angew. Chem., Int. Ed.* **2015**, *54*, 4895–4898.

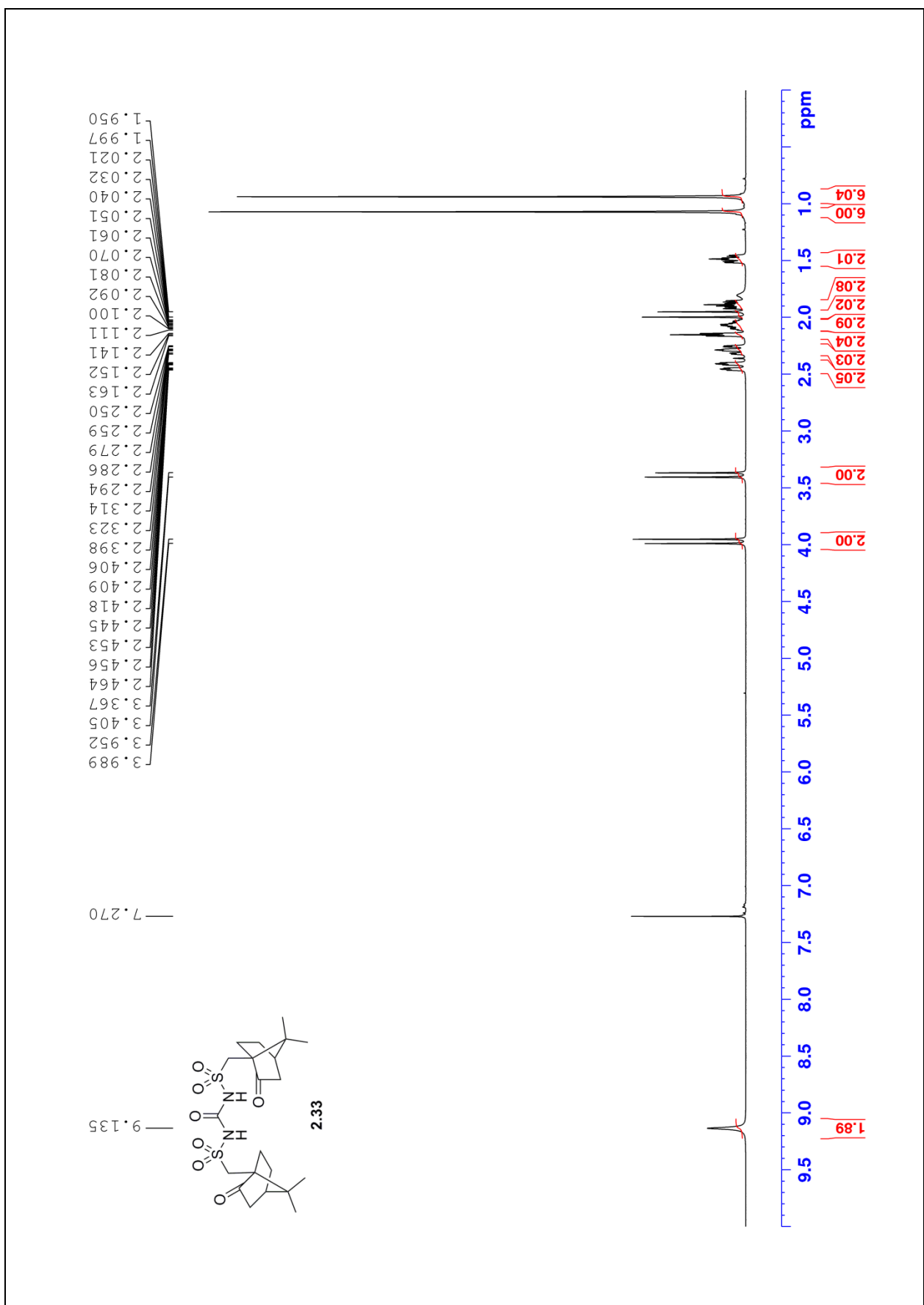
35 Xue, M. X.; Guo, C.; Gong, L. Z. *Synlett* **2009**, 2191–2197.

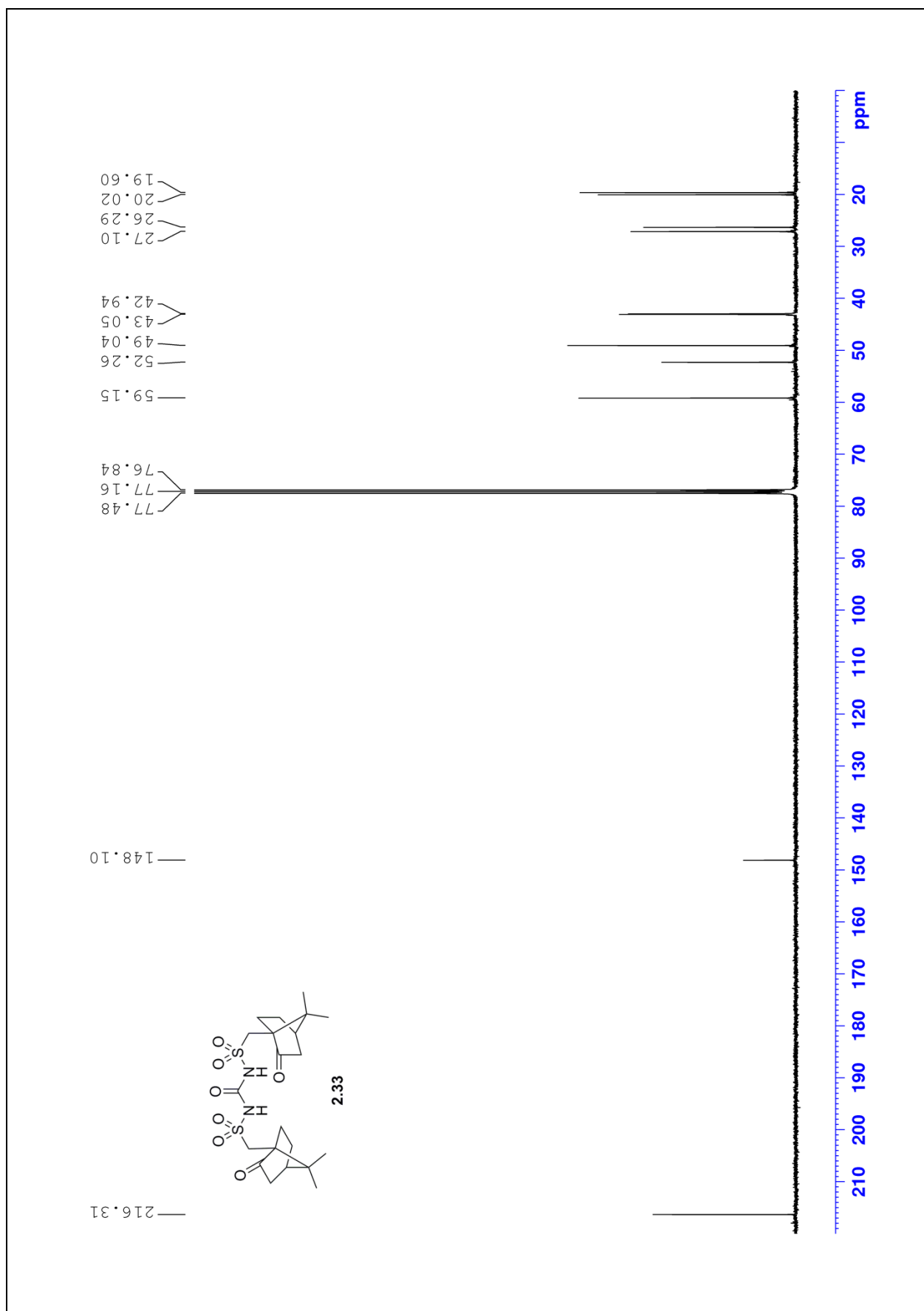
36 Verma, S. K.; Acharya, B. N.; Kaushik, M. P. *Org. Lett.* **2010**, *12*, 4232–4235.

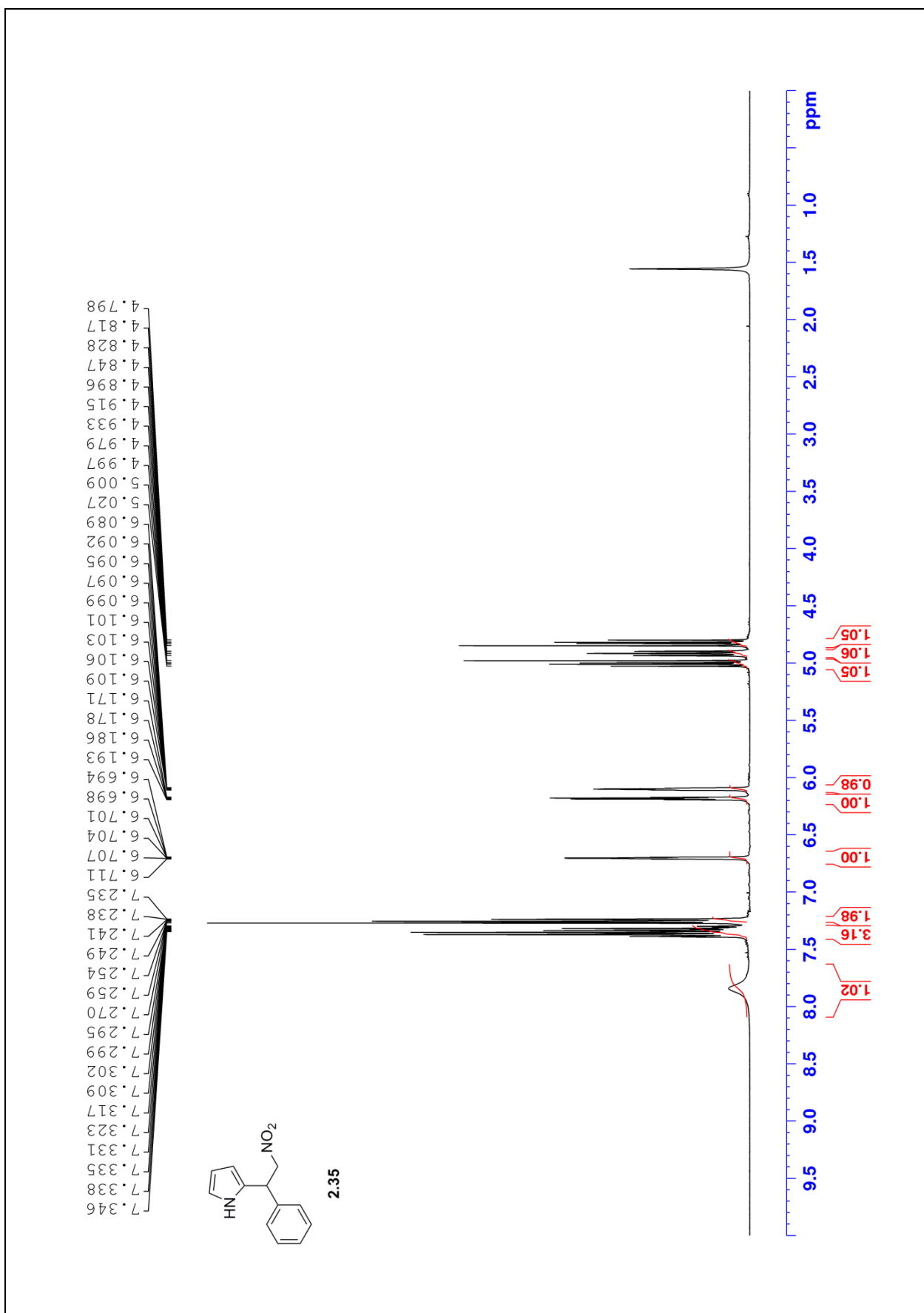
37 Sarkar, D.; Harman, K.; Ghosh, S.; Headley, A. D. *Tetrahedron: Asymmetry* **2011**, *22*, 1051–1054.

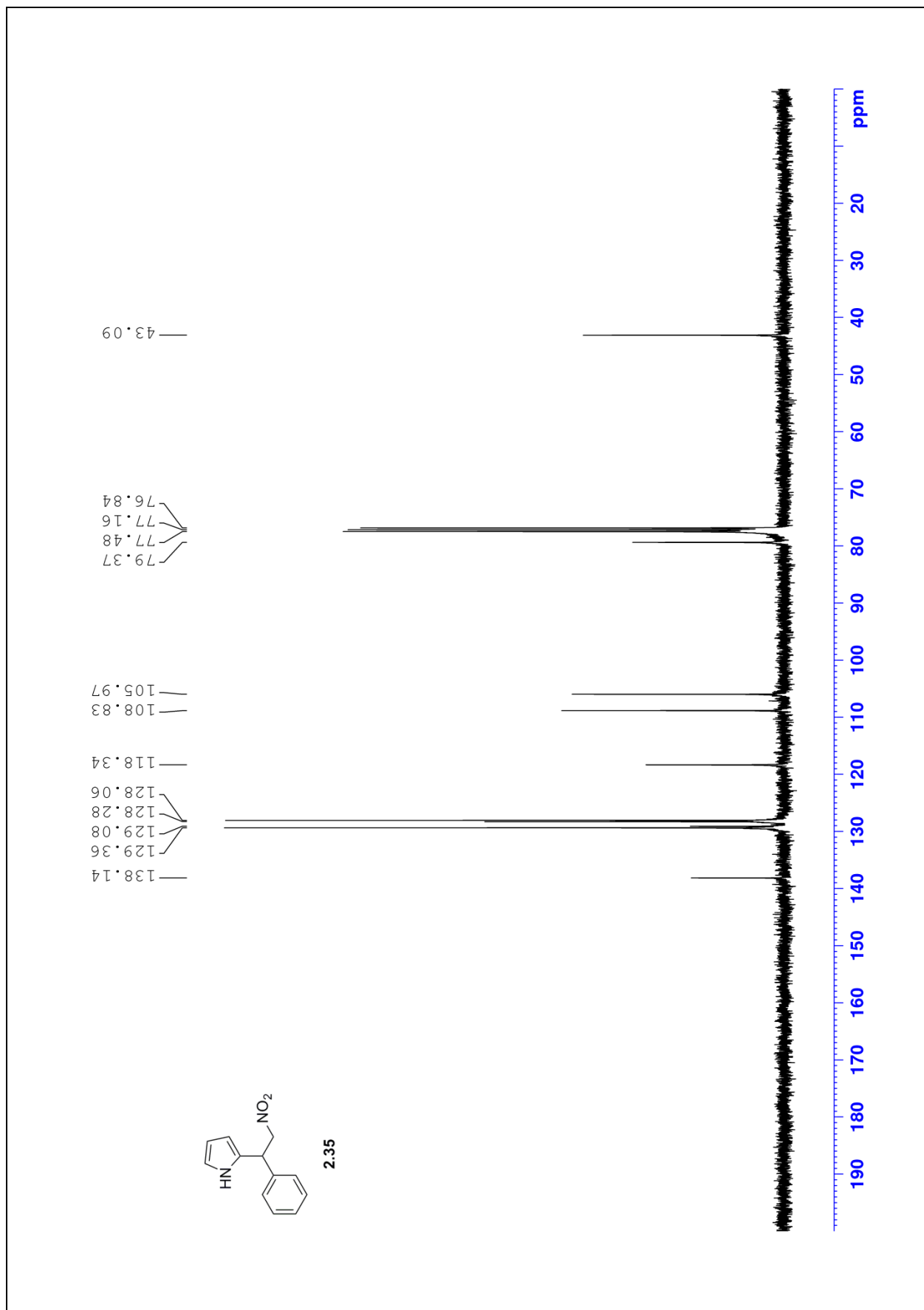
Appendix 1

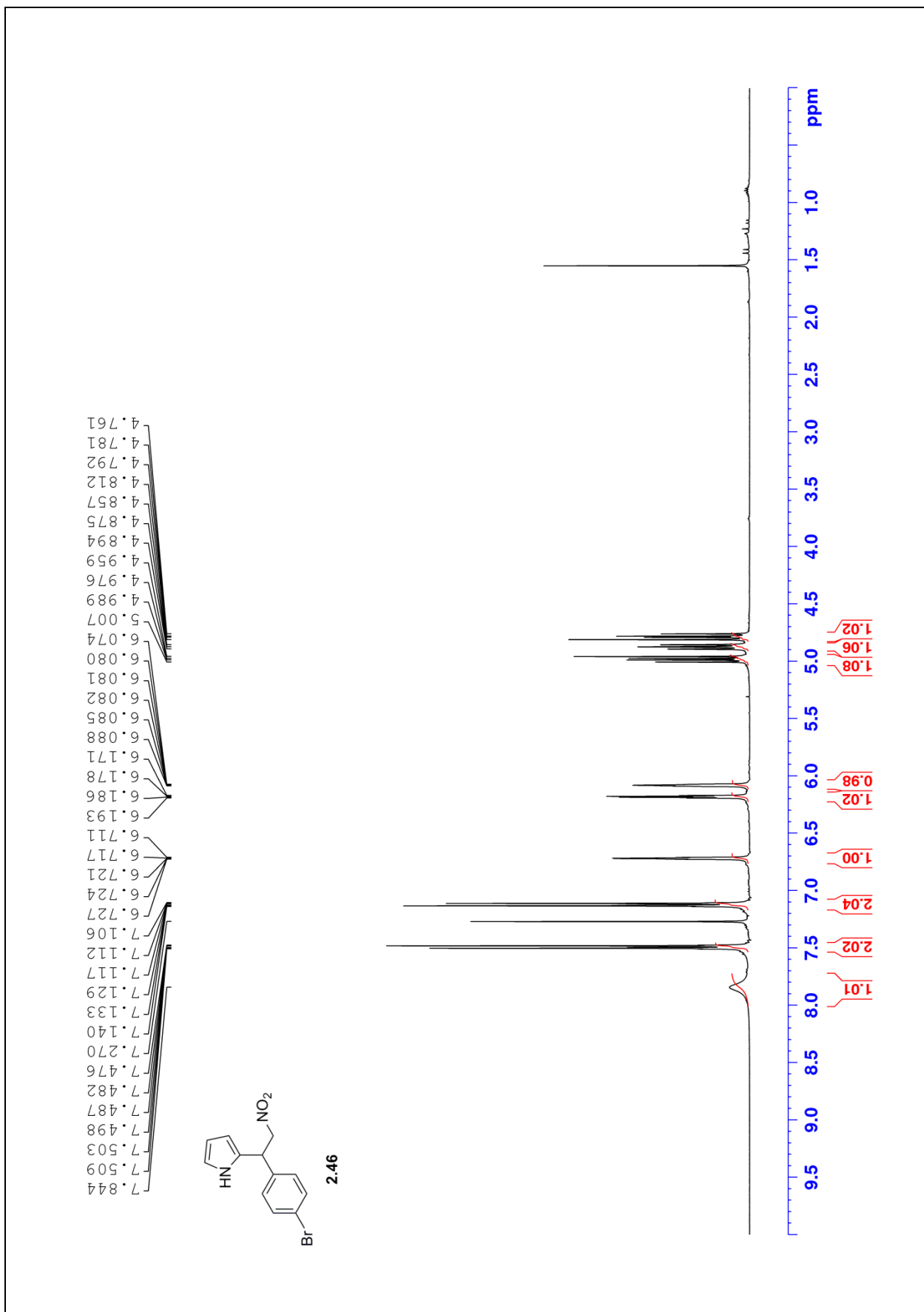
NMRs

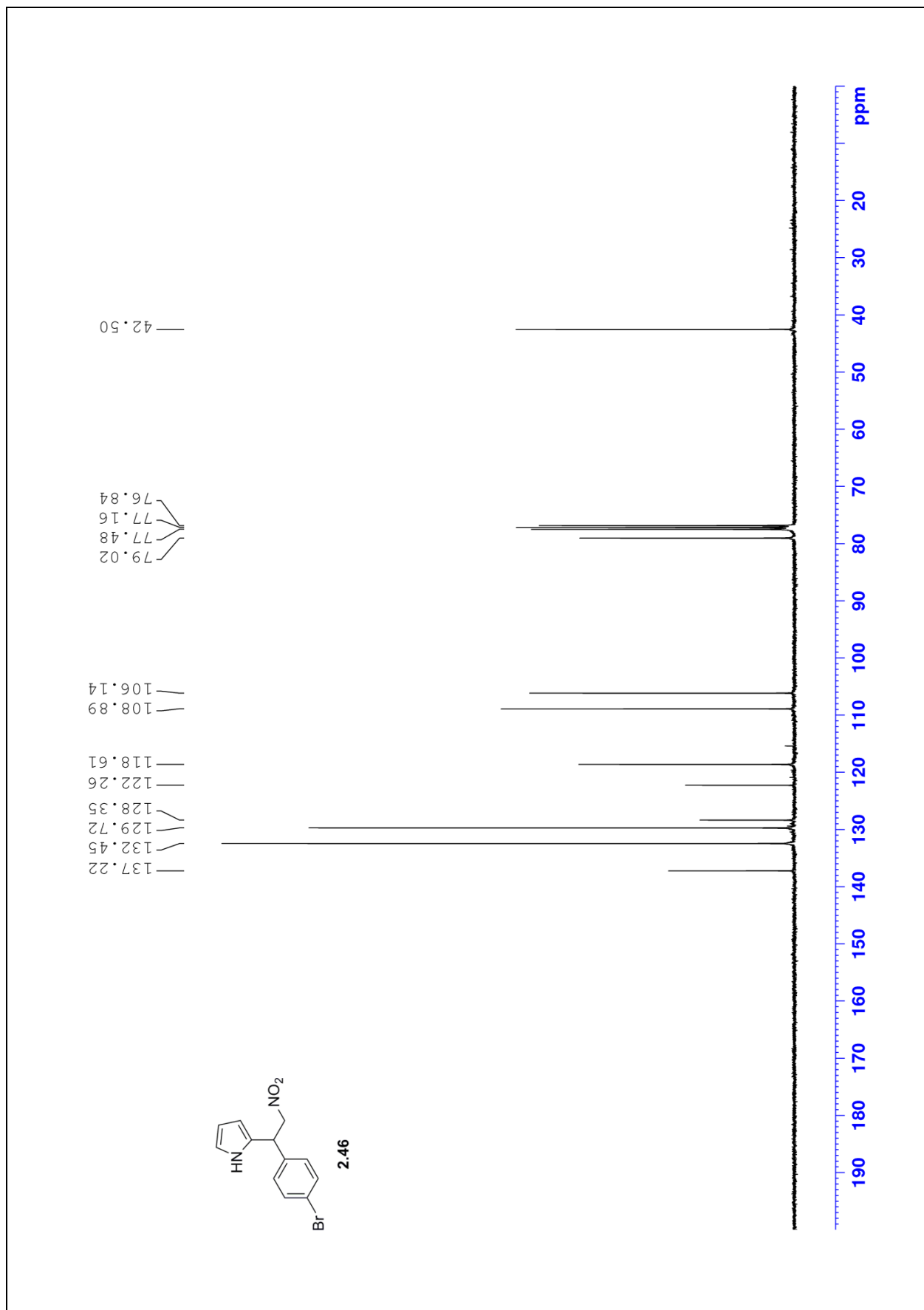


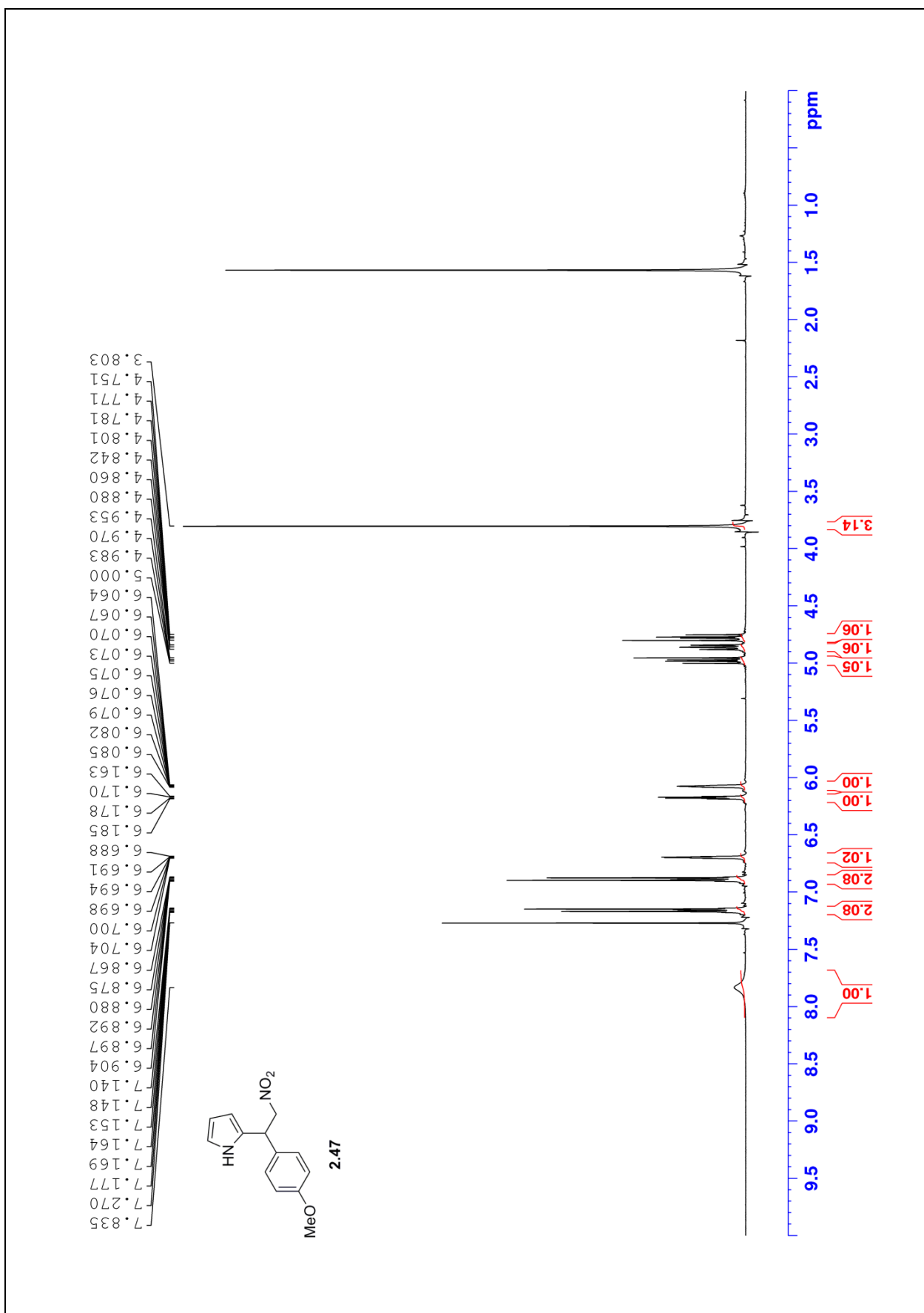


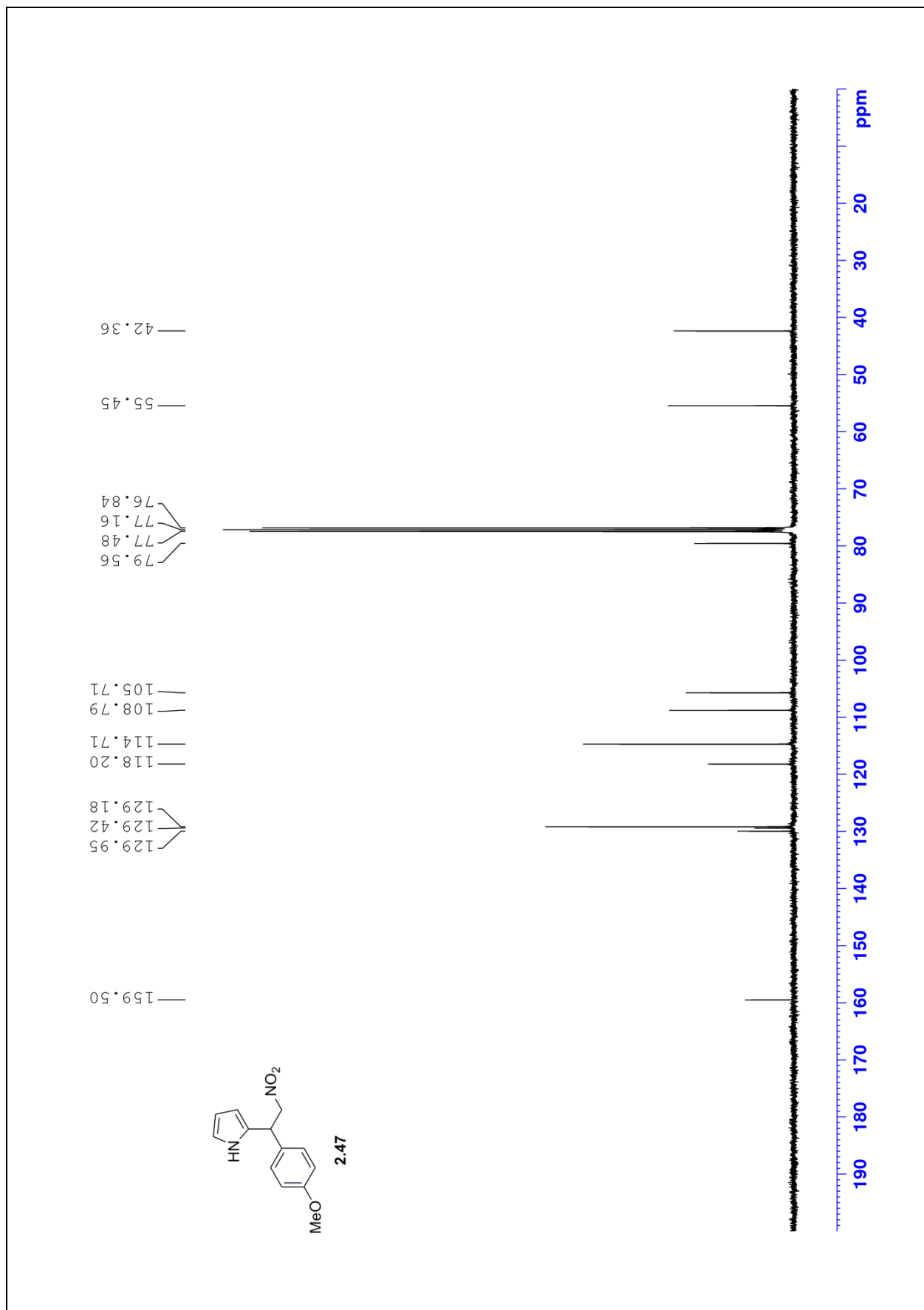


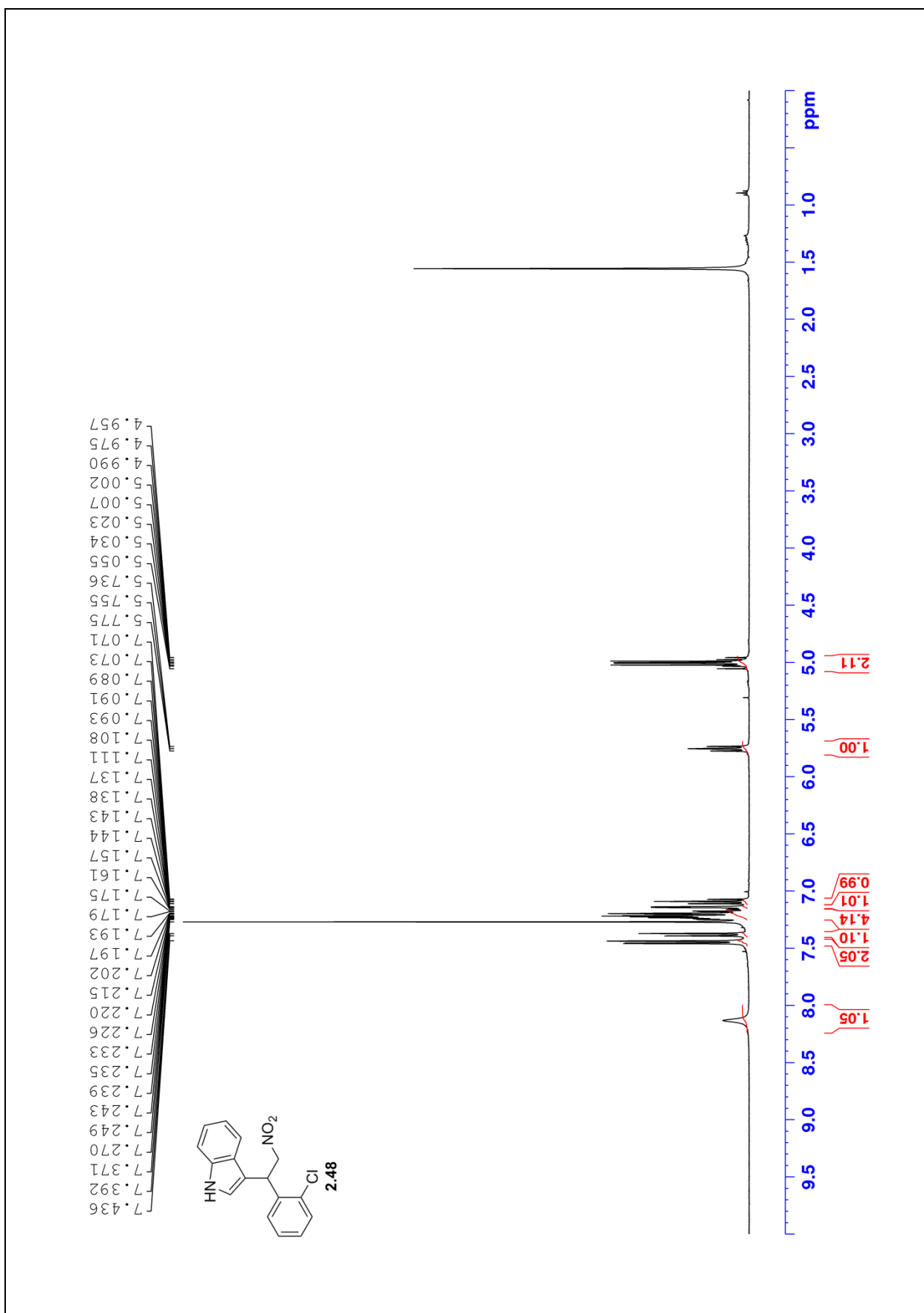


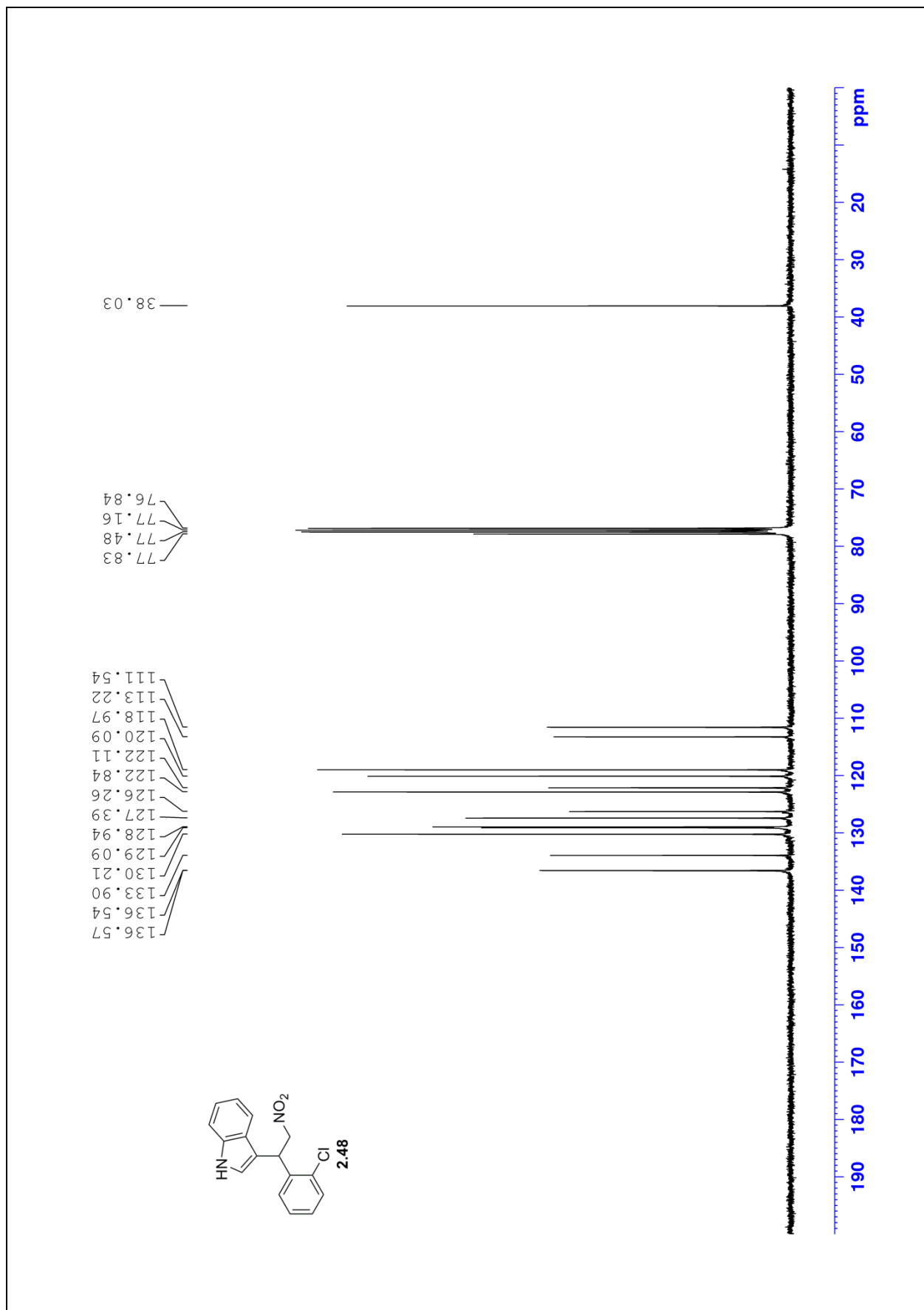


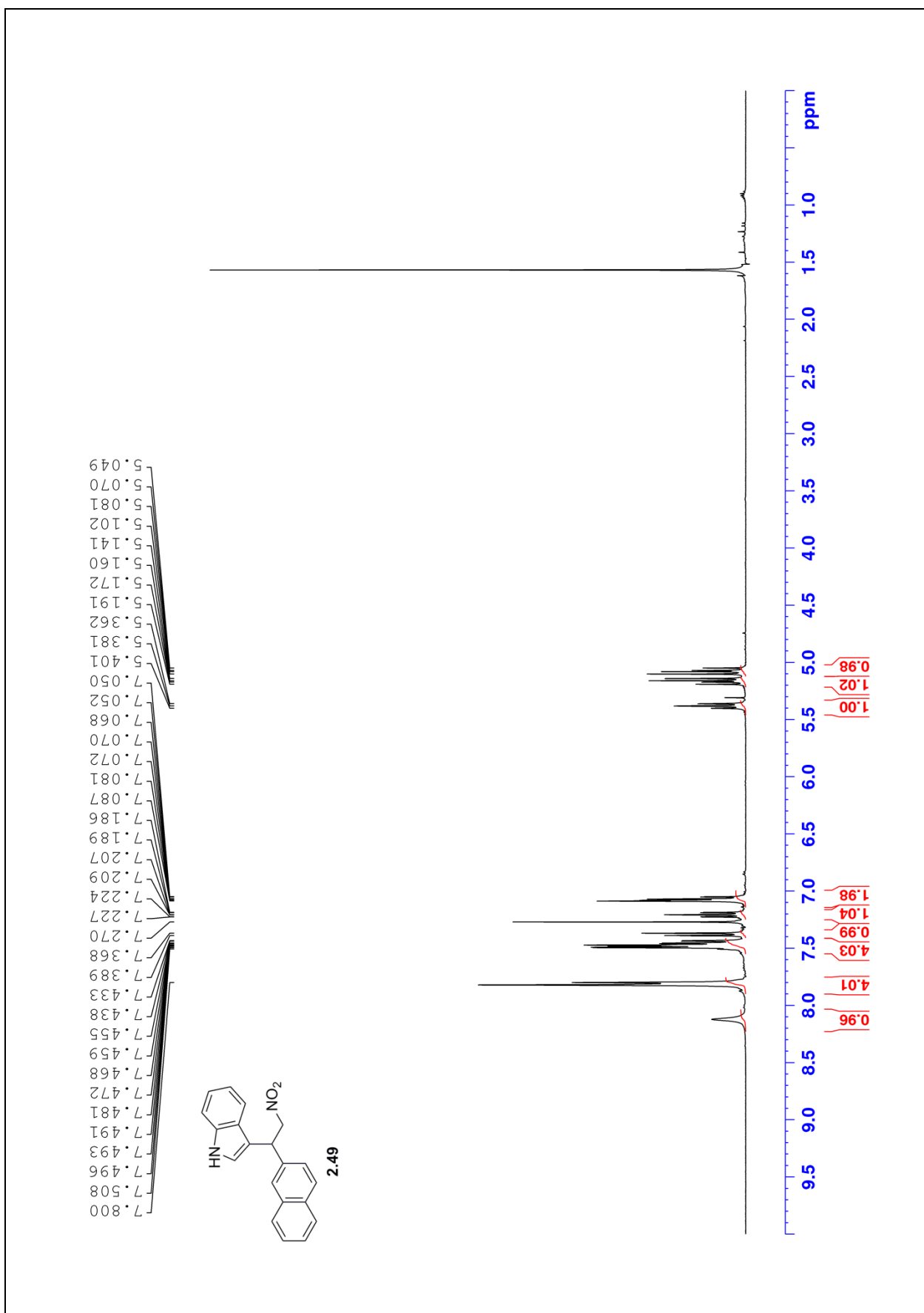


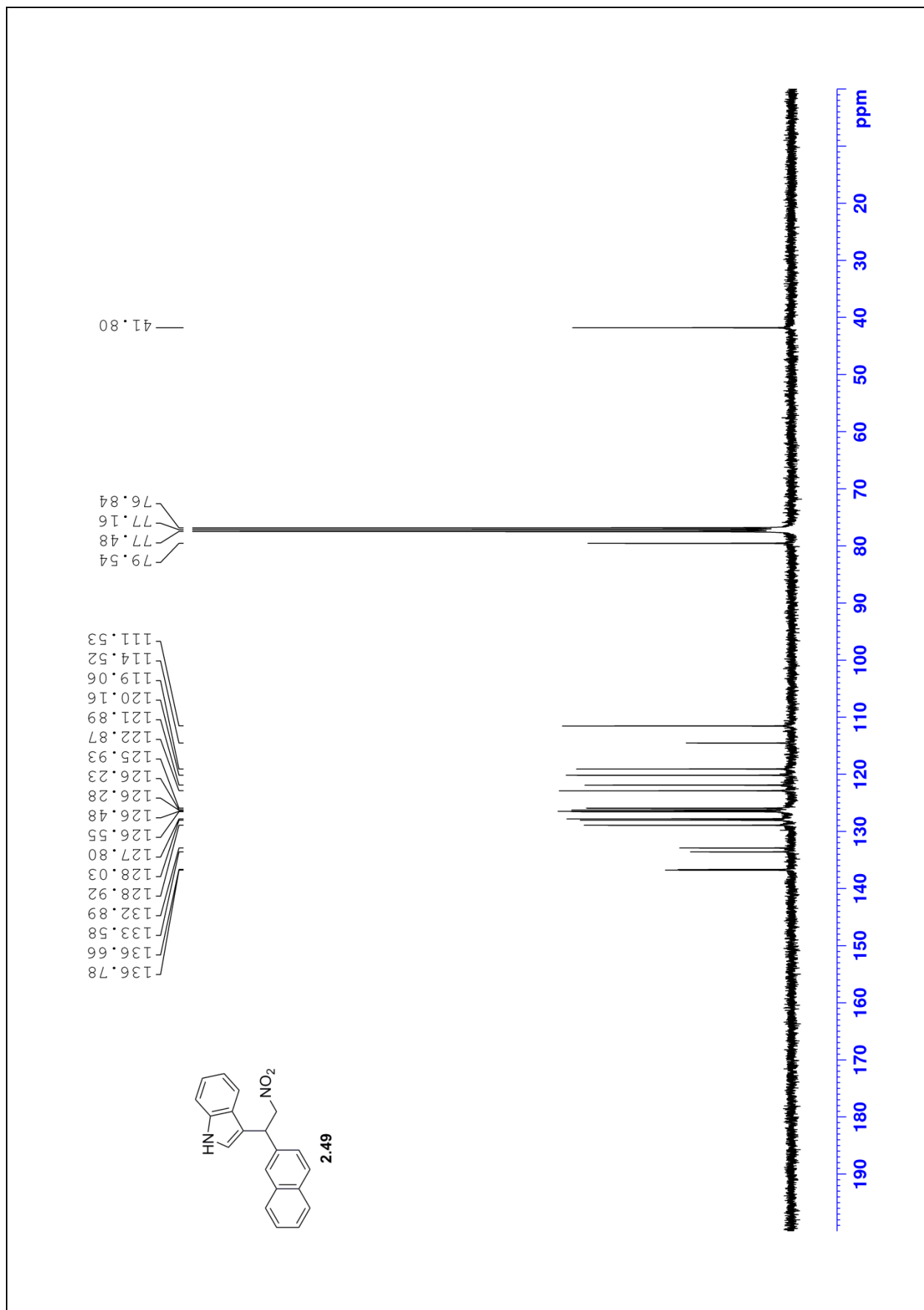


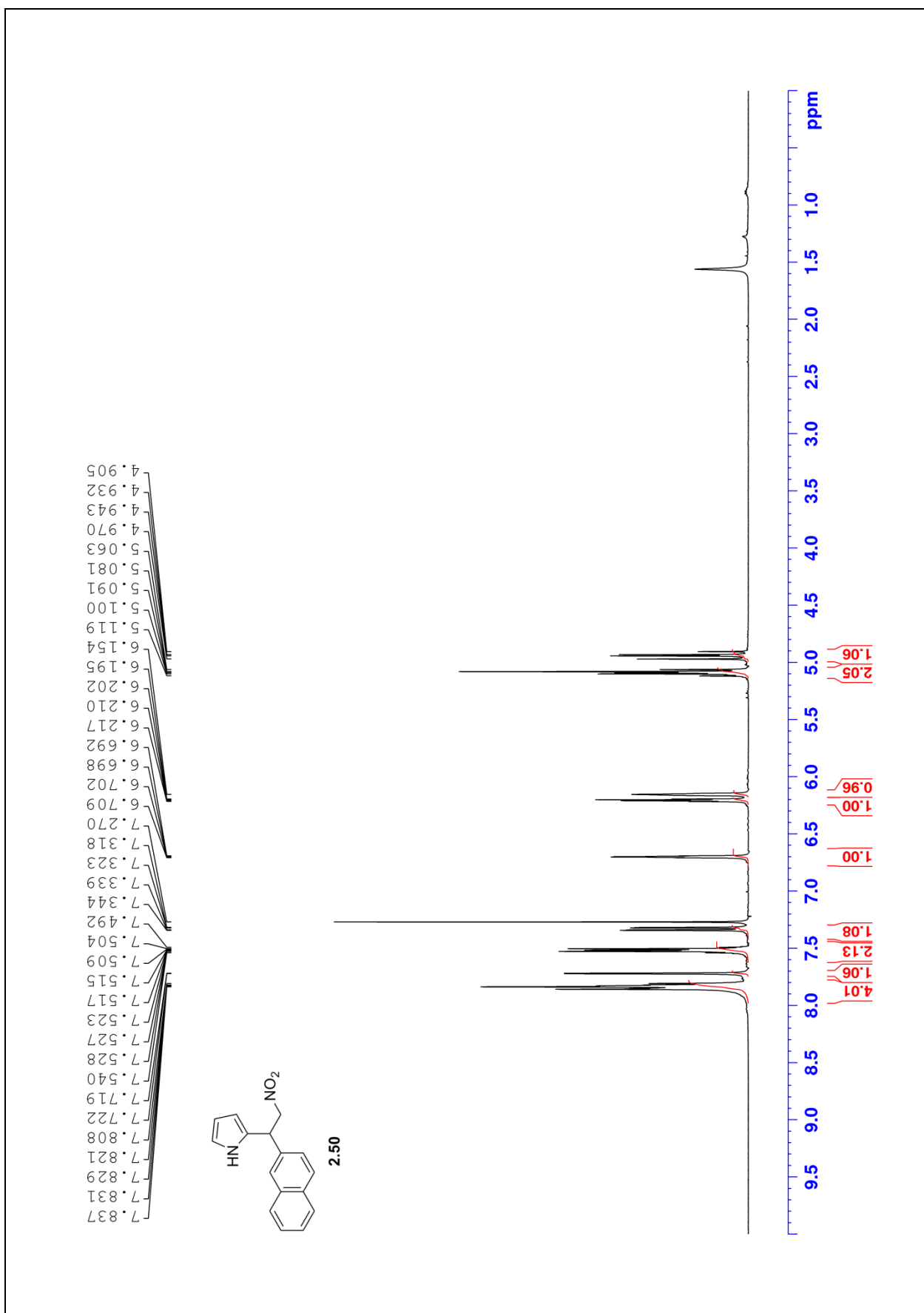


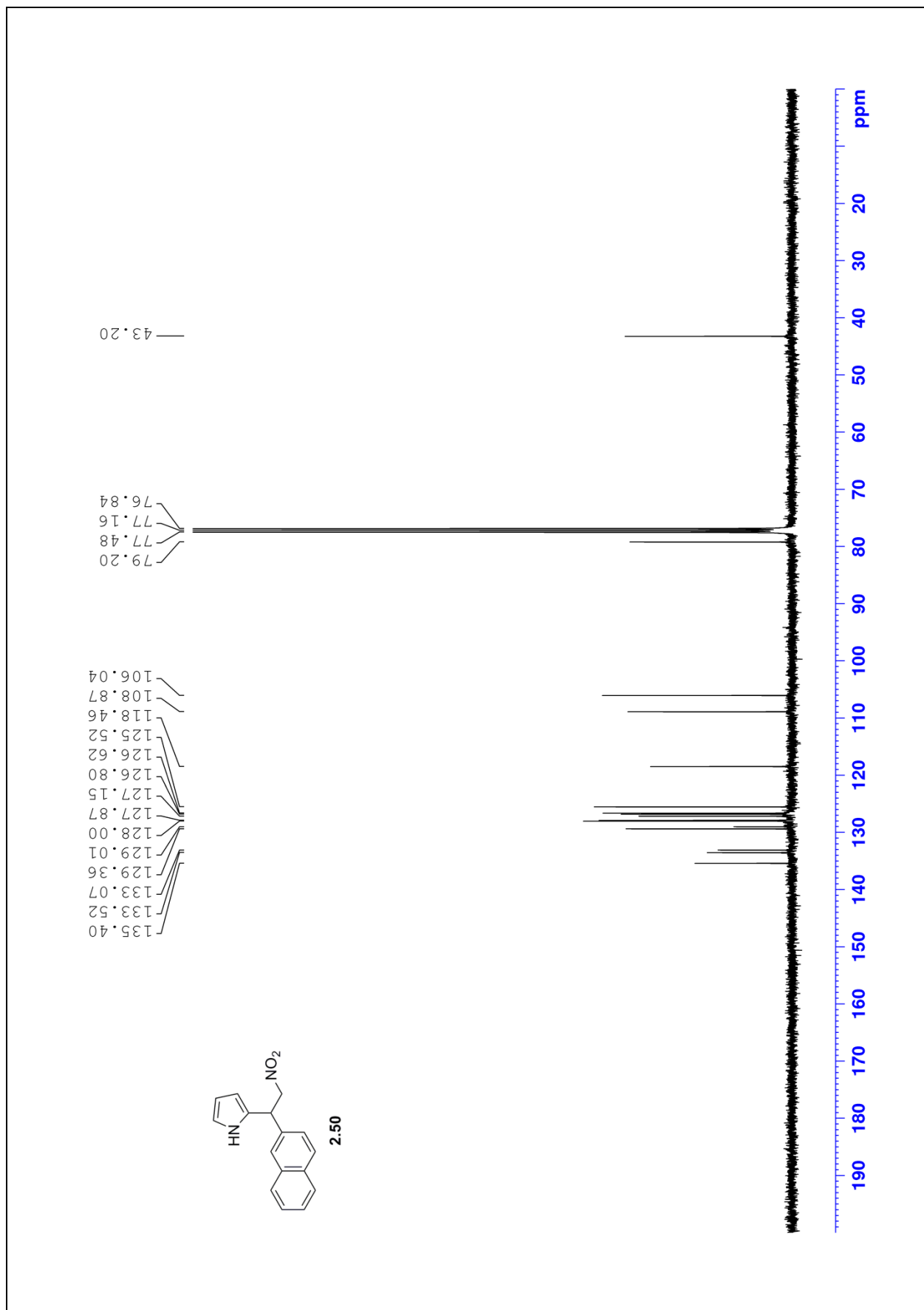


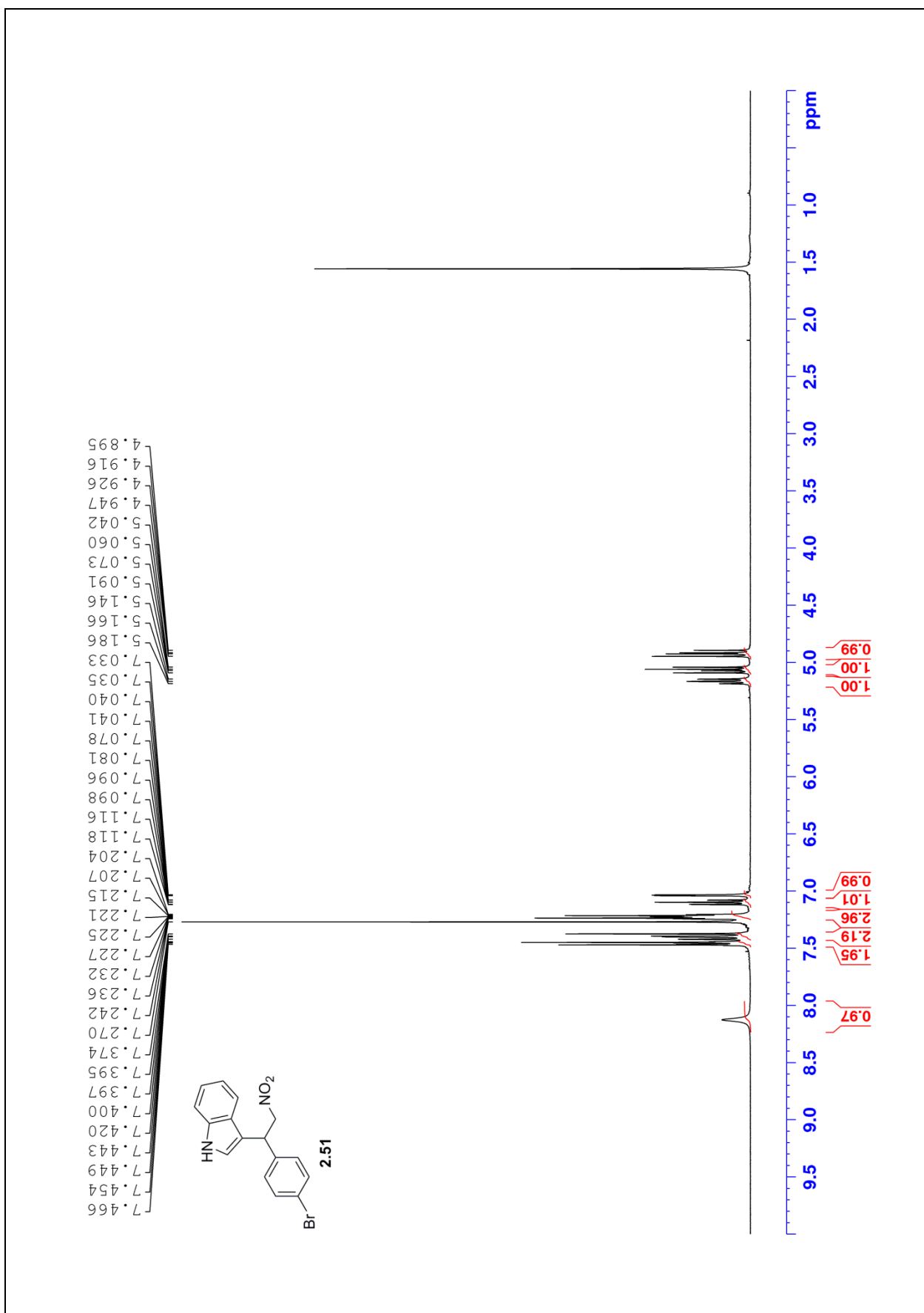


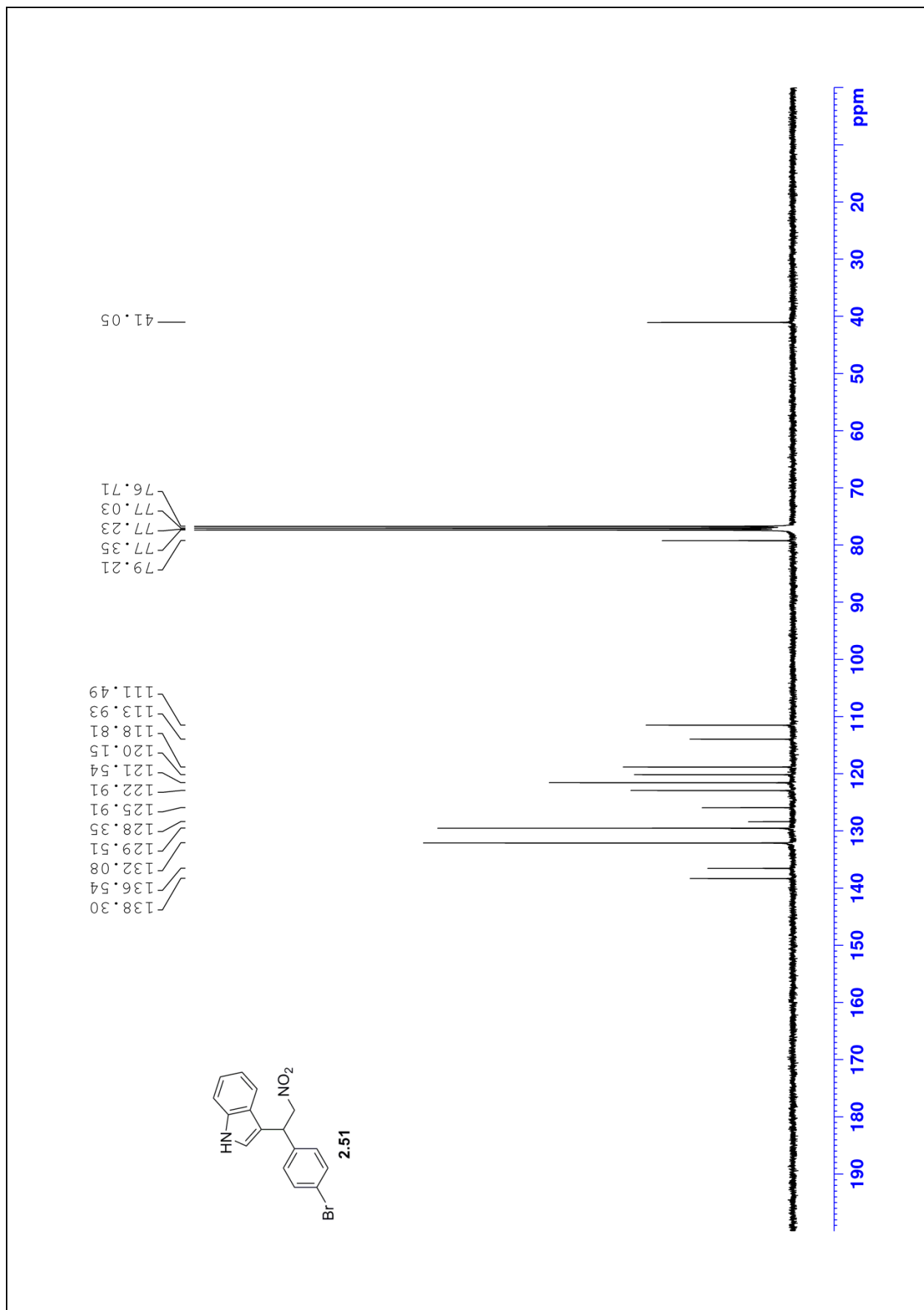


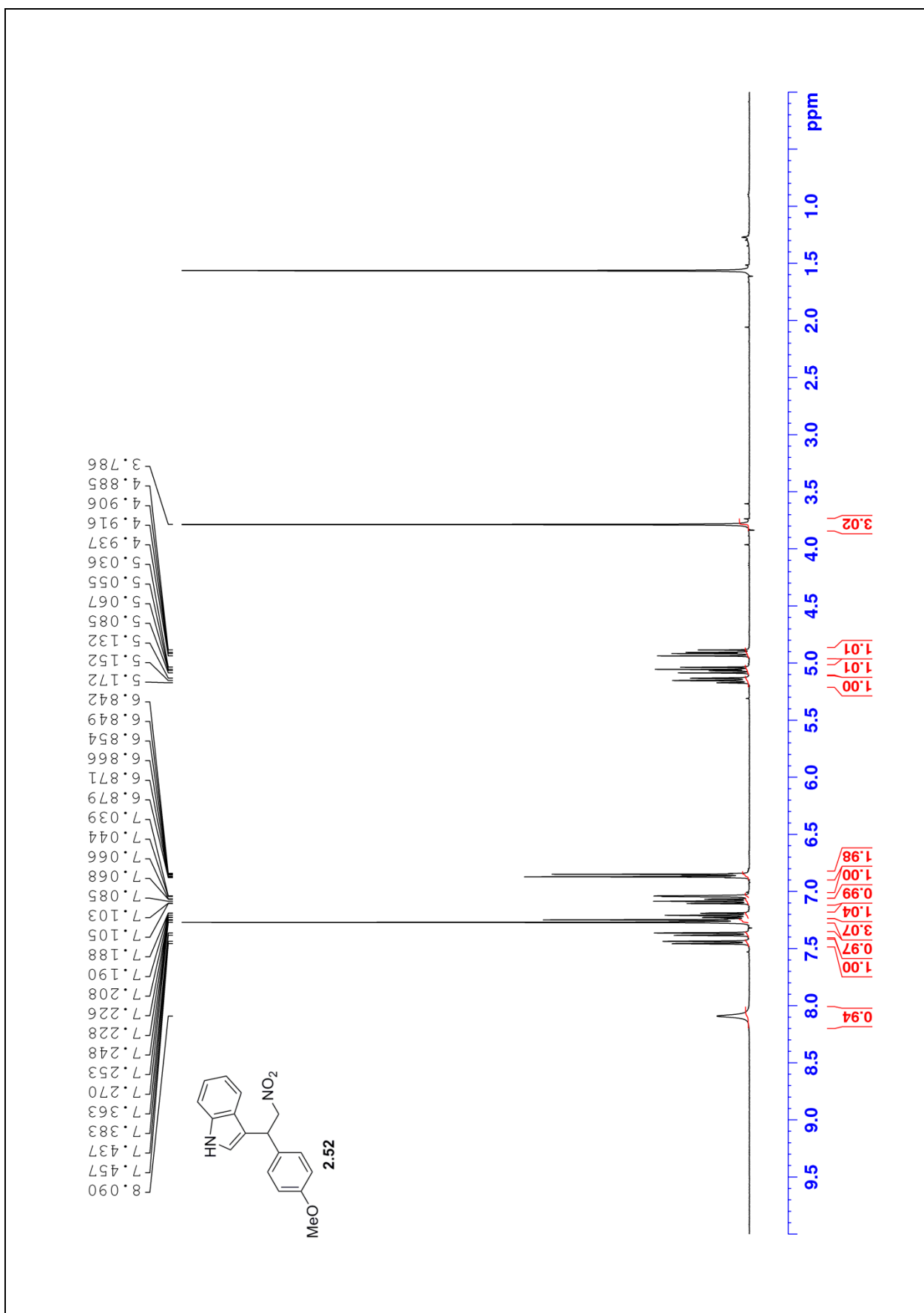


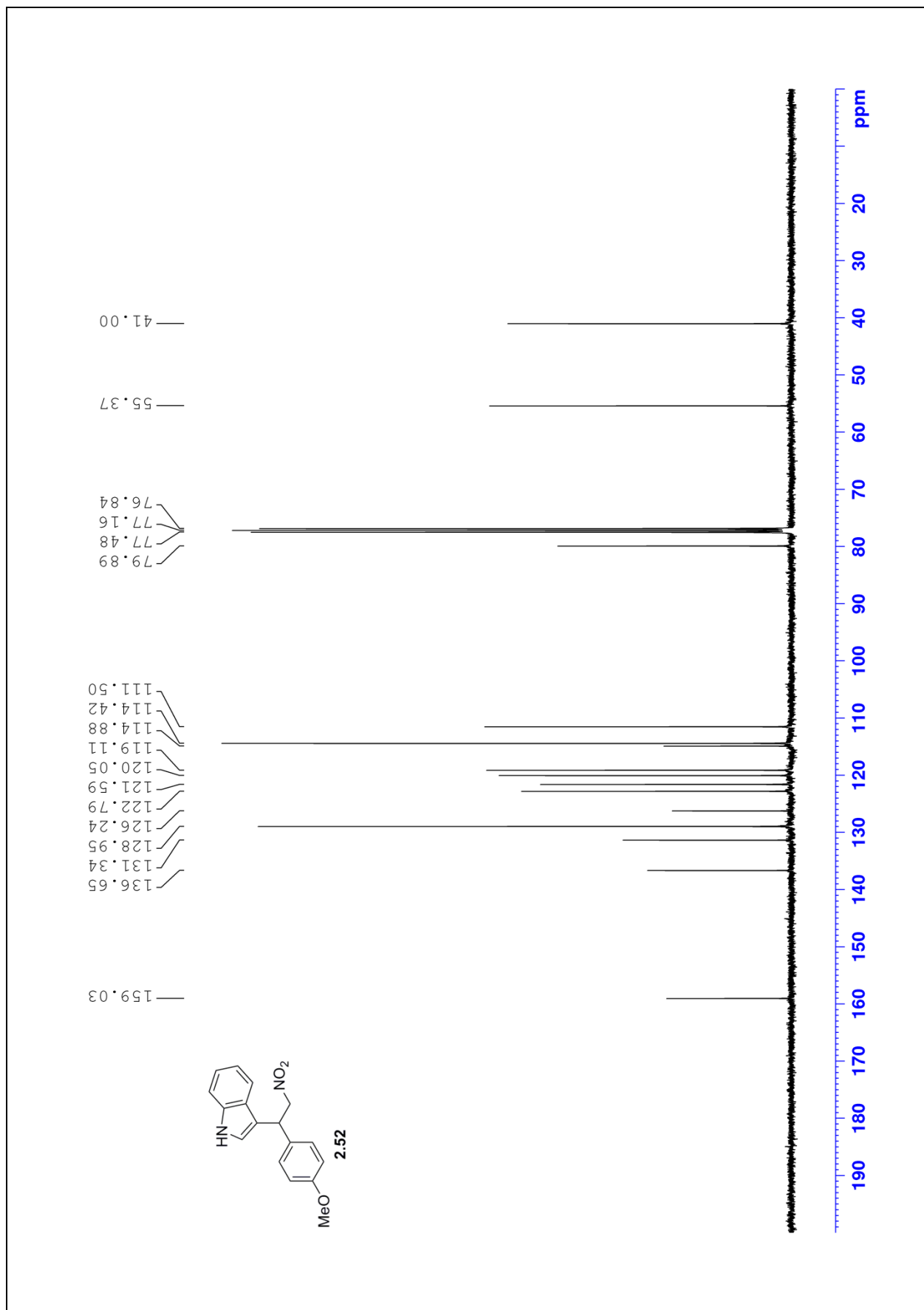


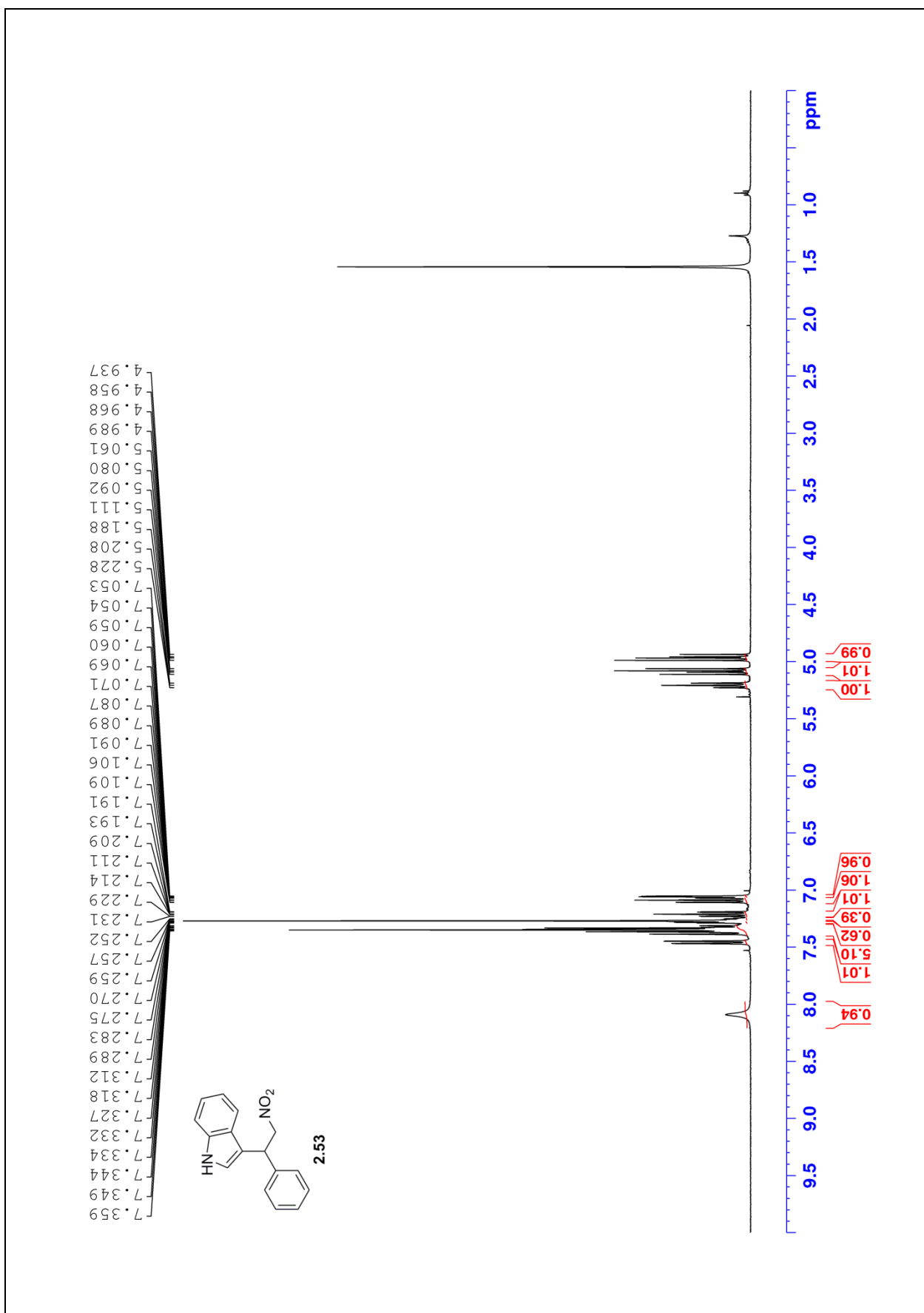


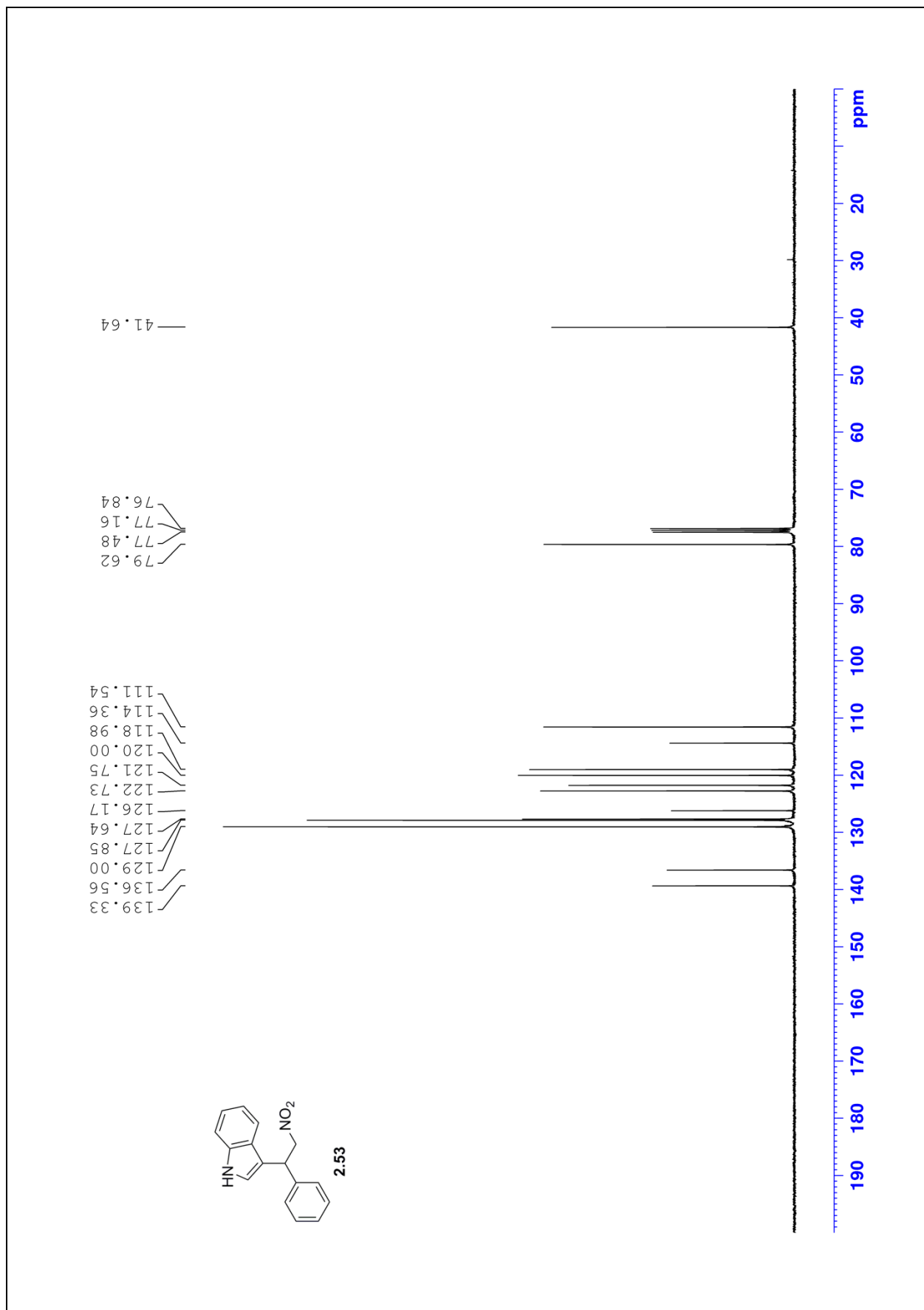


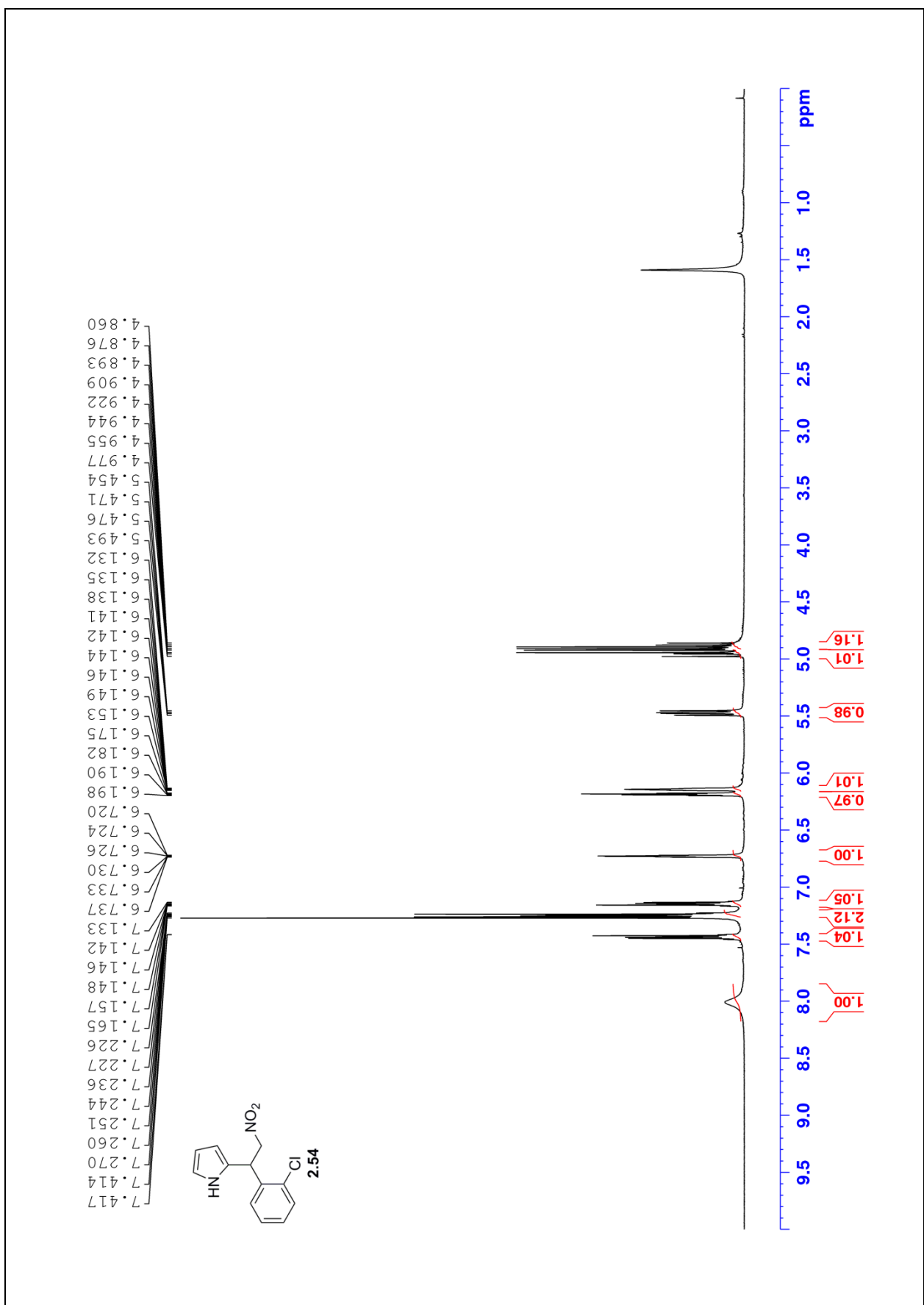


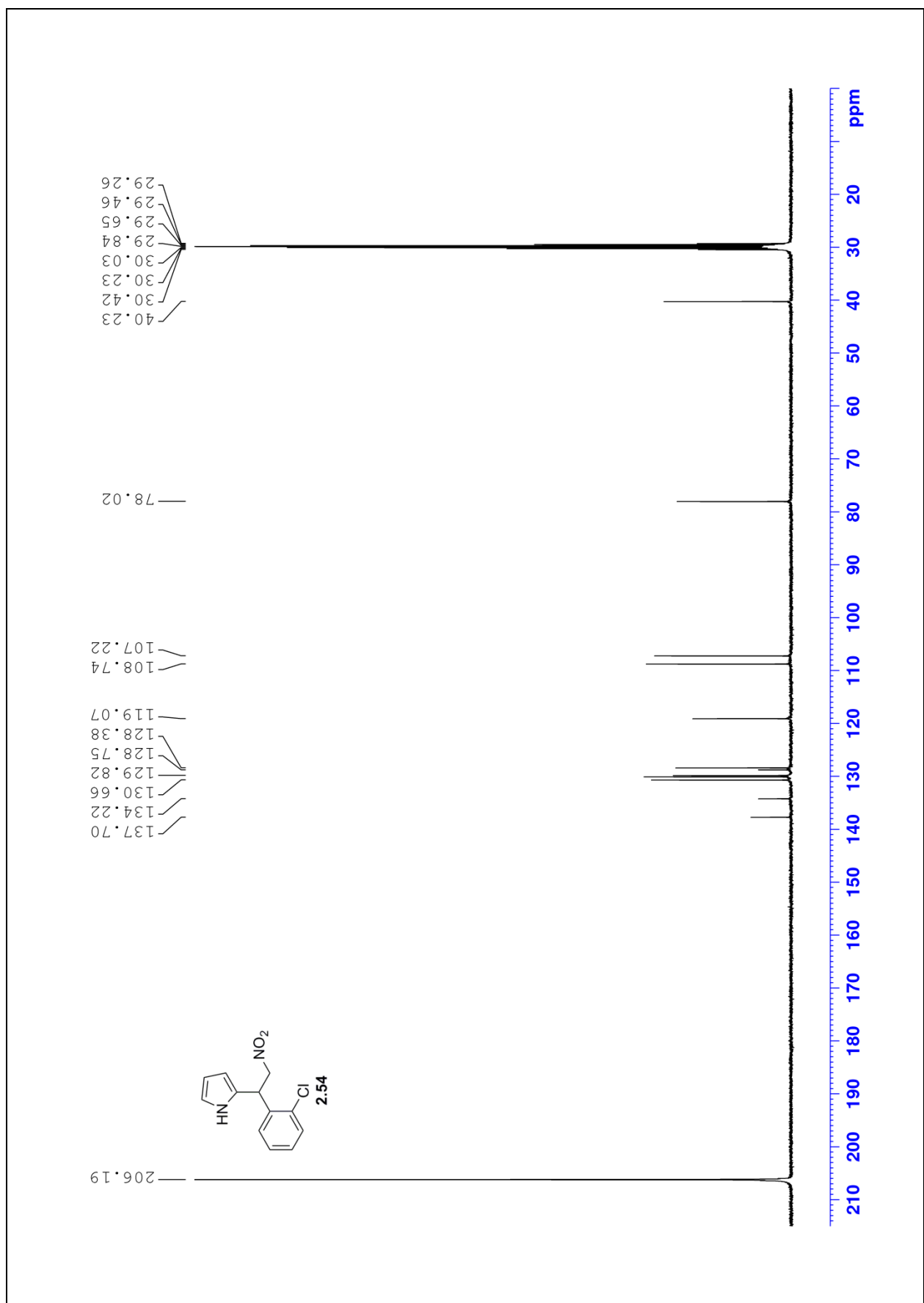


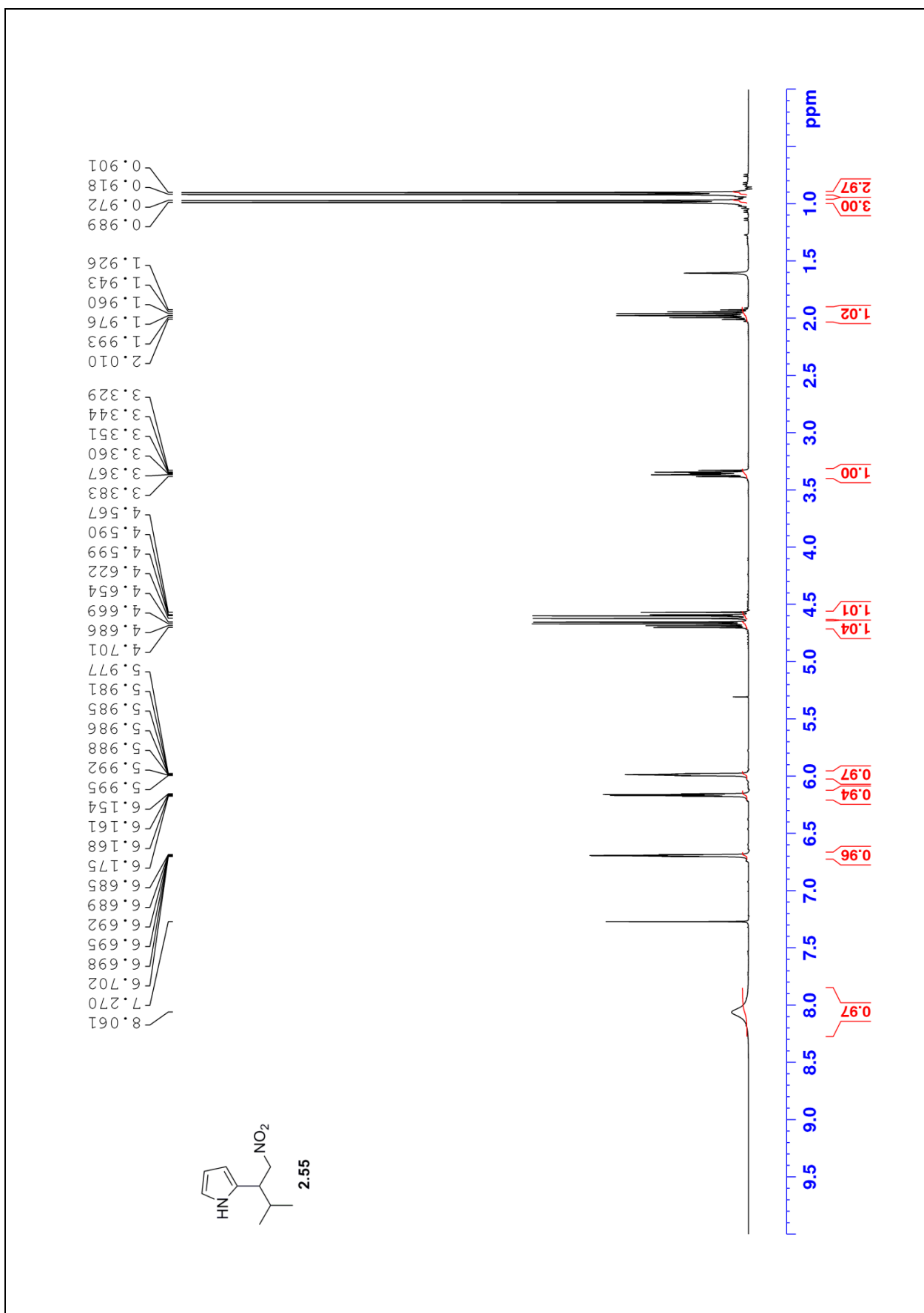


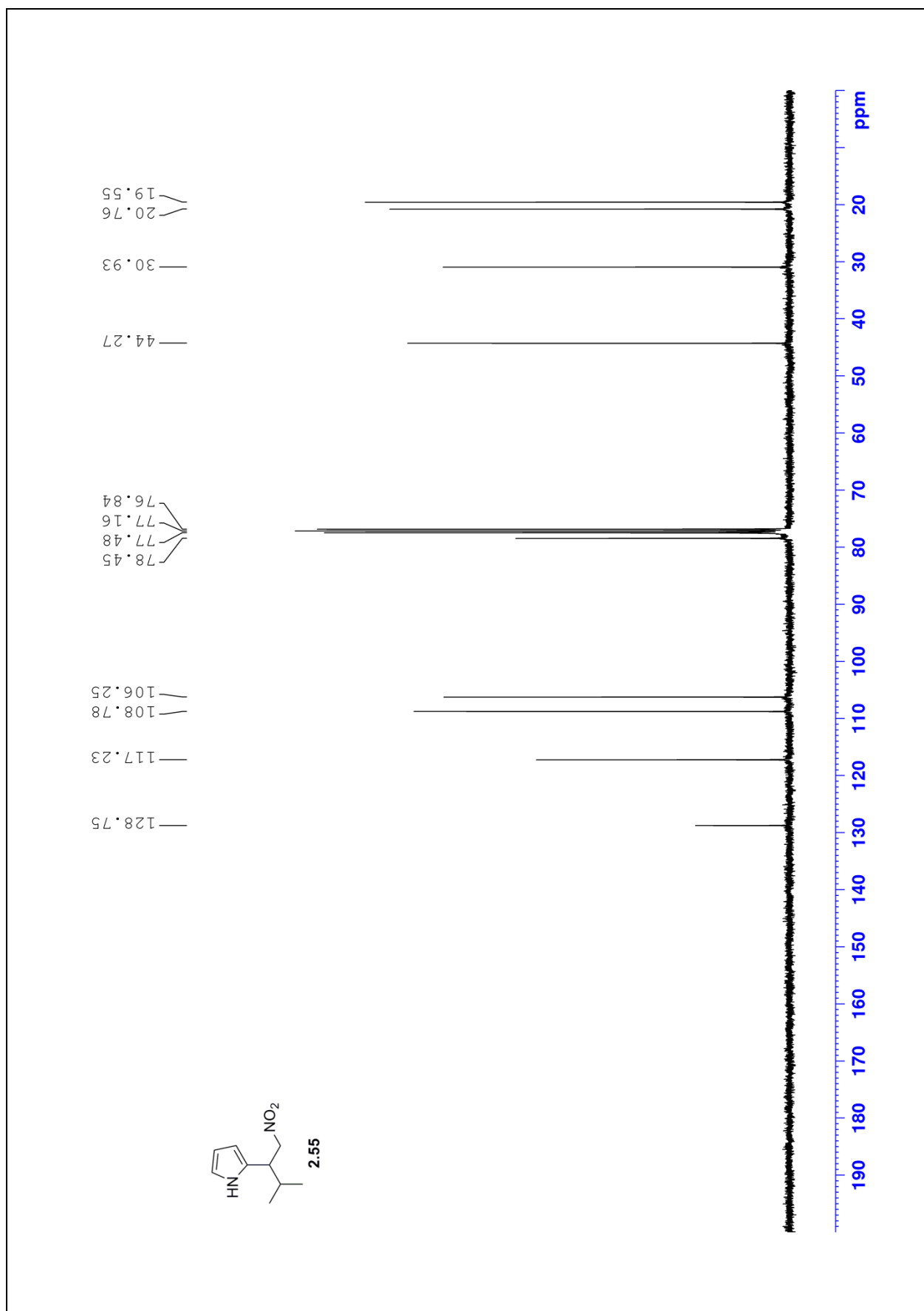


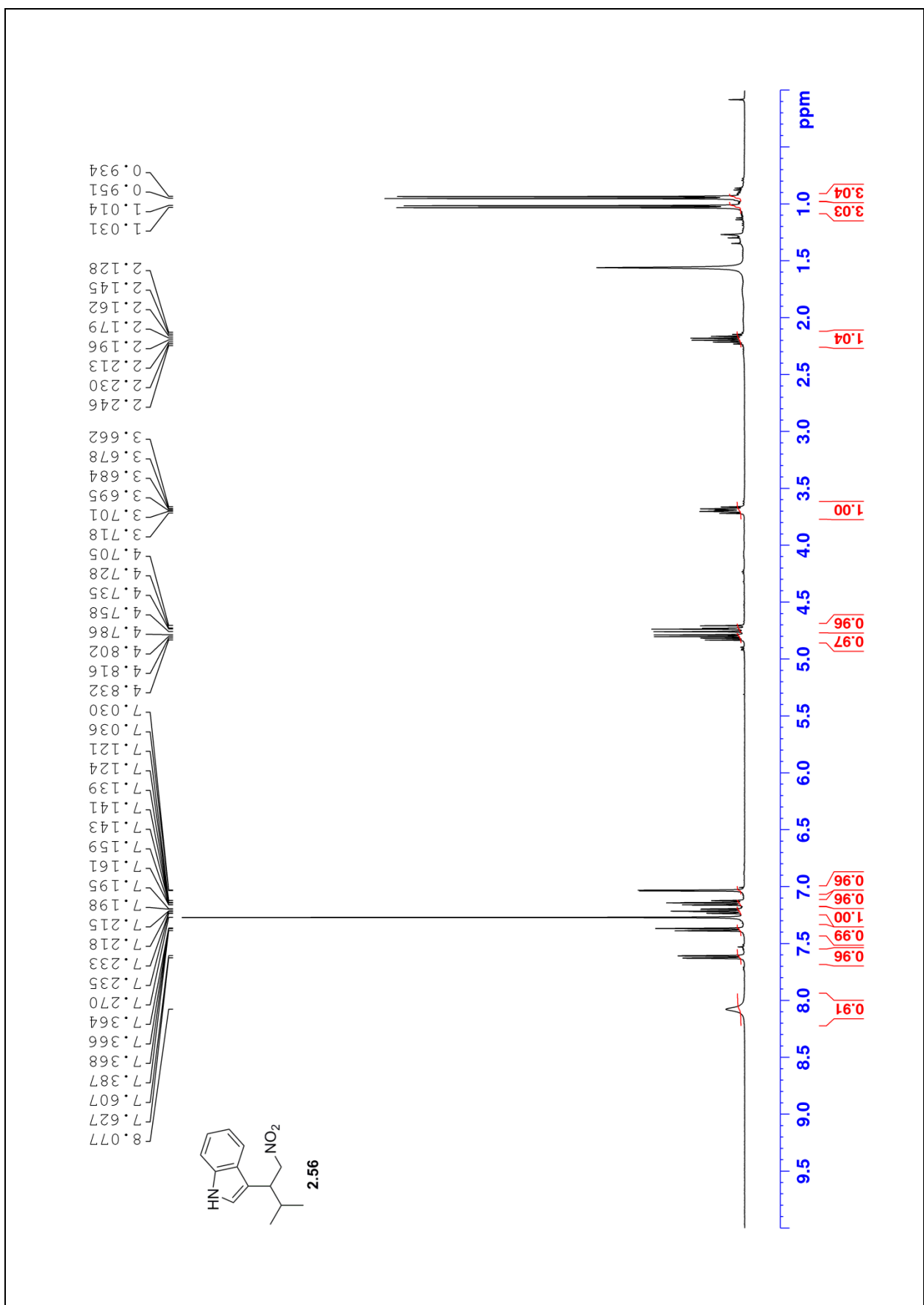


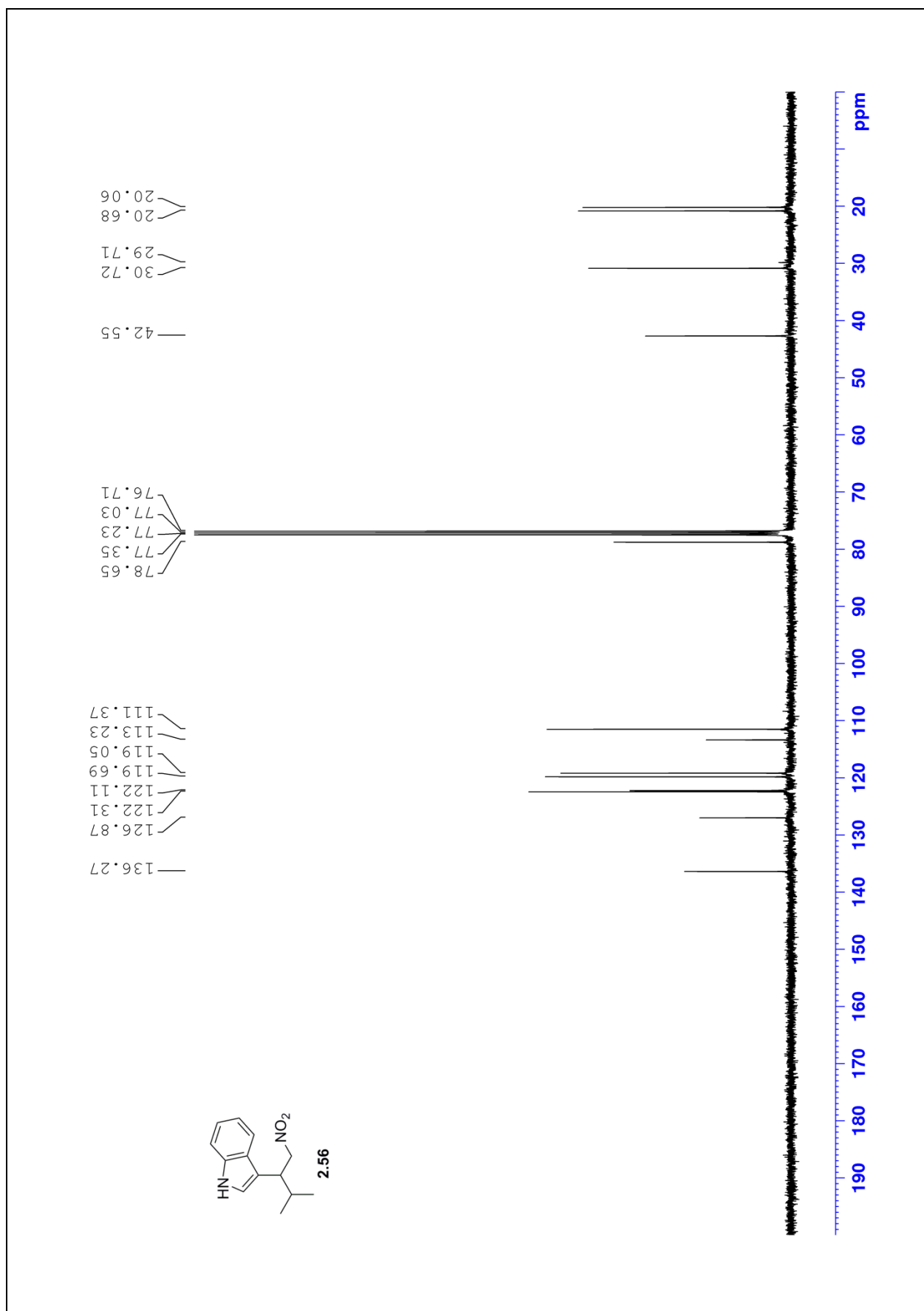


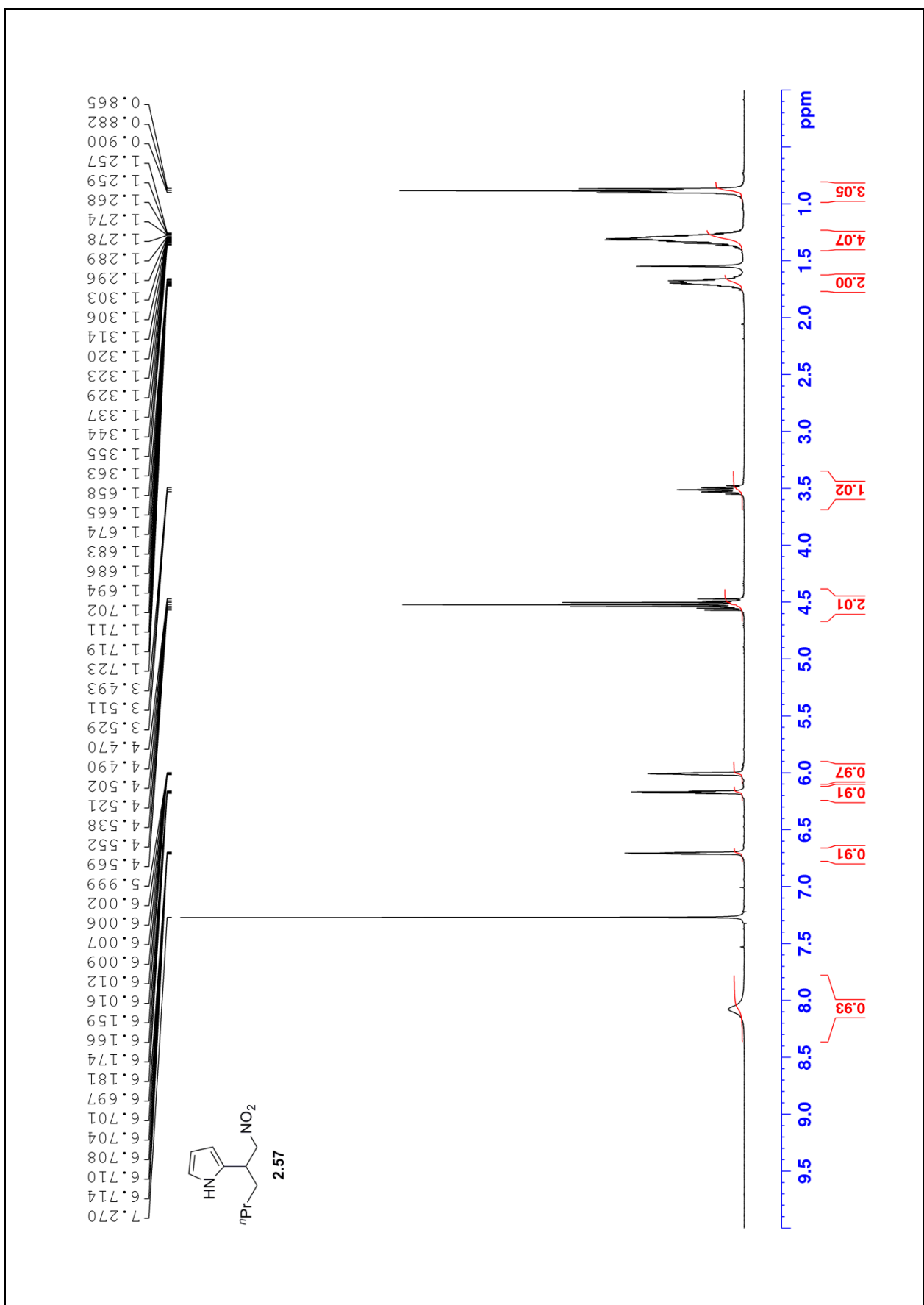


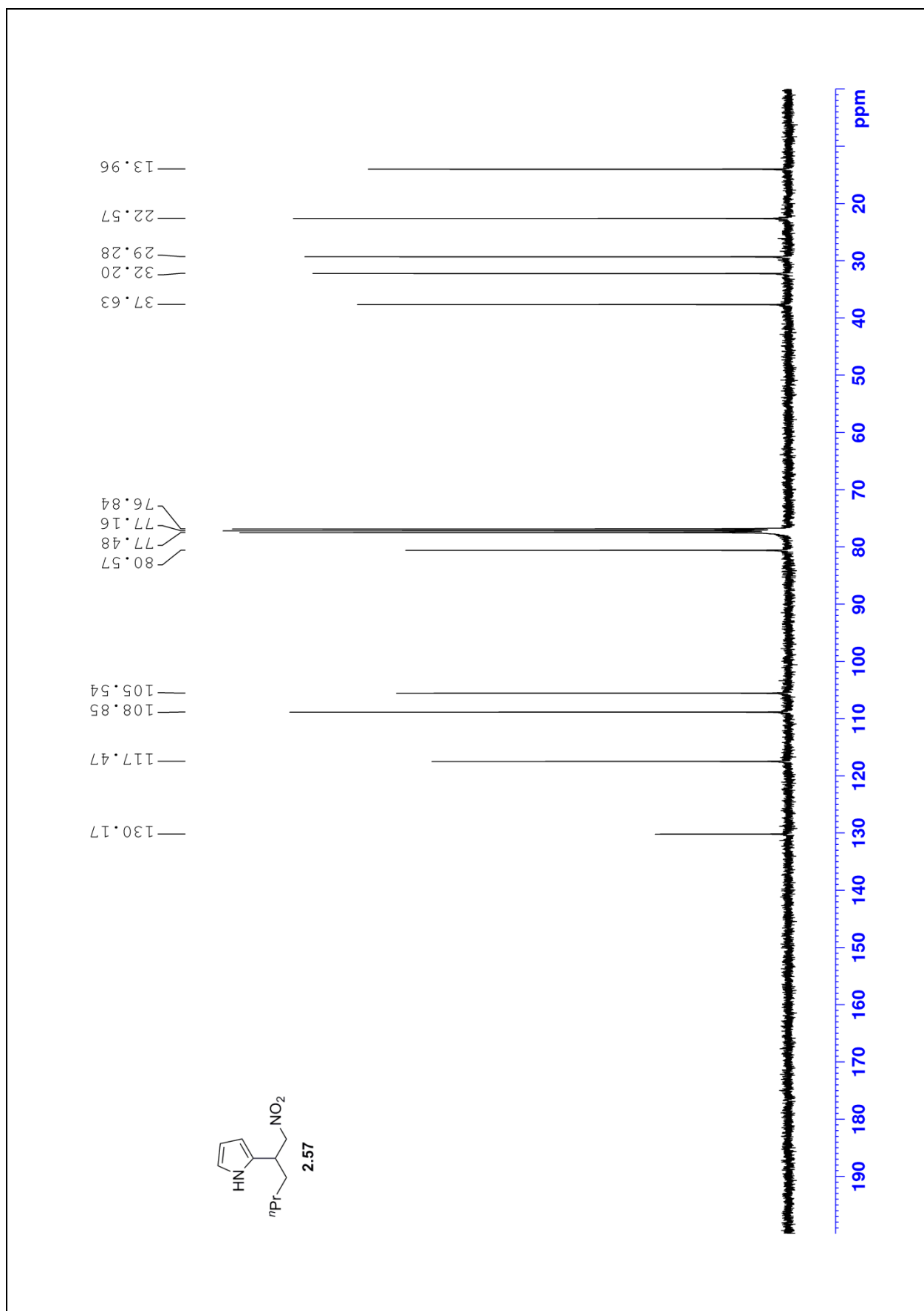


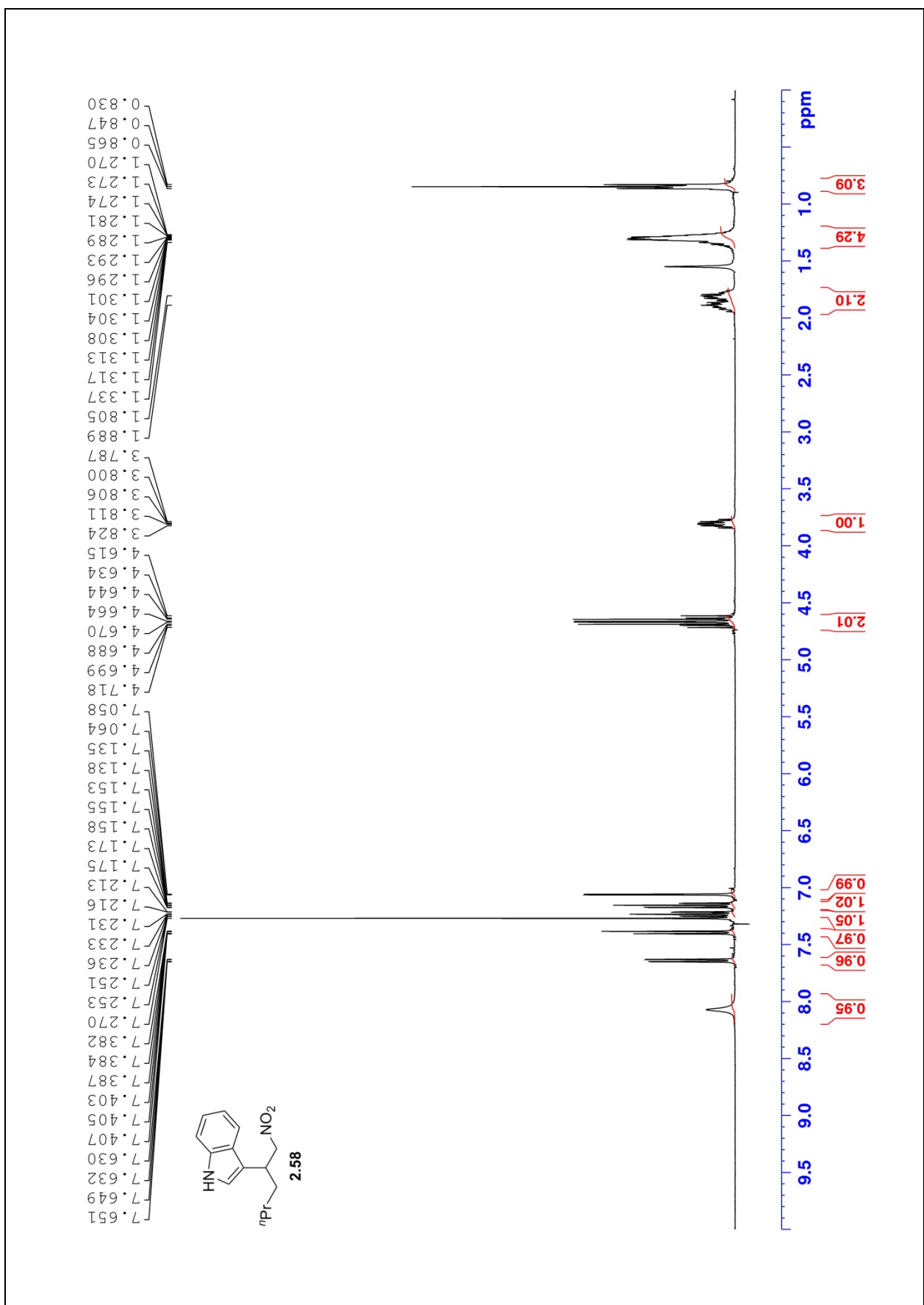


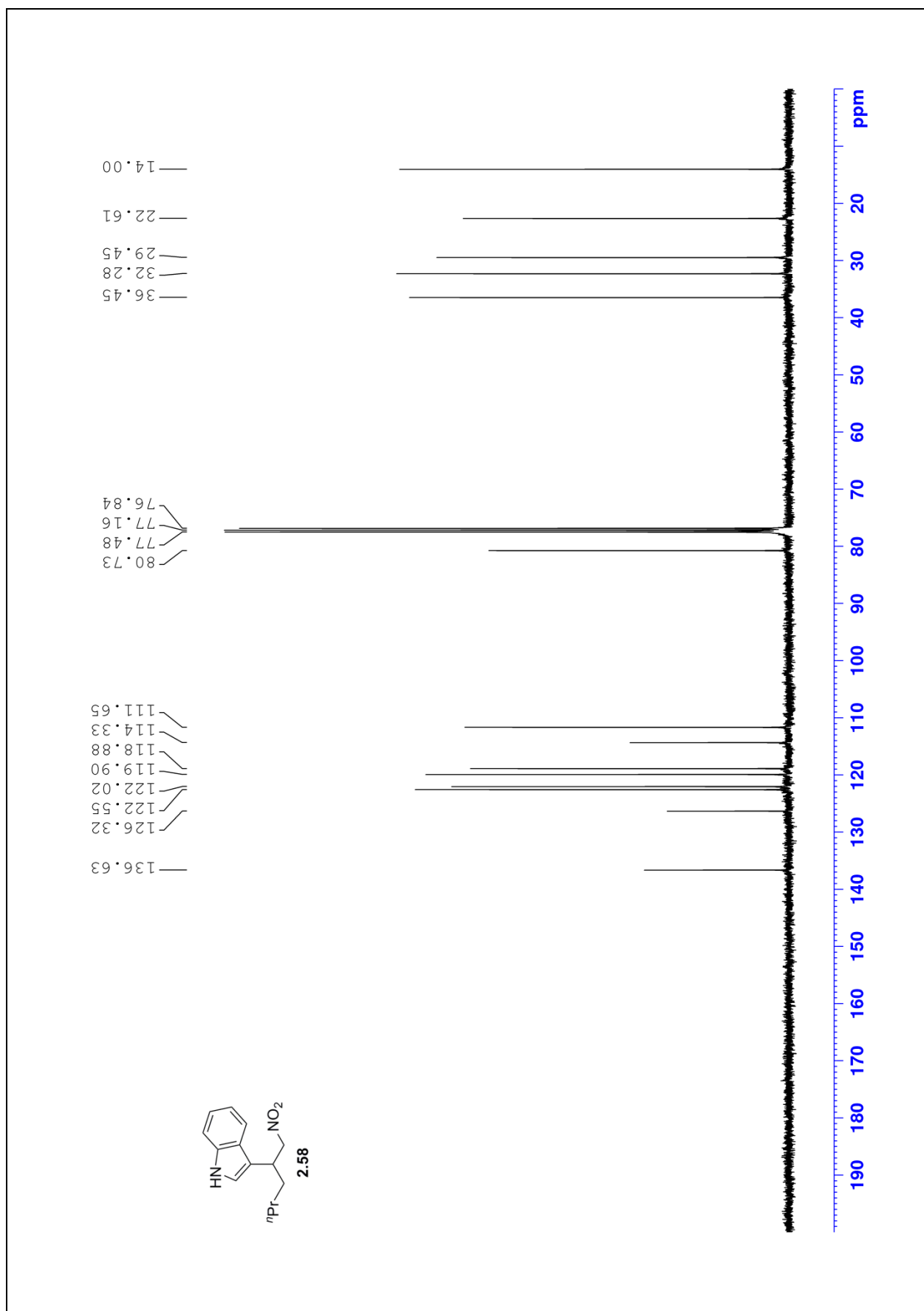


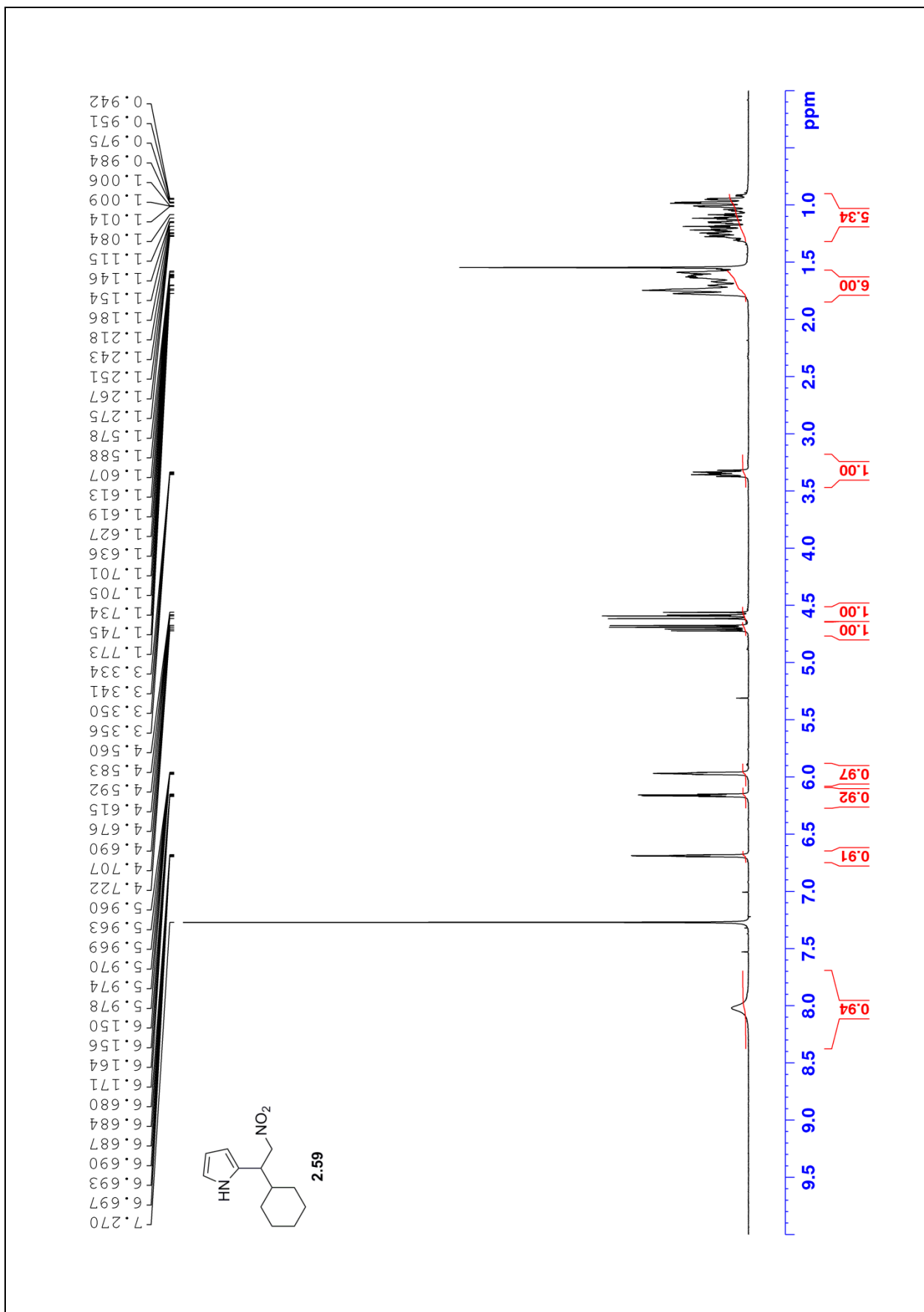


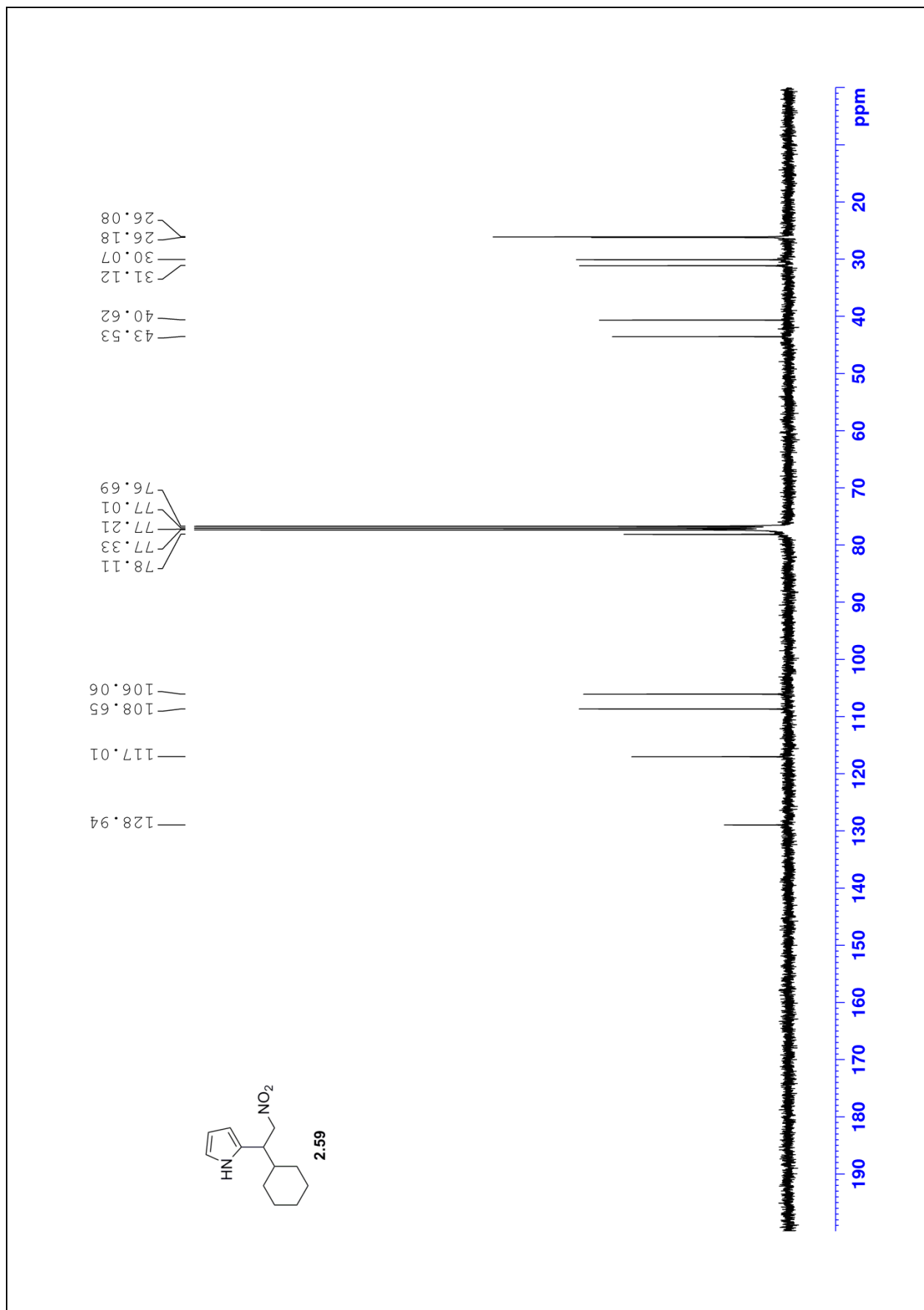


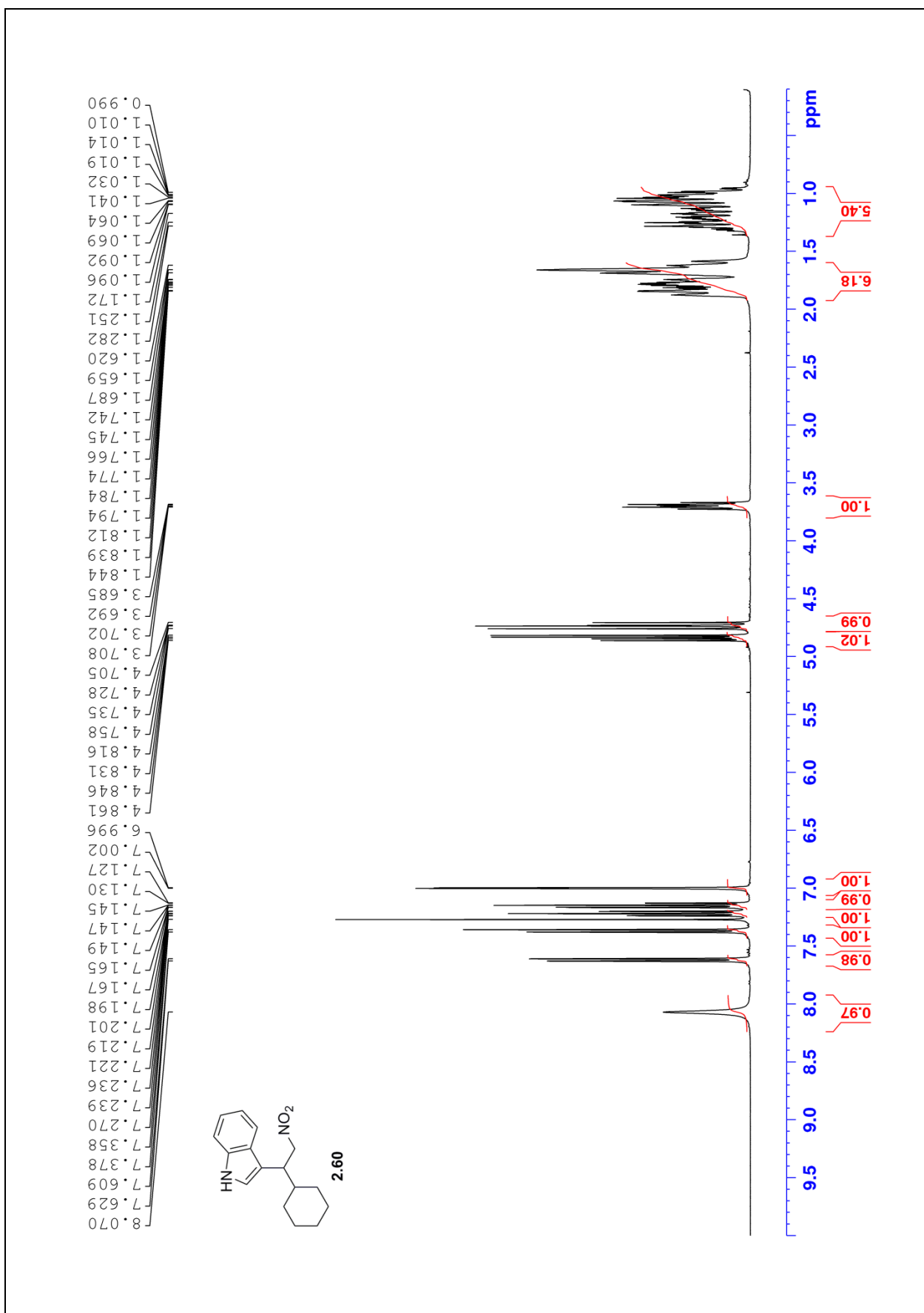


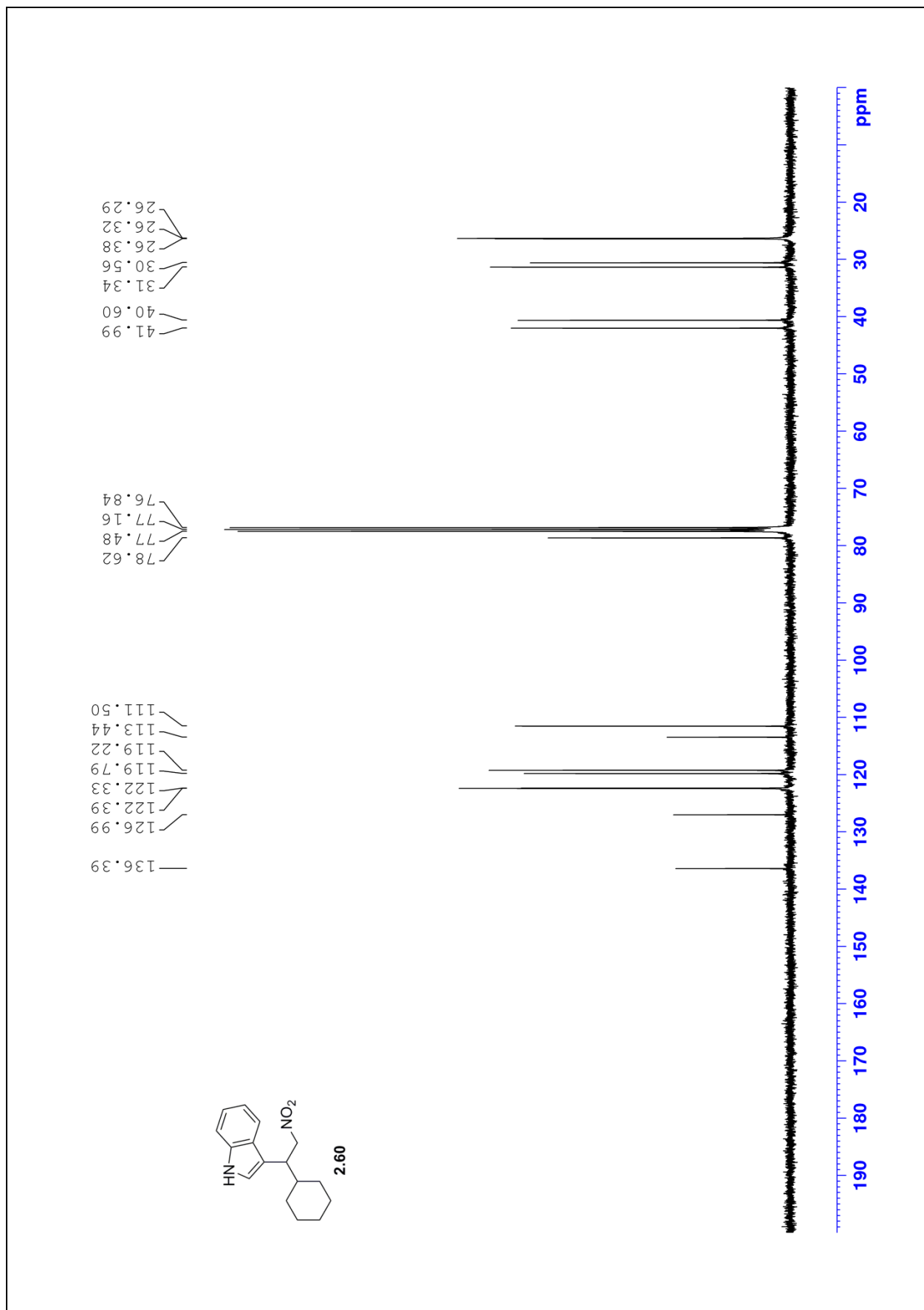


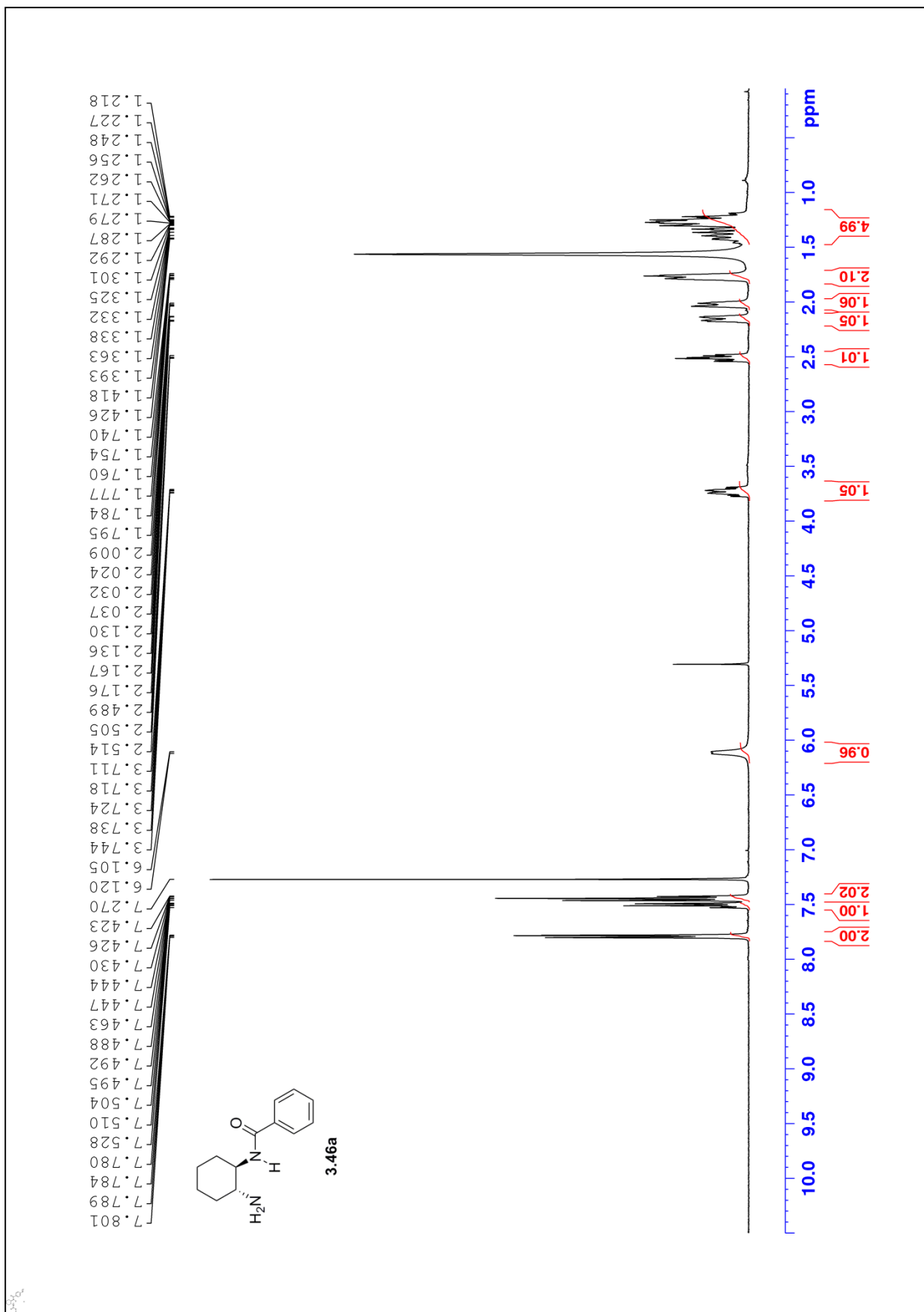


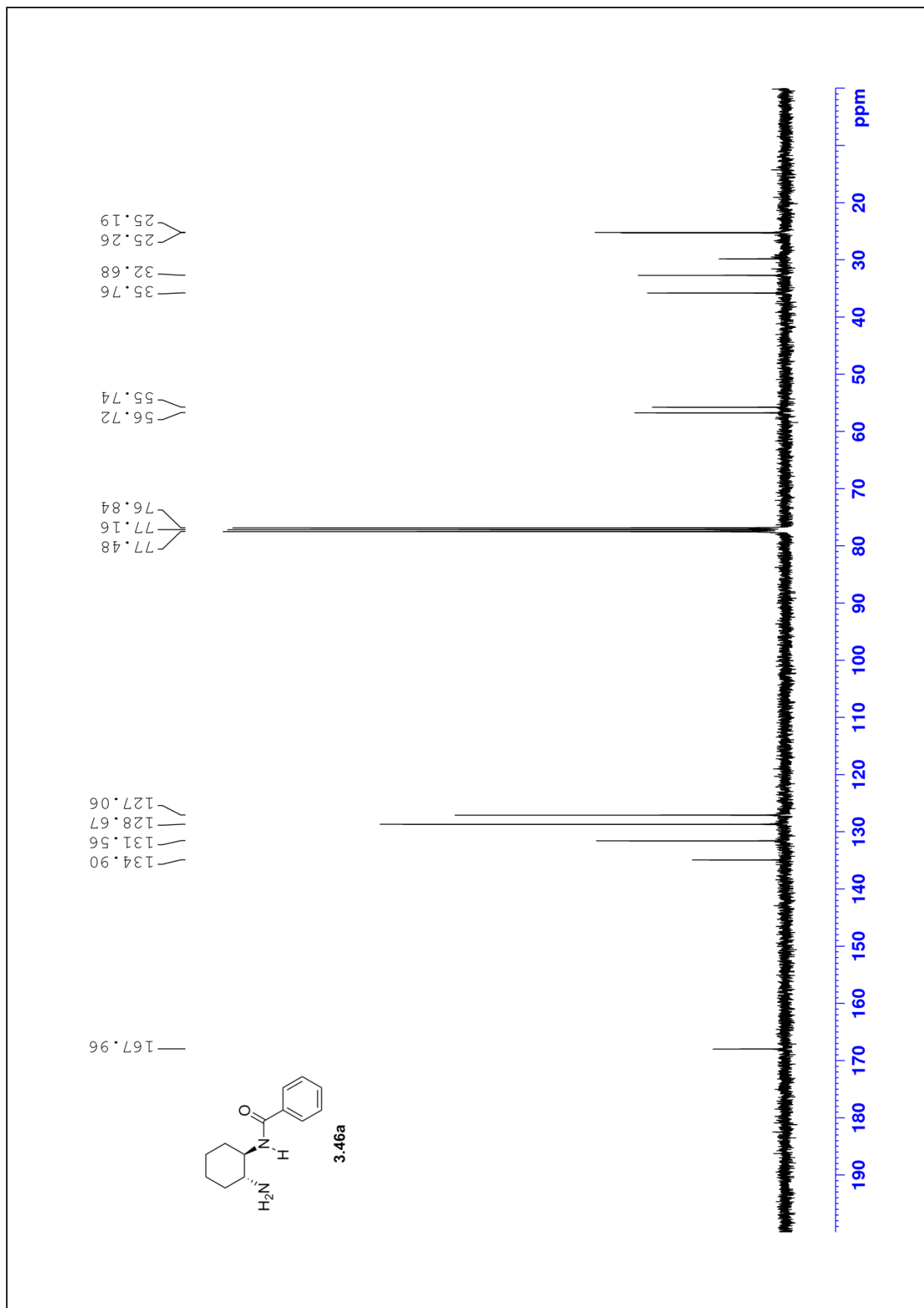


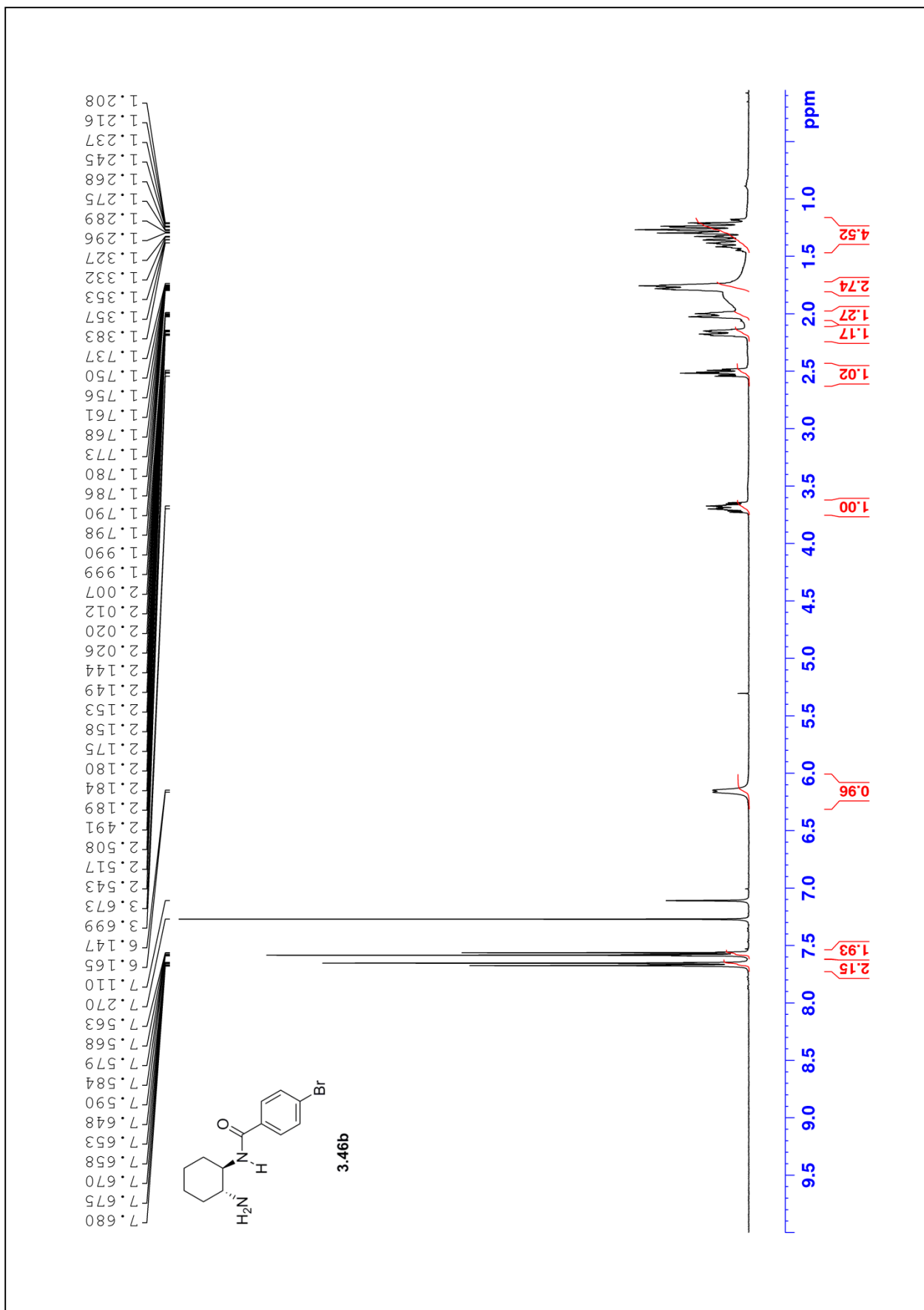


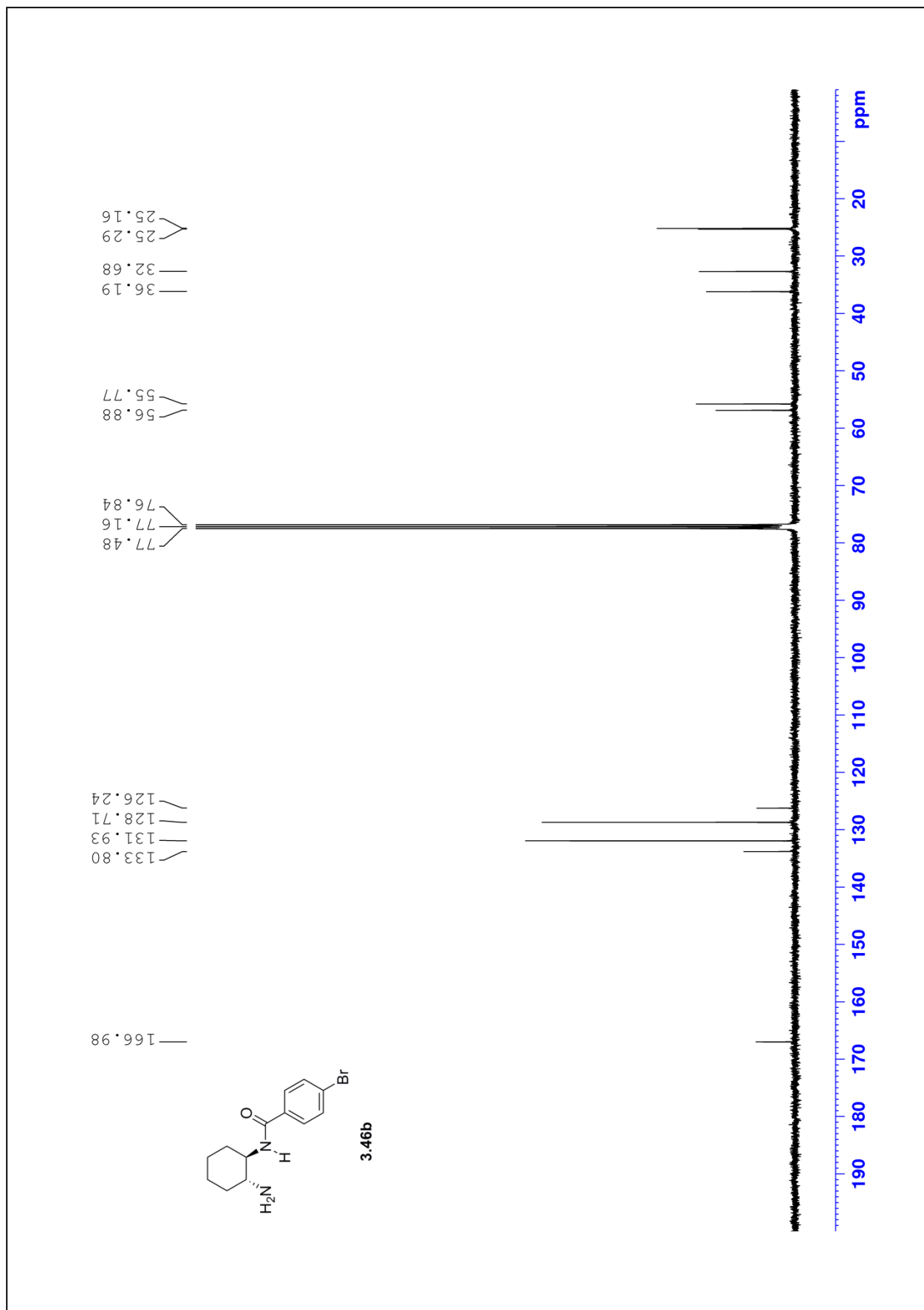


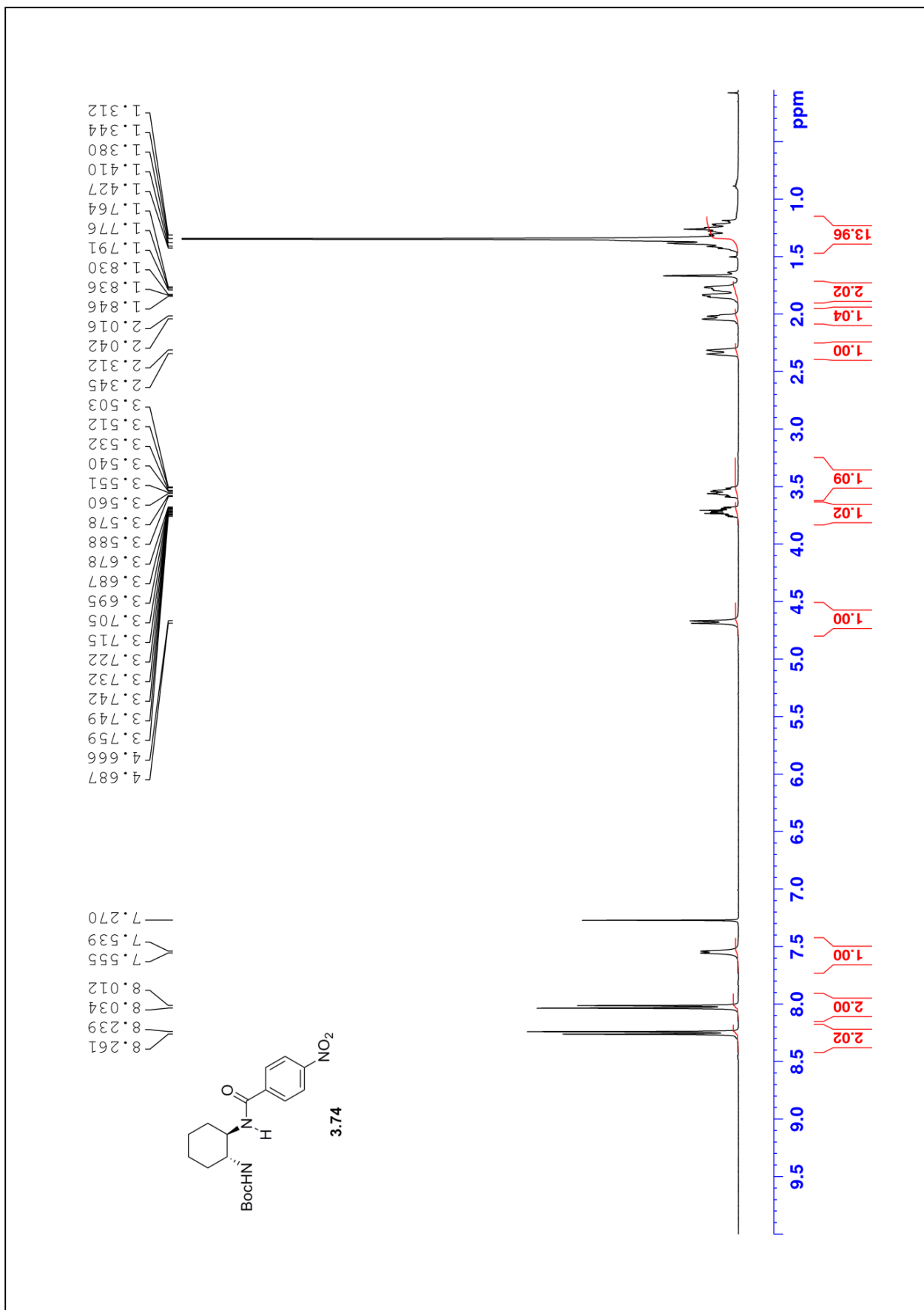


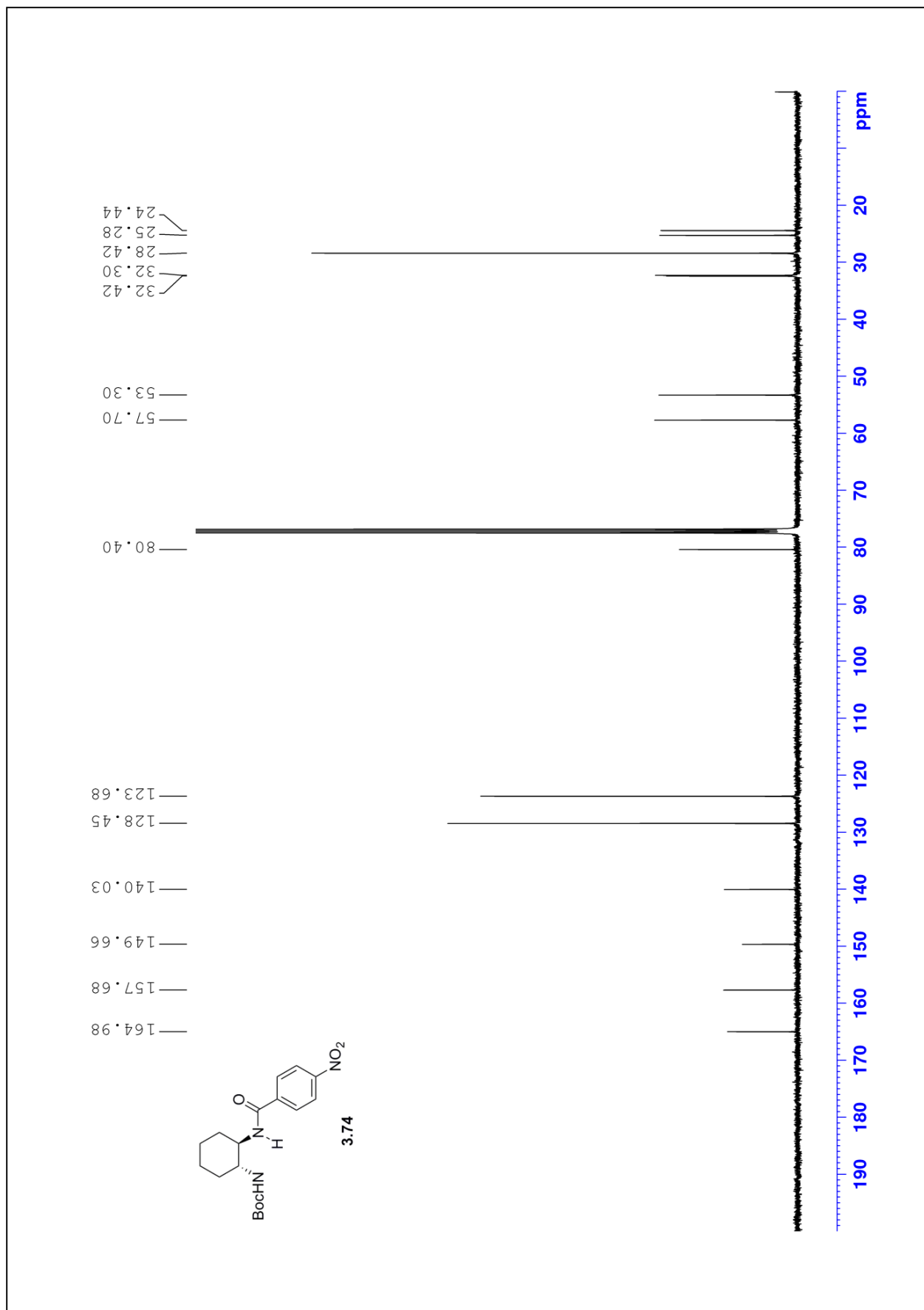


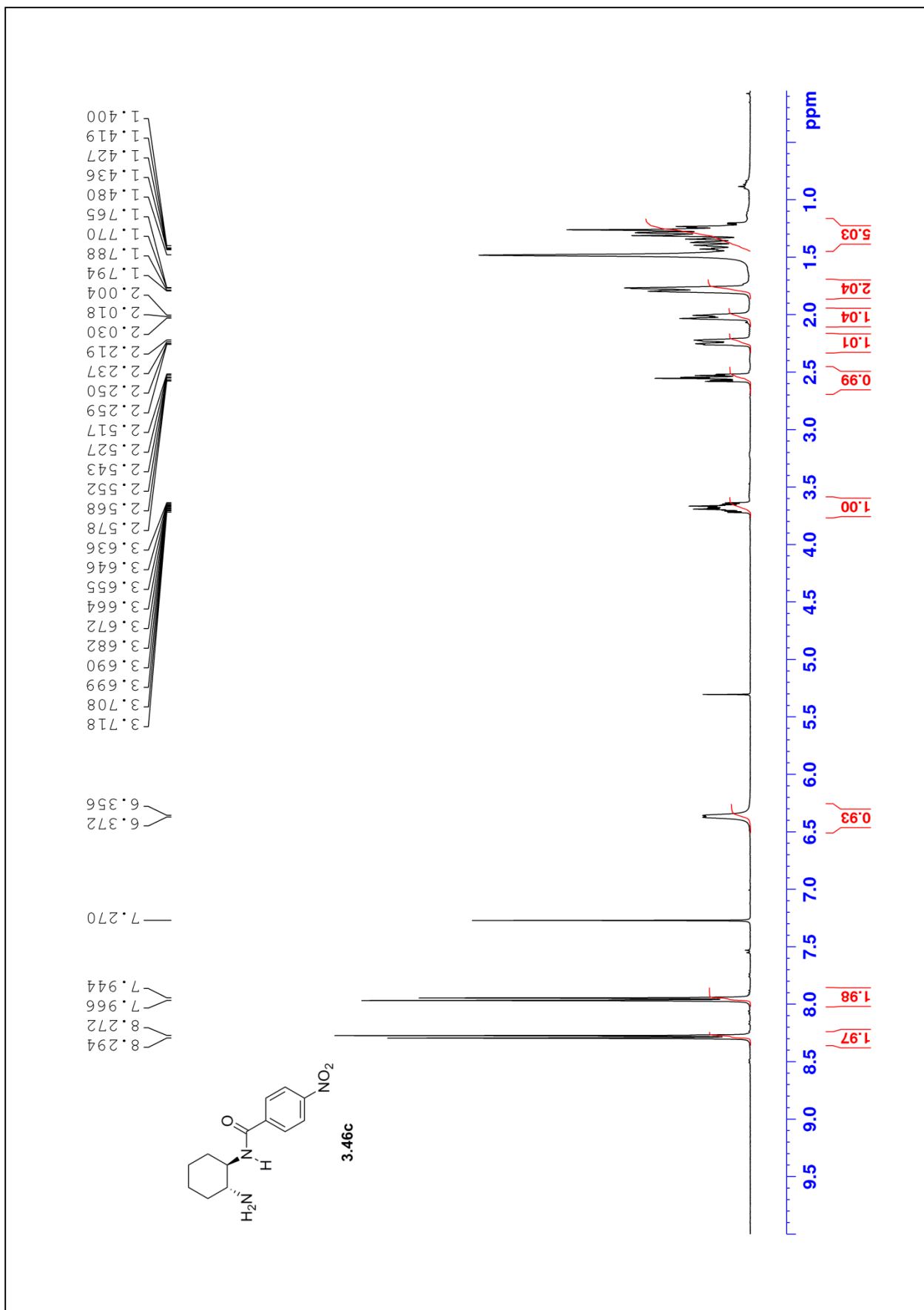


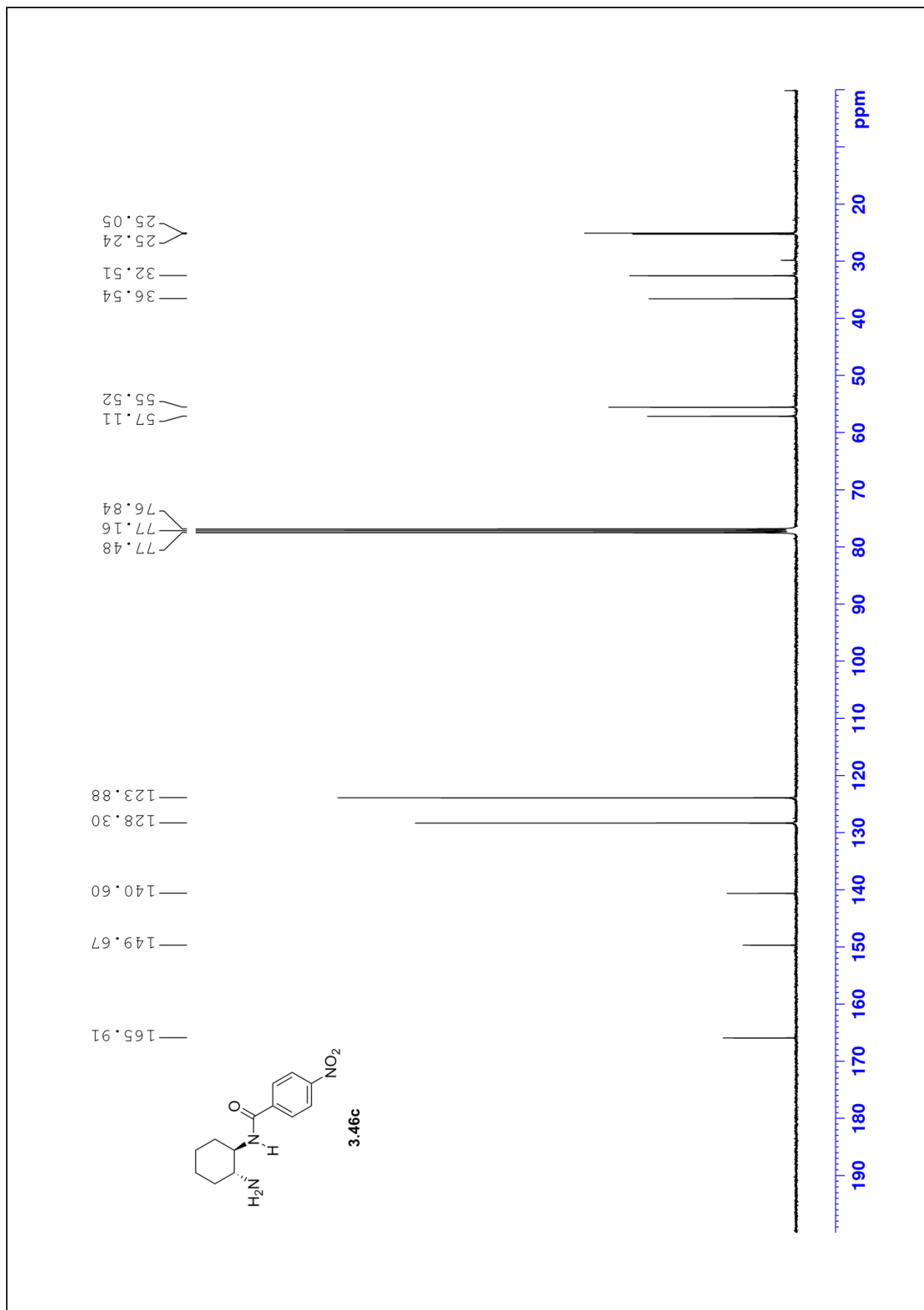


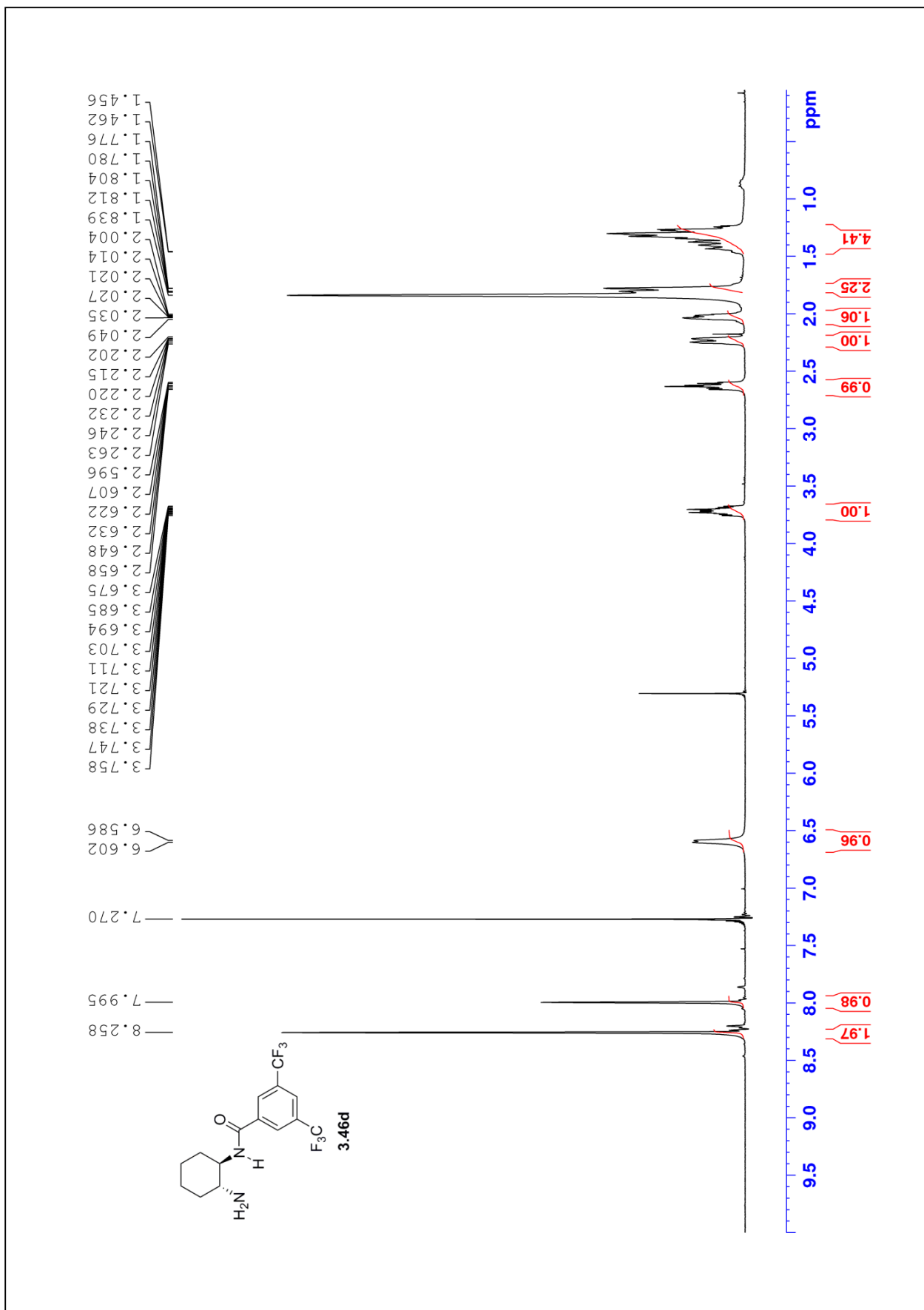


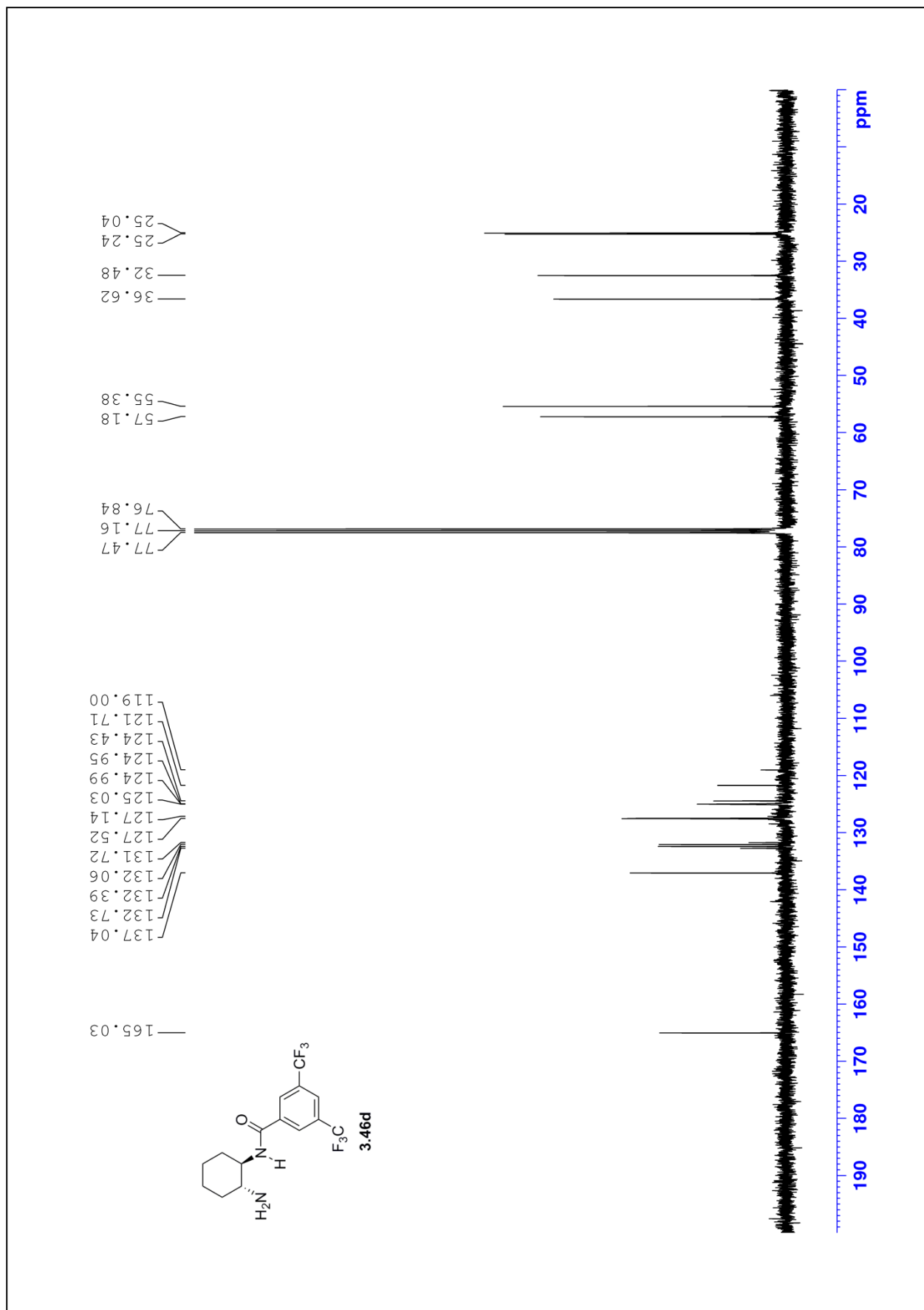


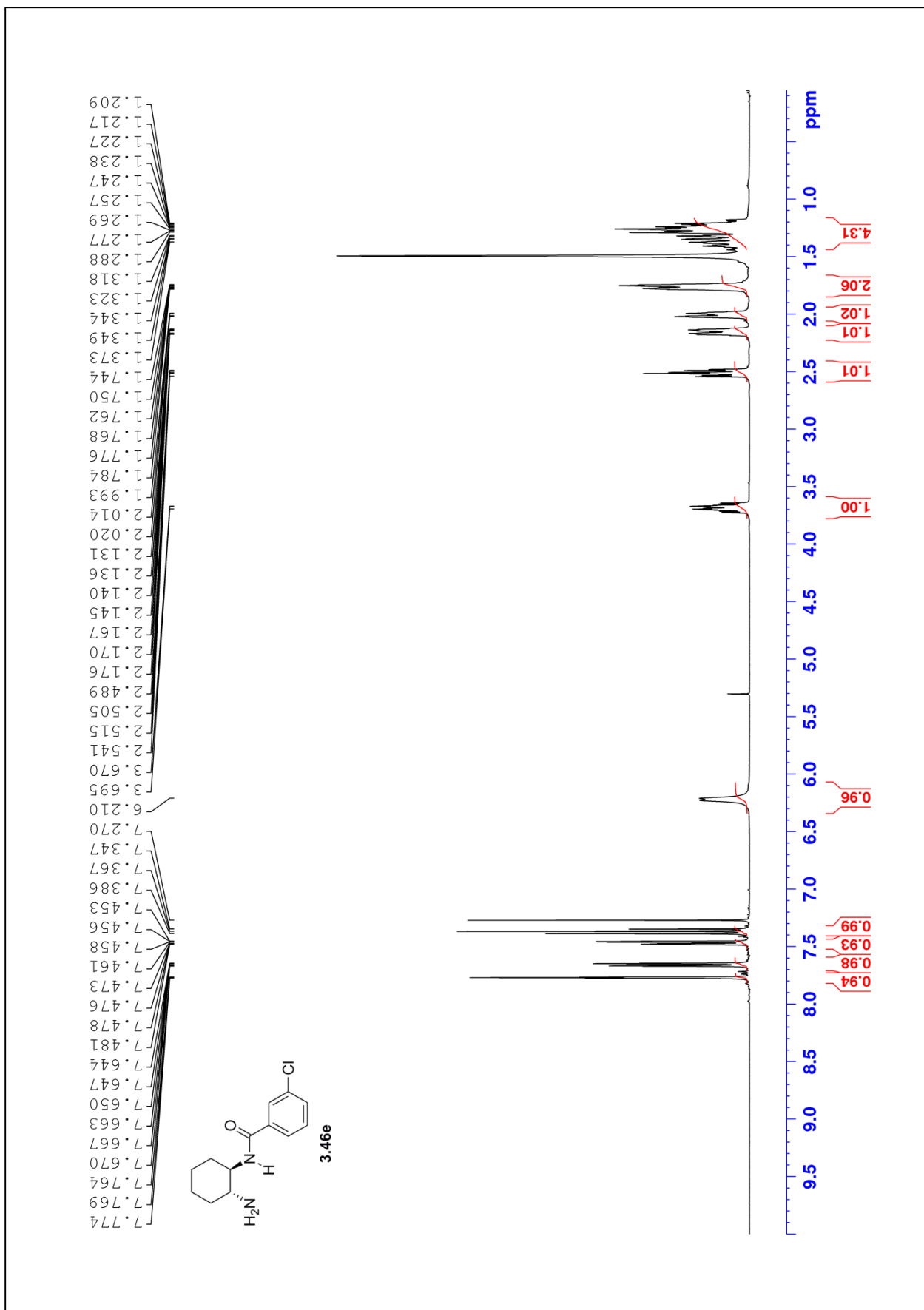


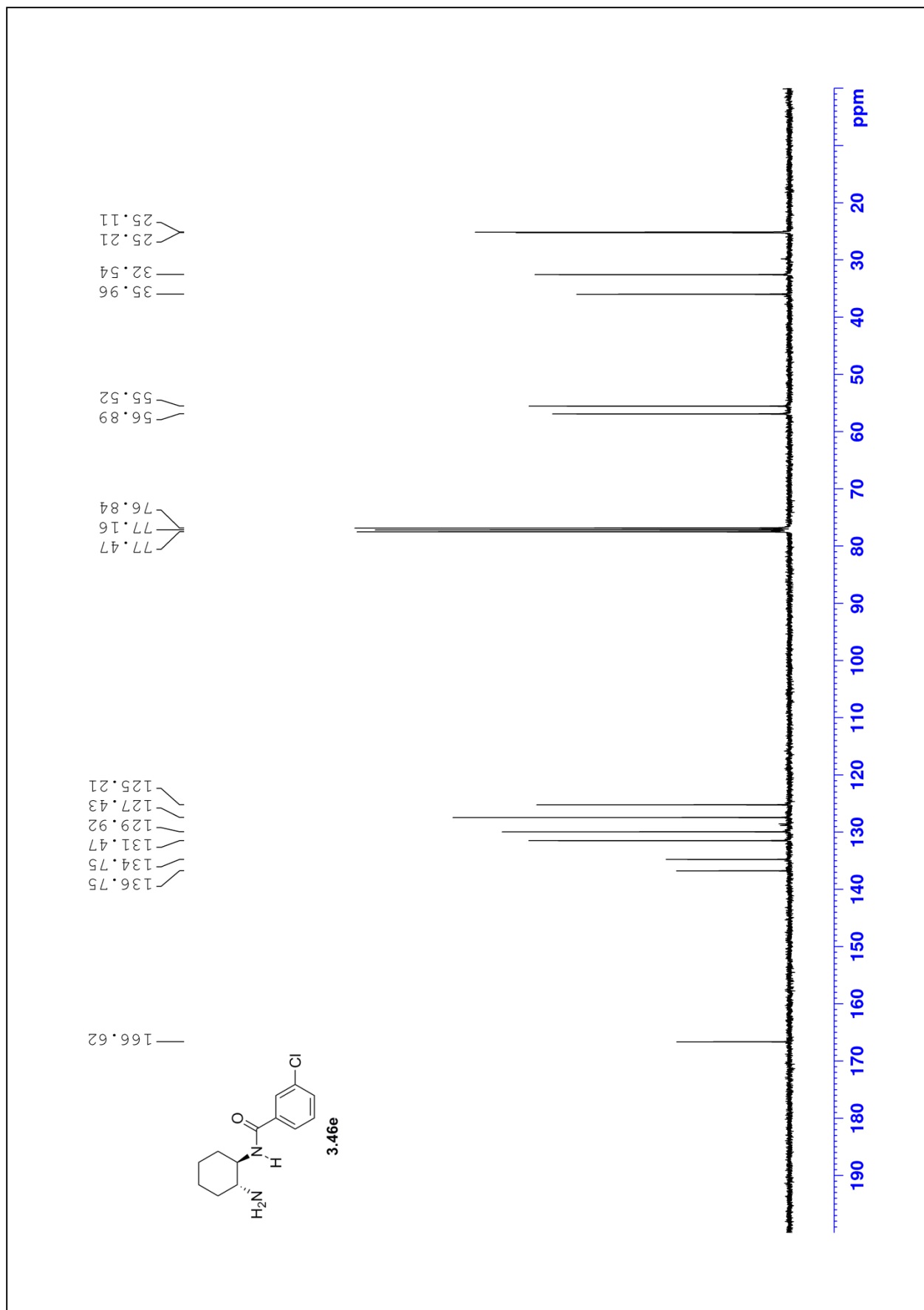


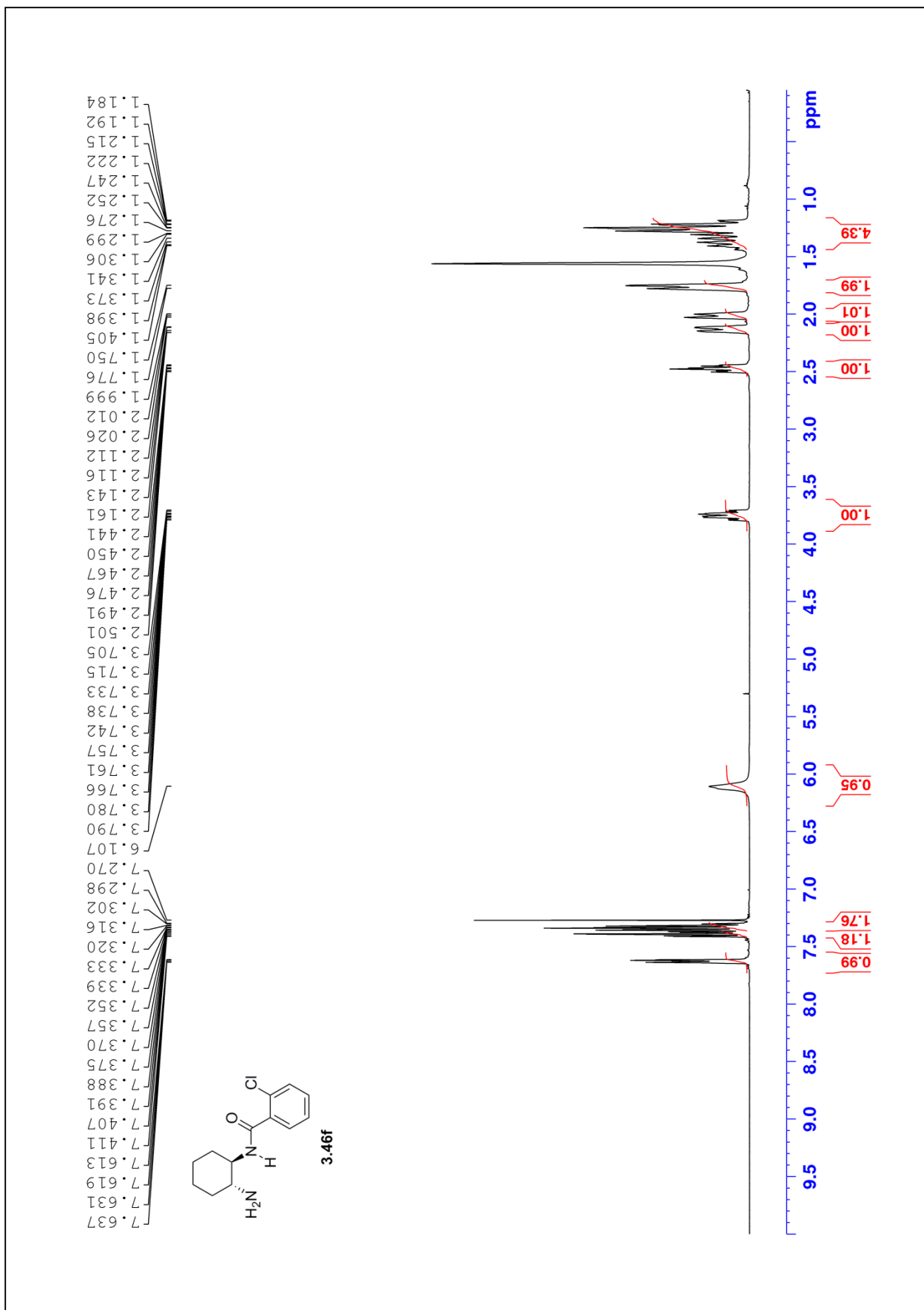


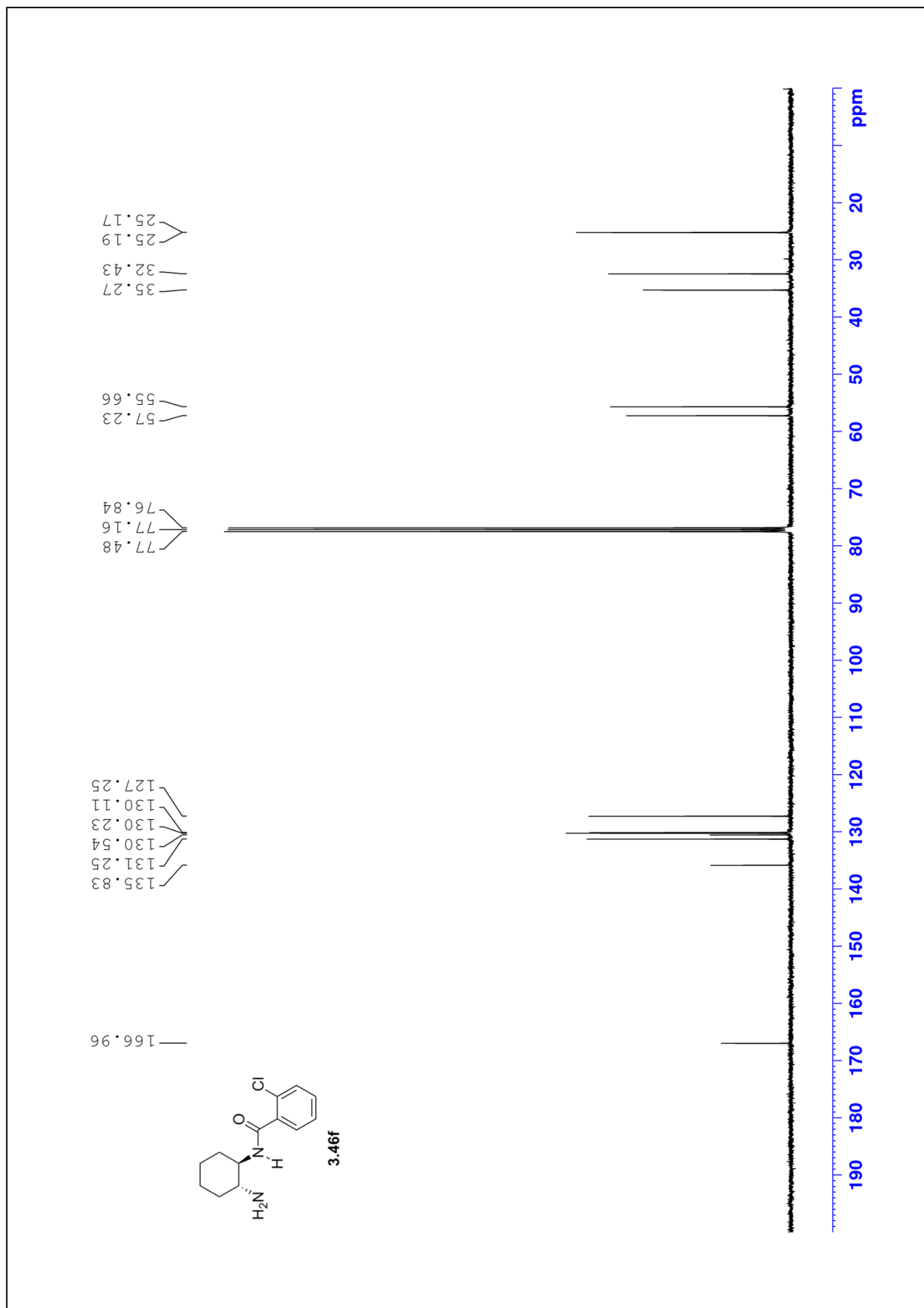


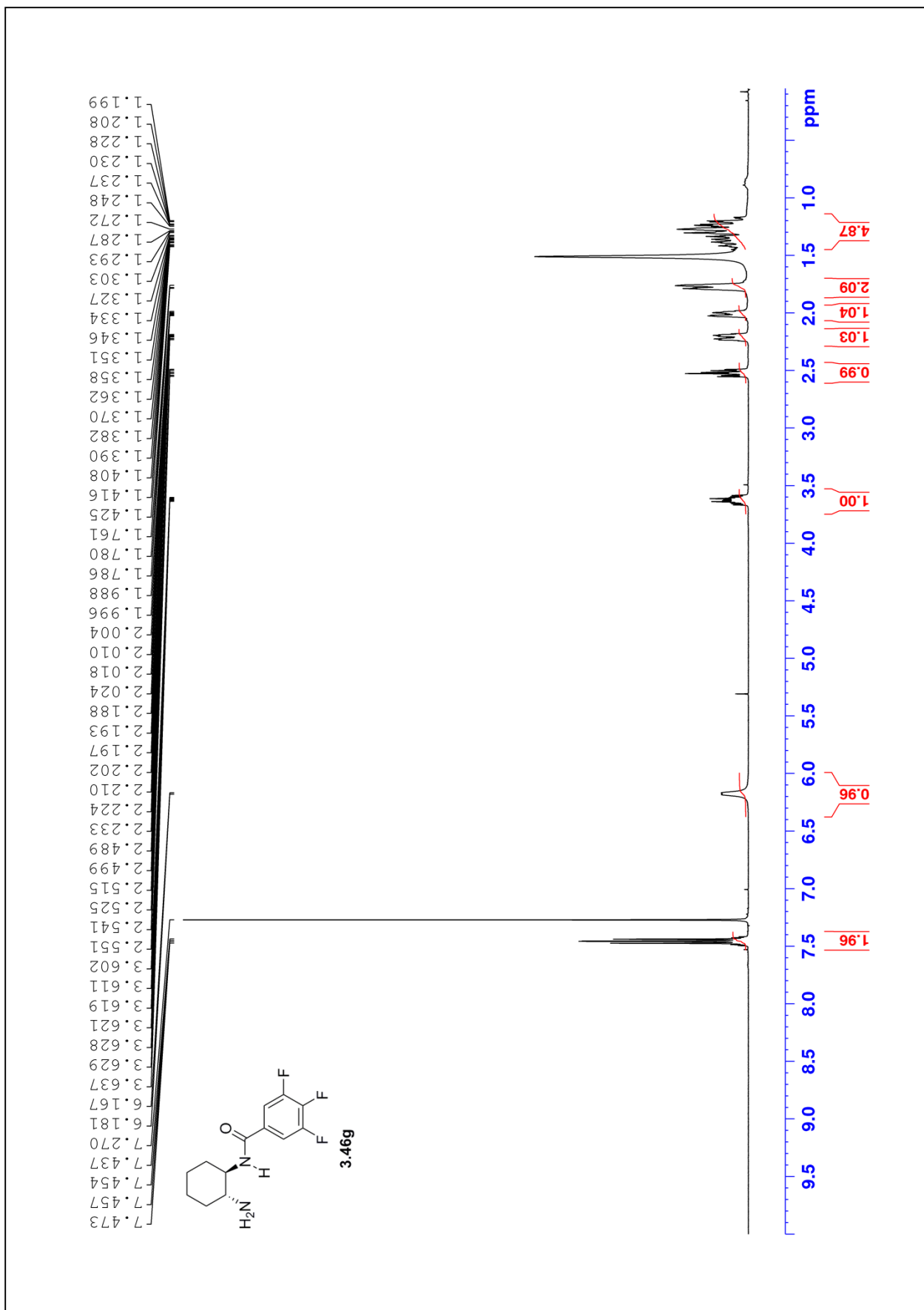


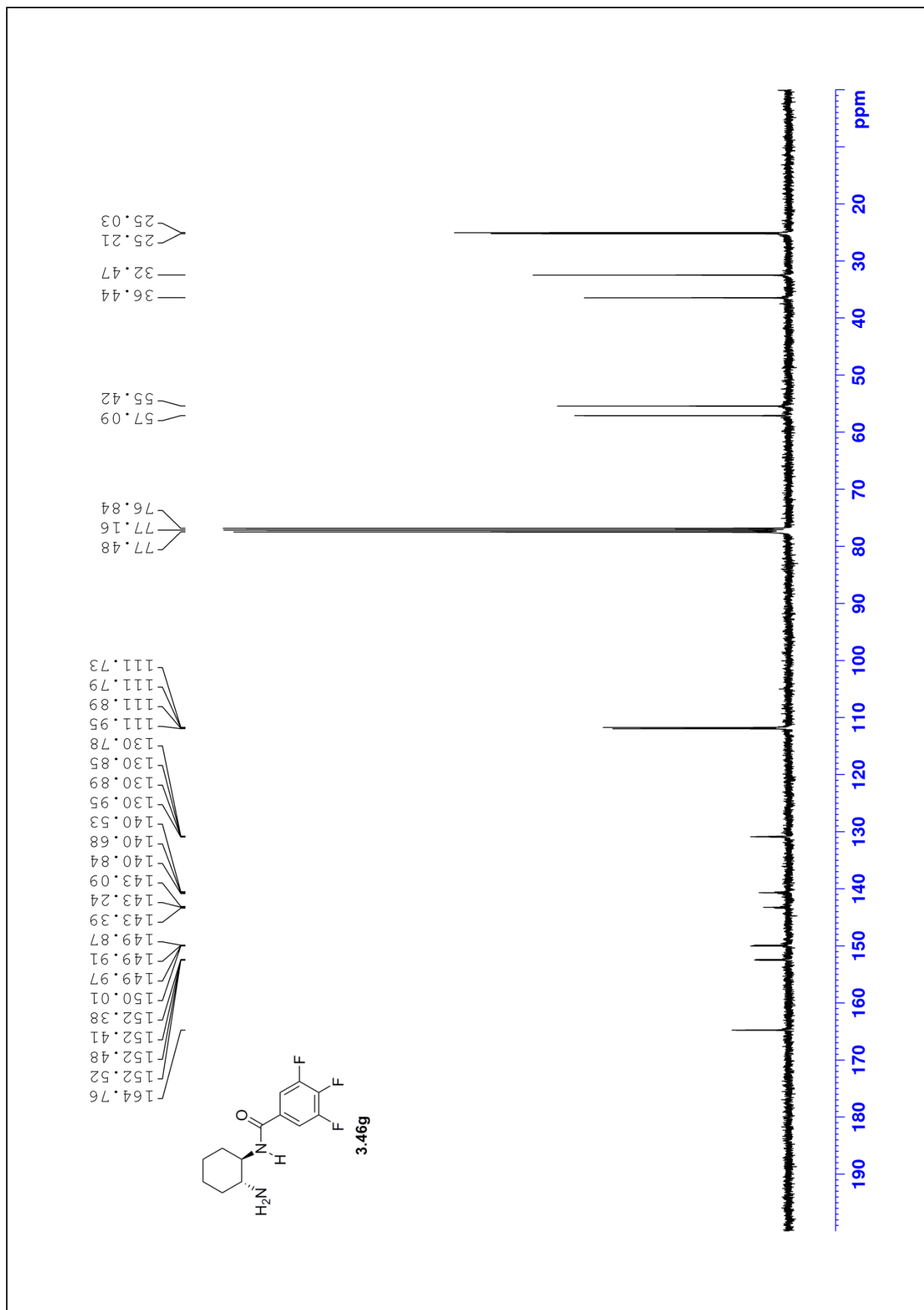


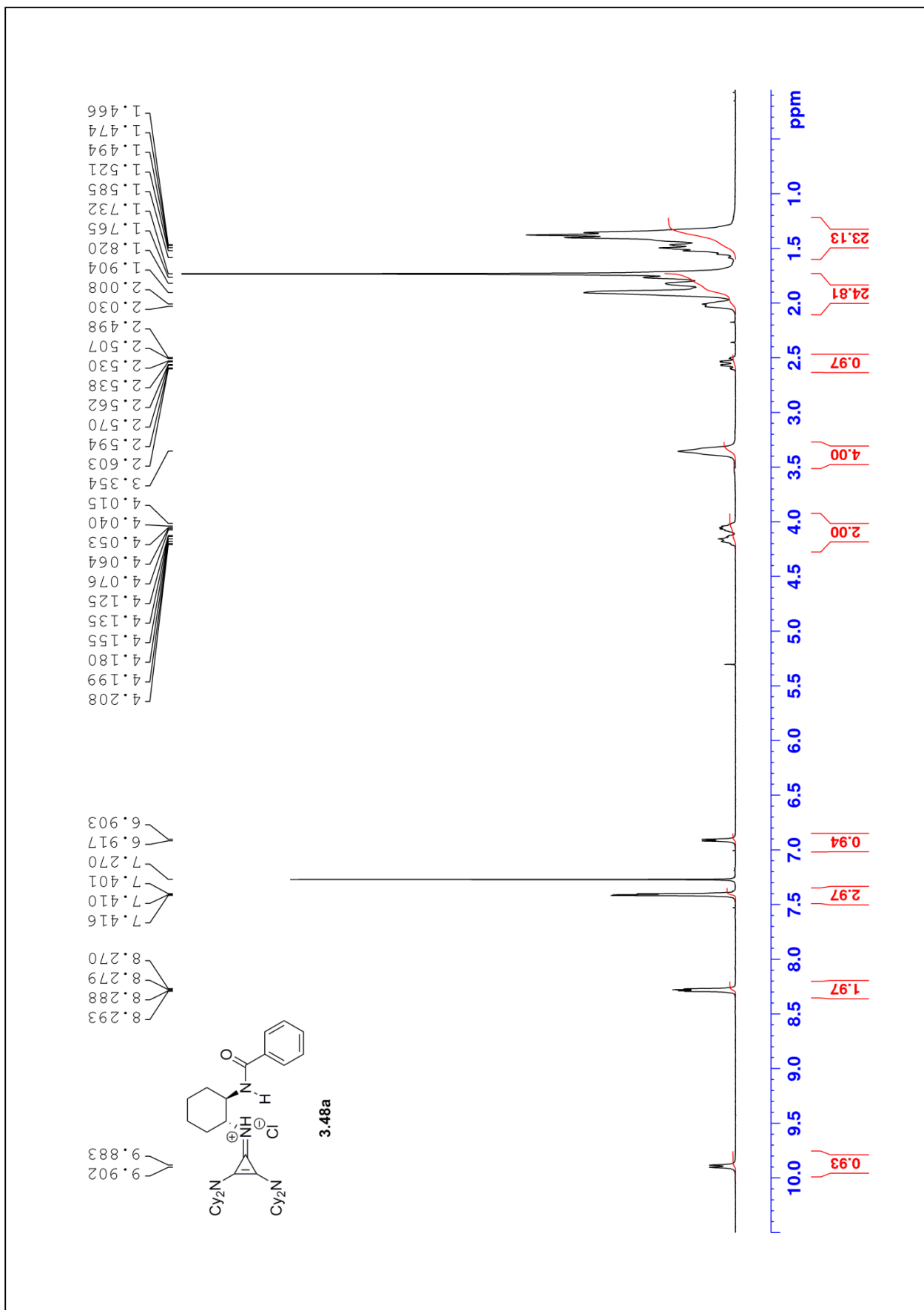


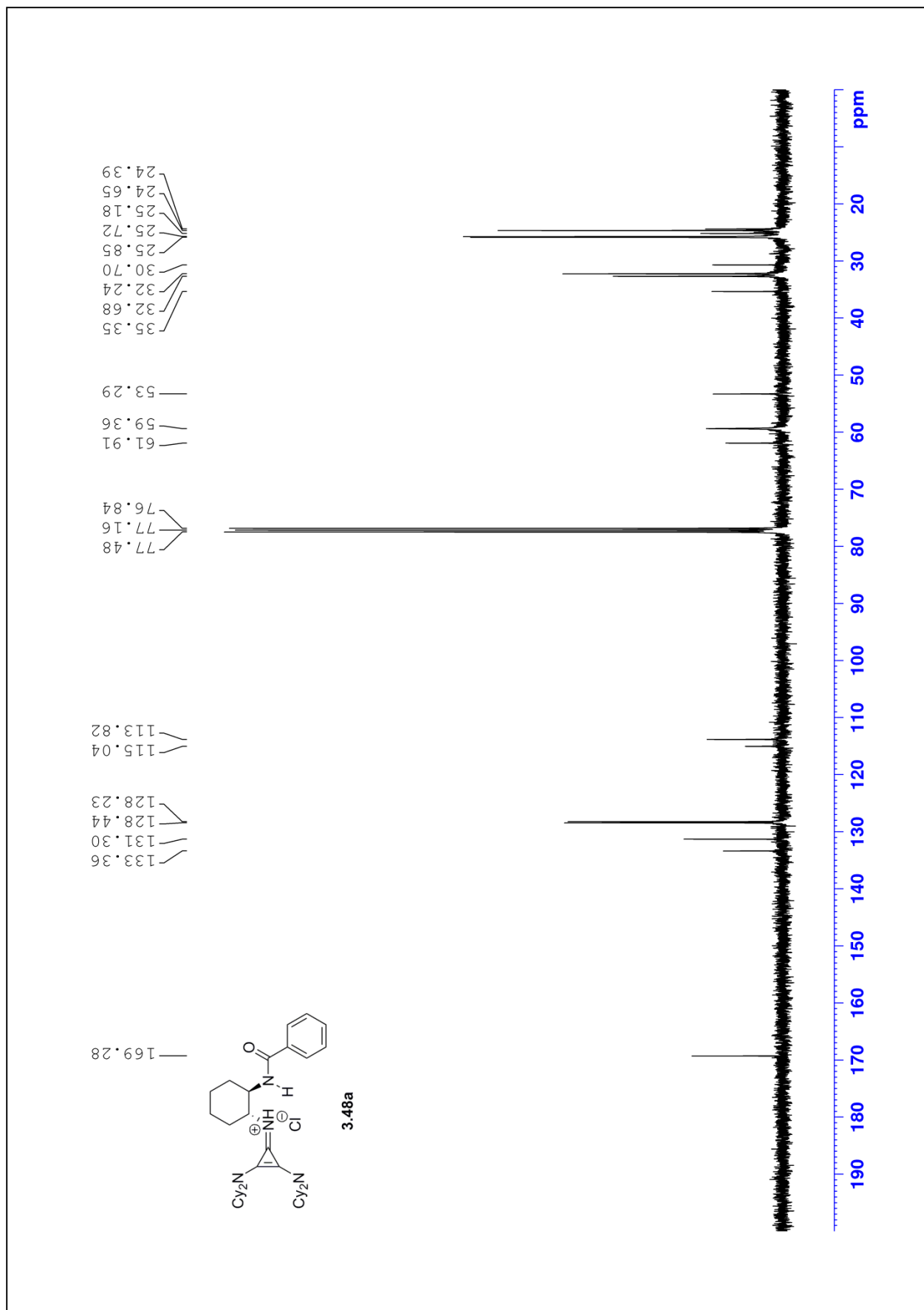


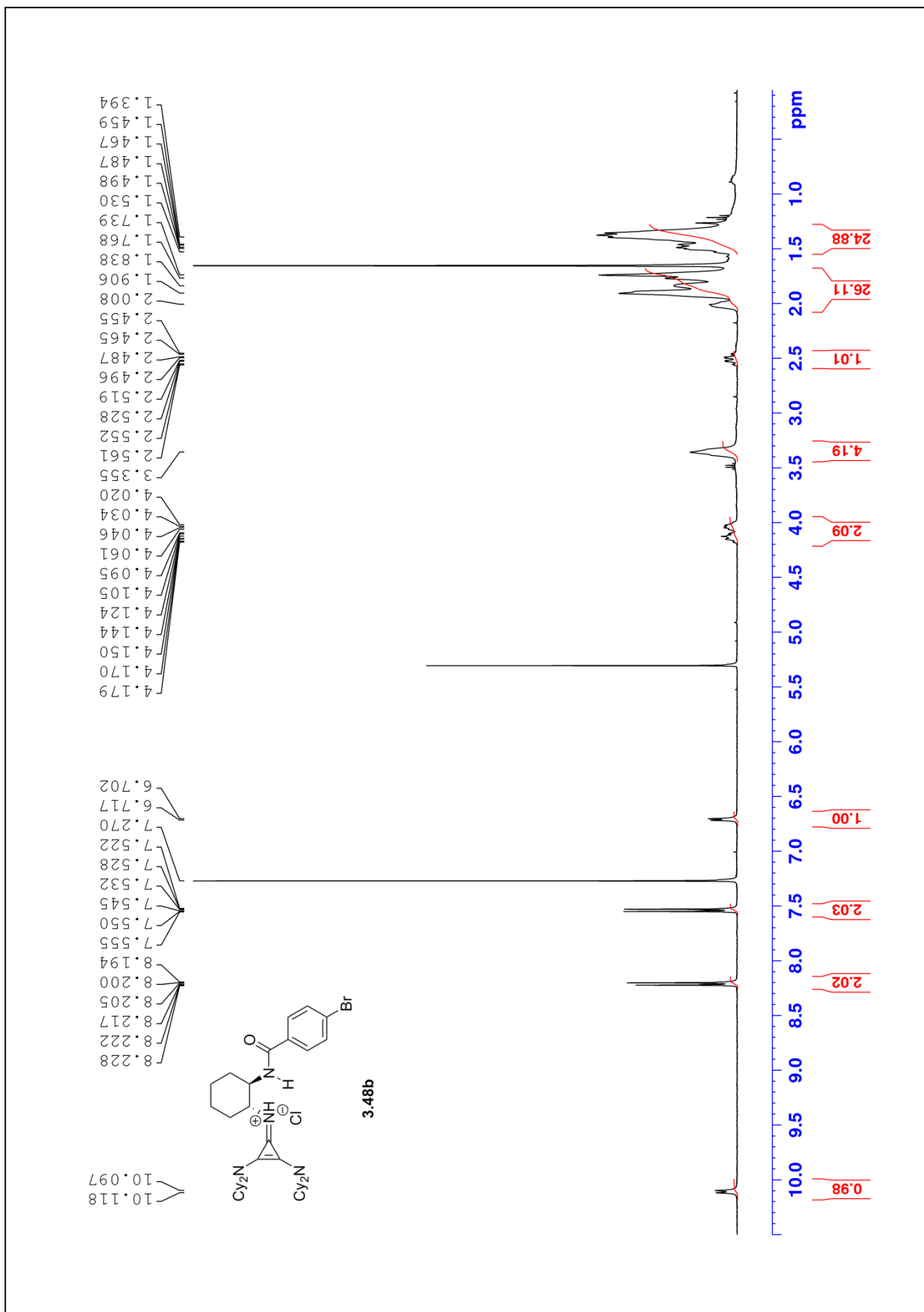


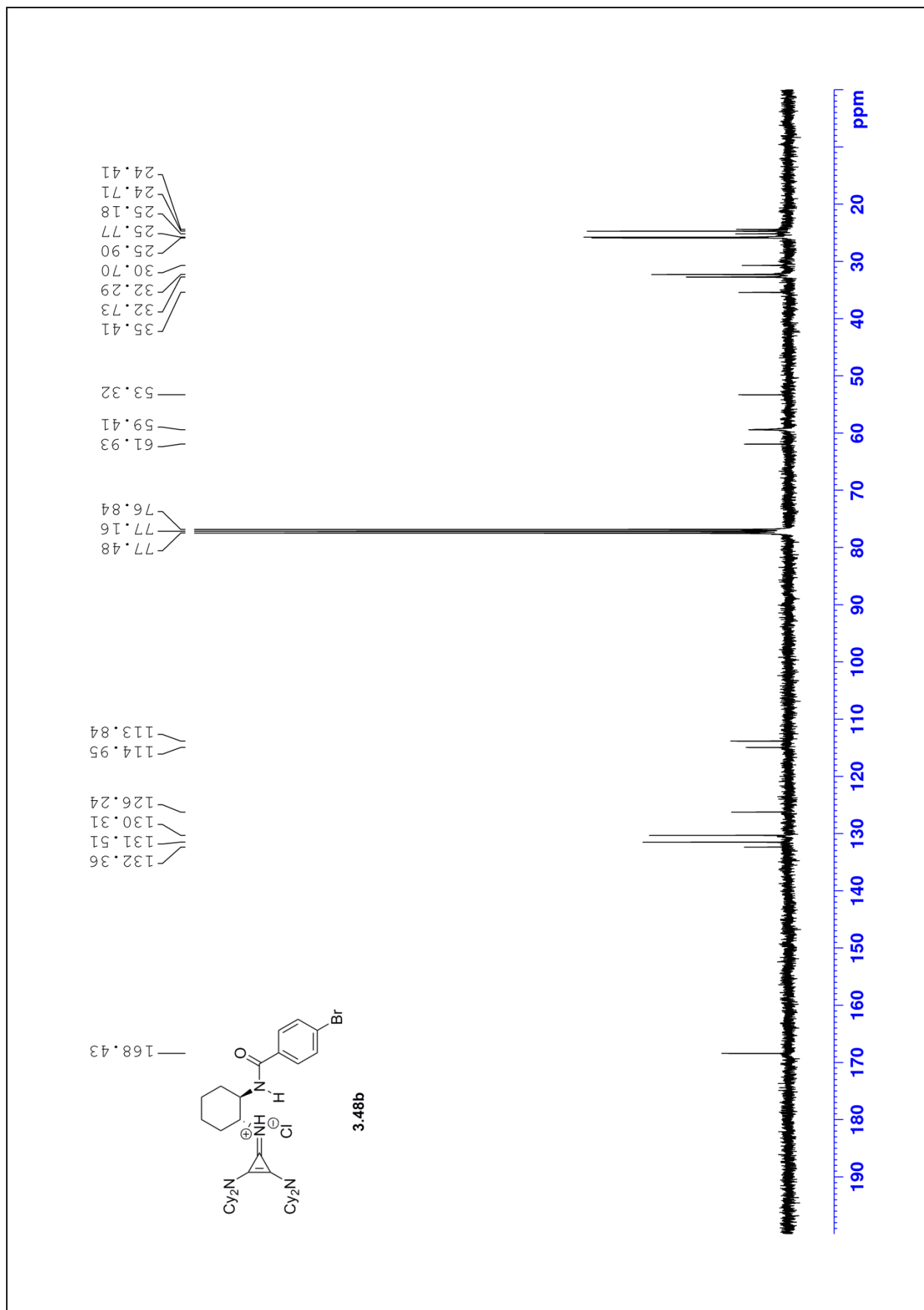


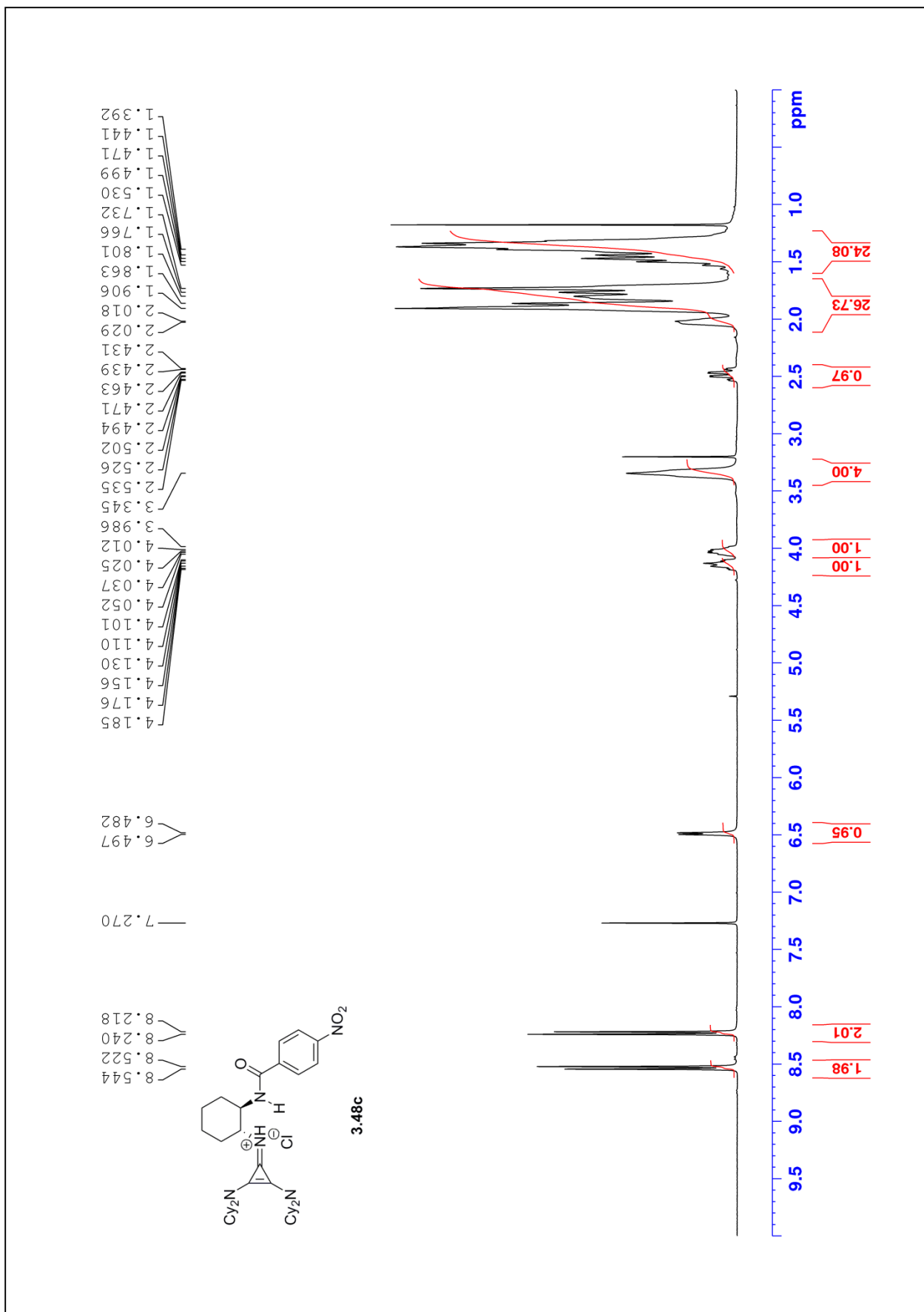


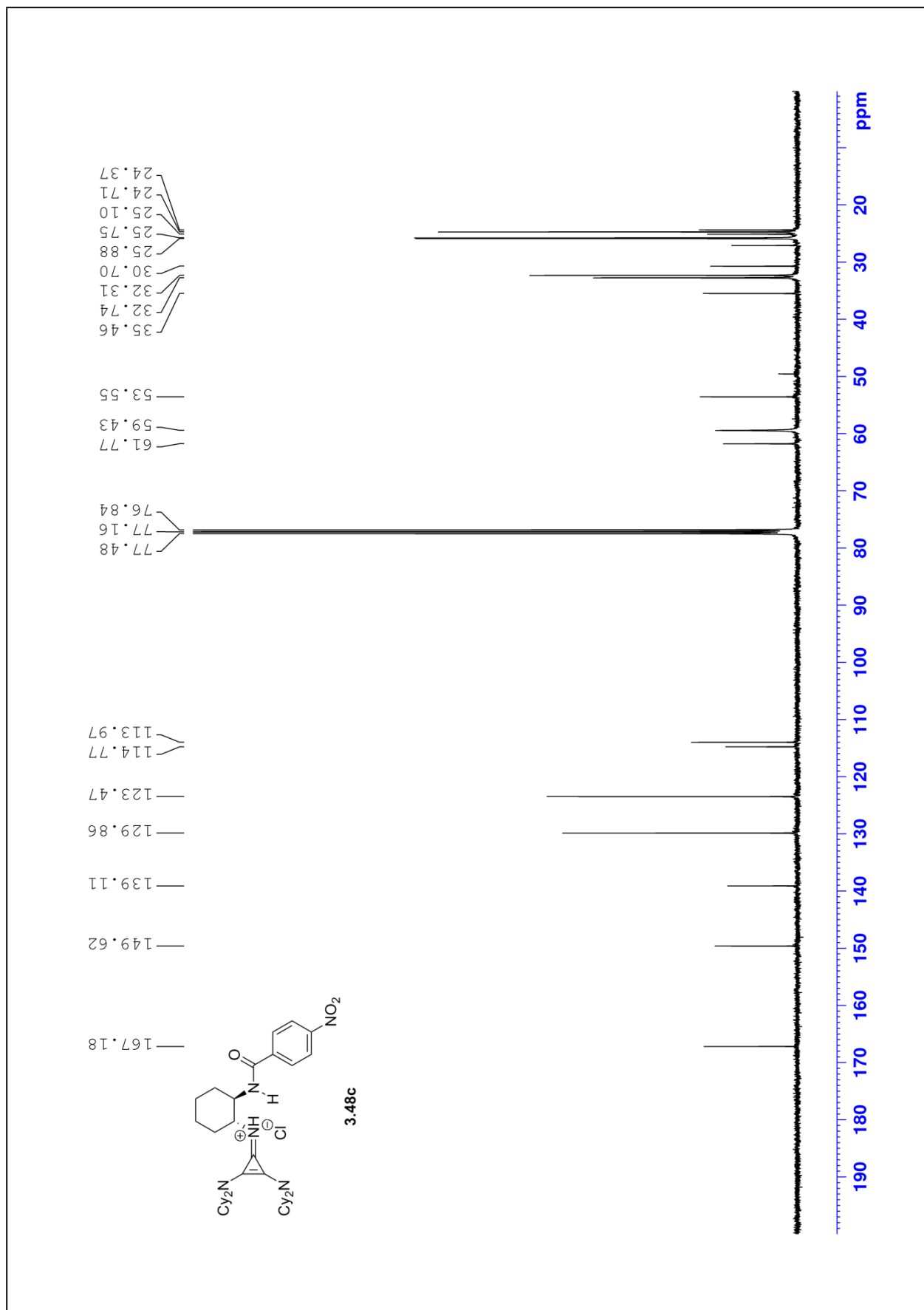


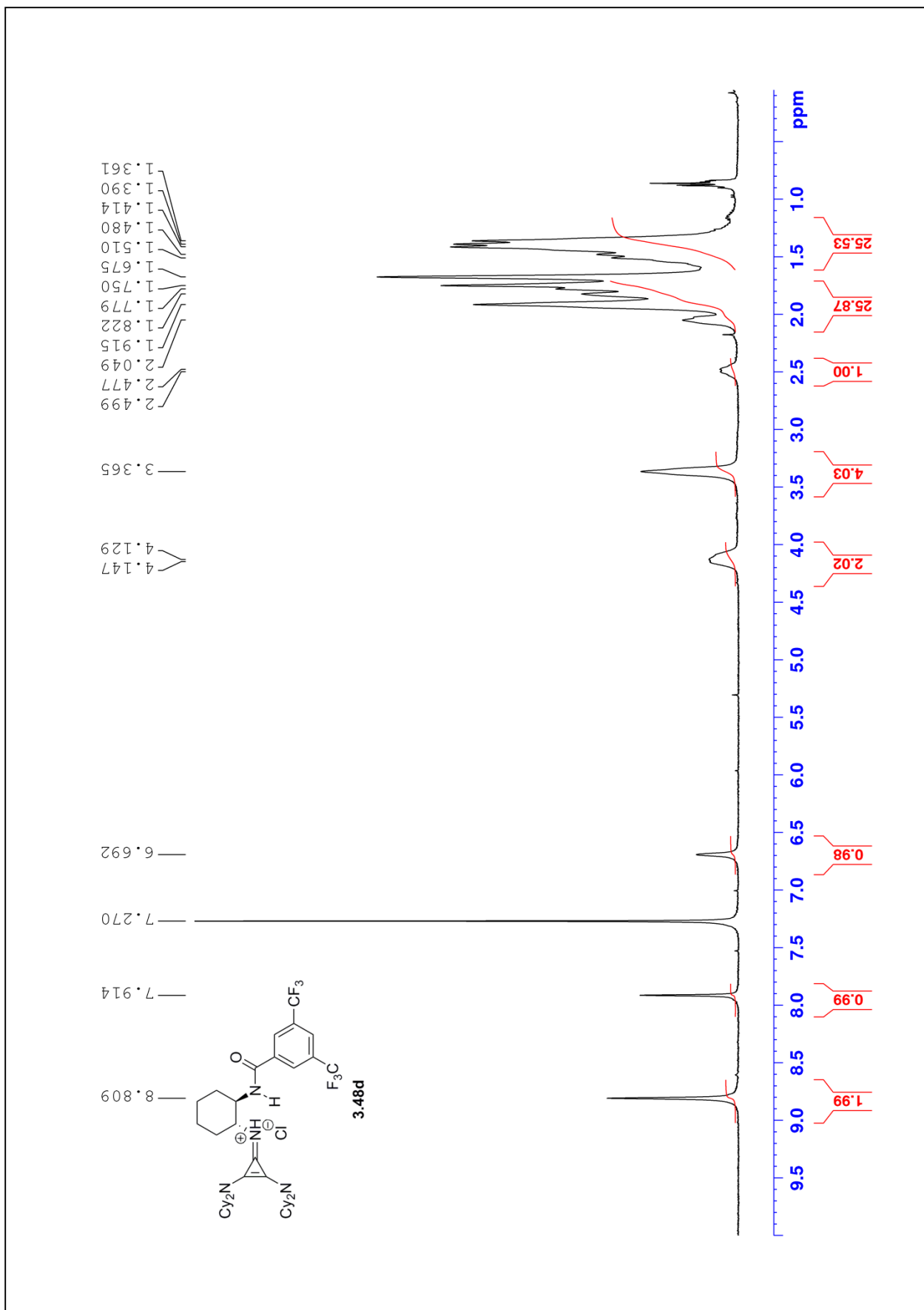


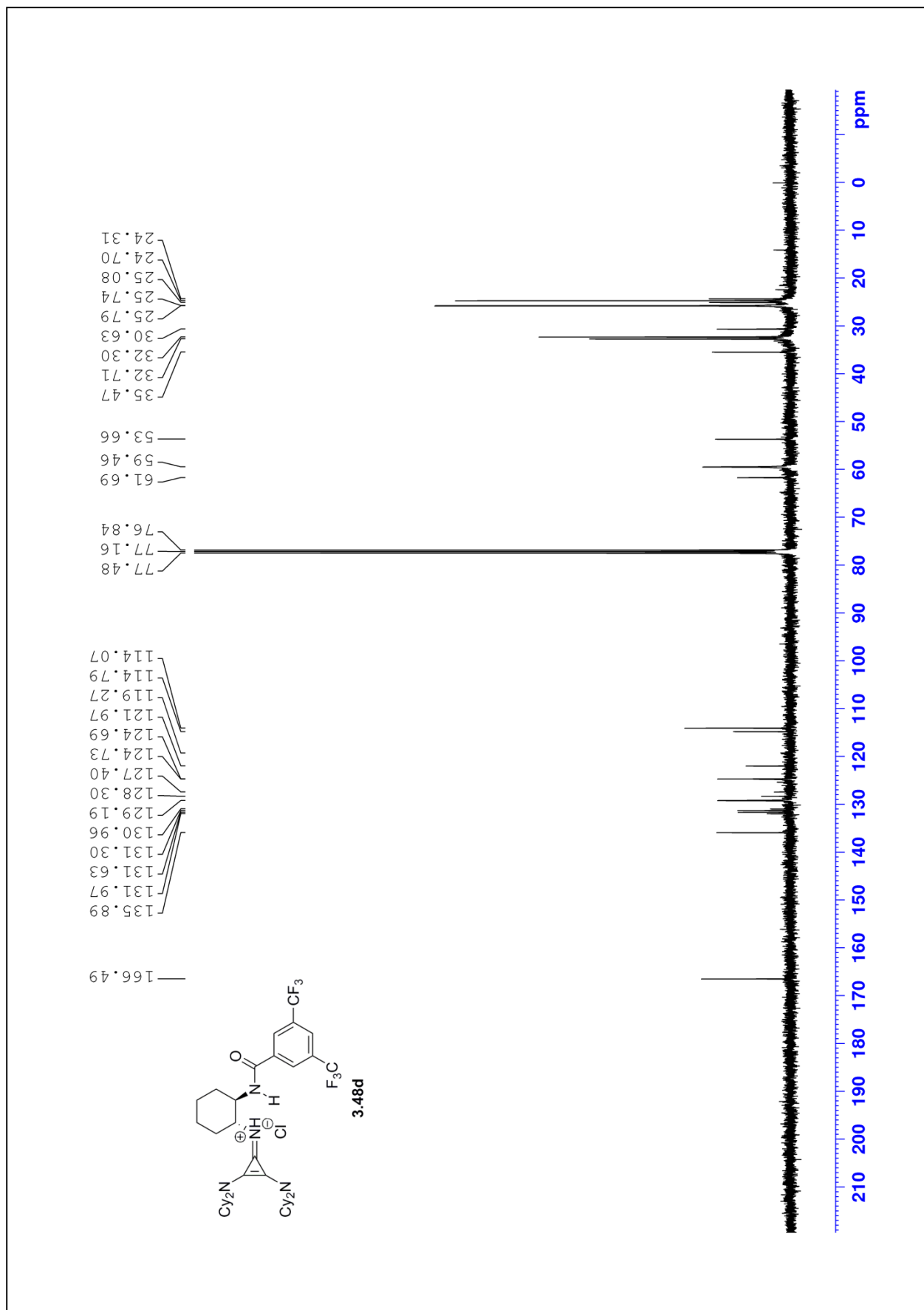


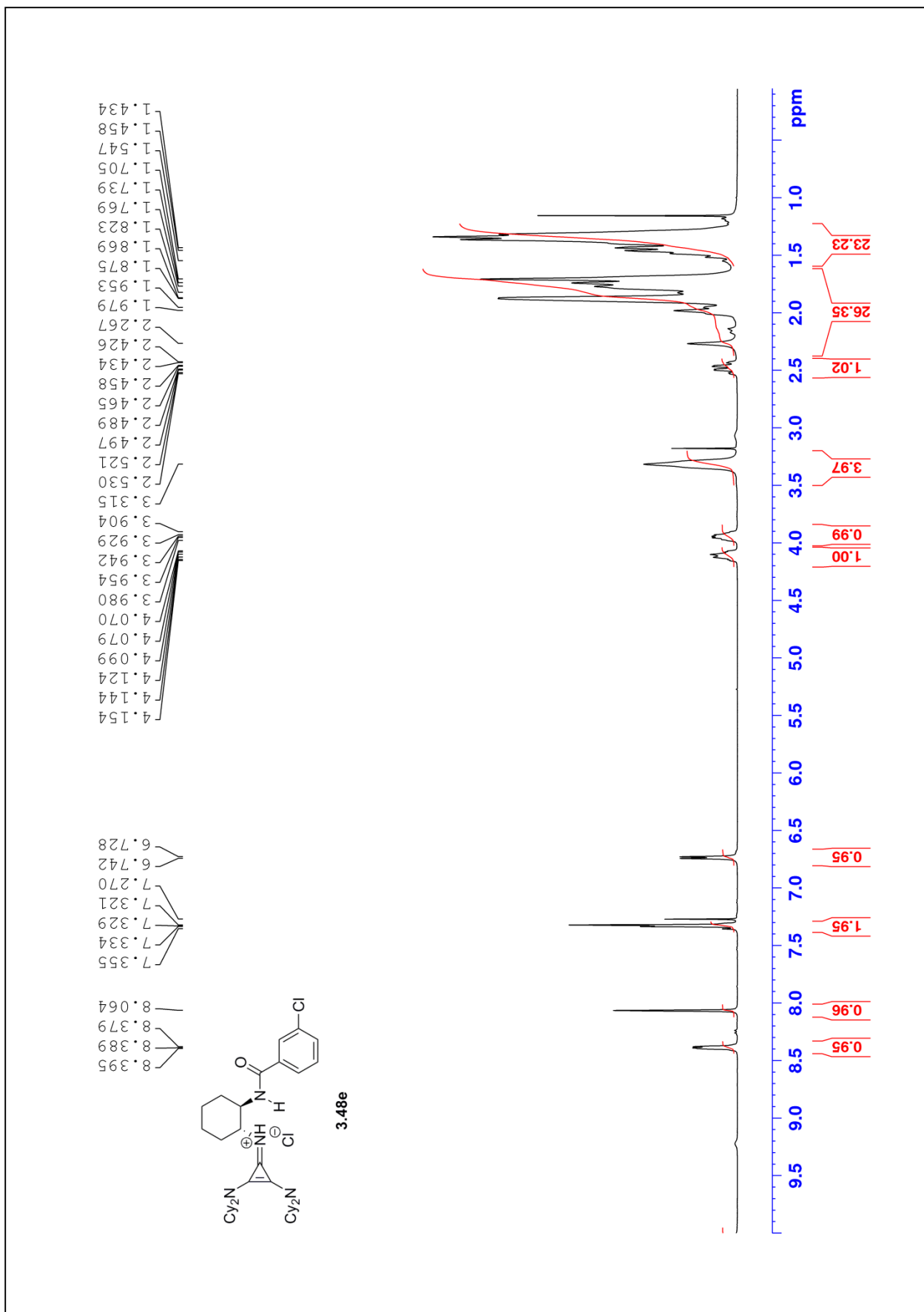


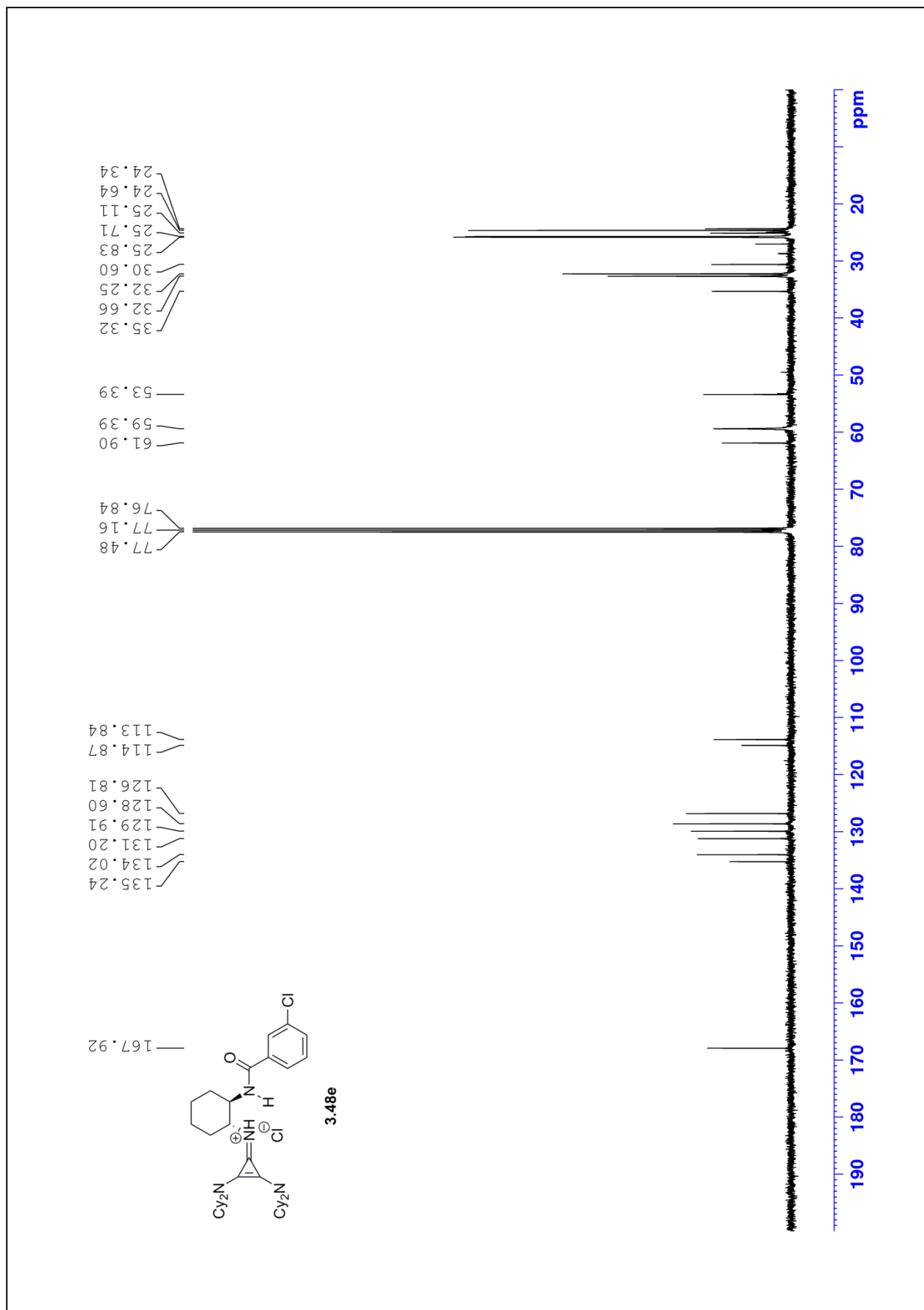


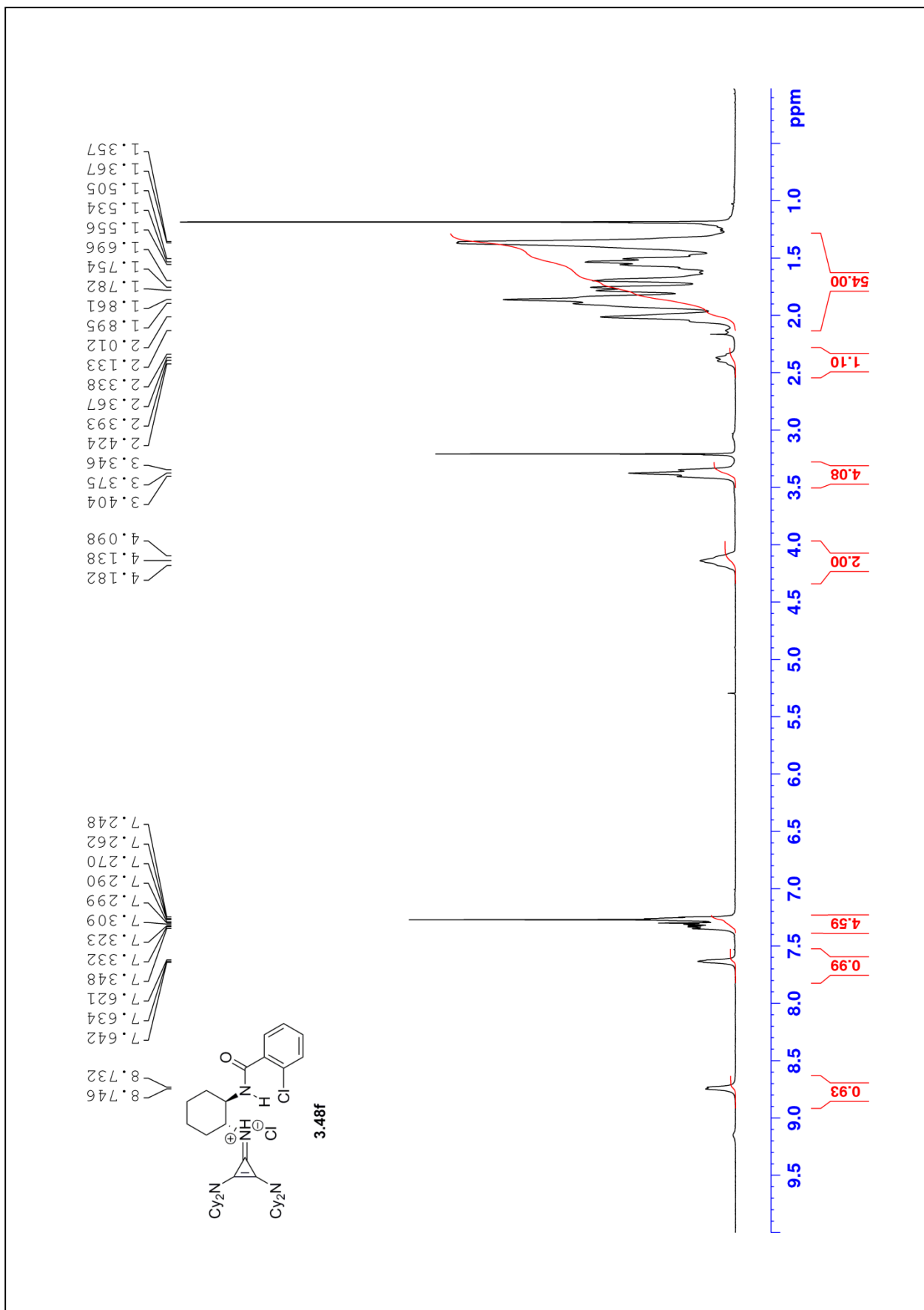


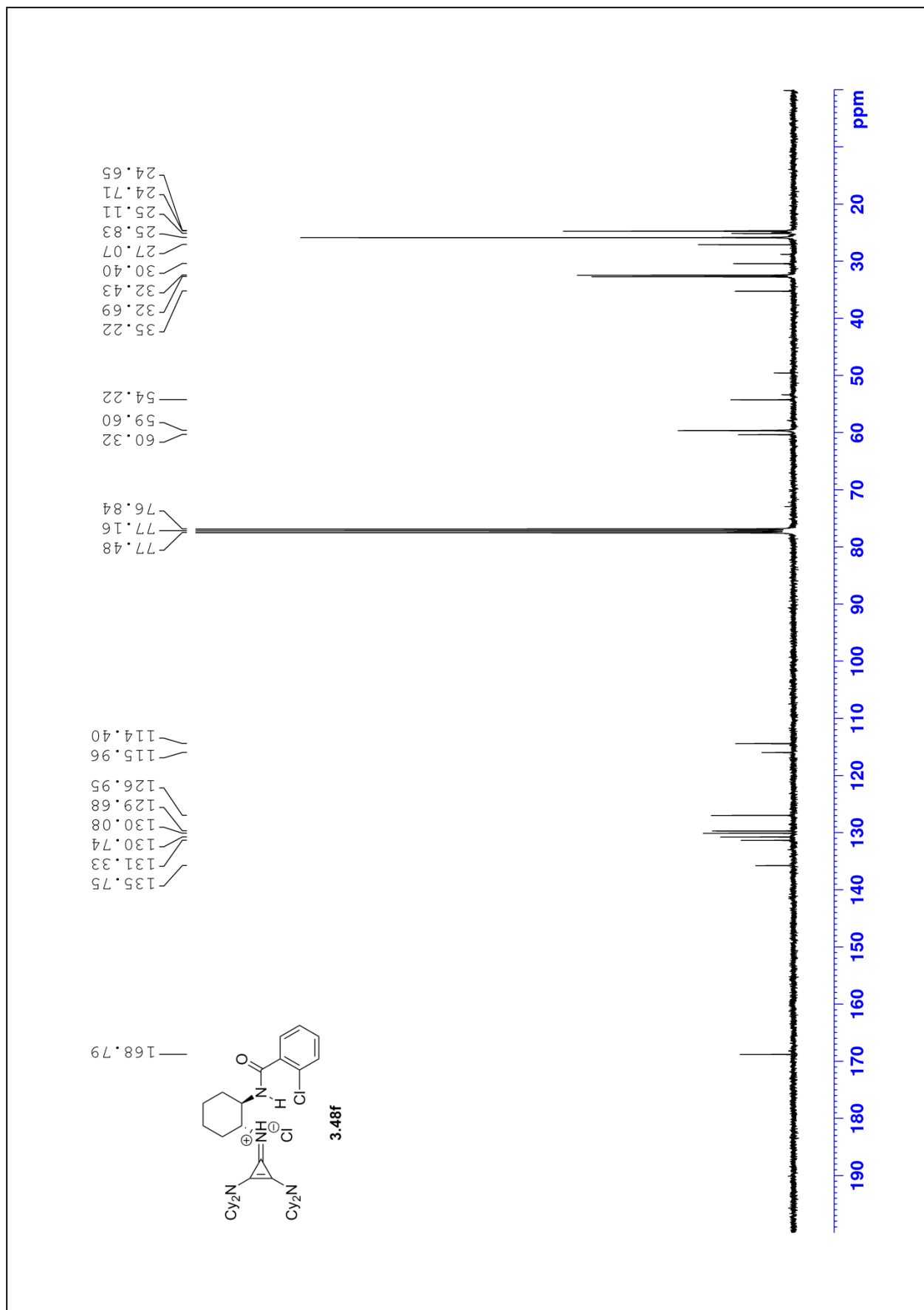


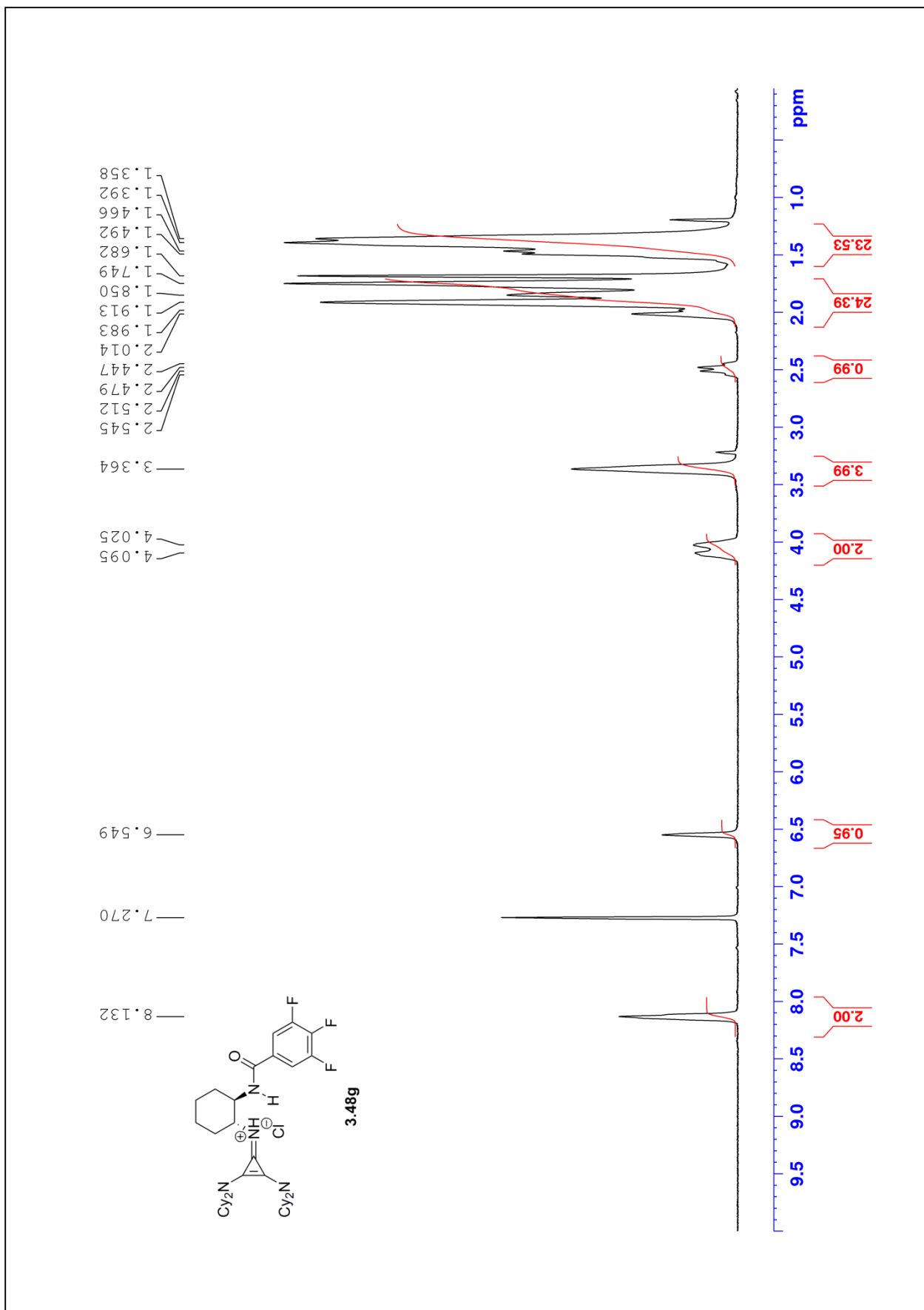


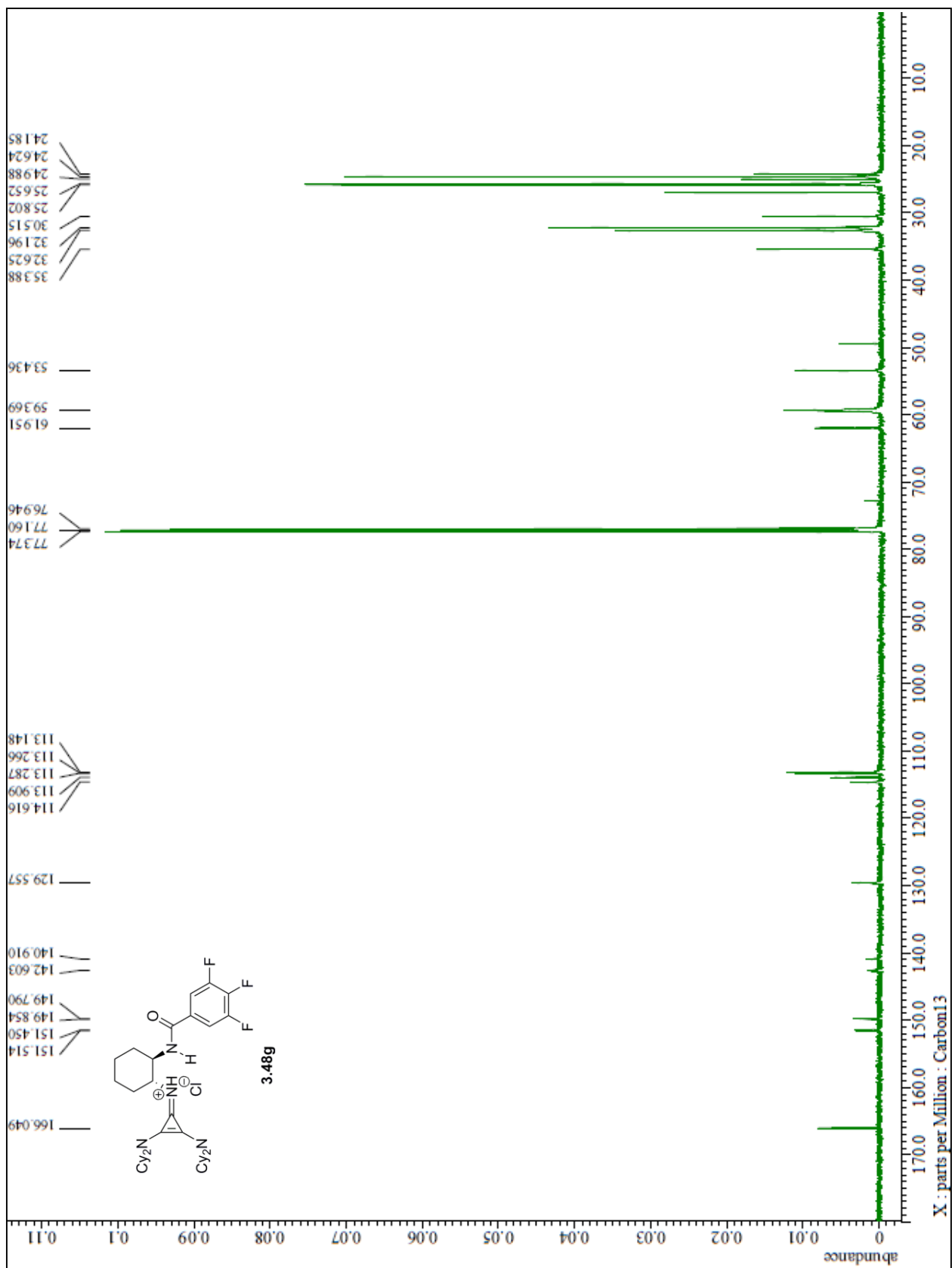


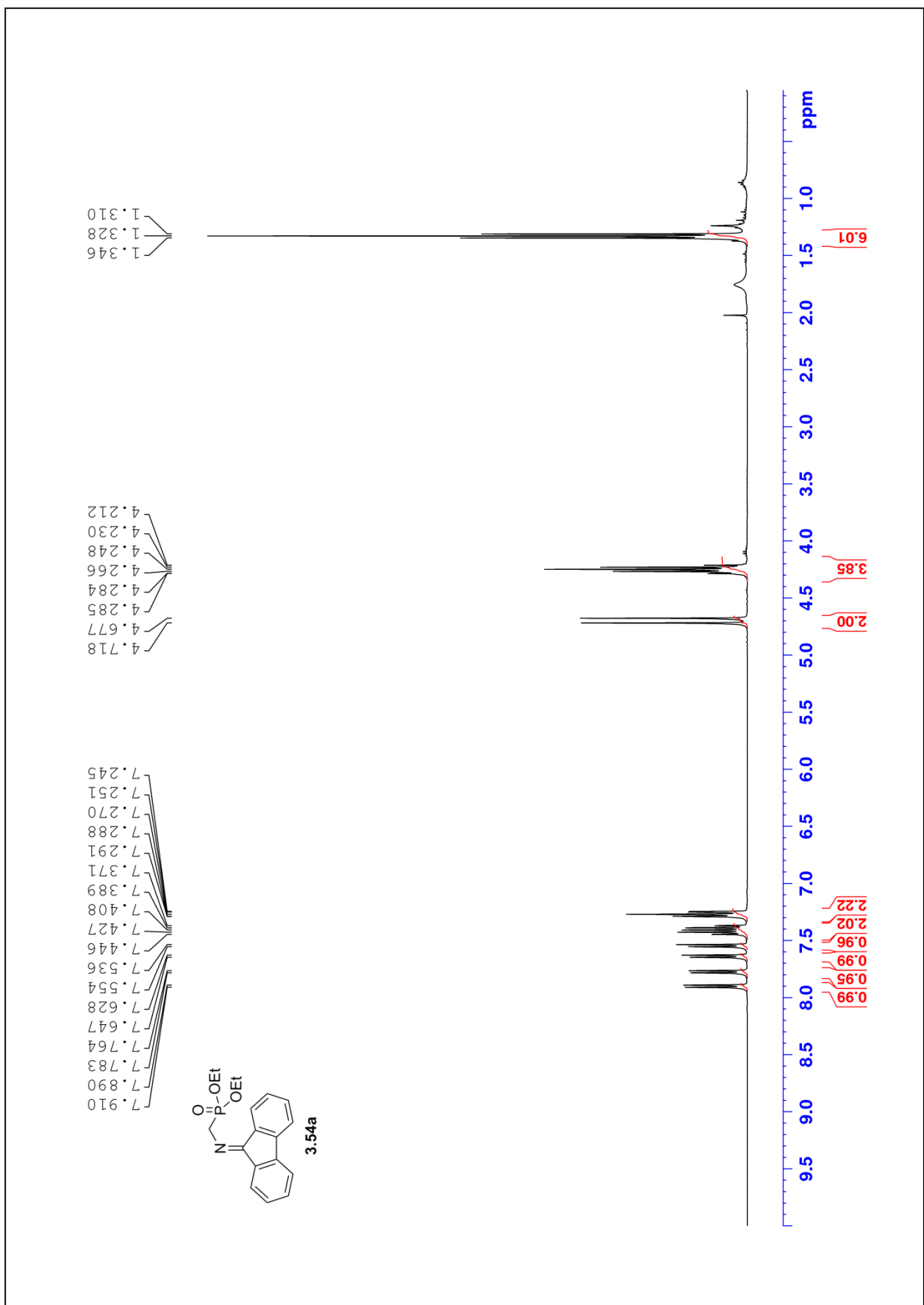


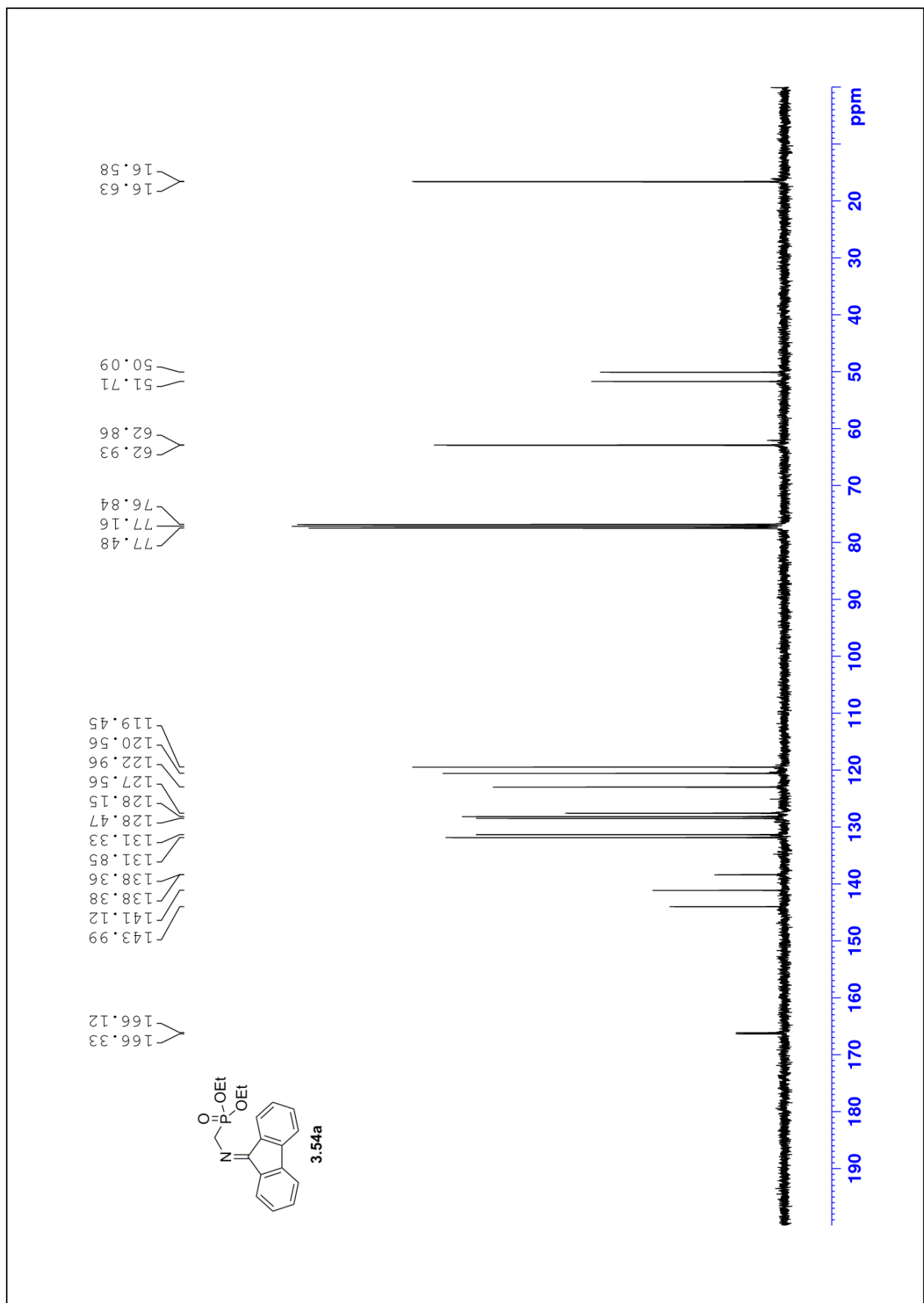


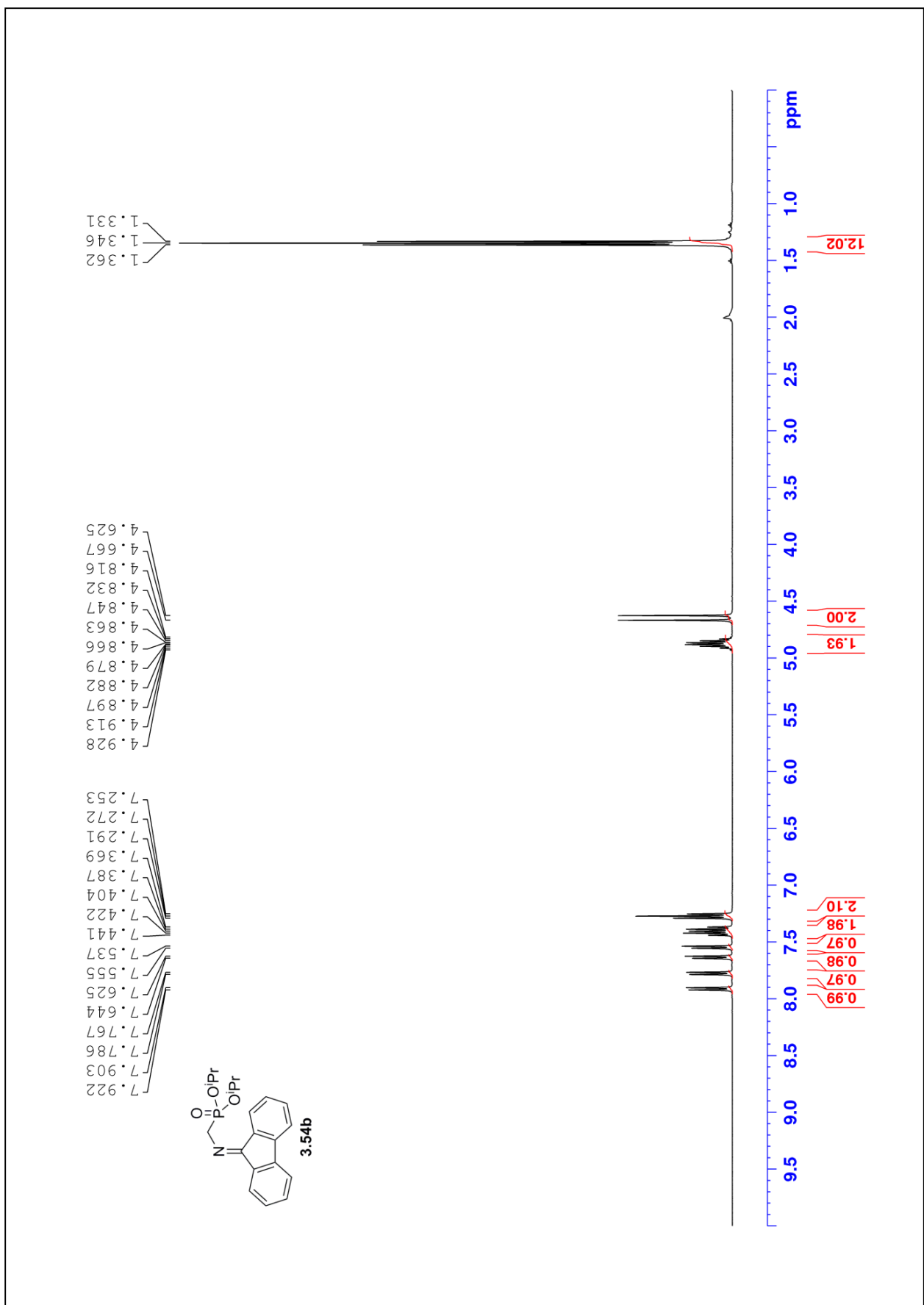


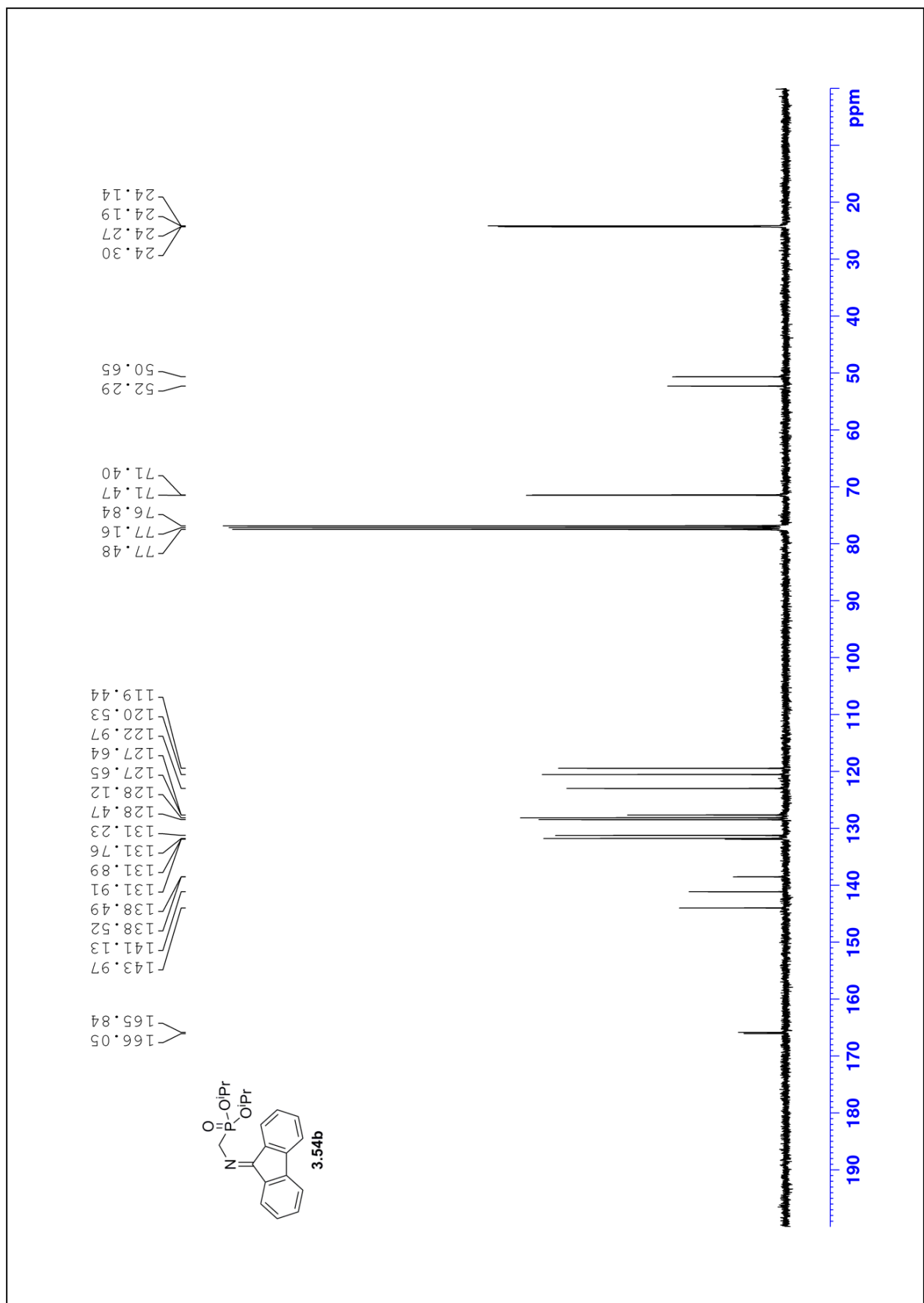


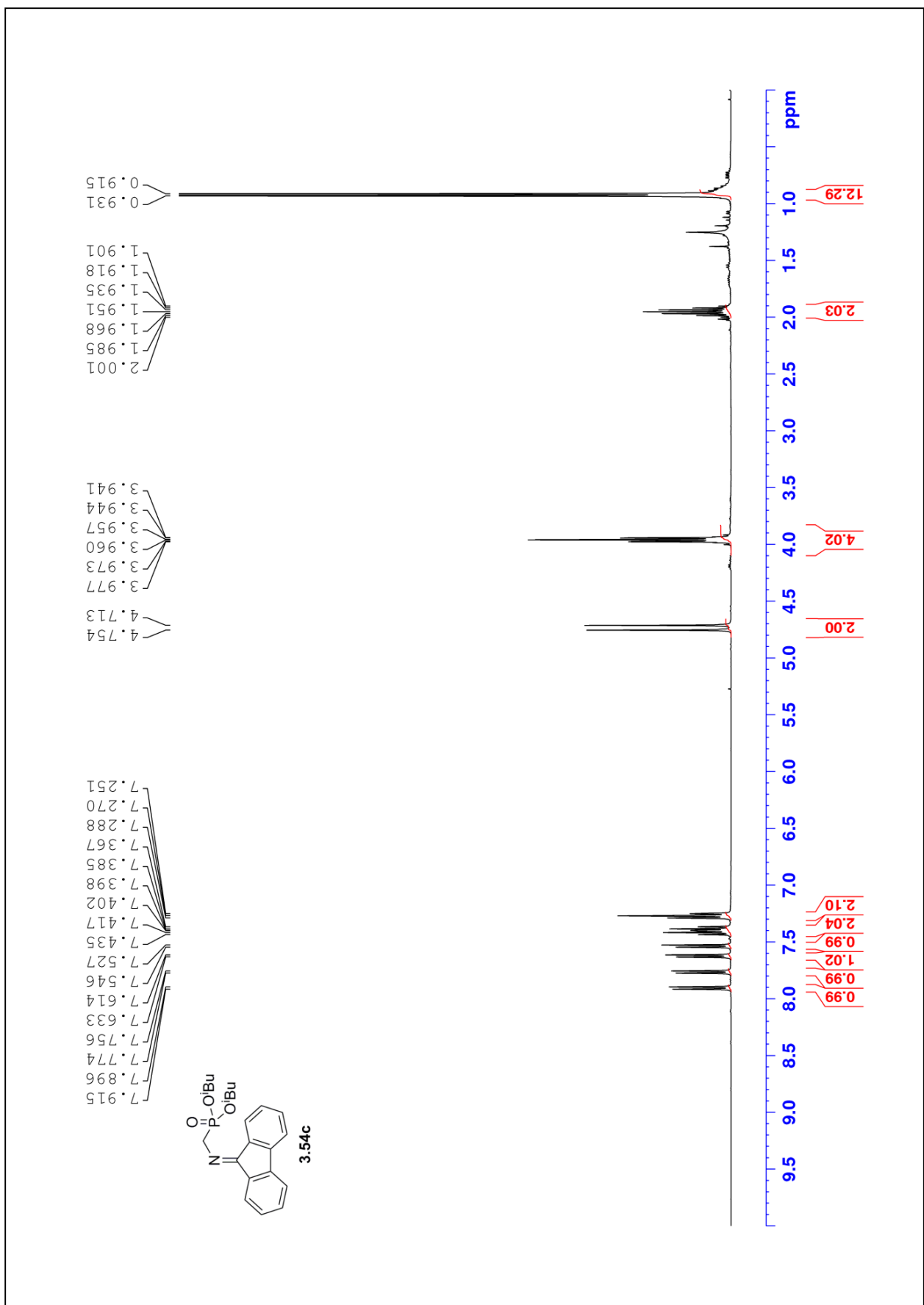


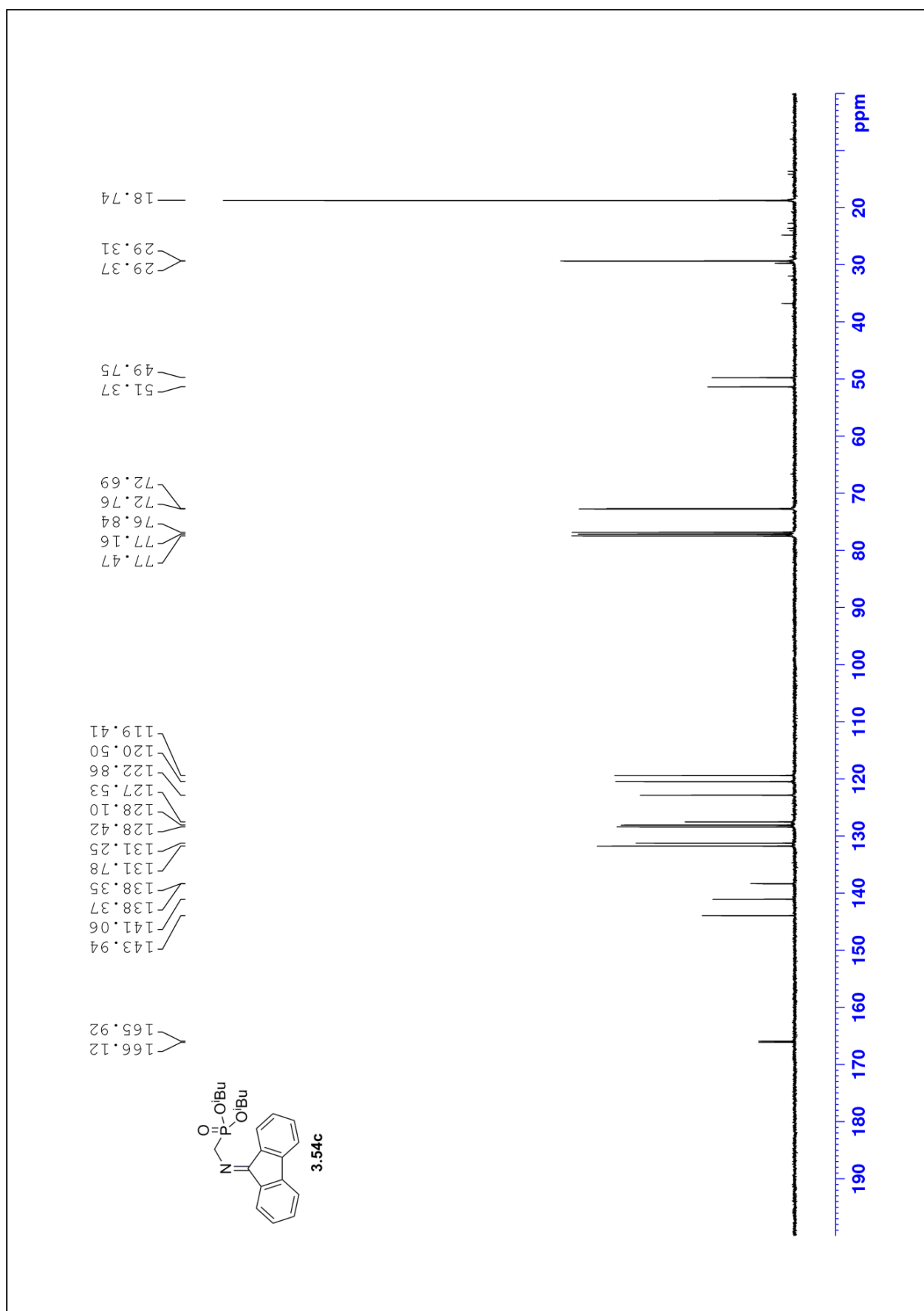


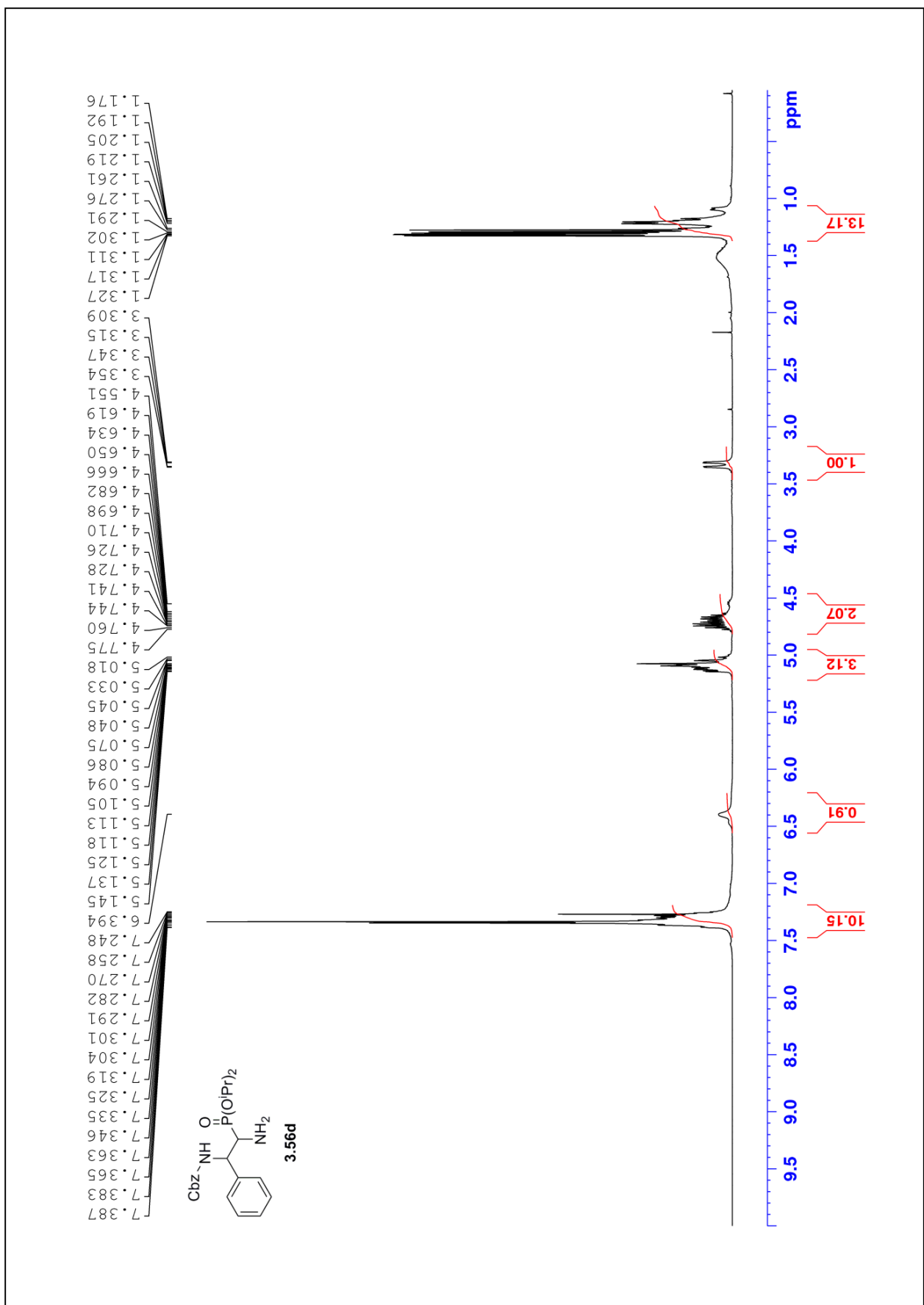


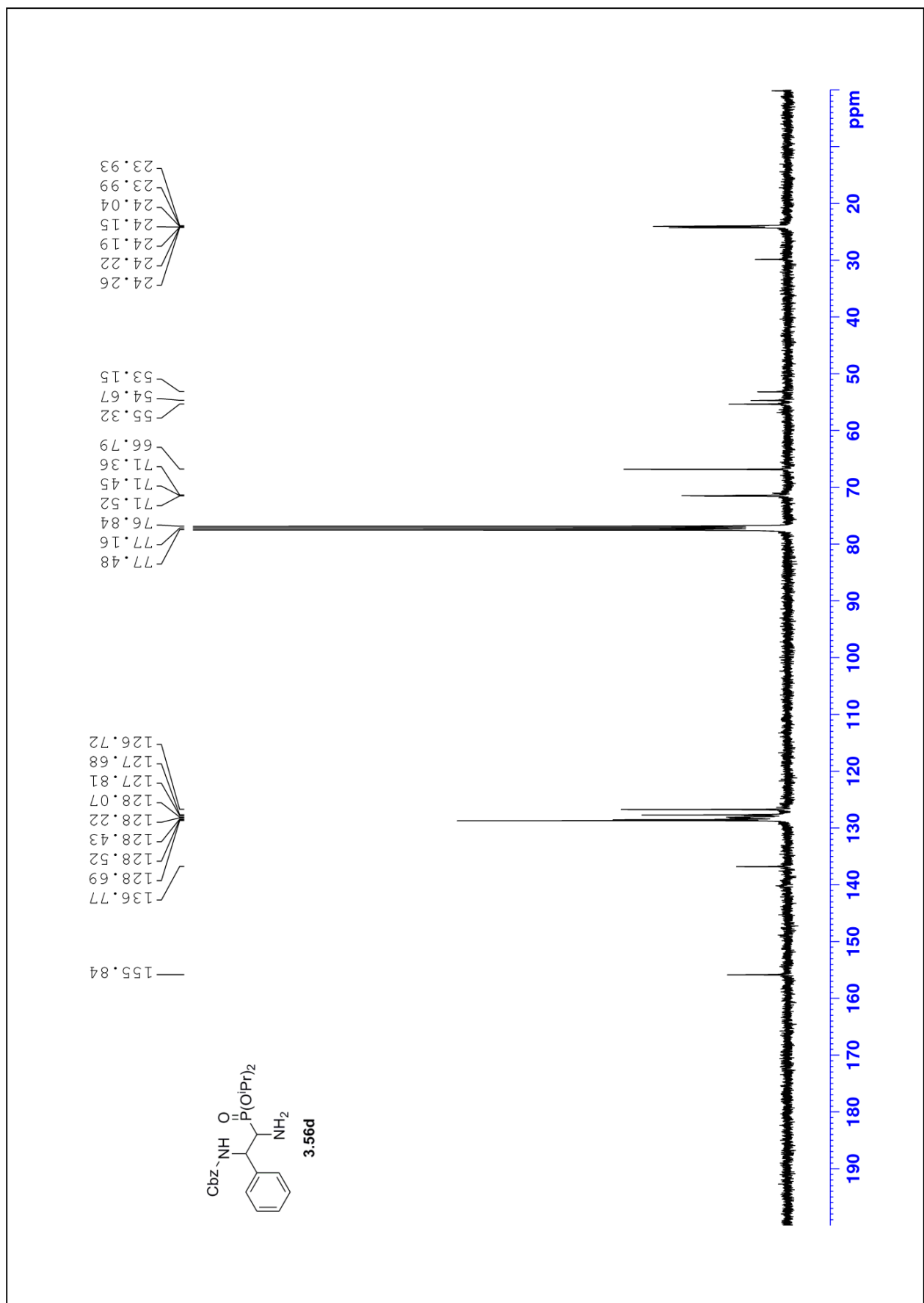


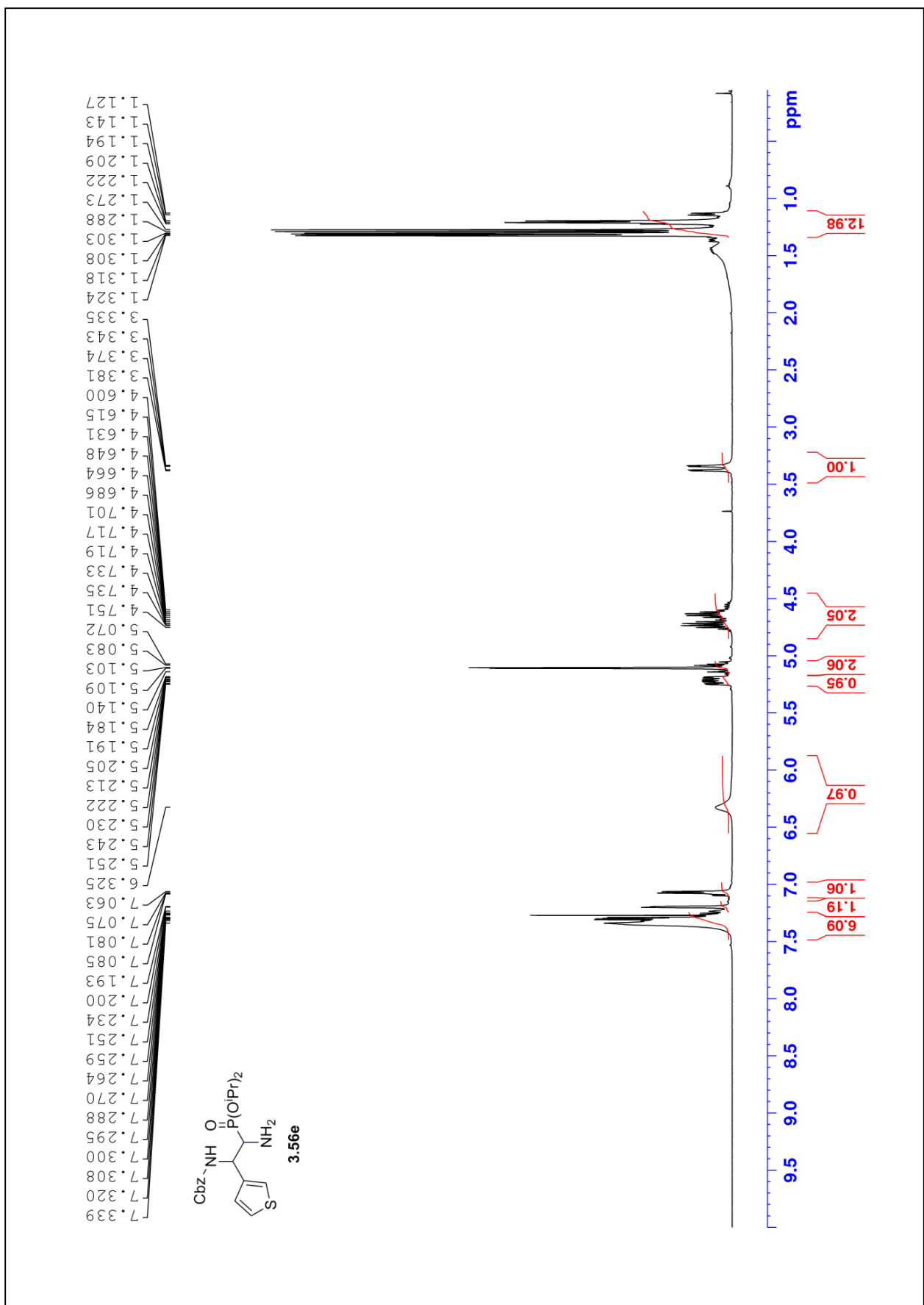


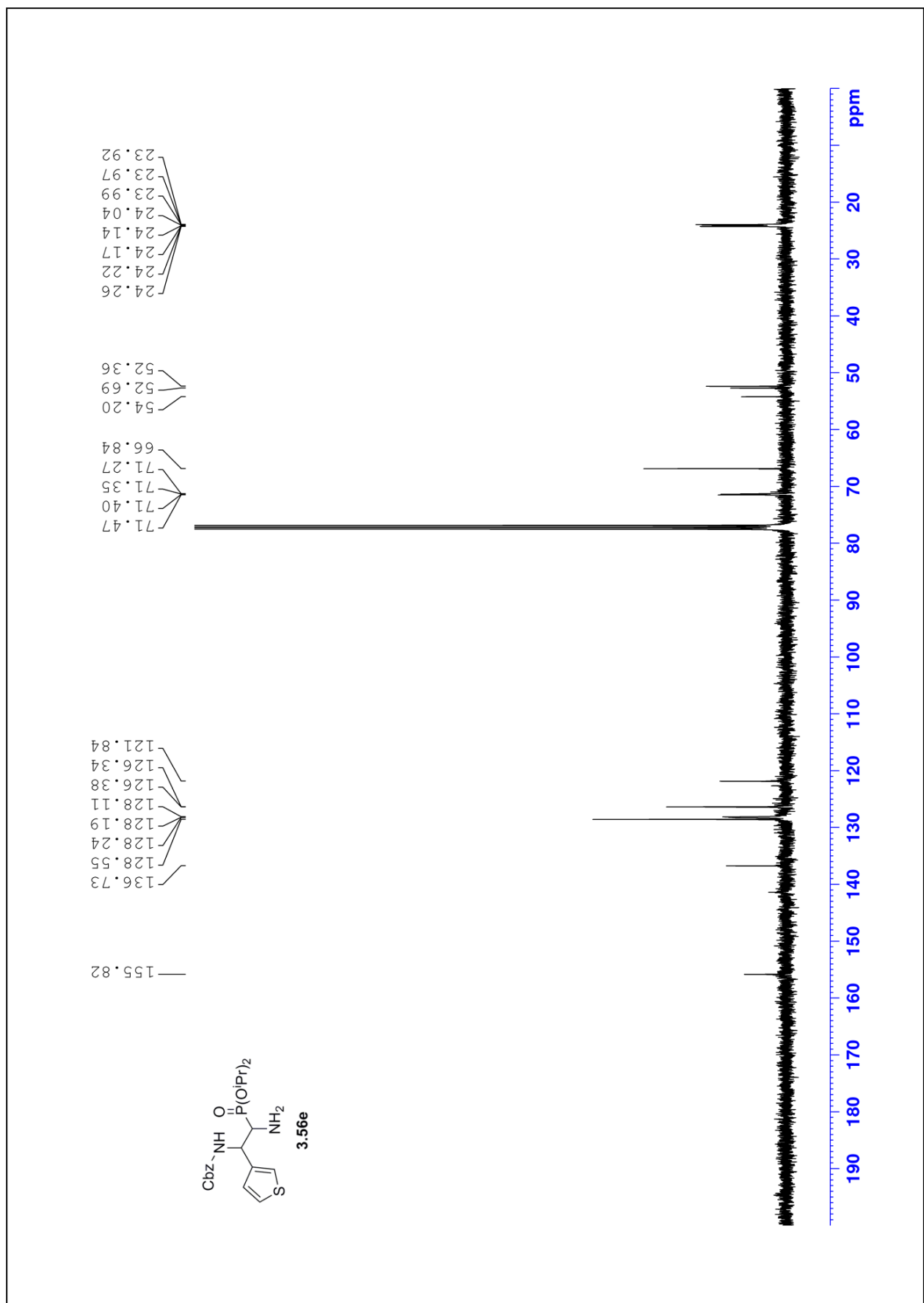


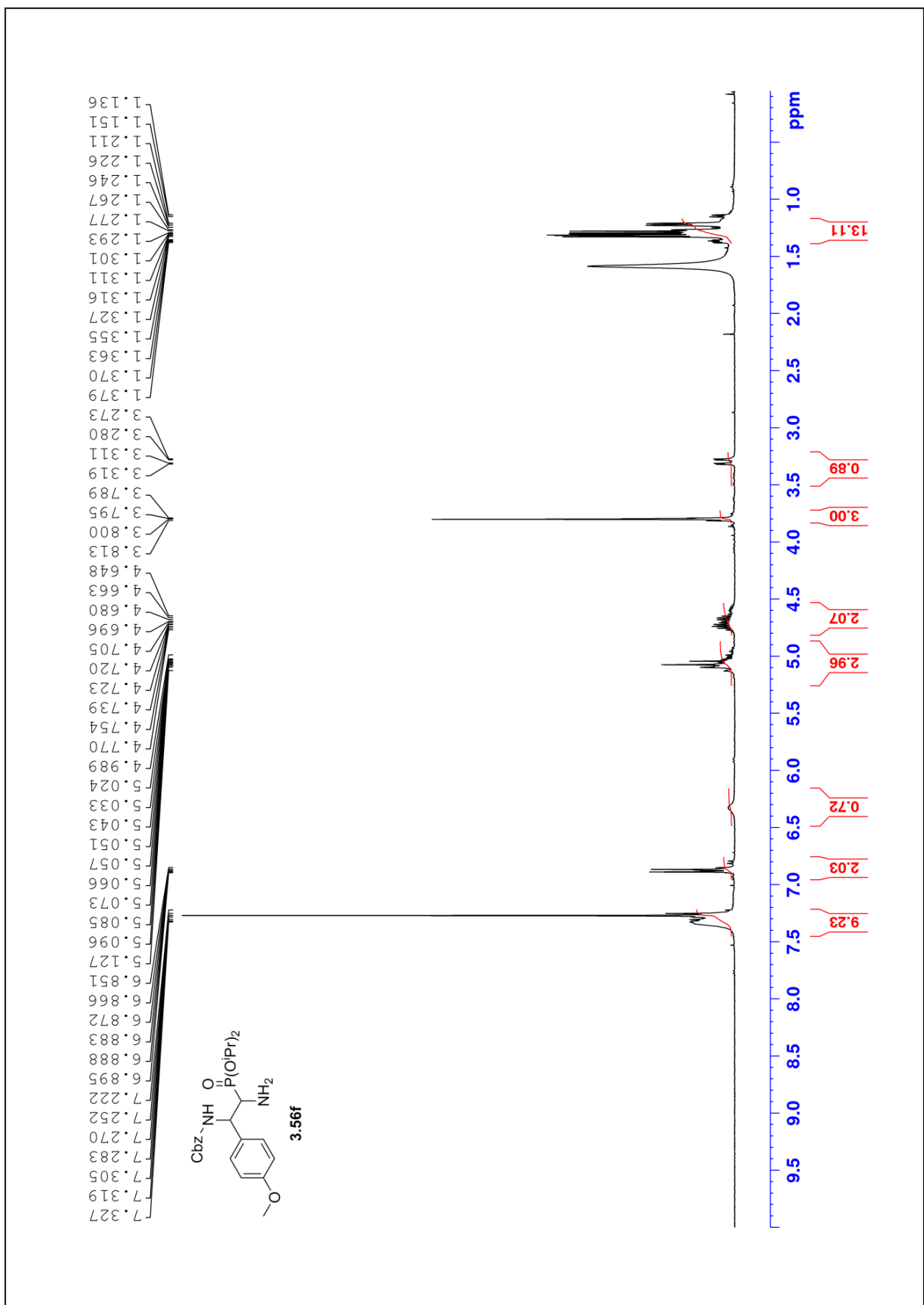


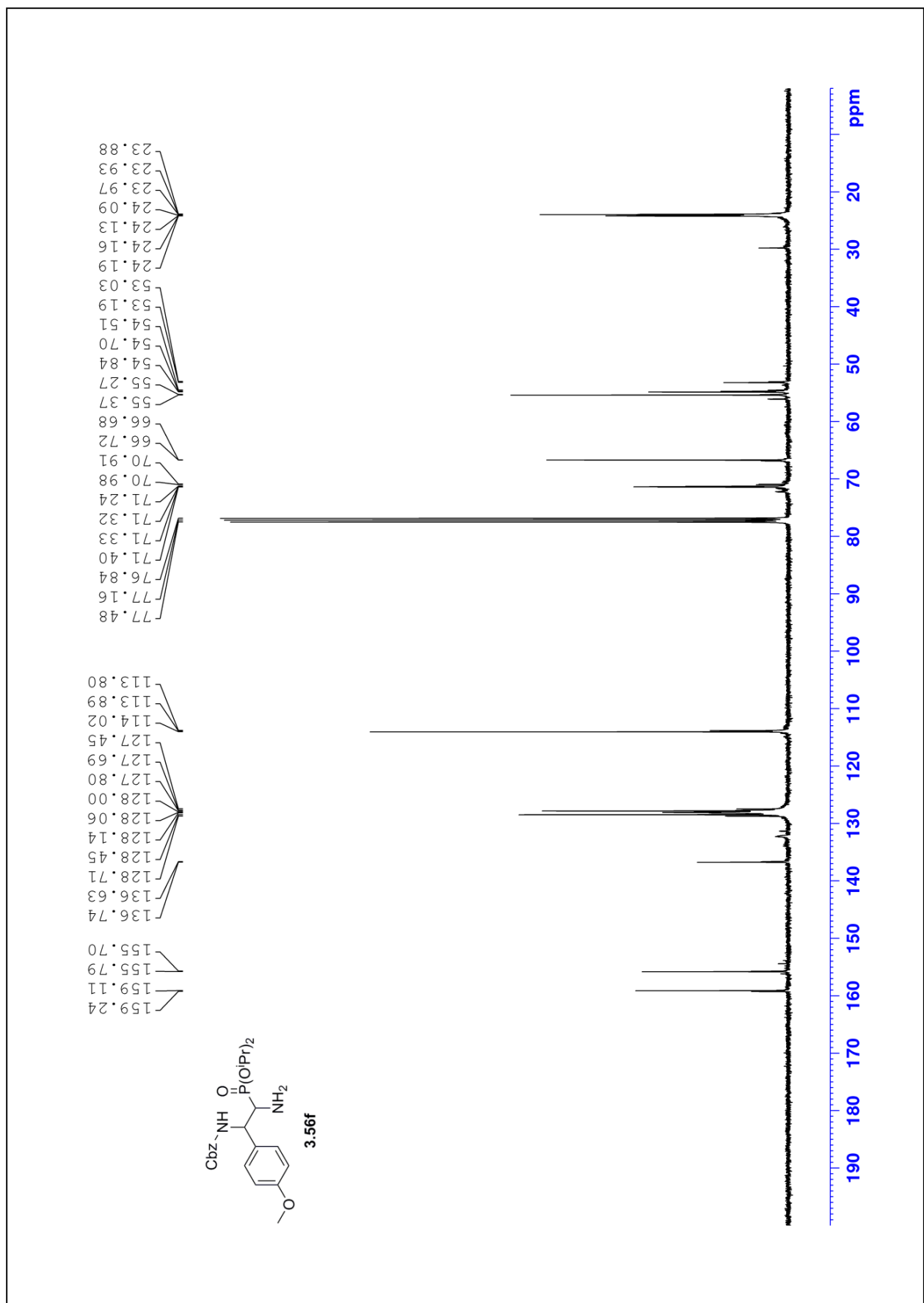


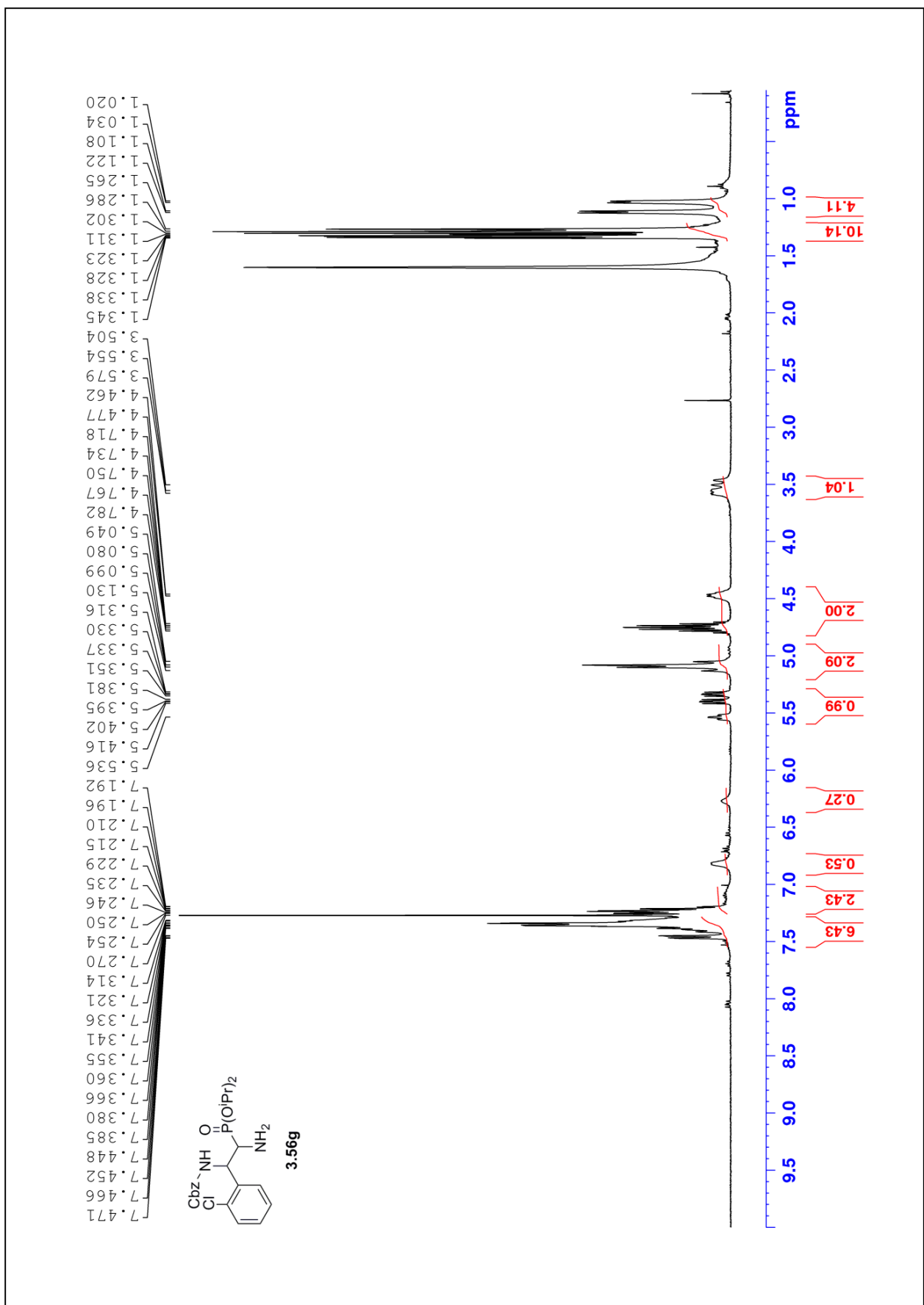


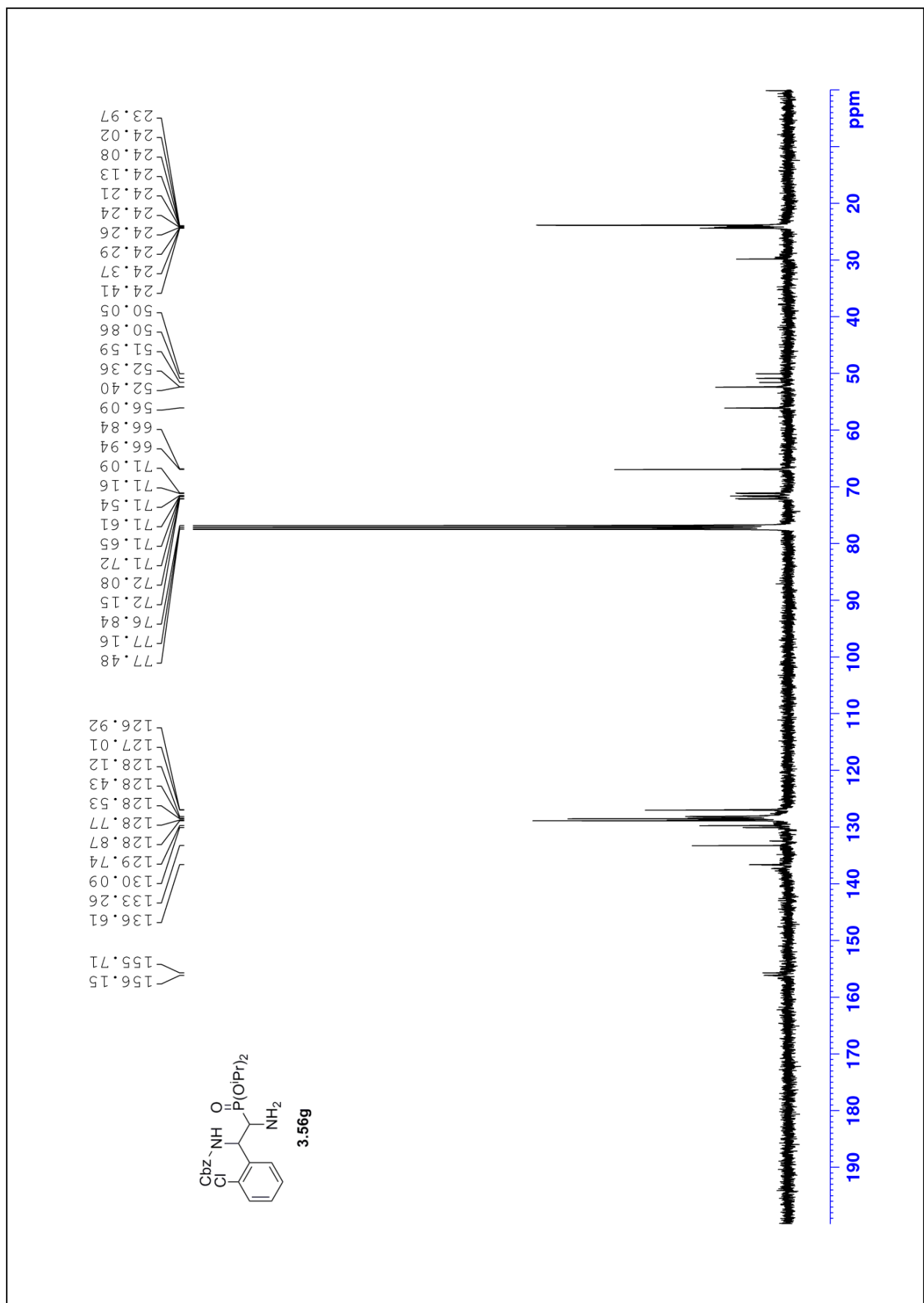


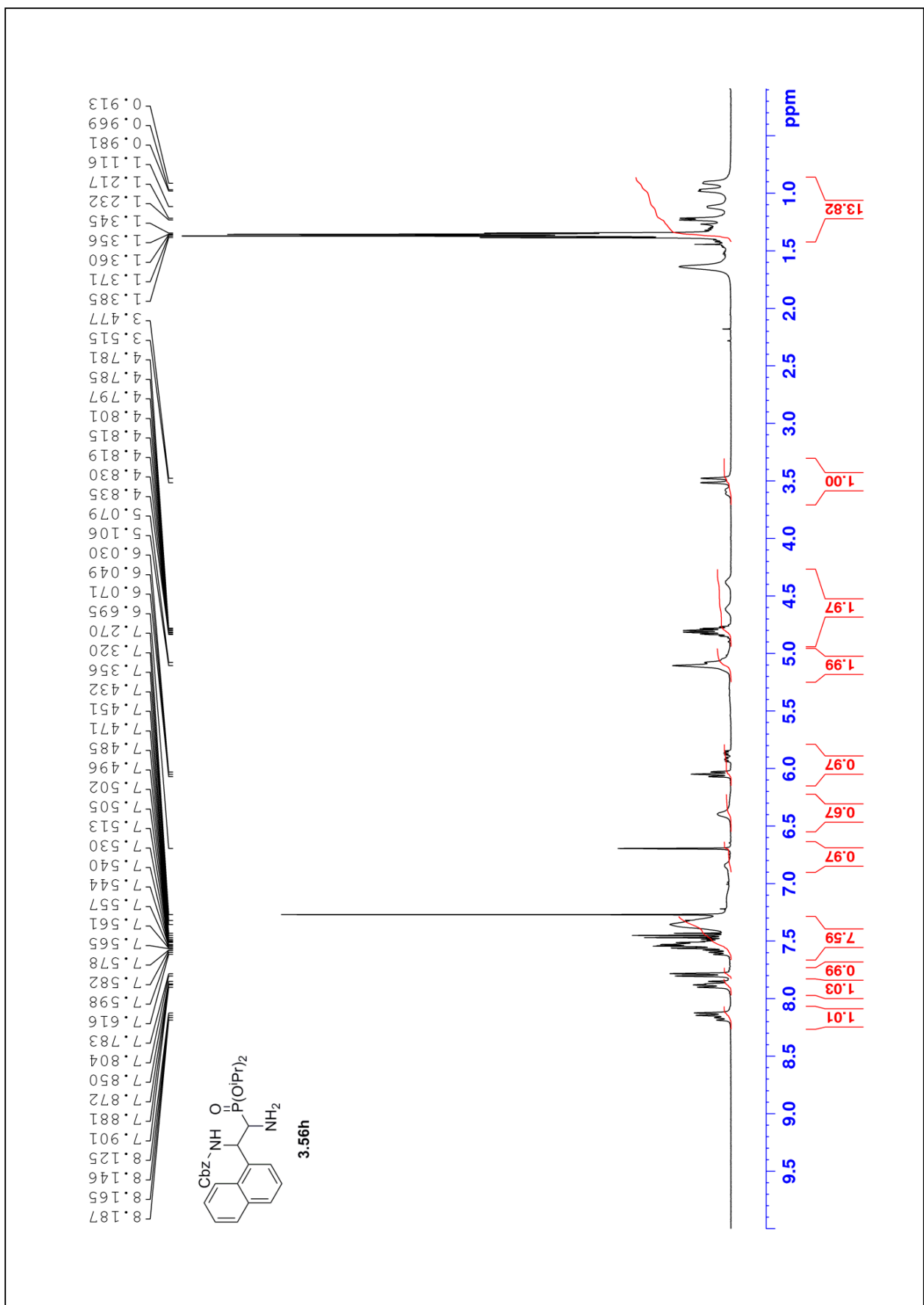


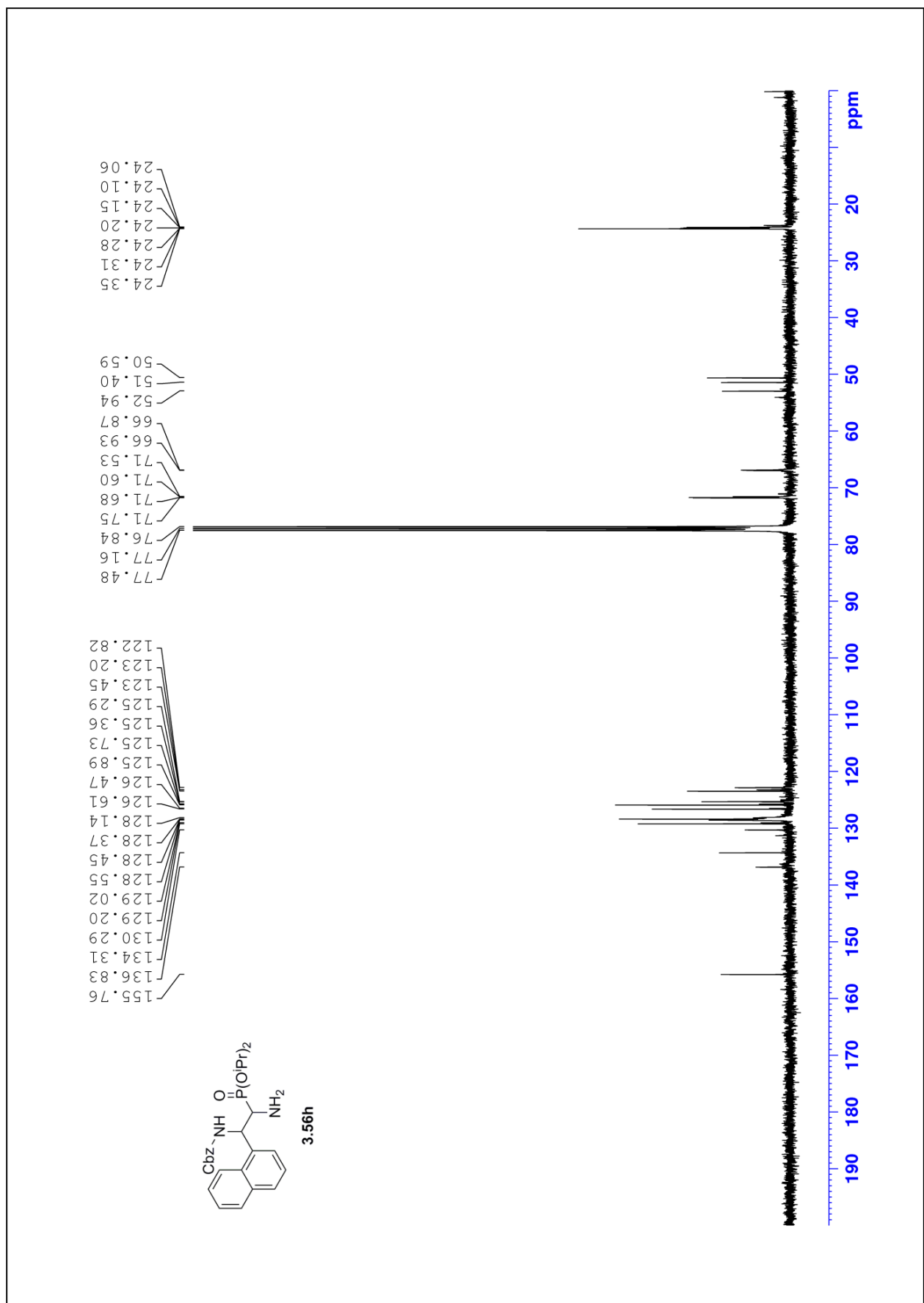


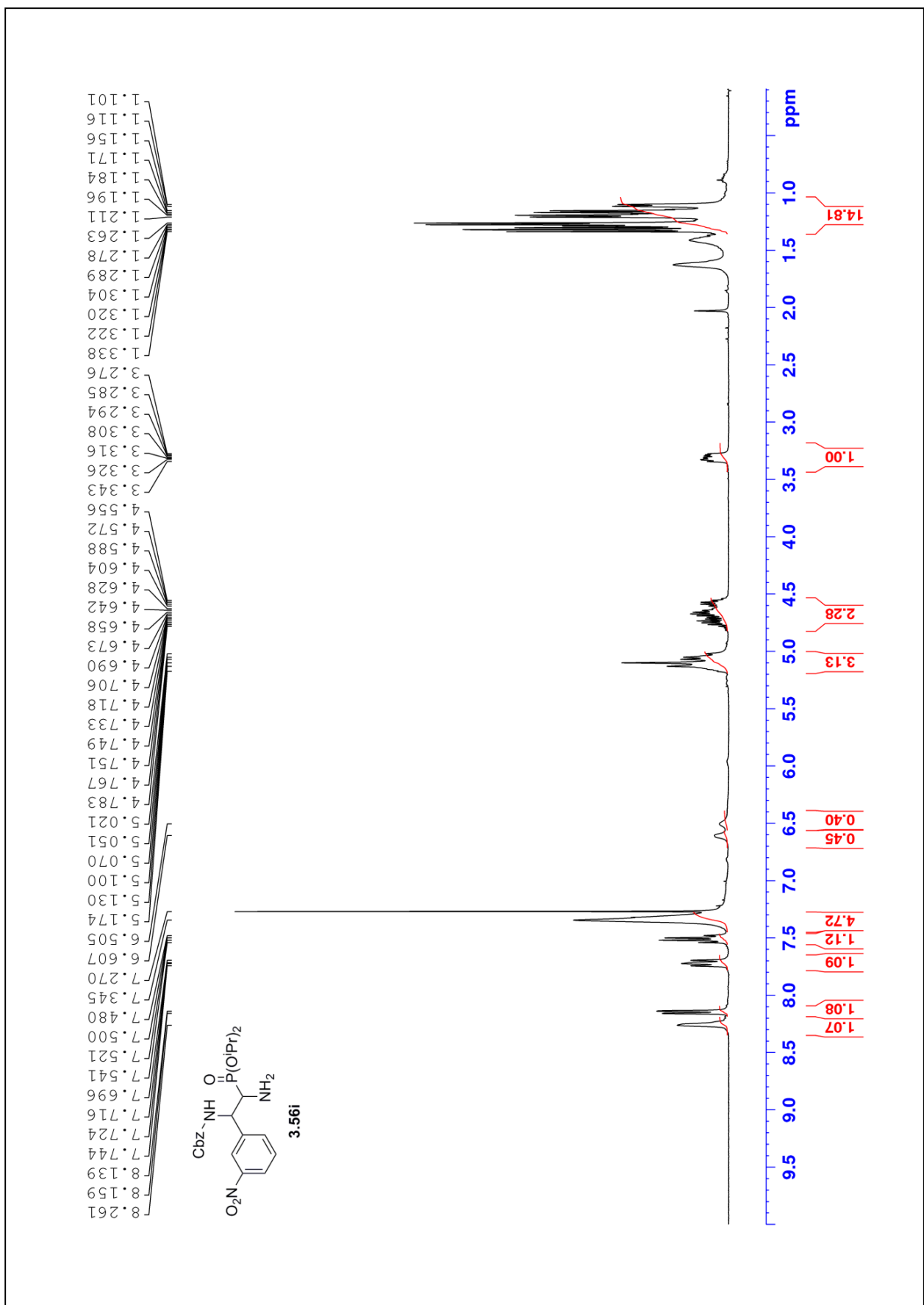


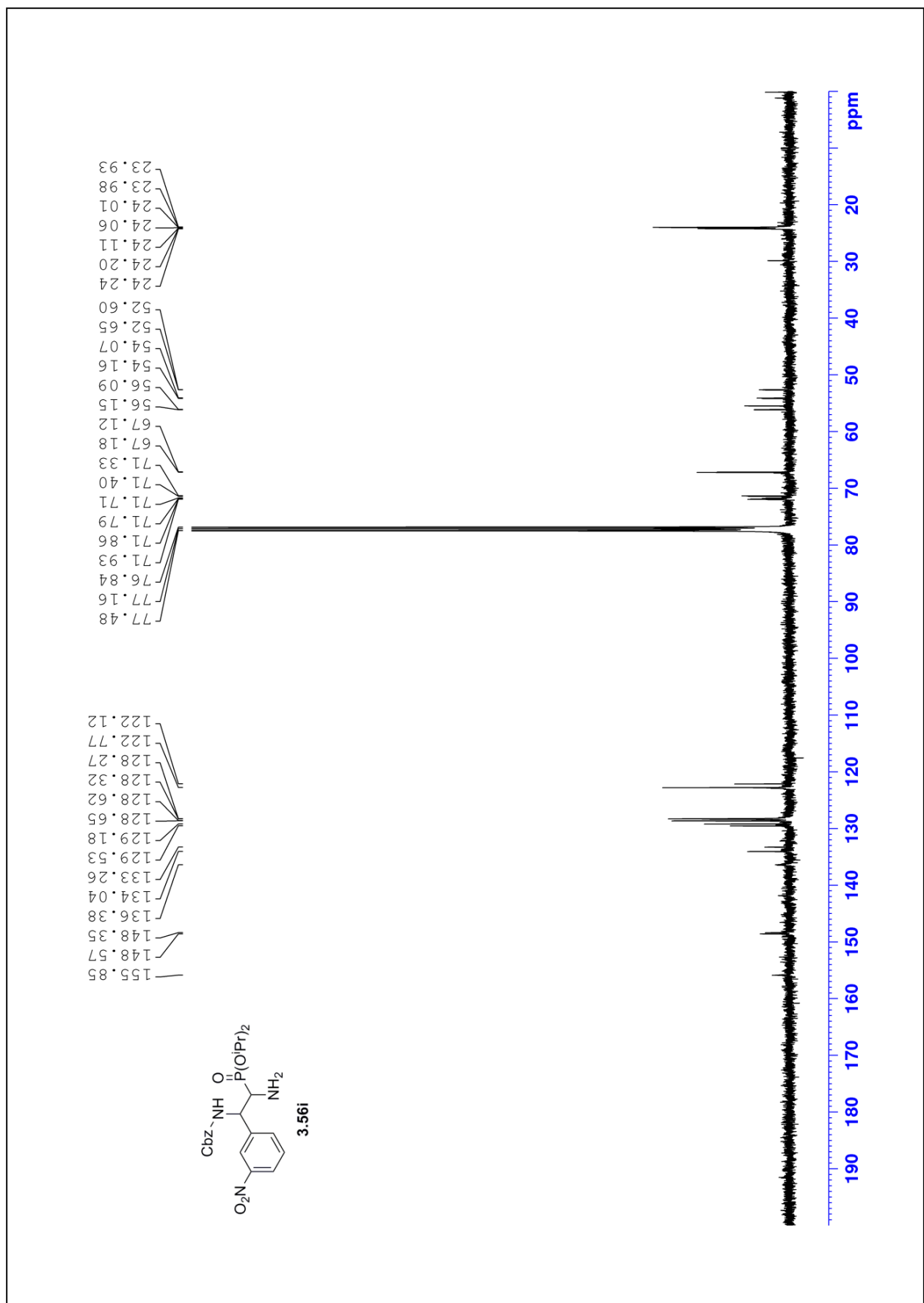


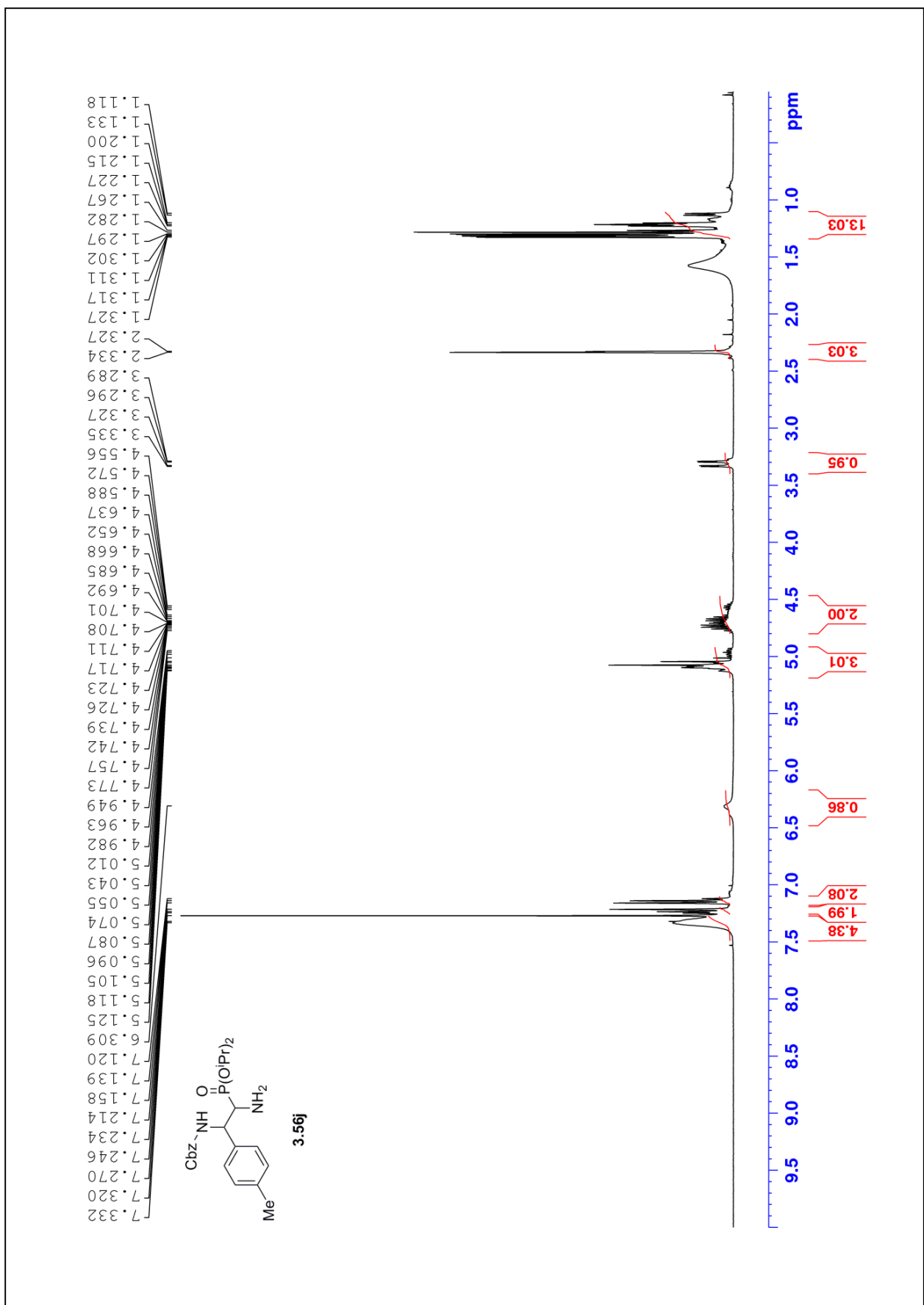


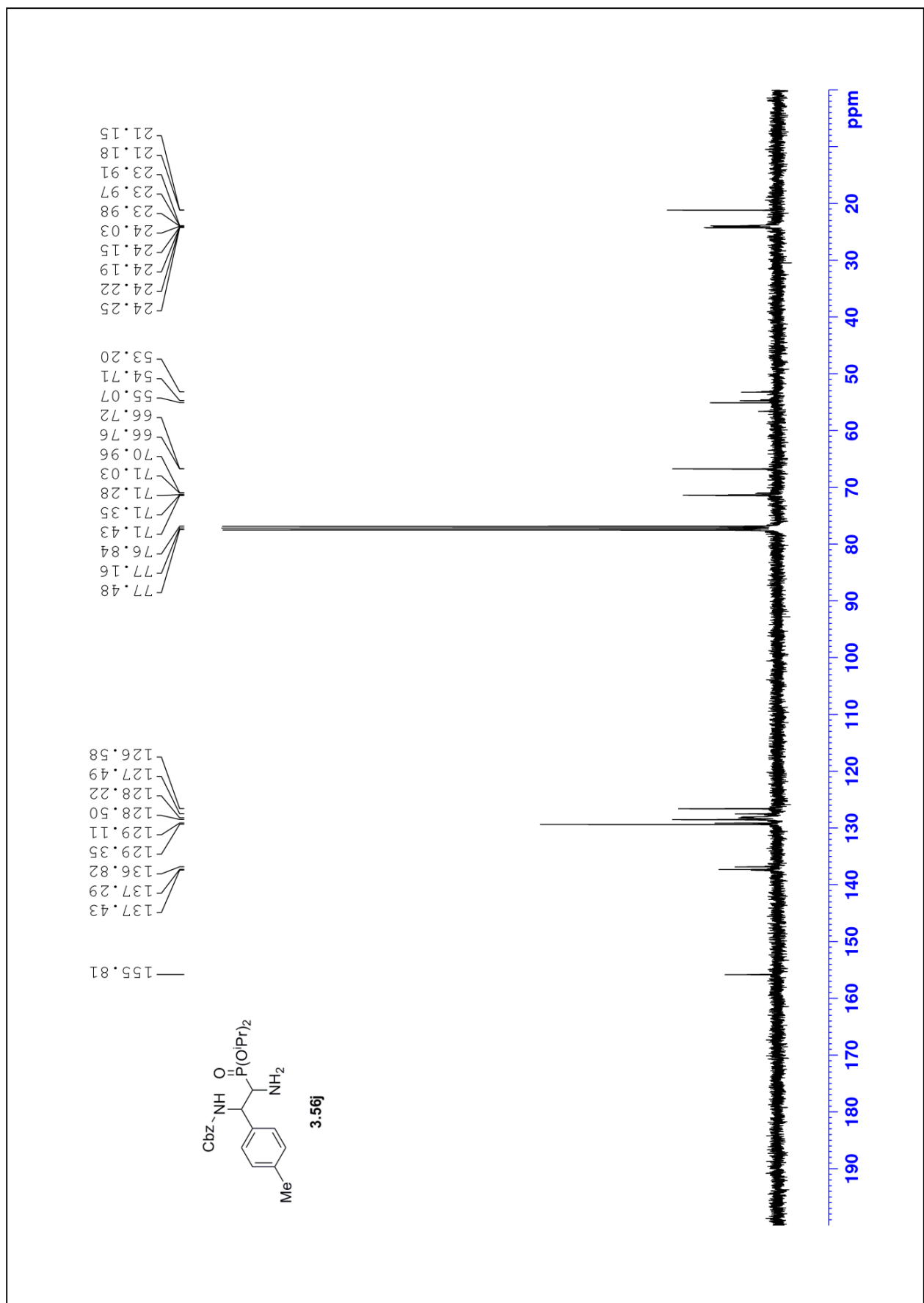


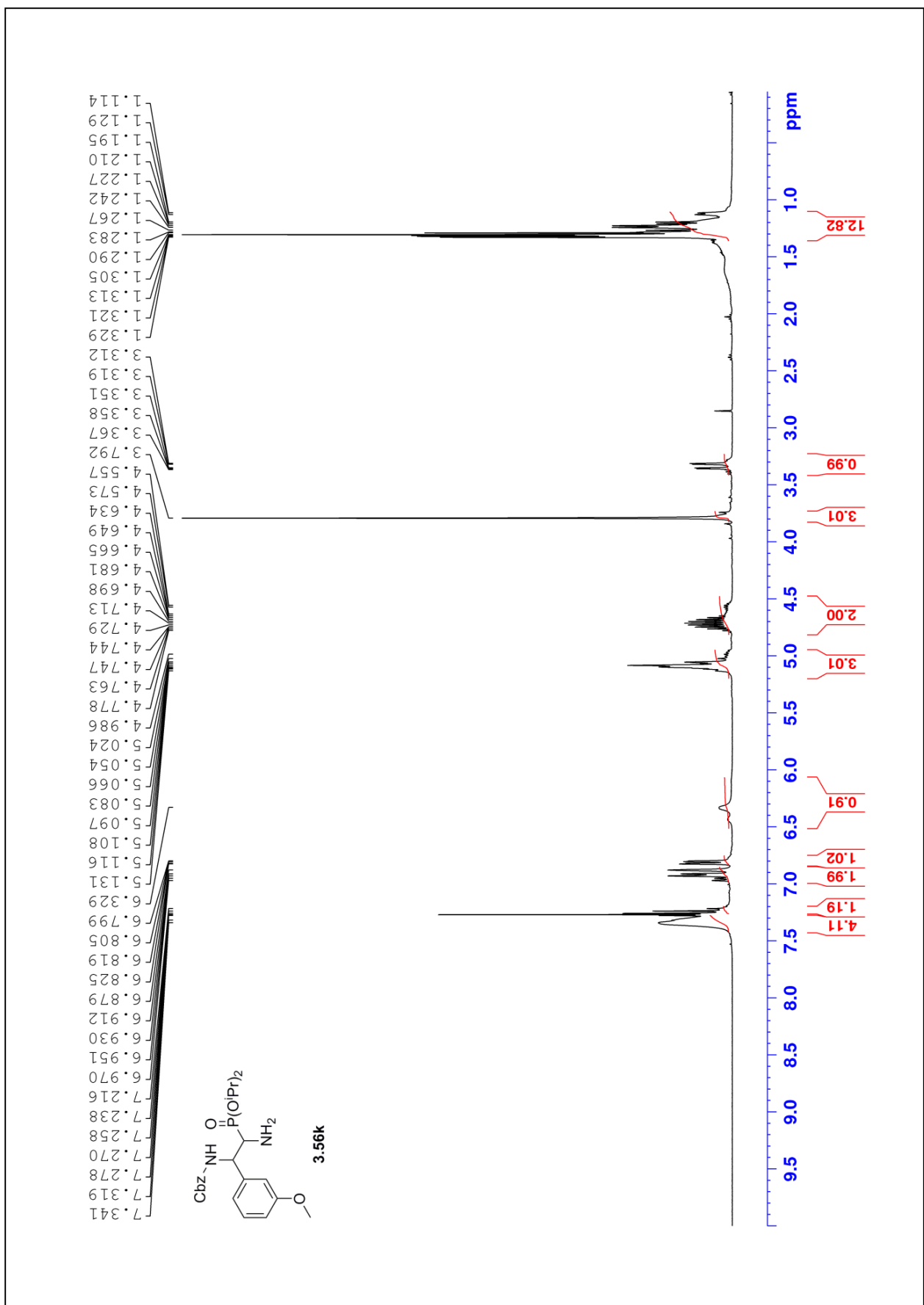


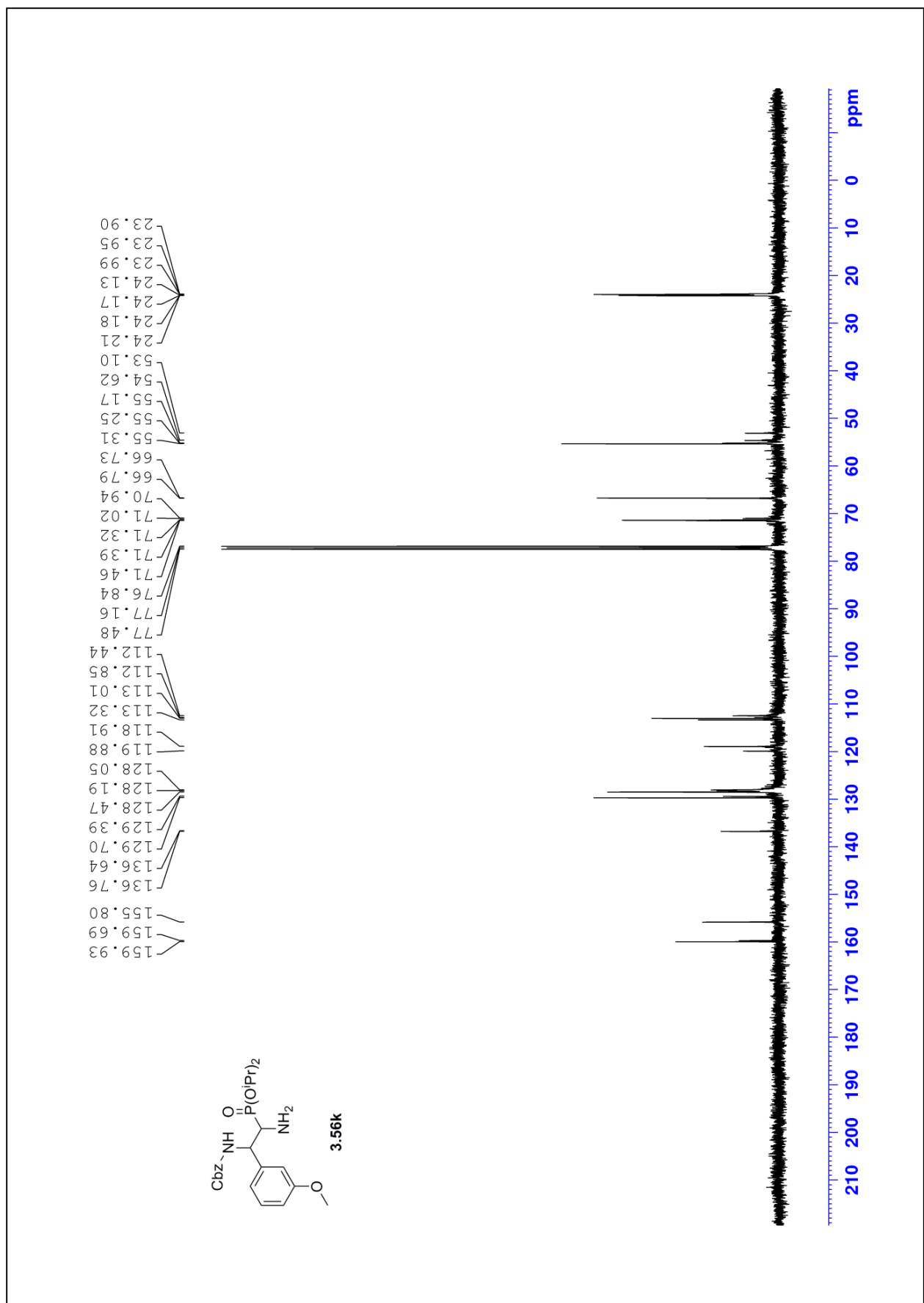


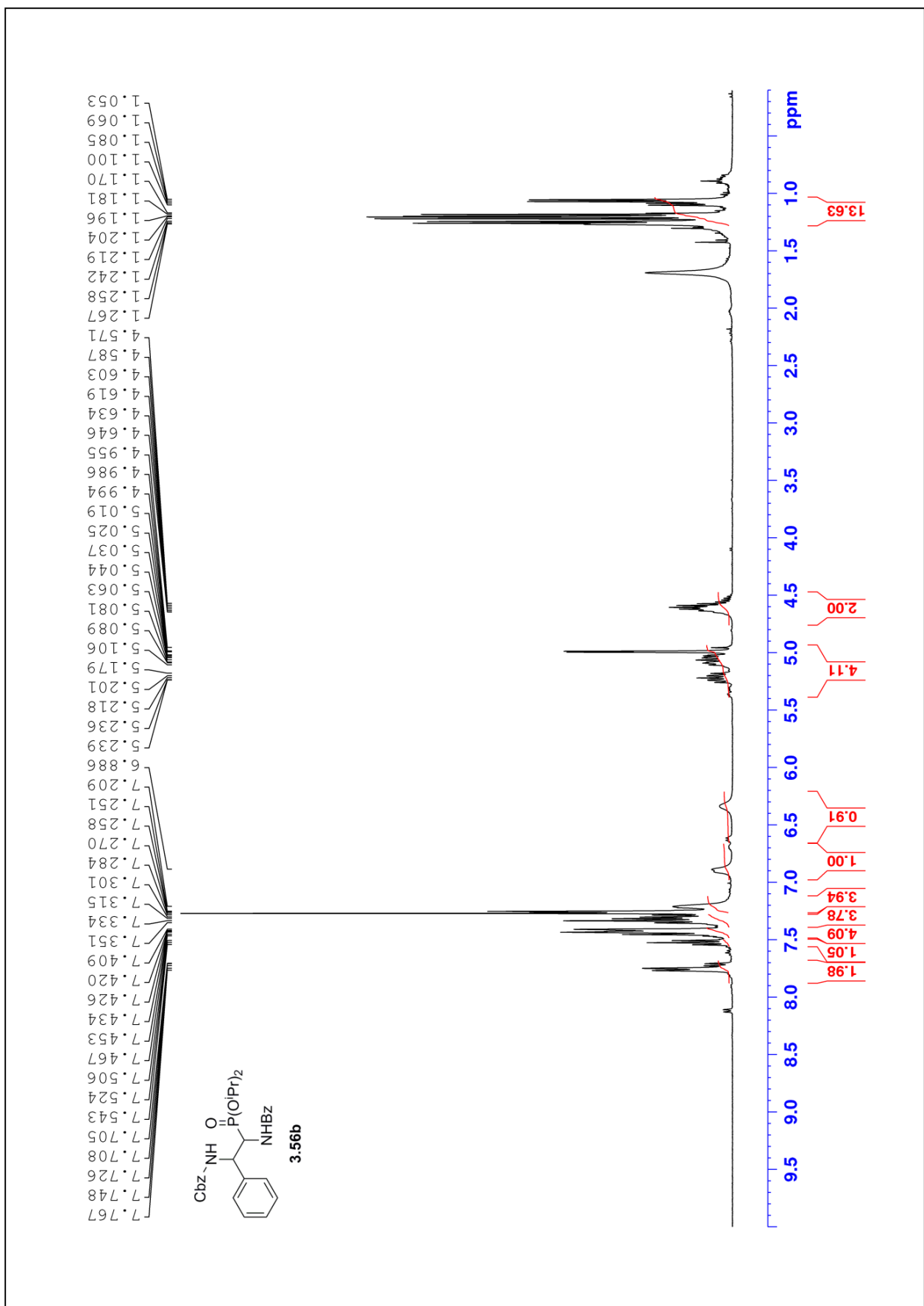


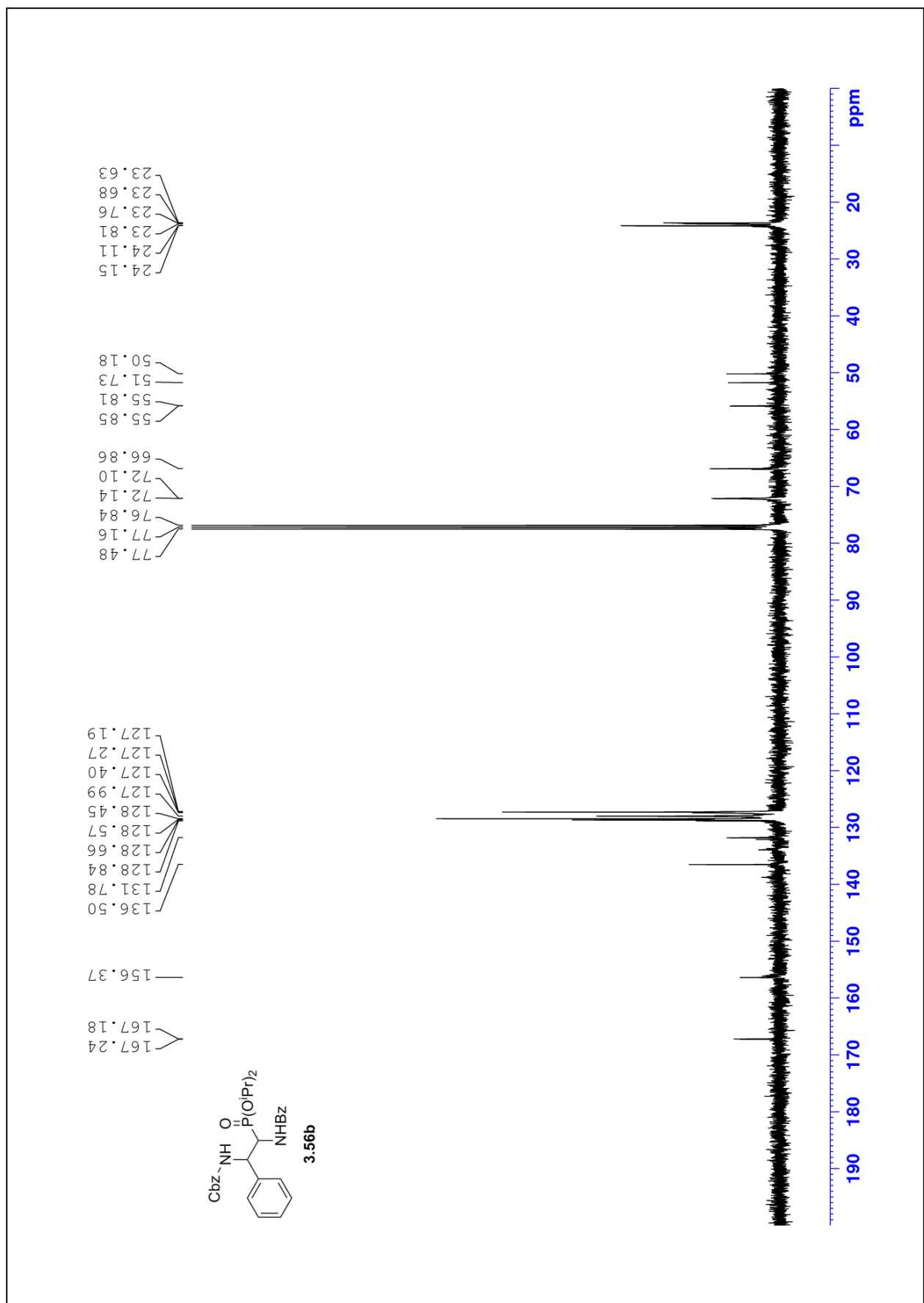


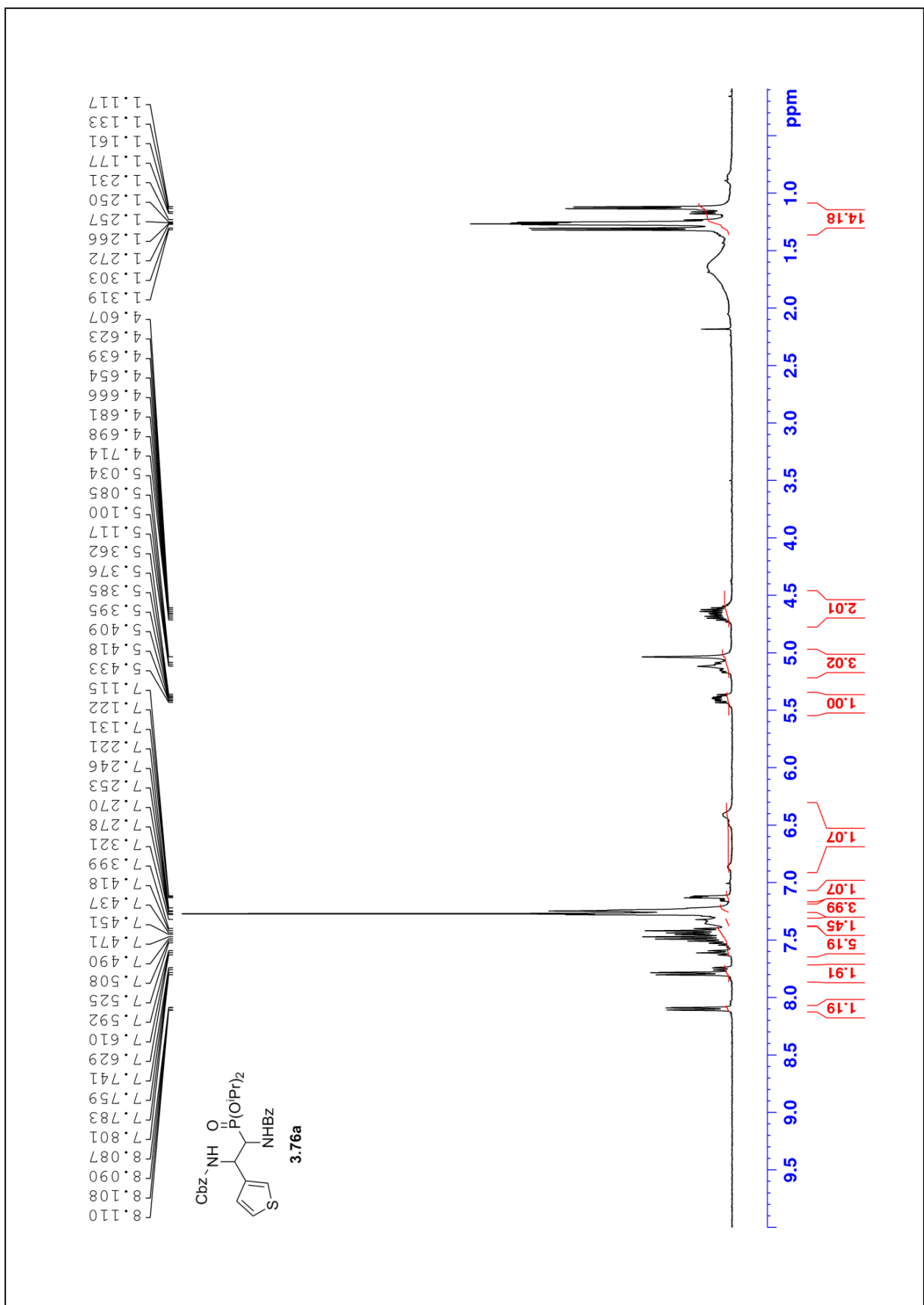


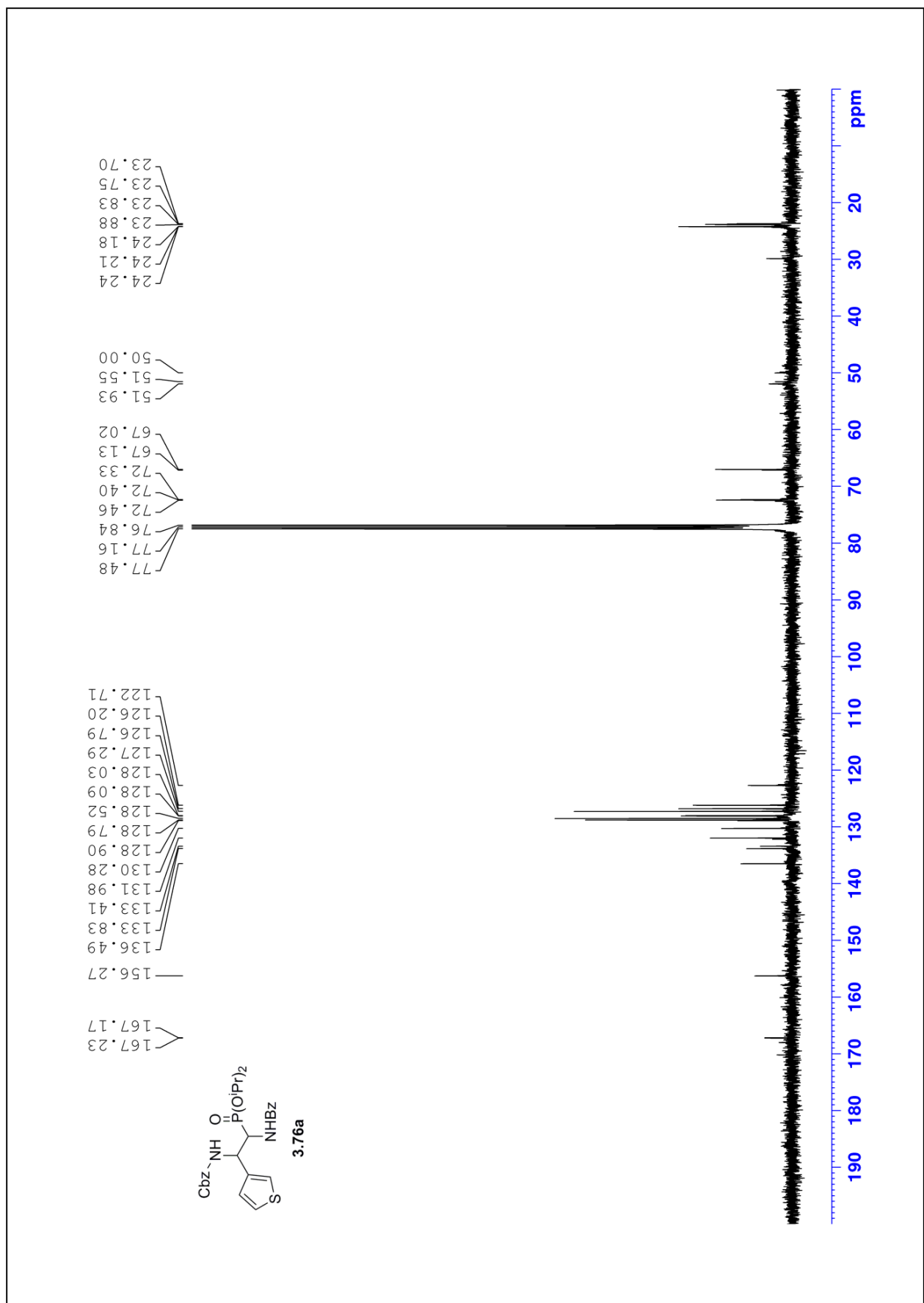


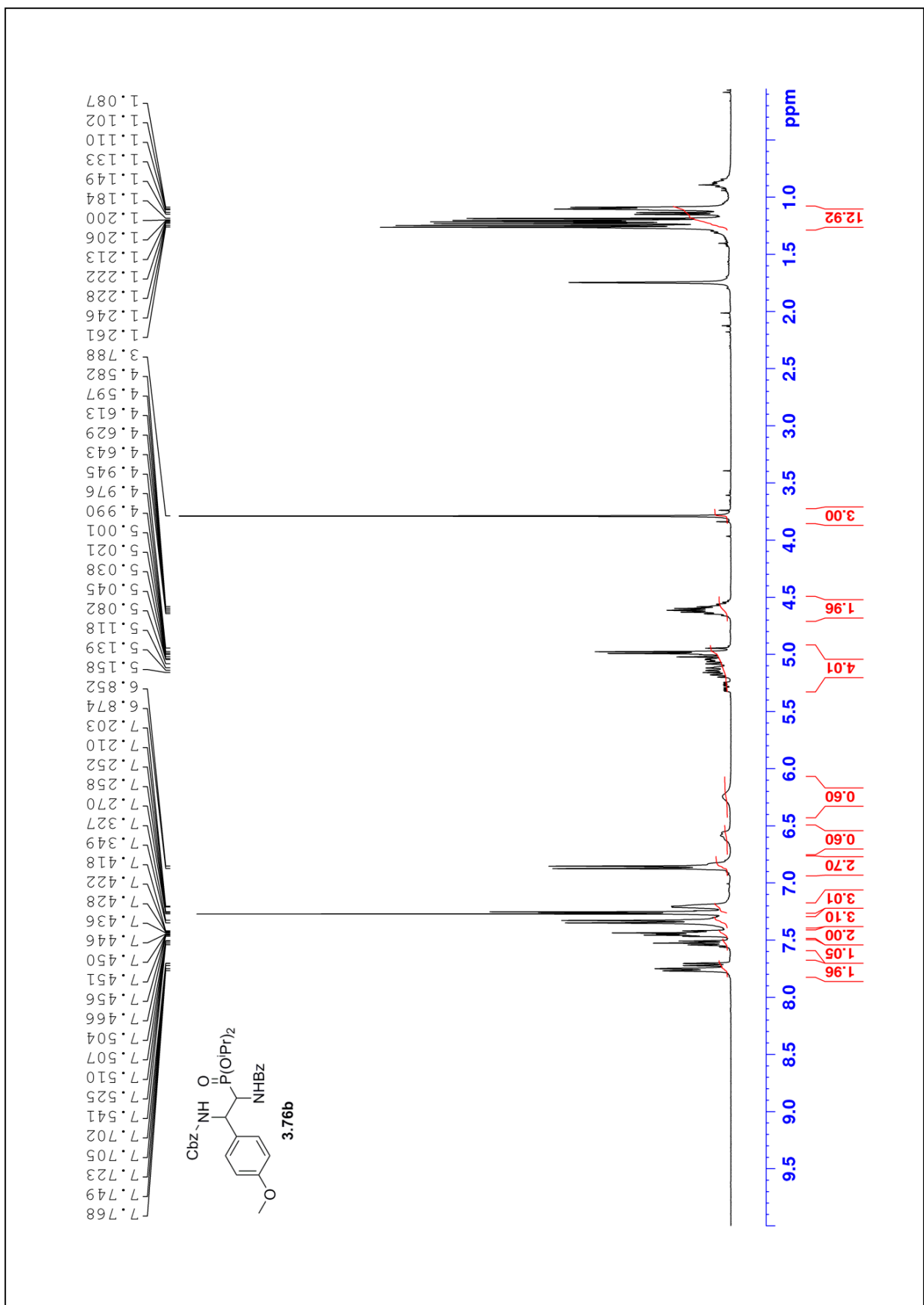


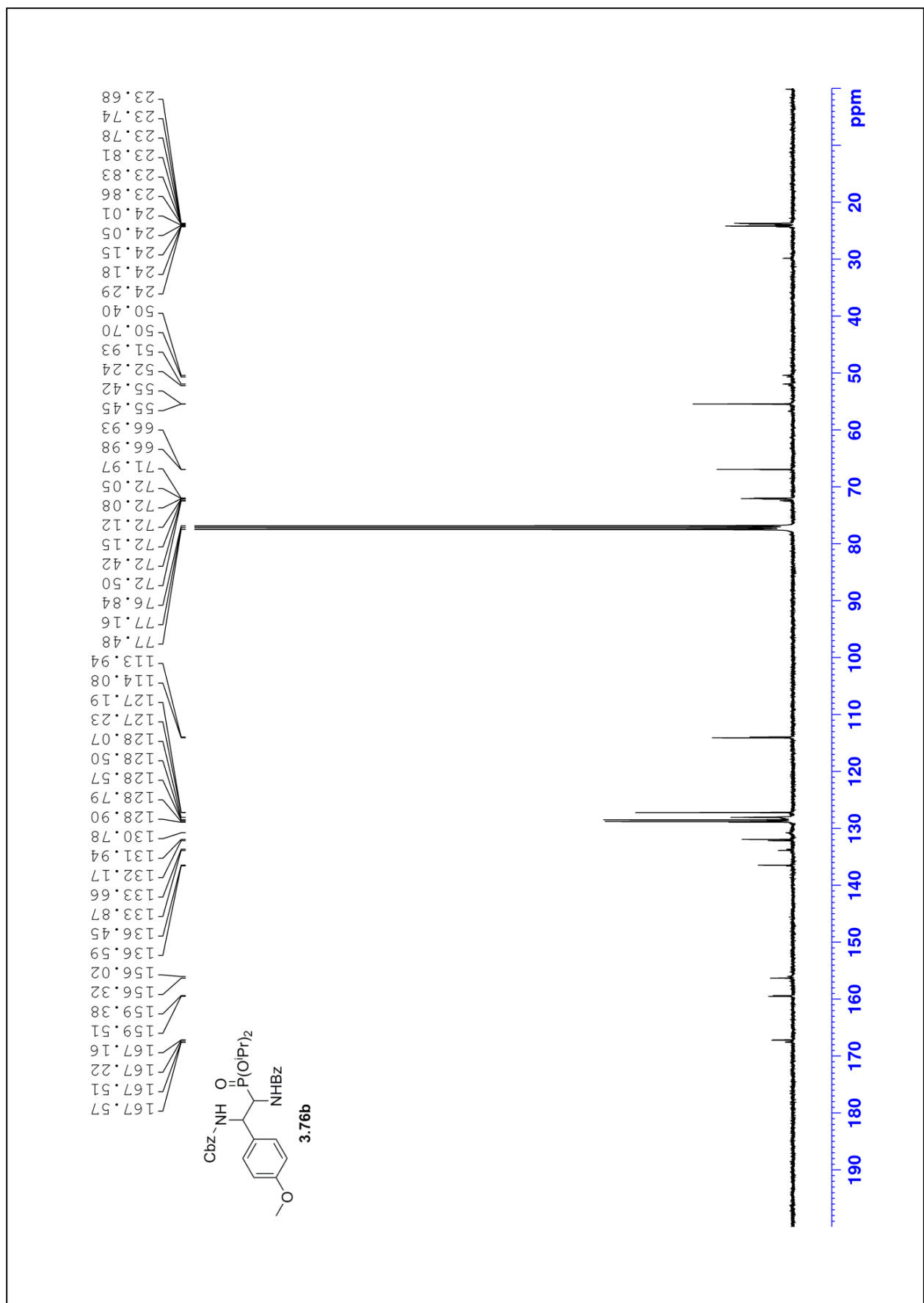


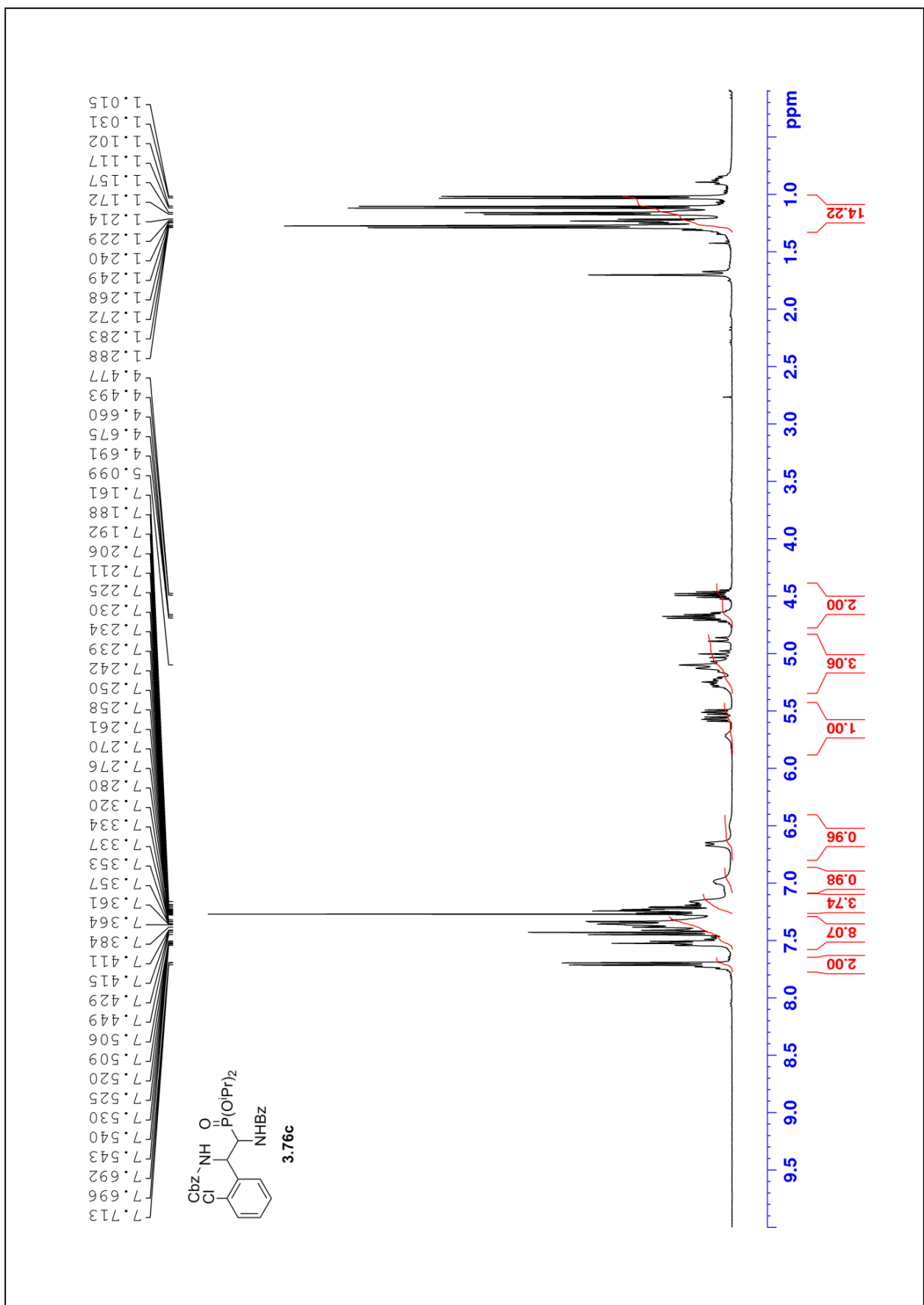


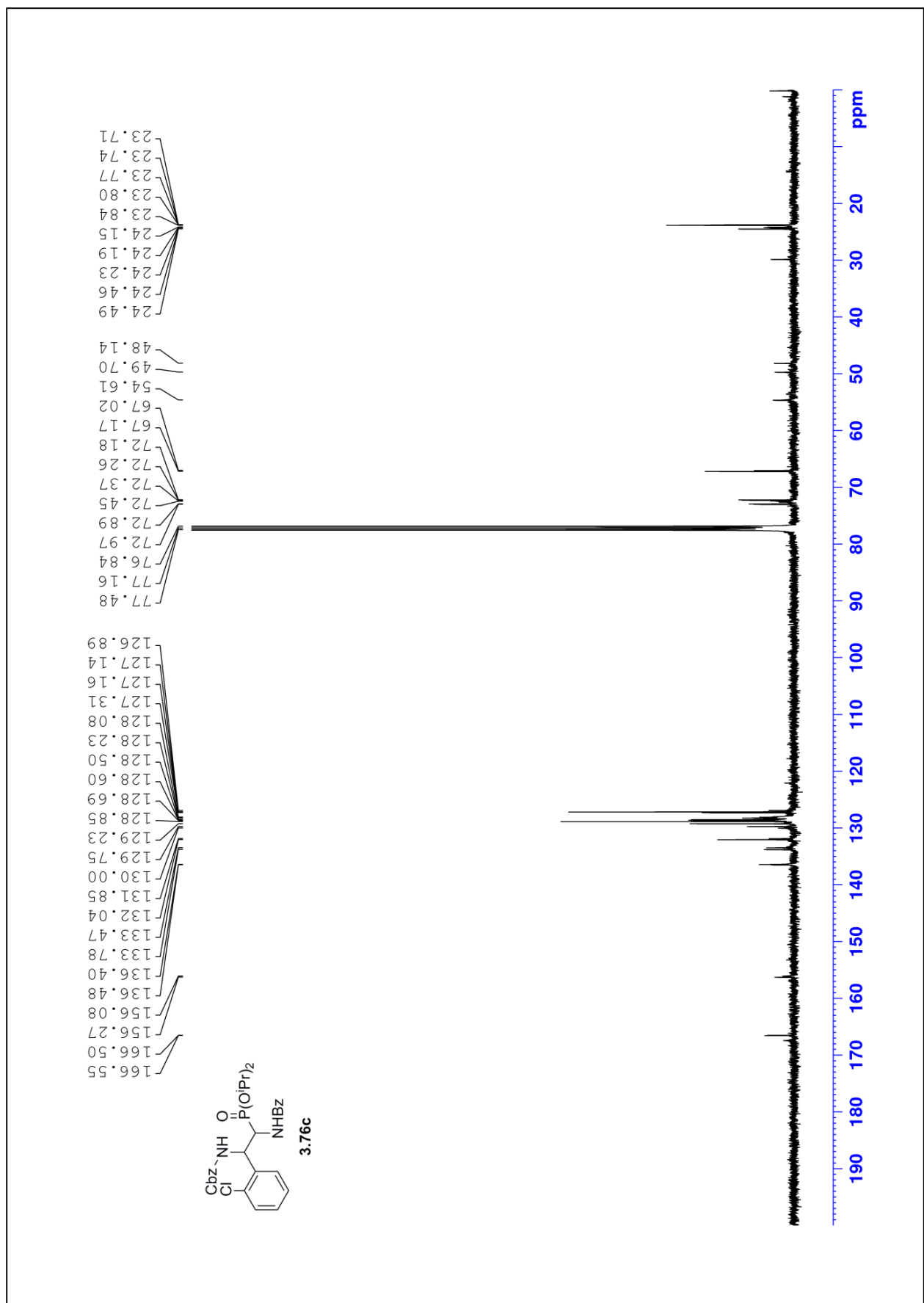


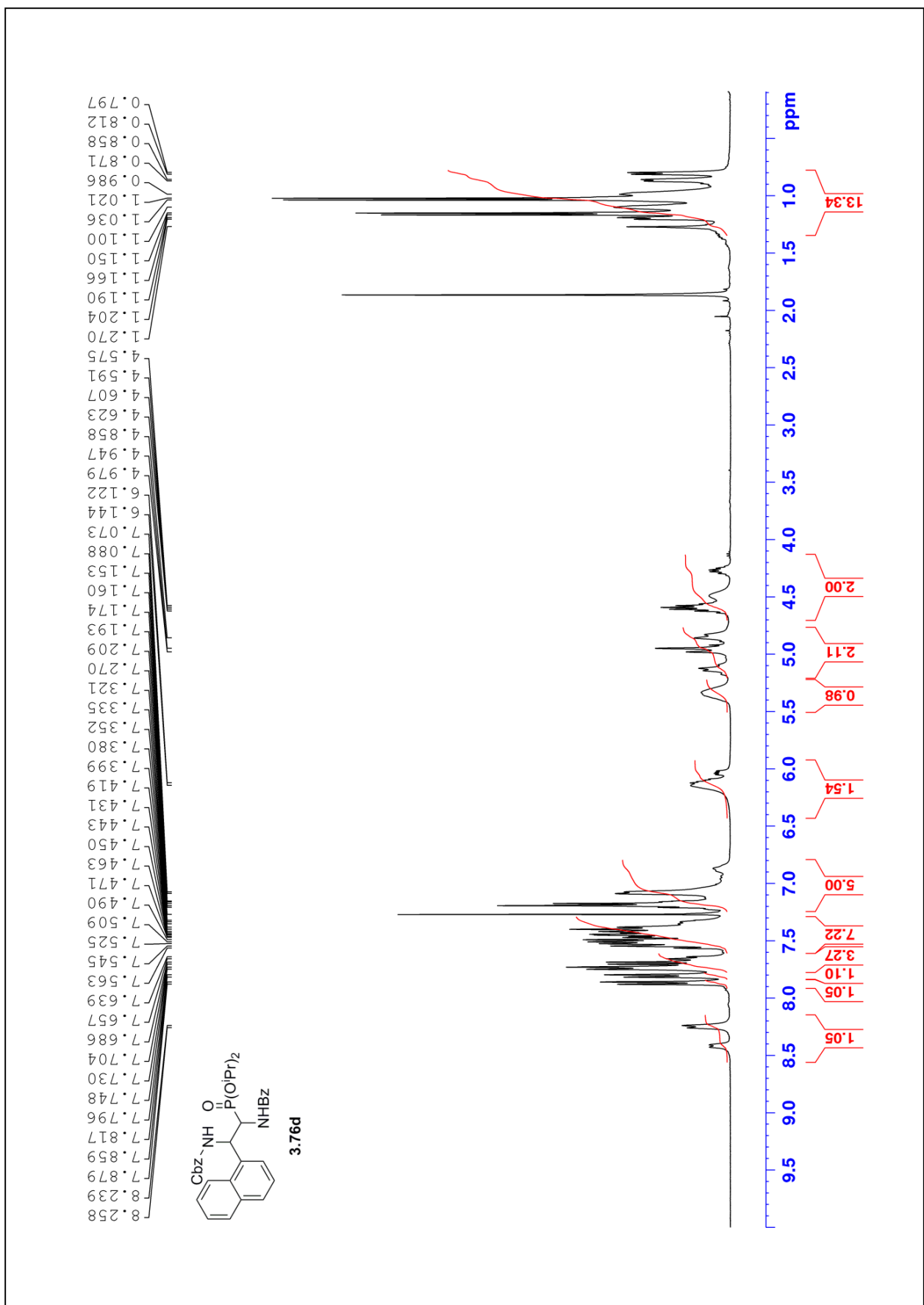


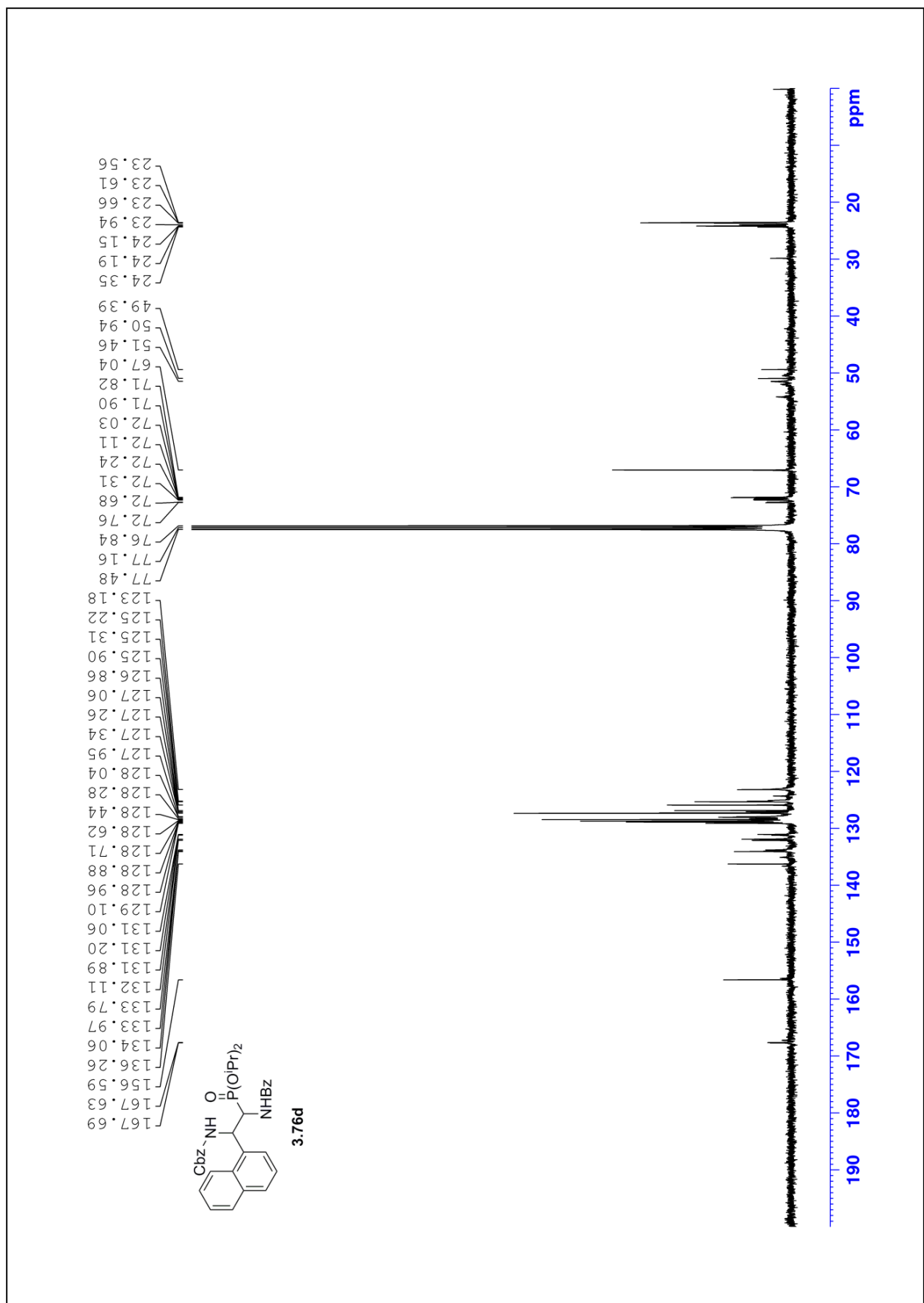


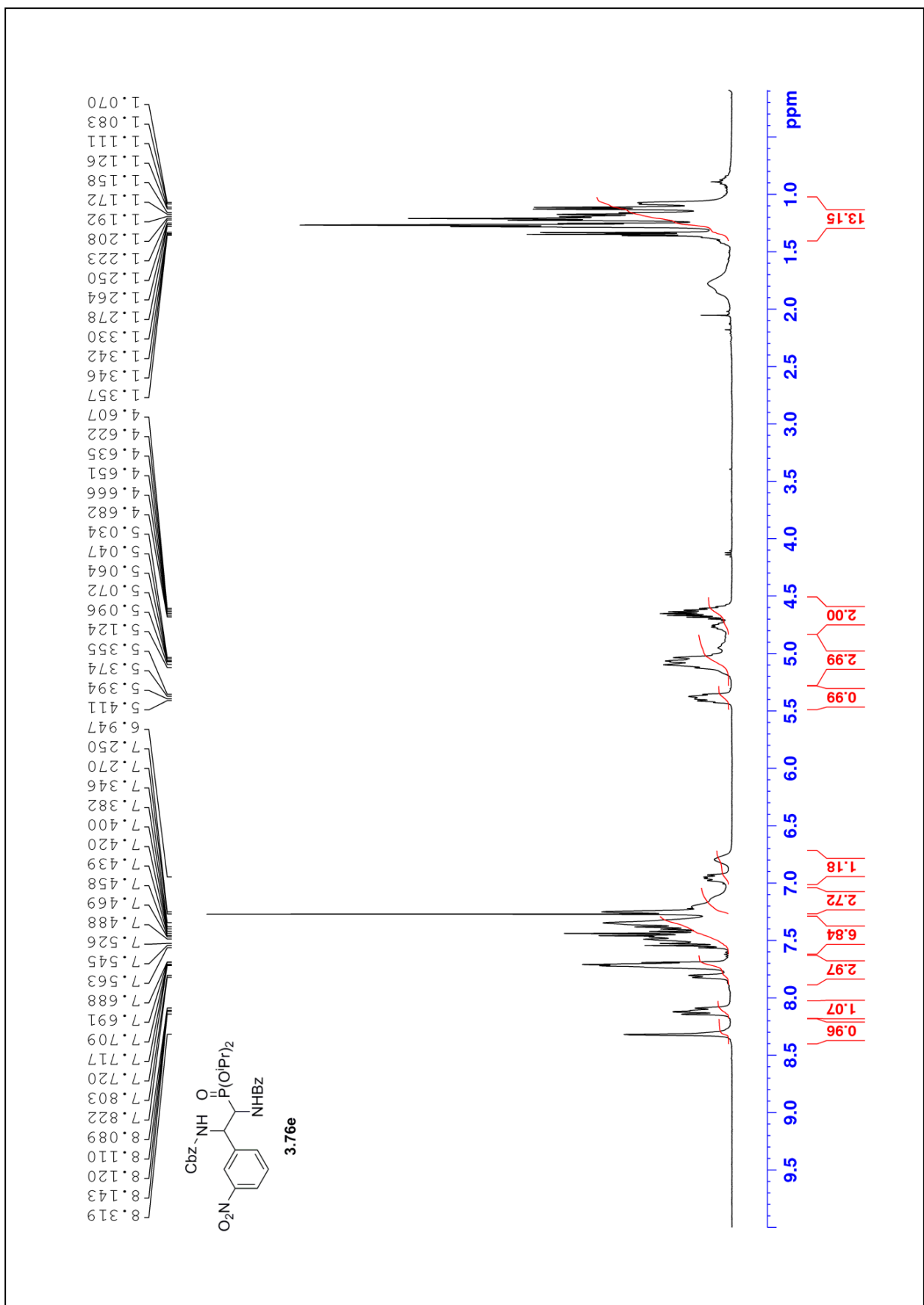


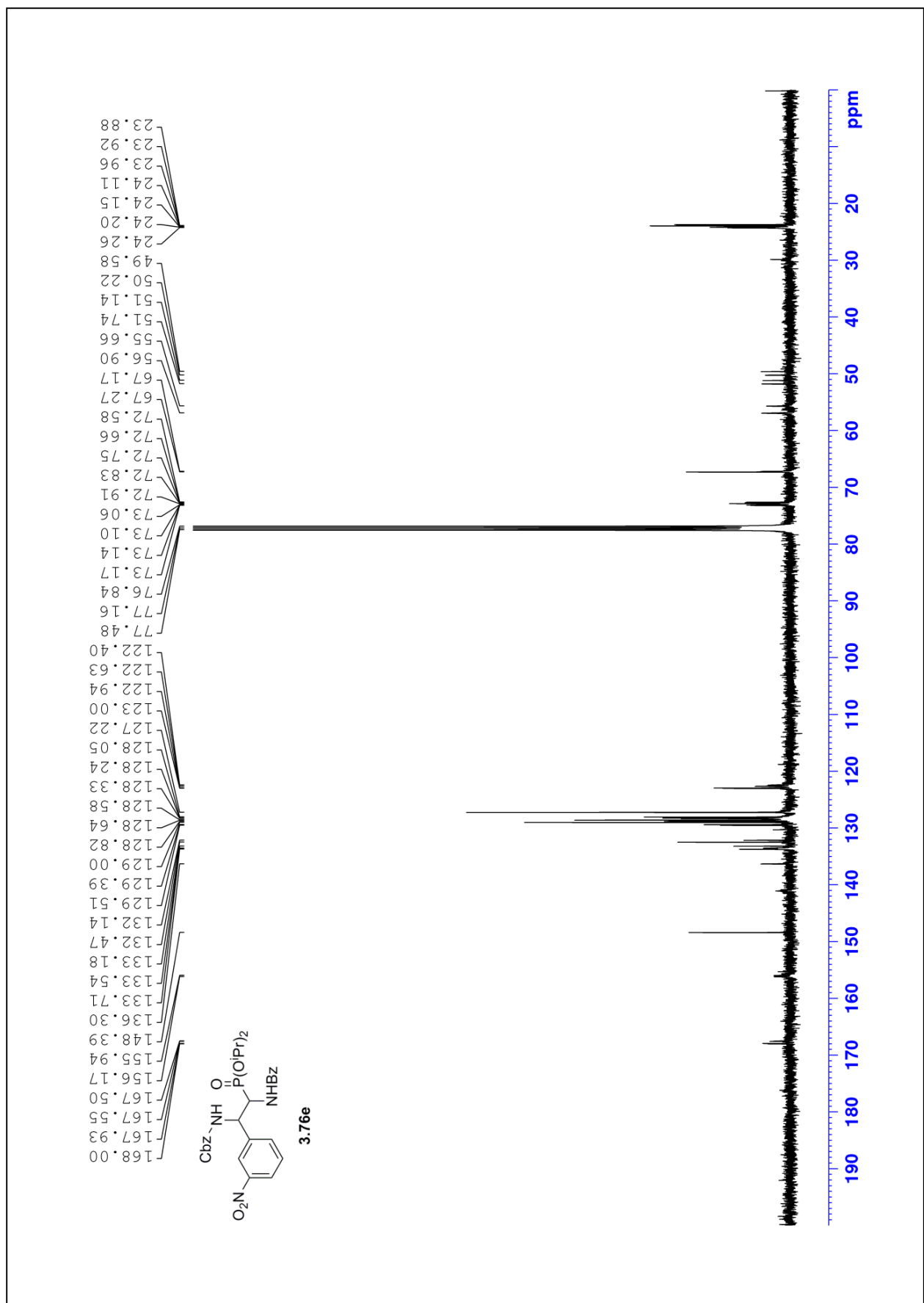


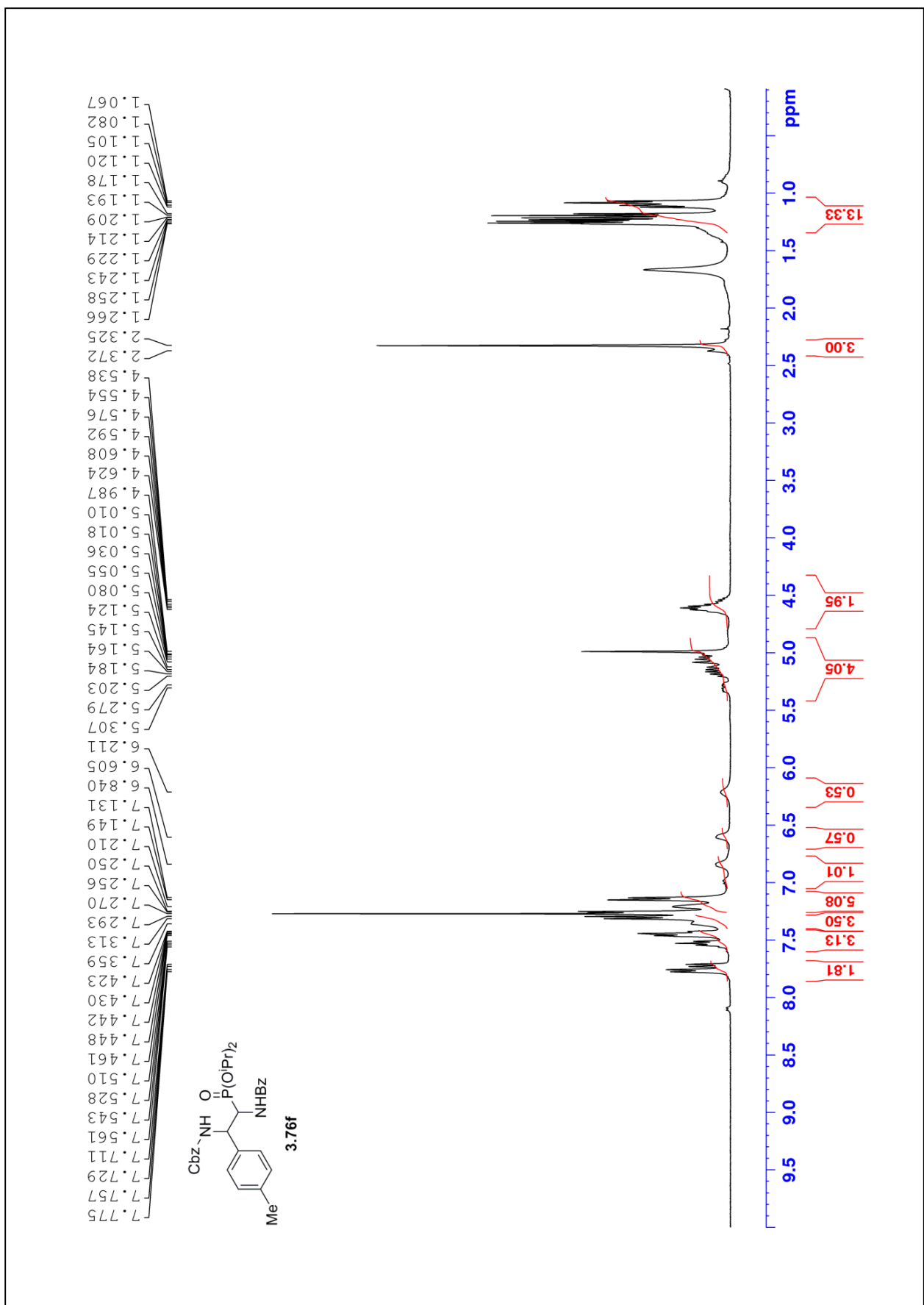


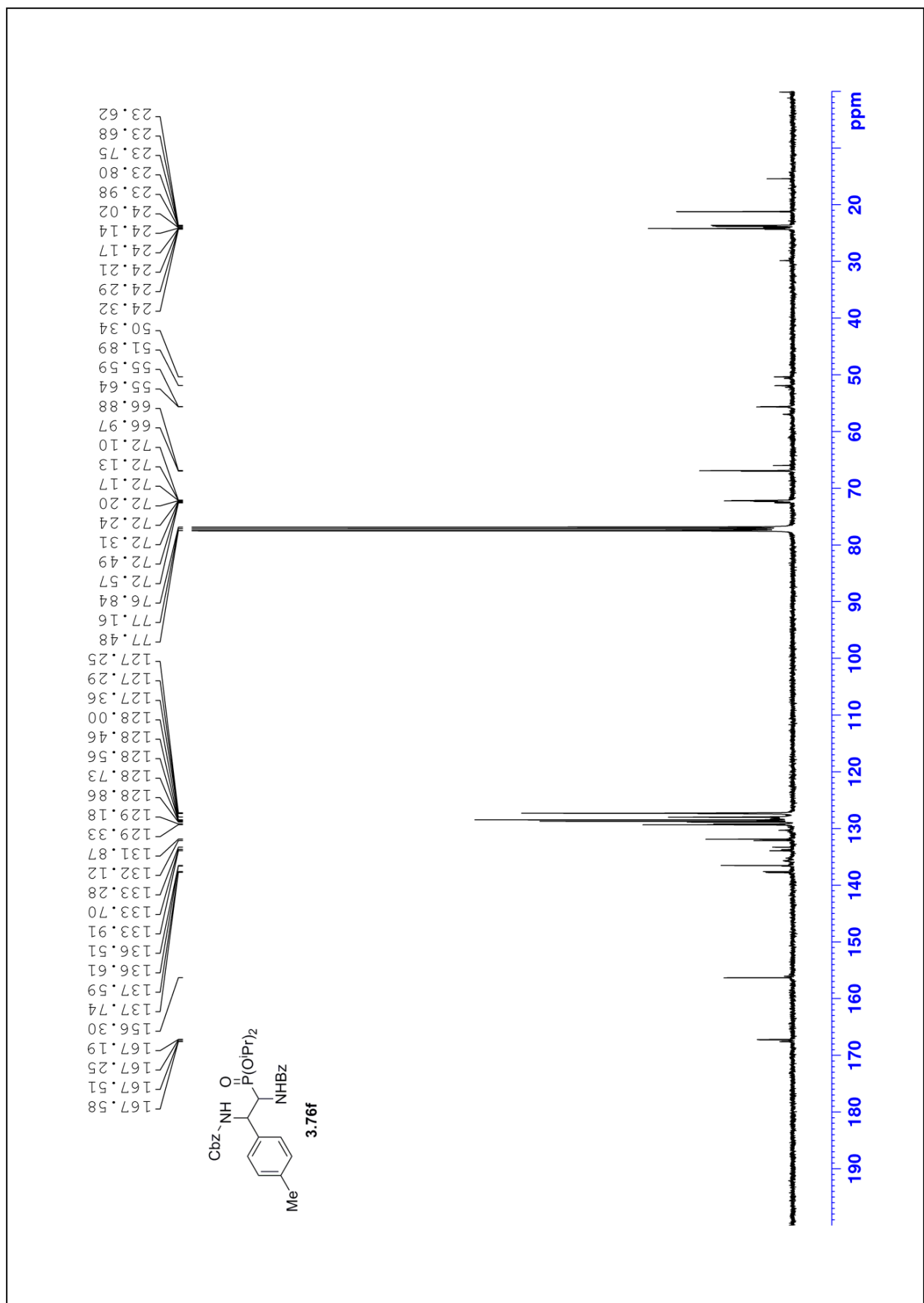


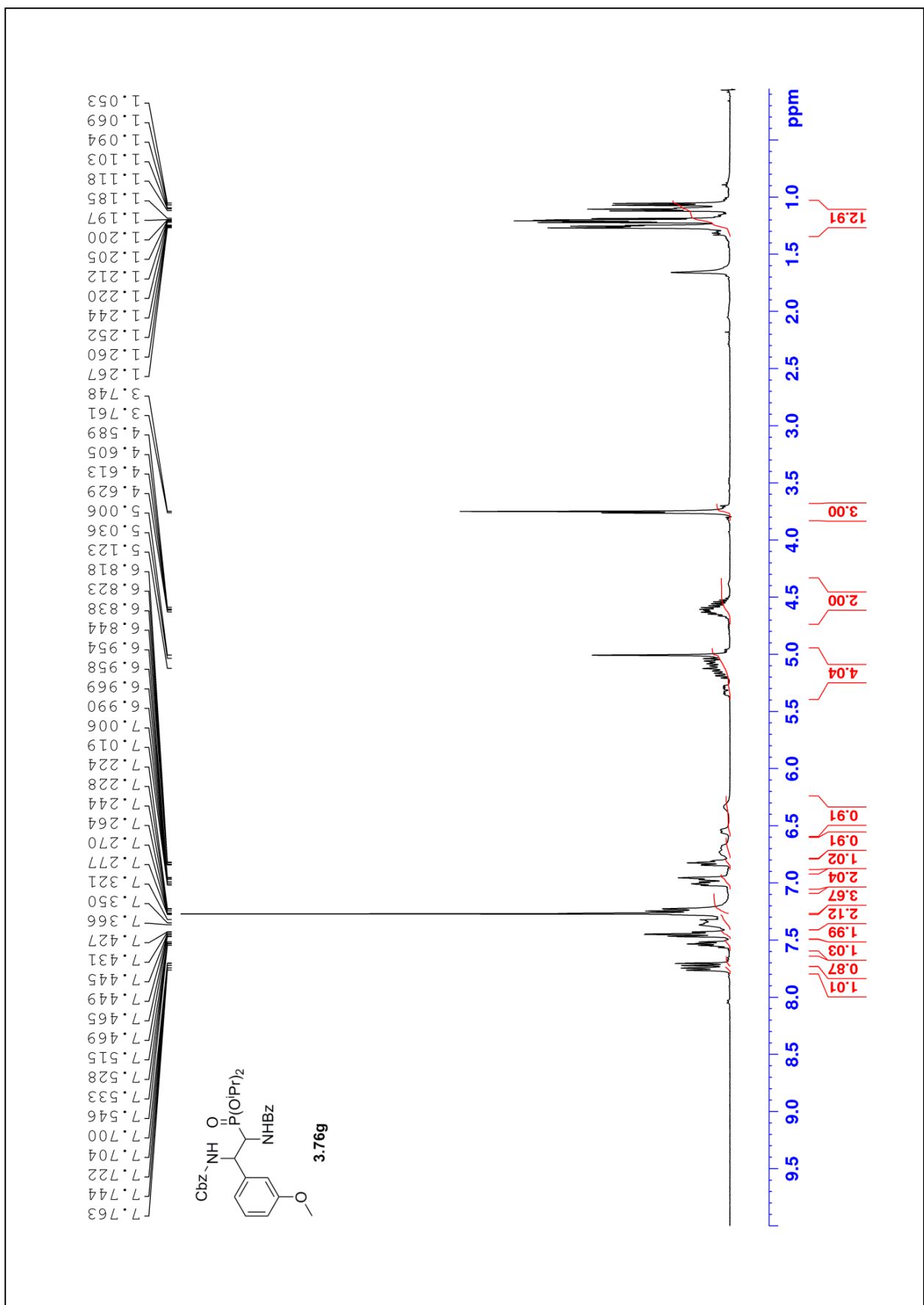


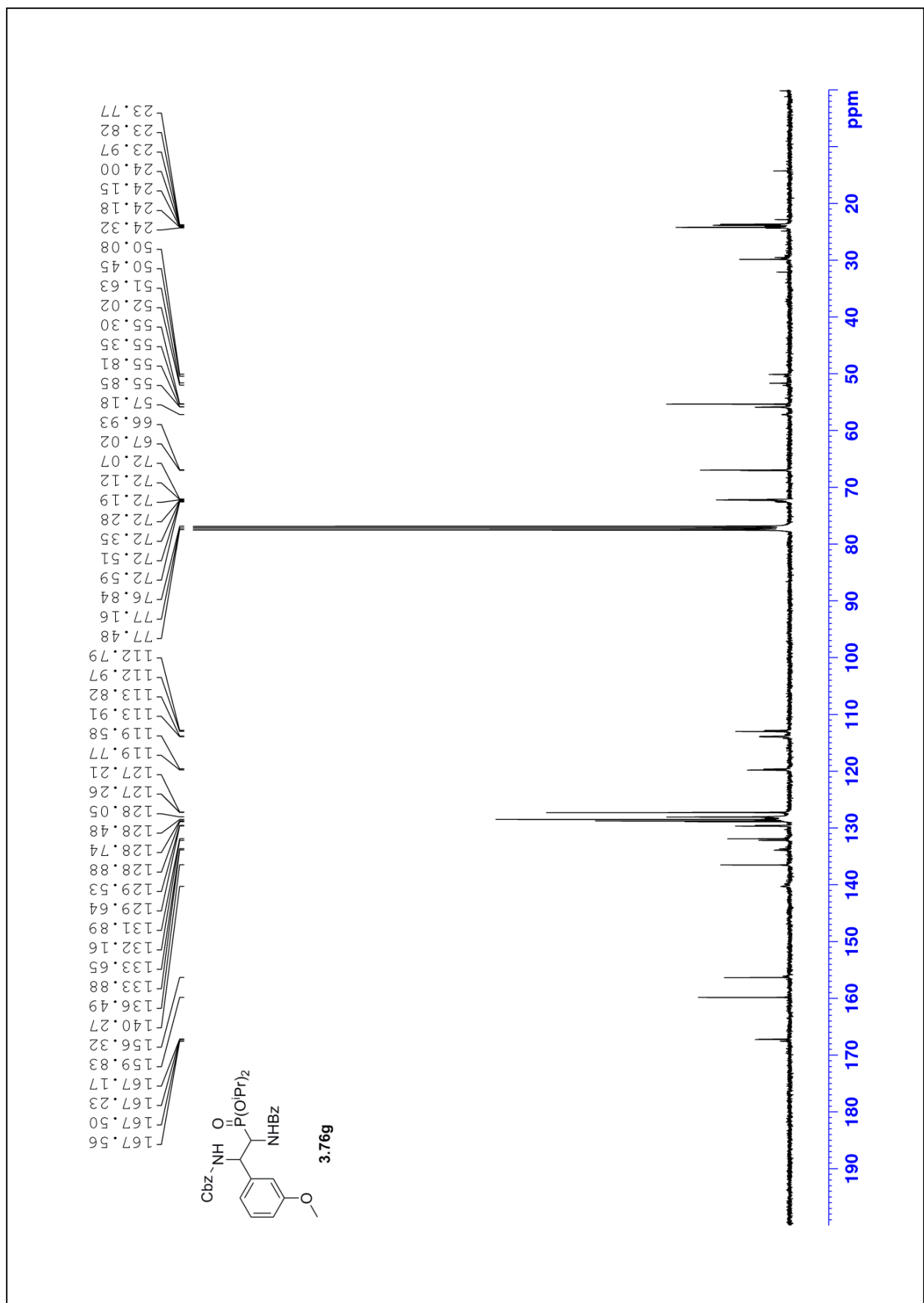


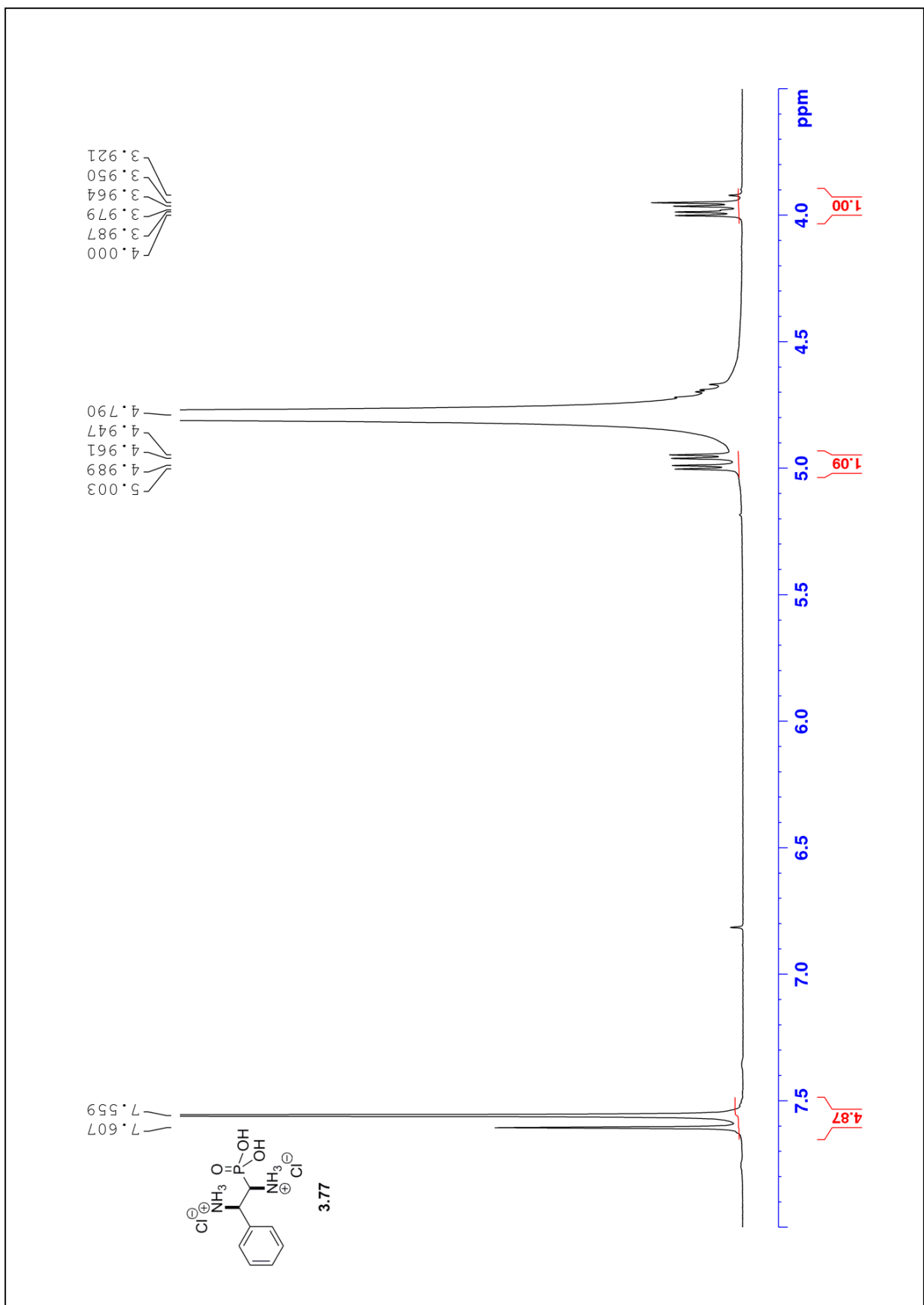








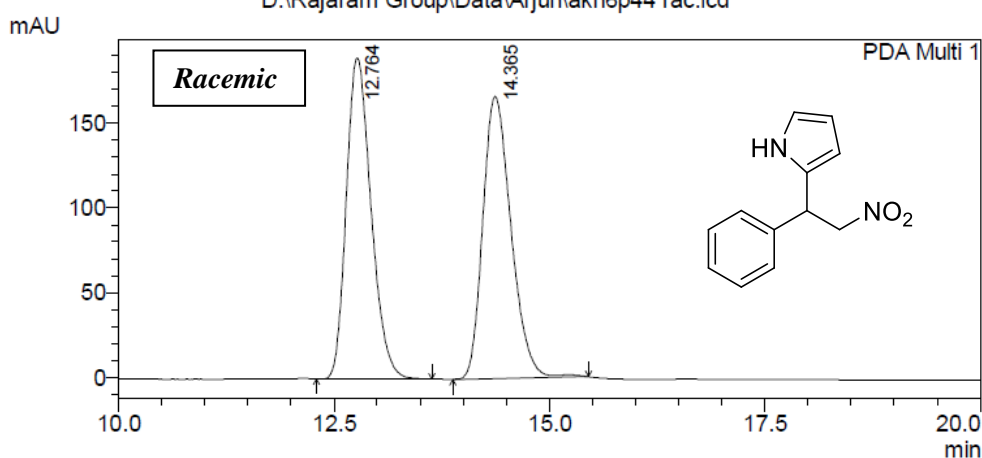




Appendix 2
HPLC Traces

Column: Phenomenex Cellulose1
Hexanes:2-propanol 85:15, 1.0 mL/min

D:\Rajaram Group\Data\Arjun\akn6p44 rac.lcd



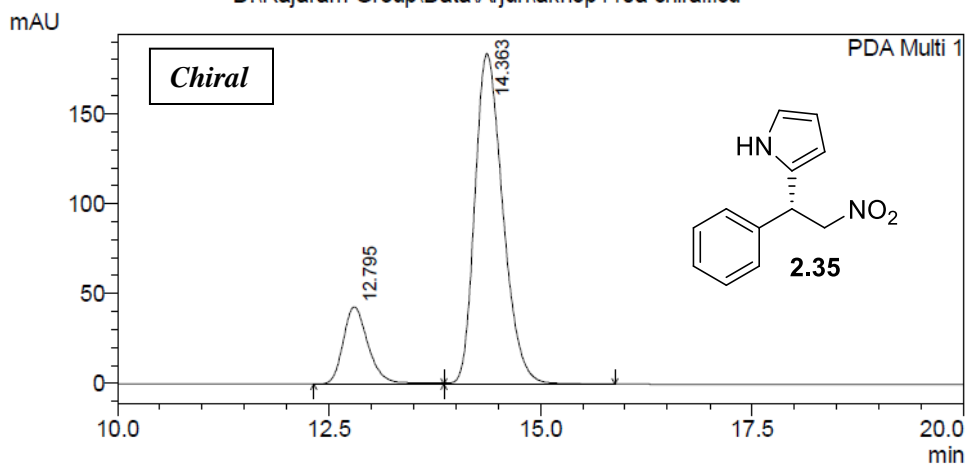
1 PDA Multi 1/254nm 4nm

PeakTable

PDA Ch1 254nm 4nm

Peak#	Ret. Time	Area	Height	Area %	Height %
1	12.764	3797664	189607	49.986	53.227
2	14.365	3799765	166617	50.014	46.773
Total		7597429	356224	100.000	100.000

D:\Rajaram Group\Data\Arjun\akn5p110a chiral.lcd



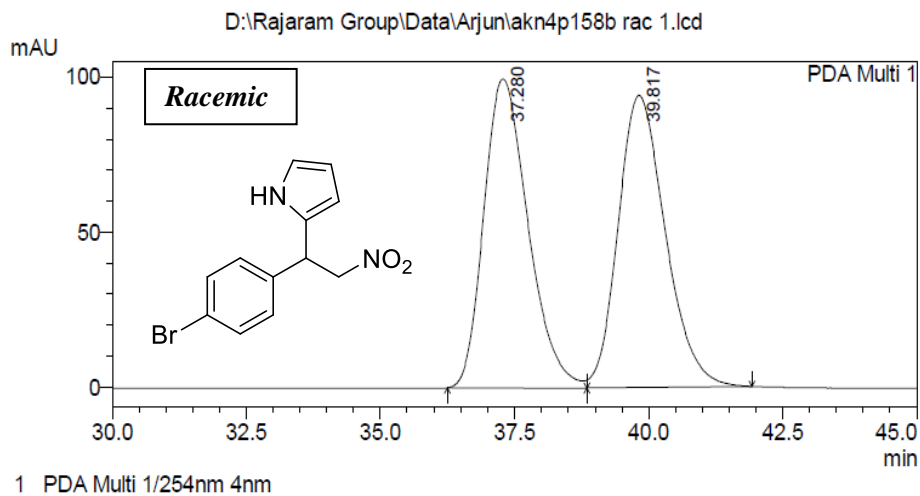
1 PDA Multi 1/254nm 4nm

PeakTable

PDA Ch1 254nm 4nm

Peak#	Ret. Time	Area	Height	Area %	Height %
1	12.795	897596	43033	17.467	18.967
2	14.363	4241130	183855	82.533	81.033
Total		5138727	226888	100.000	100.000

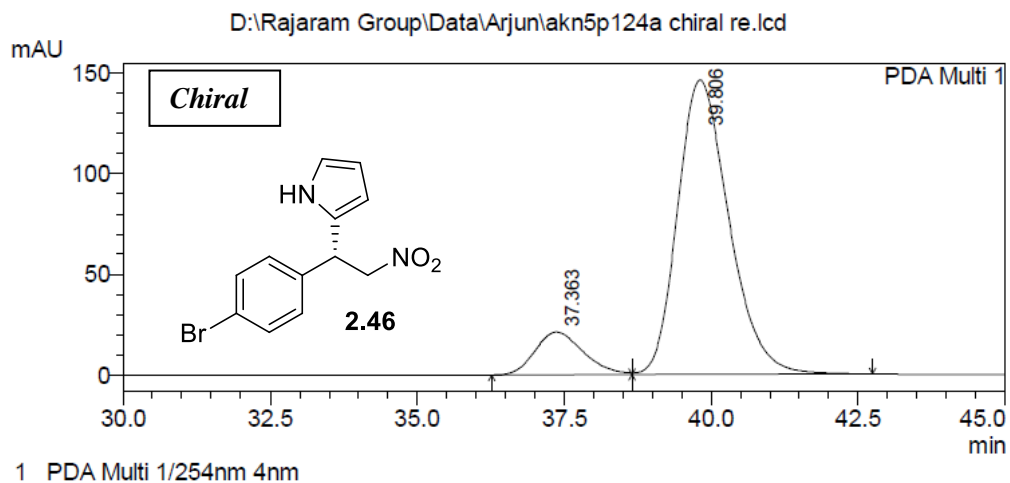
Column: Phenomenex Cellulose1
Hexanes:2-propanol 85:15, 0.5 mL/min



PeakTable

PDA Ch1 254nm 4nm

Peak#	Ret. Time	Area	Height	Area %	Height %
1	37.280	5719438	99537	49.857	51.418
2	39.817	5752135	94047	50.143	48.582
Total		11471573	193583	100.000	100.000



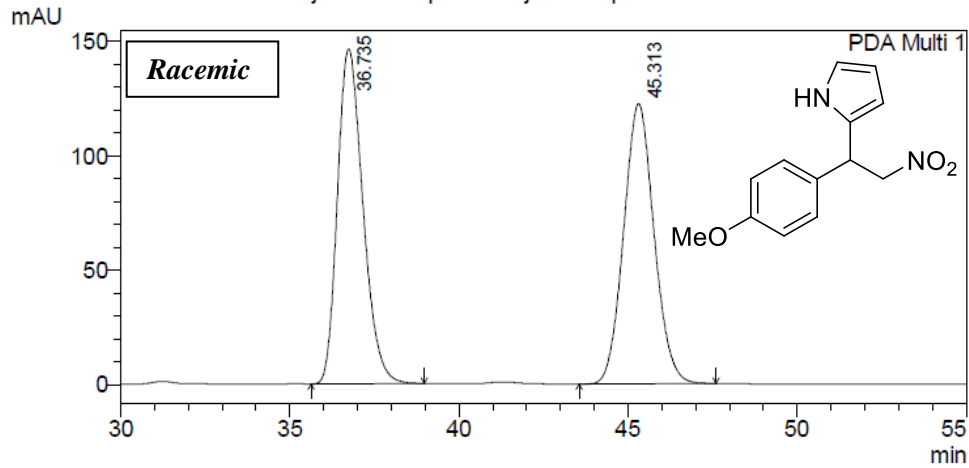
PeakTable

PDA Ch1 254nm 4nm

Peak#	Ret. Time	Area	Height	Area %	Height %
1	37.363	1202072	21095	11.928	12.614
2	39.806	8876071	146140	88.072	87.386
Total		10078143	167235	100.000	100.000

Column: Phenomenex Cellulose1
Hexanes:2-propanol 85:15, 0.5 mL/min

D:\Rajaram Group\Data\Arjun\akn5p44 rac.lcd

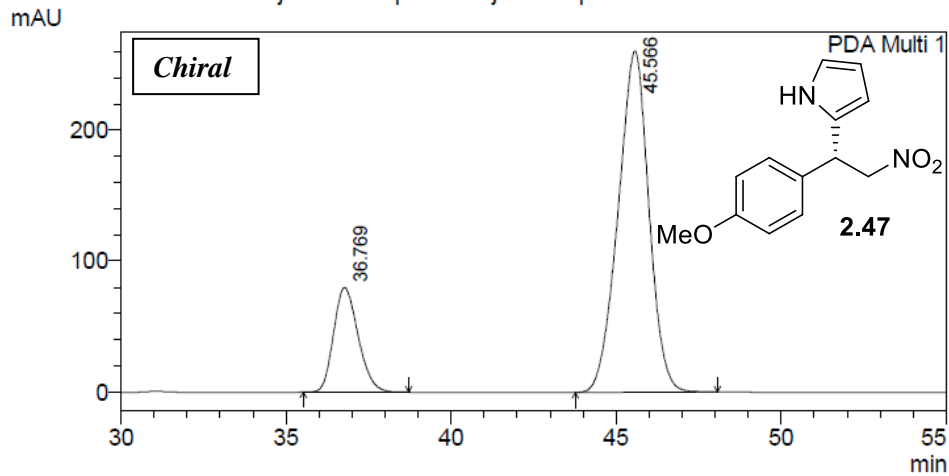


PeakTable

PDA Ch1 254nm 4nm

Peak#	Ret. Time	Area	Height	Area %	Height %
1	36.735	7666264	146146	50.102	54.462
2	45.313	7635057	122199	49.898	45.538
Total		15301321	268345	100.000	100.000

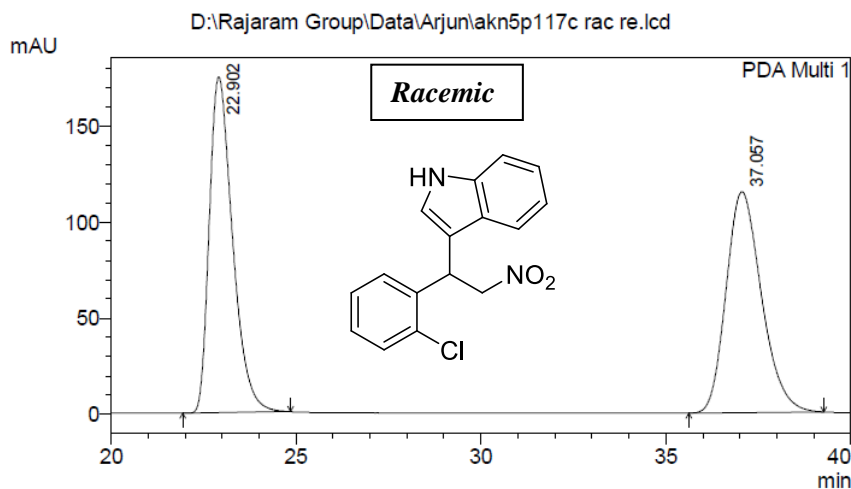
D:\Rajaram Group\Data\Arjun\akn5p114b chiral.lcd



PDA Ch1 254nm 4nm

Peak#	Ret. Time	Area	Height	Area %	Height %
1	36.769	4137827	79828	19.665	23.458
2	45.566	16903735	260473	80.335	76.542
Total		21041562	340301	100.000	100.000

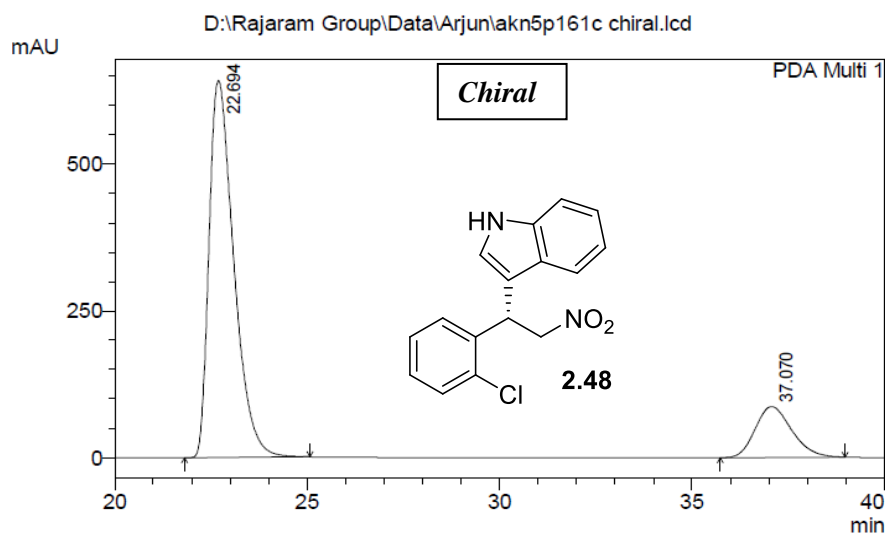
Column: Phenomenex Cellulose1
Hexanes:2-propanol 80:20, 1.0 mL/min



PeakTable

PDA Ch1 254nm 4mm

Peak#	Ret. Time	Area	Height	Area %	Height %
1	22.902	7650435	174863	49.973	60.302
2	37.057	7658647	115114	50.027	39.698
Total		15309082	289977	100.000	100.000



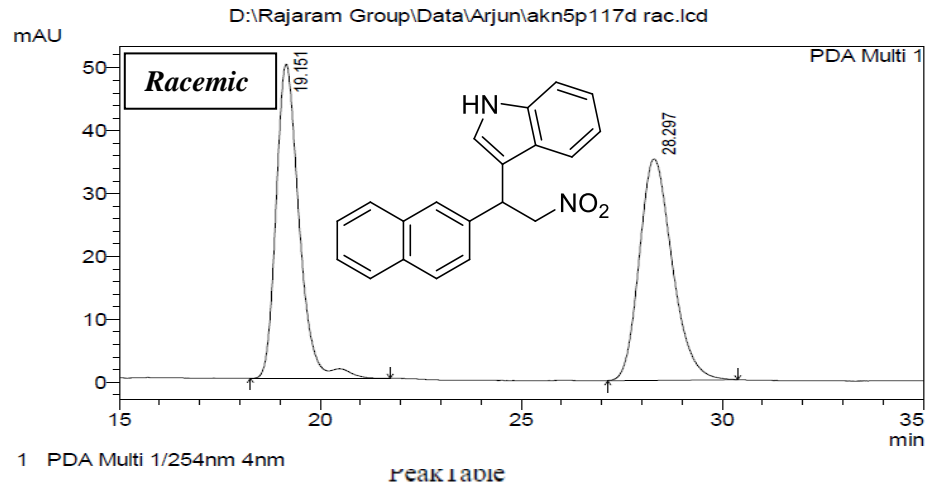
1 PDA Multi 1/254nm 4mm

PeakTable

PDA Ch1 254nm 4mm

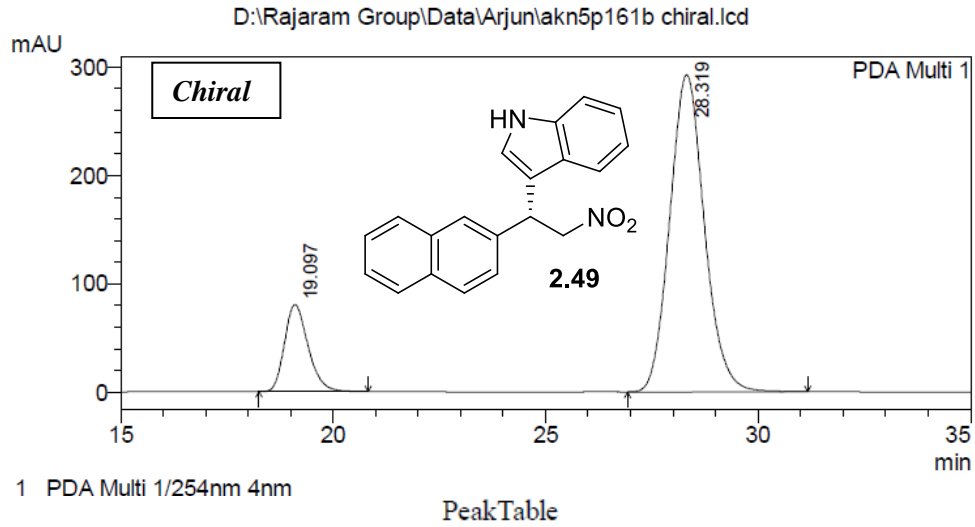
Peak#	Ret. Time	Area	Height	Area %	Height %
1	22.694	28731449	642602	83.306	88.083
2	37.070	5757551	86936	16.694	11.917
Total		34489000	729538	100.000	100.000

Column: Phenomenex Cellulose1
Hexanes:2-propanol 60:40, 1.0 mL/min



PDA Ch1 254nm 4nm

Peak#	Ret. Time	Area	Height	Area %	Height %
1	19.151	1994870	49957	49.873	58.679
2	28.297	2005030	35179	50.127	41.321
Total		3999900	85136	100.000	100.000

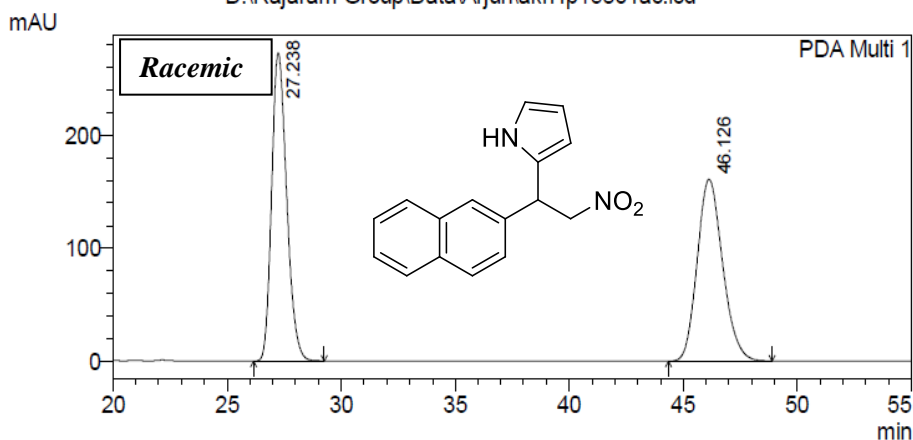


PDA Ch1 254nm 4nm

Peak#	Ret. Time	Area	Height	Area %	Height %
1	19.097	3124845	80520	15.841	21.561
2	28.319	16601466	292923	84.159	78.439
Total		19726311	373442	100.000	100.000

Column: Phenomenex Cellulose1
Hexanes:2-propanol 80:20, 1.0 mL/min

D:\Rajaram Group\Data\Arjun\akn4p158c rac.lcd

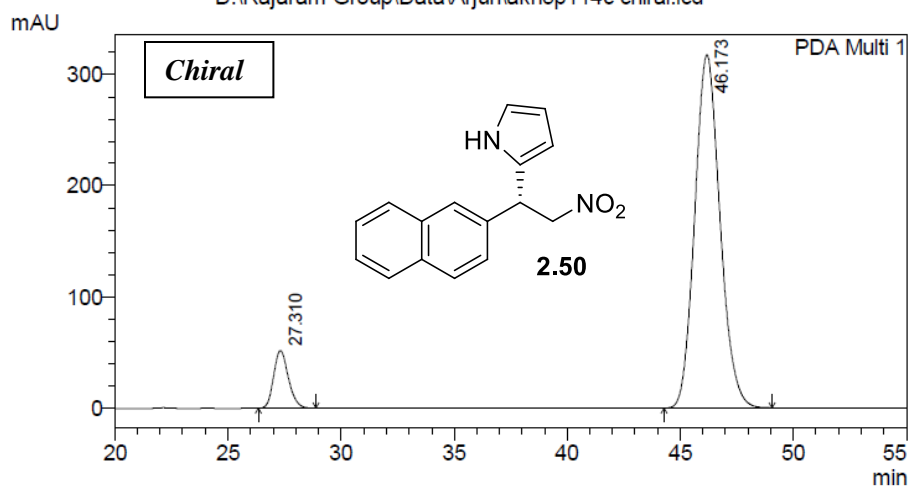


PeakTable

PDA Ch1 254nm 4nm

Peak#	Ret. Time	Area	Height	Area %	Height %
1	27.238	12501885	273231	49.971	62.883
2	46.126	12516546	161274	50.029	37.117
Total		25018432	434506	100.000	100.000

D:\Rajaram Group\Data\Arjun\akn5p114c chiral.lcd



1 PDA Multi 1/254nm 4nm

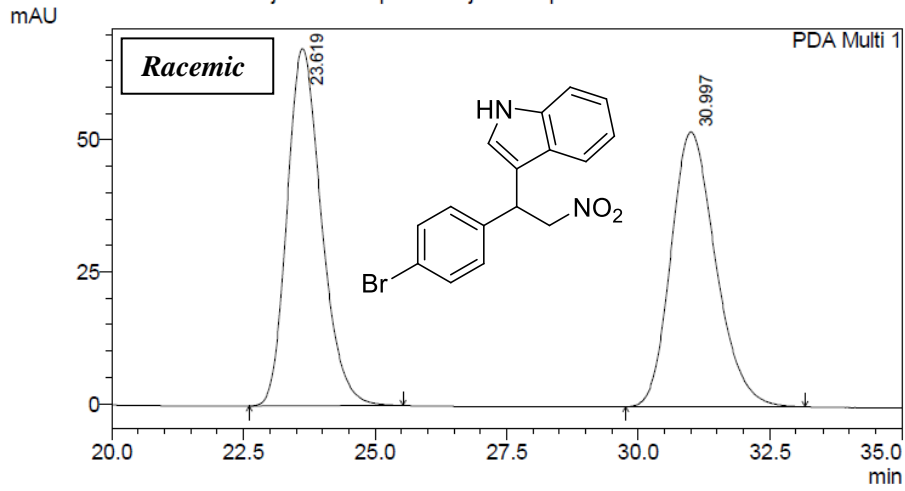
PeakTable

PDA Ch1 254nm 4nm

Peak#	Ret. Time	Area	Height	Area %	Height %
1	27.310	2344271	51784	8.678	14.027
2	46.173	24669986	317389	91.322	85.973
Total		27014256	369173	100.000	100.000

Column: Phenomenex Cellulose1
Hexanes:2-propanol 70:30, 1.0 mL/min

D:\Rajaram Group\Data\Arjun\lkn5p117a rac 1.lcd

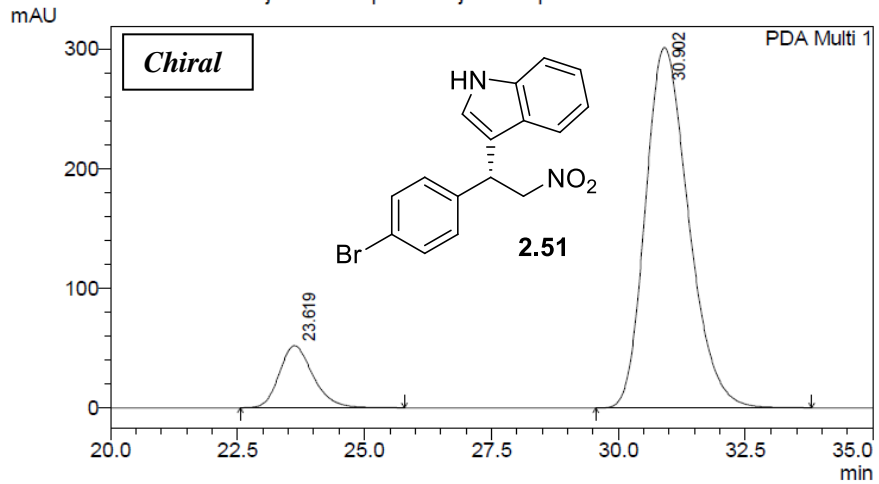


PeakTable

PDA Ch1 254nm 4nm

Peak#	Ret. Time	Area	Height	Area %	Height %
1	23.619	3070929	67565	49.956	56.504
2	30.997	3076395	52011	50.044	43.496
Total		6147324	119576	100.000	100.000

D:\Rajaram Group\Data\Arjun\lkn6p25b chiral.lcd

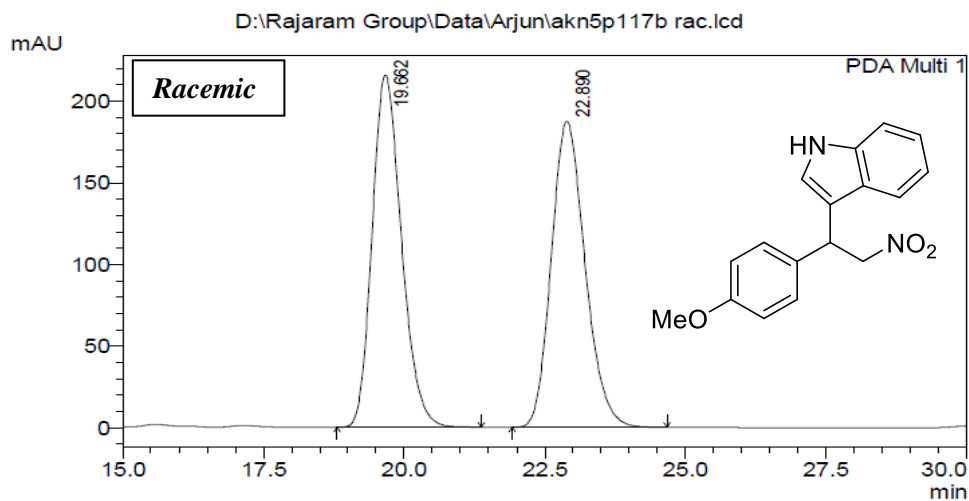


PeakTable

PDA Ch1 254nm 4nm

Peak#	Ret. Time	Area	Height	Area %	Height %
1	23.619	2390236	51682	11.840	14.656
2	30.902	17796735	300942	88.160	85.344
Total		20186971	352624	100.000	100.000

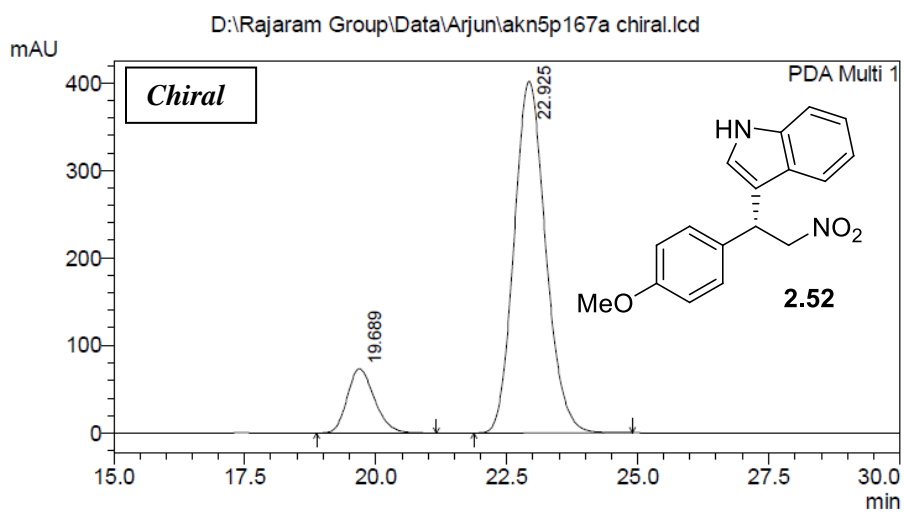
Column: Phenomenex Cellulose1
Hexanes:2-propanol 70:30, 1.0 mL/min



PeakTable

PDA Ch1 254nm 4nm

Peak#	Ret. Time	Area	Height	Area %	Height %
1	19.662	7815488	215725	49.954	53.537
2	22.890	7829929	187224	50.046	46.463
Total		15645417	402948	100.000	100.000



1 PDA Multi 1/254nm 4nm

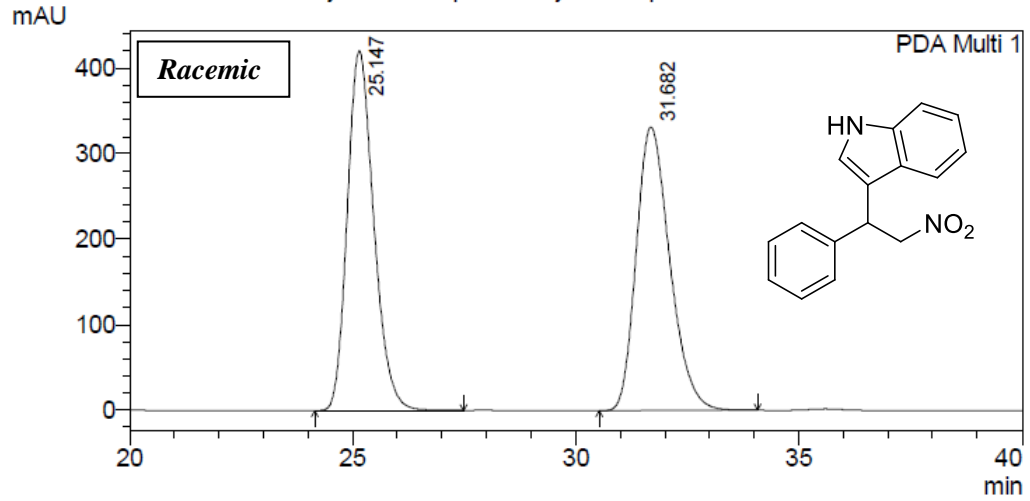
PeakTable

PDA Ch1 254nm 4nm

Peak#	Ret. Time	Area	Height	Area %	Height %
1	19.689	2644426	73269	13.564	15.423
2	22.925	16851943	401783	86.436	84.577
Total		19496369	475052	100.000	100.000

Column: Phenomenex Cellulose1
Hexanes:2-propanol 70:30, 0.7 mL/min

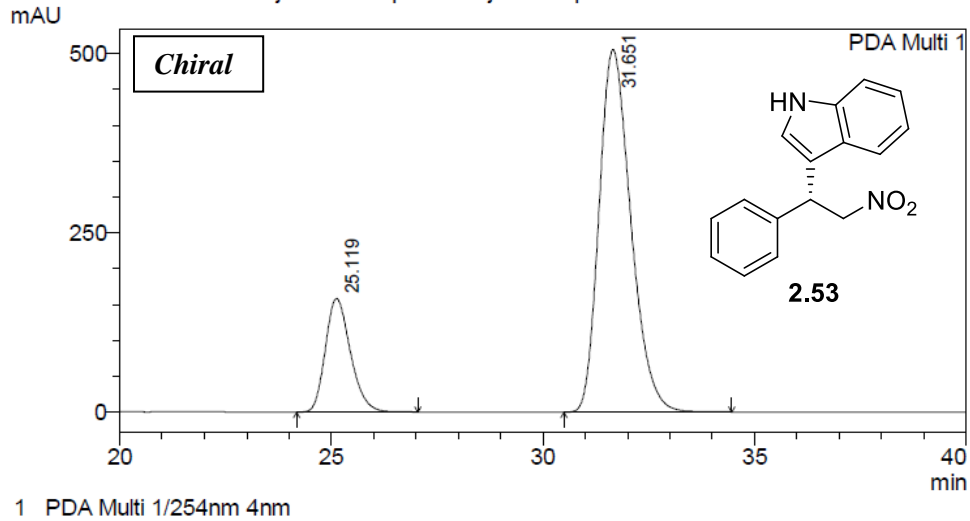
D:\Rajaram Group\Data\Arjun\akn6p48 rac.lcd



PDA Ch1 254nm 4nm

Peak#	Ret. Time	Area	Height	Area %	Height %
1	25.147	17338914	420677	49.984	55.914
2	31.682	17350082	331684	50.016	44.086
Total		34688996	752361	100.000	100.000

D:\Rajaram Group\Data\Arjun\akn5p106b chiral re.lcd

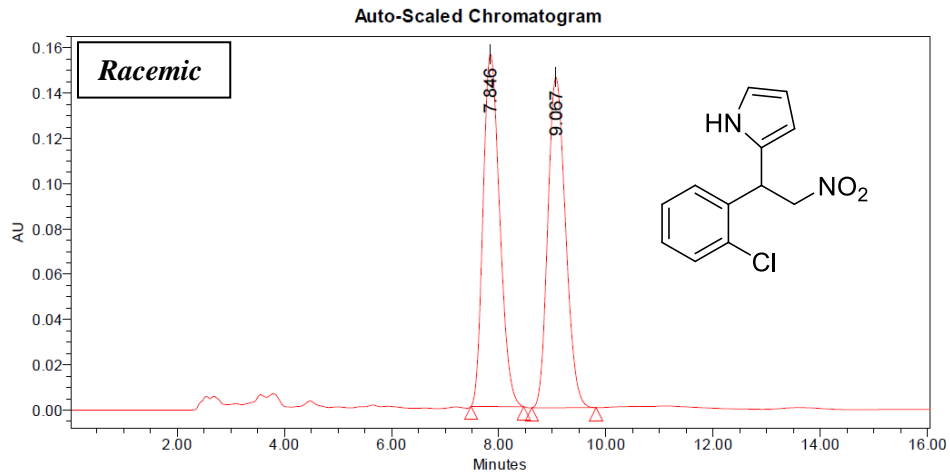


PeakTable

PDA Ch1 254nm 4nm

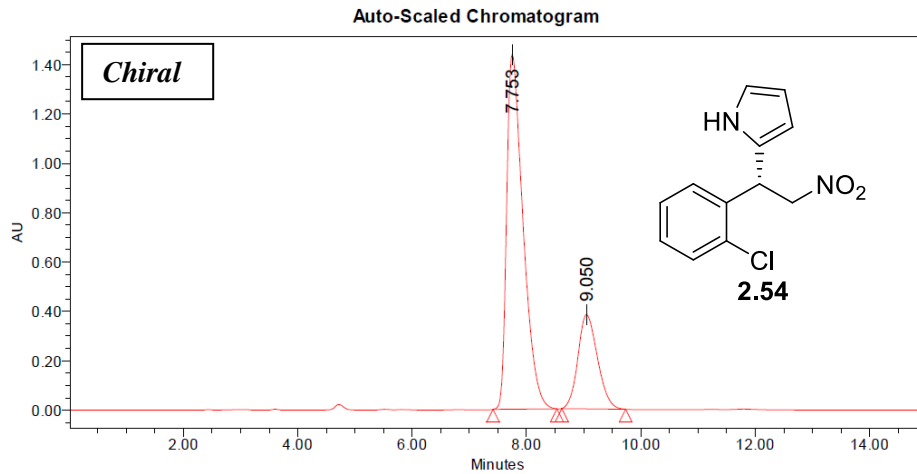
Peak#	Ret. Time	Area	Height	Area %	Height %
1	25.119	6529807	158456	19.825	23.867
2	31.651	26407512	505447	80.175	76.133
Total		32937320	663902	100.000	100.000

Column: Daicel Chiralpak AD-H
n-Hexane:2-propanol 90:10, 0.8 mL/min



Peak Name:

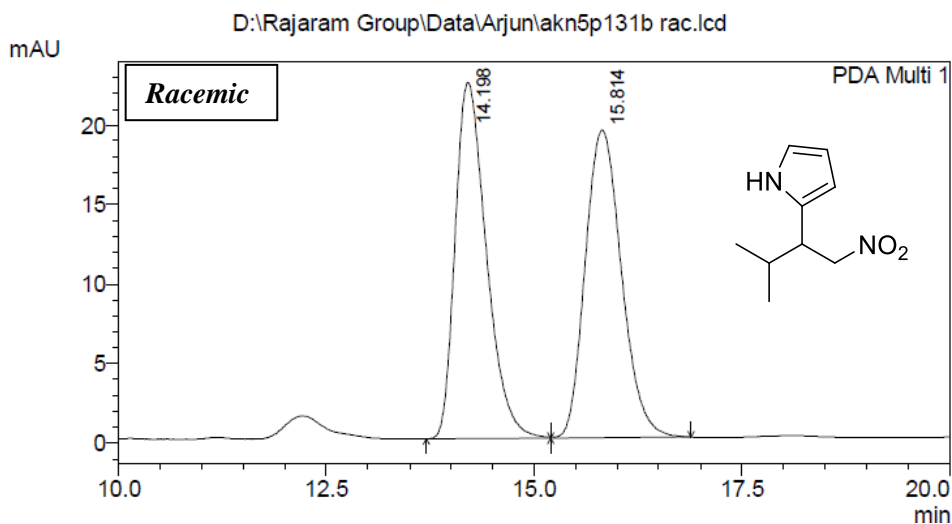
	Injection	RT	Area	% Area	Height
1	1	7.846	3336569	49.91	155611
2	1	9.067	3348522	50.09	146044



Peak Name:

	Injection	RT	Area	% Area	Height
1	1	7.753	28639552	75.96	1438863
2	1	9.050	9063094	24.04	381995

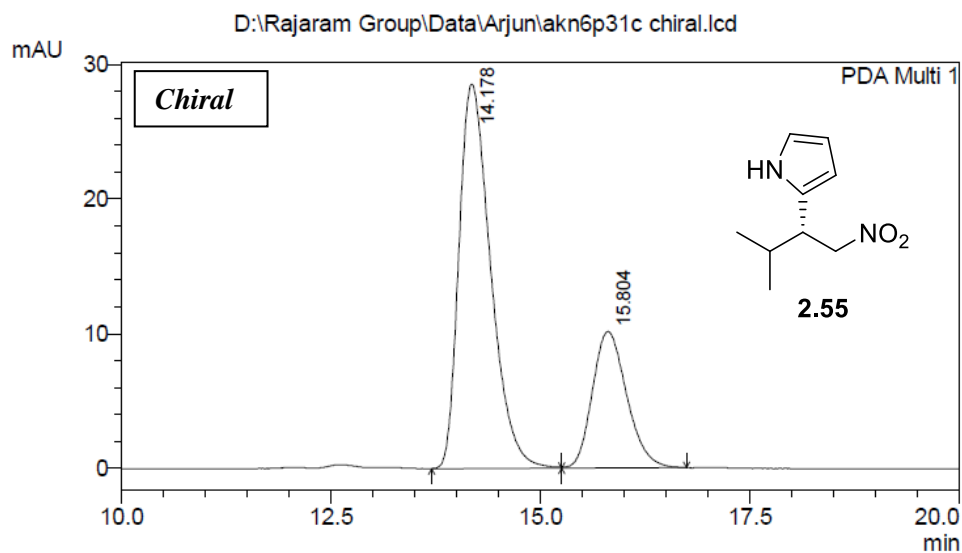
Column: Phenomenex Cellulose1
Hexanes:2-propanol 93:07, 1.0 mL/min



PeakTable

PDA Ch1 254nm 4nm

Peak#	Ret. Time	Area	Height	Area %	Height %
1	14.198	584757	22381	49.894	53.629
2	15.814	587245	19353	50.106	46.371
Total		1172002	41734	100.000	100.000

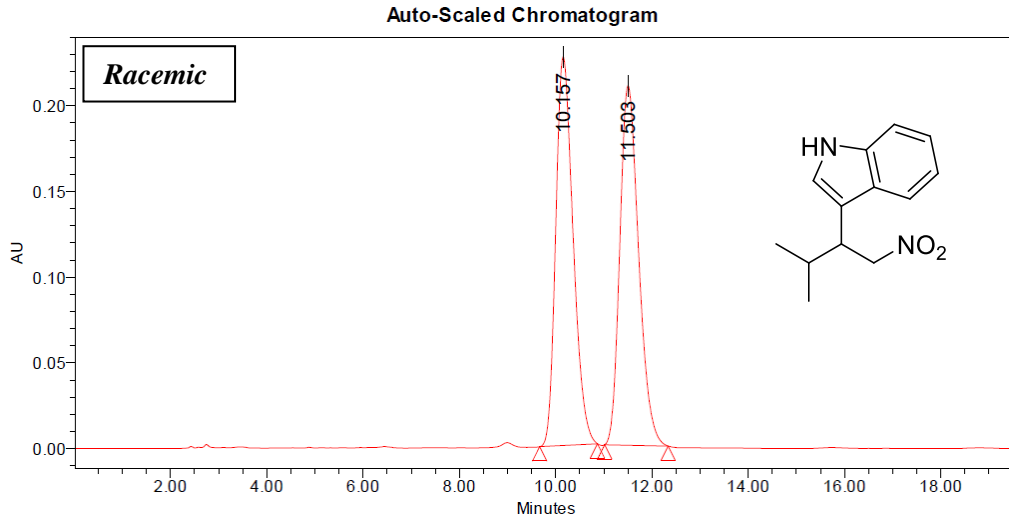


PeakTable

PDA Ch1 254nm 4nm

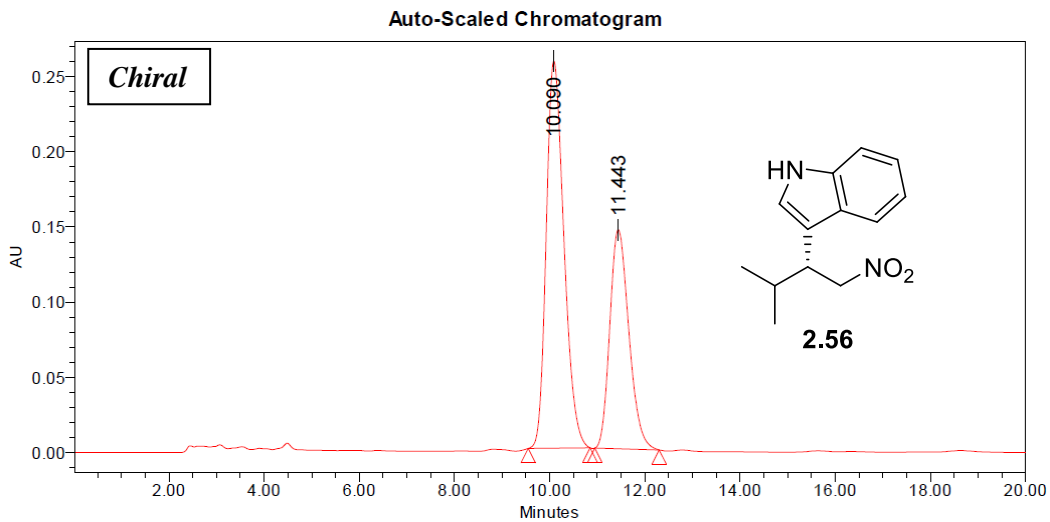
Peak#	Ret. Time	Area	Height	Area %	Height %
1	14.178	750069	28554	72.146	73.770
2	15.804	289589	10153	27.854	26.230
Total		1039659	38707	100.000	100.000

Column: Daicel Chiralpak AD-H
n-Hexane:2-propanol 90:10, 0.8 mL/min



Peak Name:

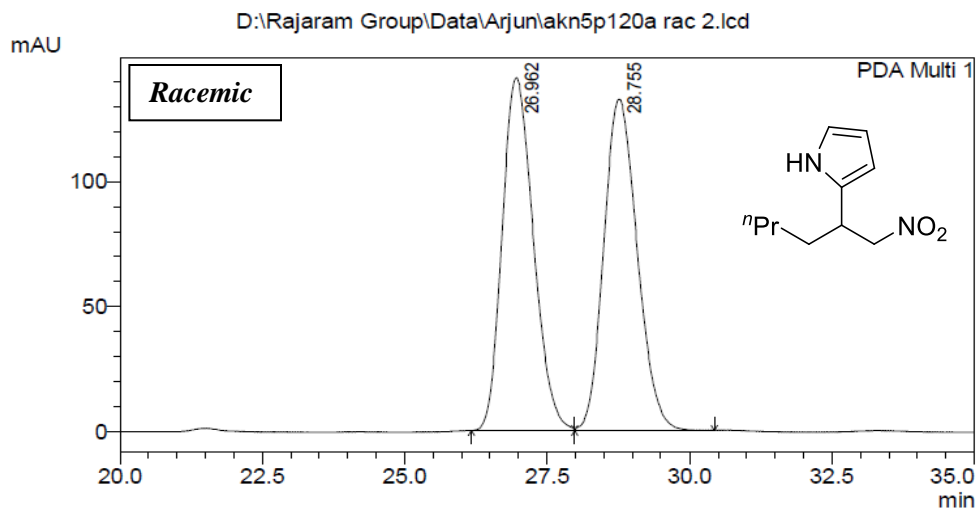
	Injection	RT	Area	% Area	Height
1	1	10.157	5673111	49.89	226957
2	1	11.503	5697088	50.11	209894



Peak Name:

	Injection	RT	Area	% Area	Height
1	1	10.090	6658771	62.13	257891
2	1	11.443	4059027	37.87	145872

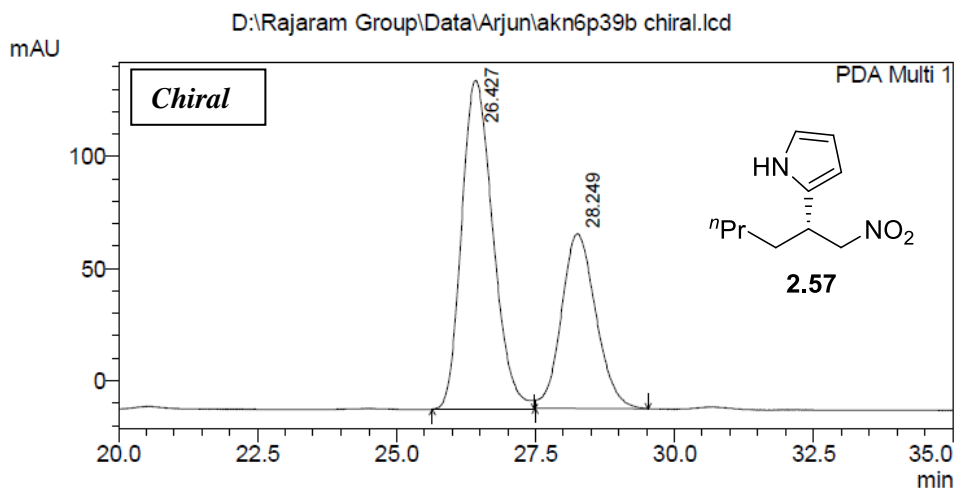
Column: Phenomenex cellulose1
Hexanes:2-propanol 93:07, 0.5 mL/min



PeakTable

PDA Ch1 254nm 4nm

Peak#	Ret. Time	Area	Height	Area %	Height %
1	26.962	5387797	141214	49.900	51.596
2	28.755	5409318	132479	50.100	48.404
Total		10797116	273693	100.000	100.000



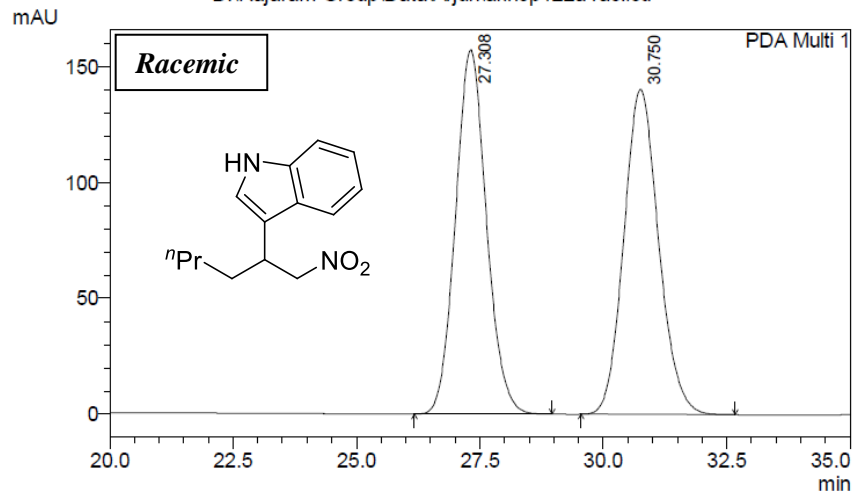
PeakTable

PDA Ch1 254nm 4nm

Peak#	Ret. Time	Area	Height	Area %	Height %
1	26.427	5756961	146638	63.188	65.283
2	28.249	3353814	77982	36.812	34.717
Total		9110775	224621	100.000	100.000

Column: Phenomenex cellulose1
Hexanes:2-propanol 90:10, 1.0 mL/min

D:\Rajaram Group\Data\Arjun\akn5p122a rac.lcd



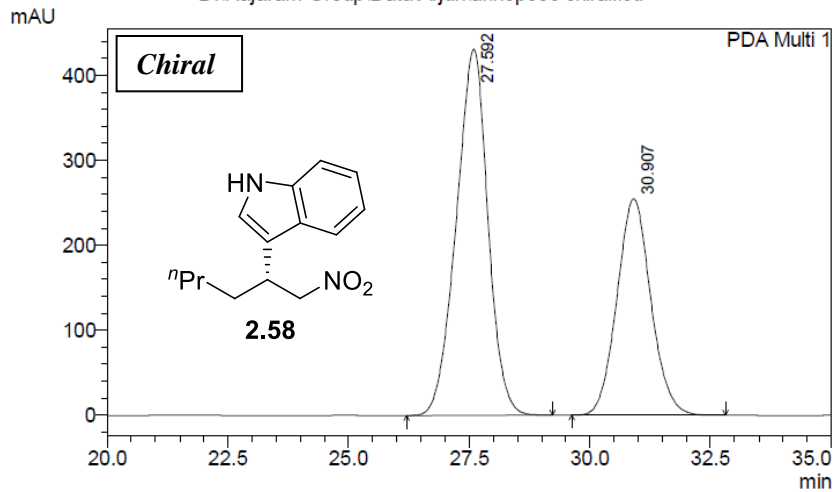
1 PDA Multi 1/254nm 4nm

PeakTable

PDA Ch1 254nm 4nm

Peak#	Ret. Time	Area	Height	Area %	Height %
1	27.308	6878805	157414	49.935	52.829
2	30.750	6896607	140554	50.065	47.171
Total		13775413	297968	100.000	100.000

D:\Rajaram Group\Data\Arjun\akn6p39c chiral.lcd



1 PDA Multi 1/254nm 4nm

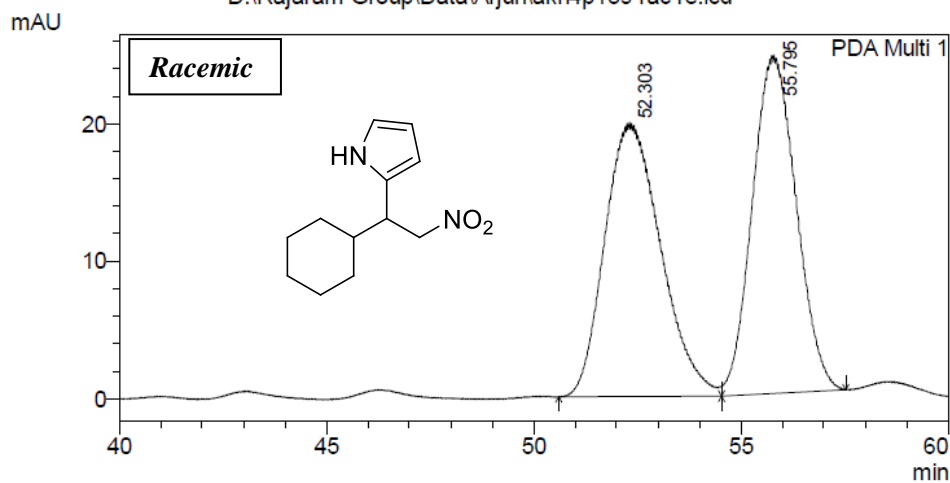
PeakTable

PDA Ch1 254nm 4nm

Peak#	Ret. Time	Area	Height	Area %	Height %
1	27.592	19661714	431304	61.196	62.851
2	30.907	12467349	254929	38.804	37.149
Total		32129064	686234	100.000	100.000

Column: Phenomenex cellulose1
Hexanes:2-propanol 95:05, 0.4 mL/min

D:\Rajaram Group\Data\Arjun\akn4p139 rac re.lcd

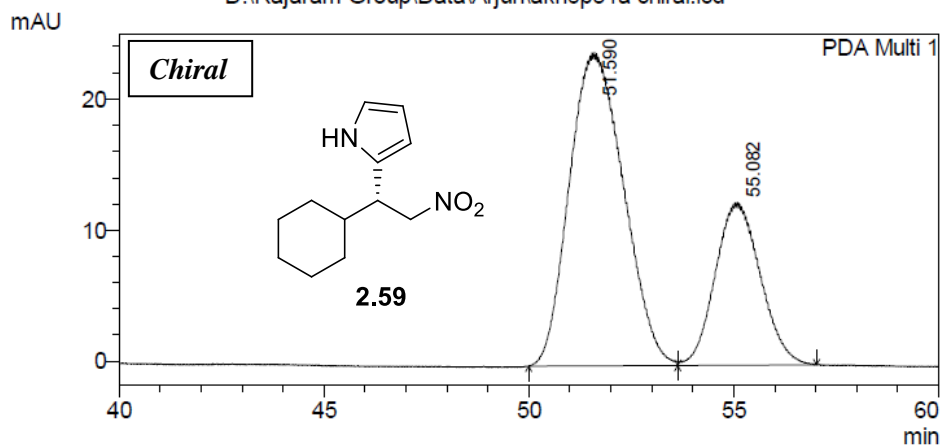


PeakTable

PDA Ch1 254nm 4nm

Peak#	Ret. Time	Area	Height	Area %	Height %
1	52.303	1868584	19964	50.692	44.732
2	55.795	1817590	24667	49.308	55.268
Total		3686174	44631	100.000	100.000

D:\Rajaram Group\Data\Arjun\akn6p31a chiral.lcd



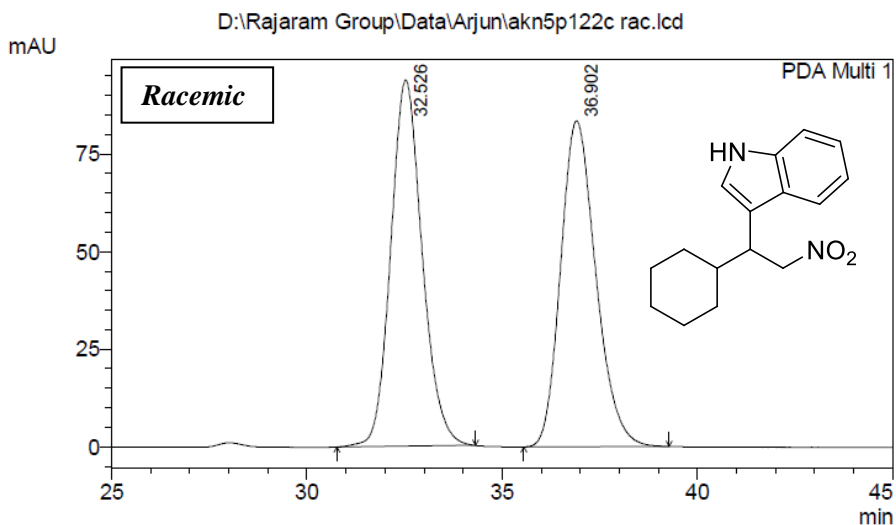
1 PDA Multi 1/254nm 4nm

PeakTable

PDA Ch1 254nm 4nm

Peak#	Ret. Time	Area	Height	Area %	Height %
1	51.590	2197150	23944	69.798	65.816
2	55.082	950736	12436	30.202	34.184
Total		3147886	36380	100.000	100.000

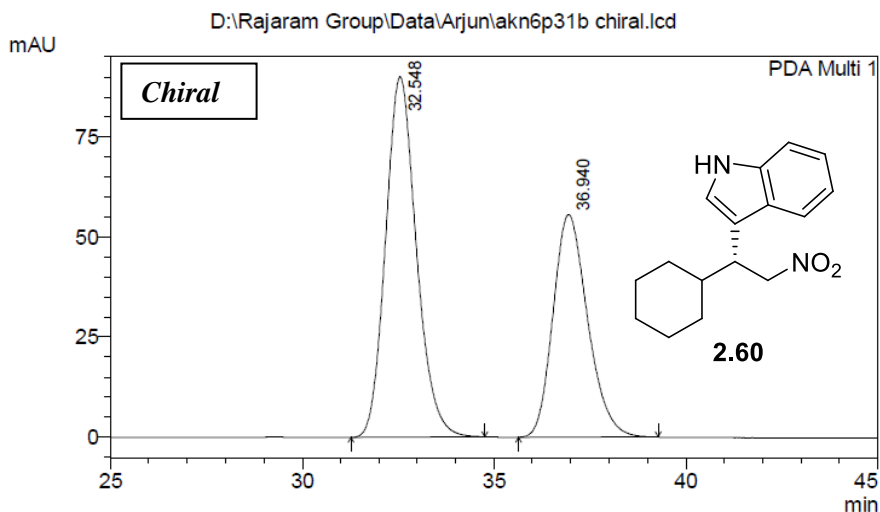
Column: Phenomenex cellulose1
Hexanes:2-propanol 90:10, 1.0 mL/min



PeakTable

PDA Ch1 254nm 4nm

Peak#	Ret. Time	Area	Height	Area %	Height %
1	32.526	5260086	93858	50.101	52.919
2	36.902	5238862	83503	49.899	47.081
Total		10498948	177361	100.000	100.000

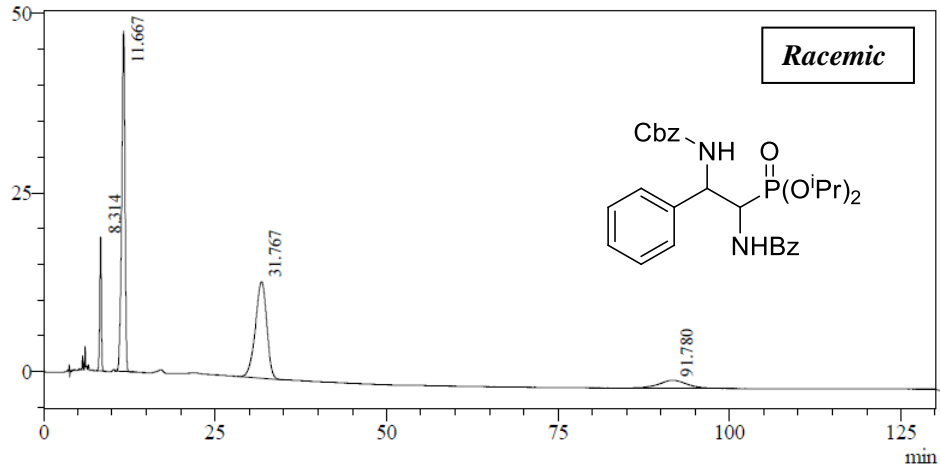


PeakTable

PDA Ch1 254nm 4nm

Peak#	Ret. Time	Area	Height	Area %	Height %
1	32.548	5037547	90180	59.028	61.836
2	36.940	3496677	55657	40.972	38.164
Total		8534224	145838	100.000	100.000

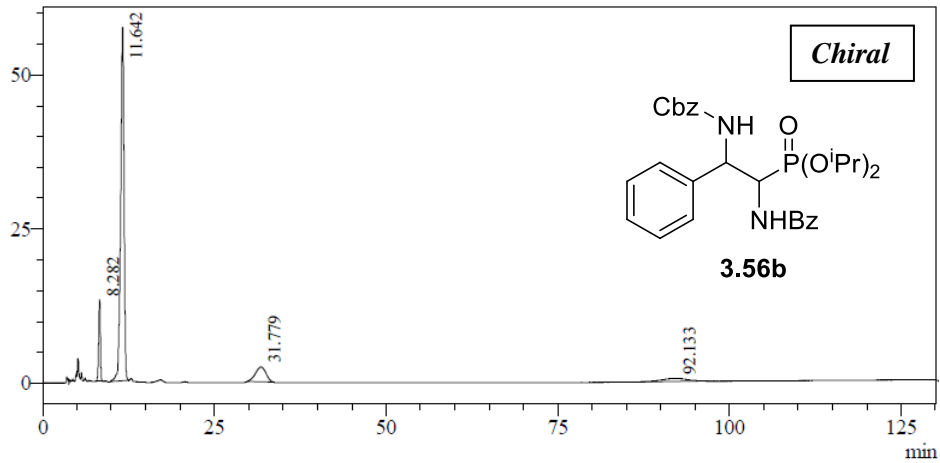
Column: Phenomenex Amylose1
Hexanes:2-propanol 80:20, 0.75 mL/min



PeakTable

PDA Ch1 254nm 4nm

Peak#	Ret. Time	Area	Height	Area %
1	8.314	297588	18672	8.053
2	11.667	1543545	47471	41.768
3	31.767	1547711	13470	41.881
4	91.780	306667	1099	8.298
Total		3695512	80713	100.000

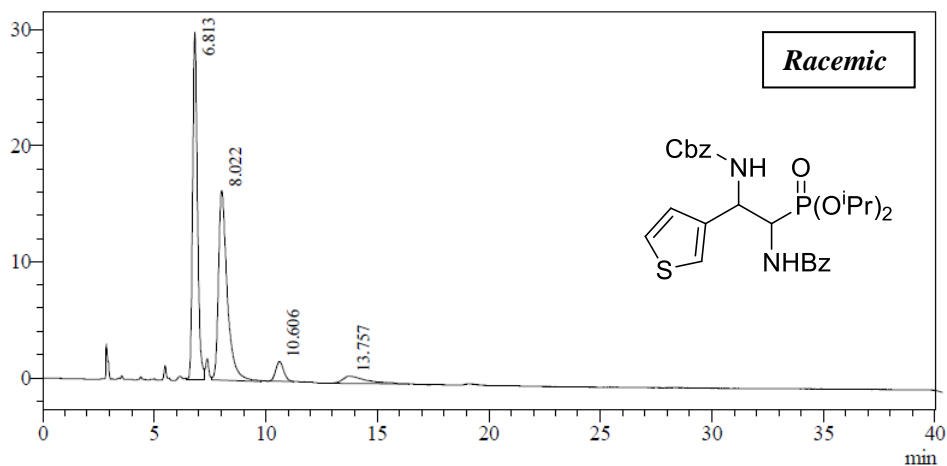


PeakTable

PDA Ch1 254nm 4nm

Peak#	Ret. Time	Area	Height	Area %
1	8.282	223342	13269	8.858
2	11.642	1914649	57351	75.941
3	31.779	255310	2414	10.126
4	92.133	127926	505	5.074
Total		2521227	73540	100.000

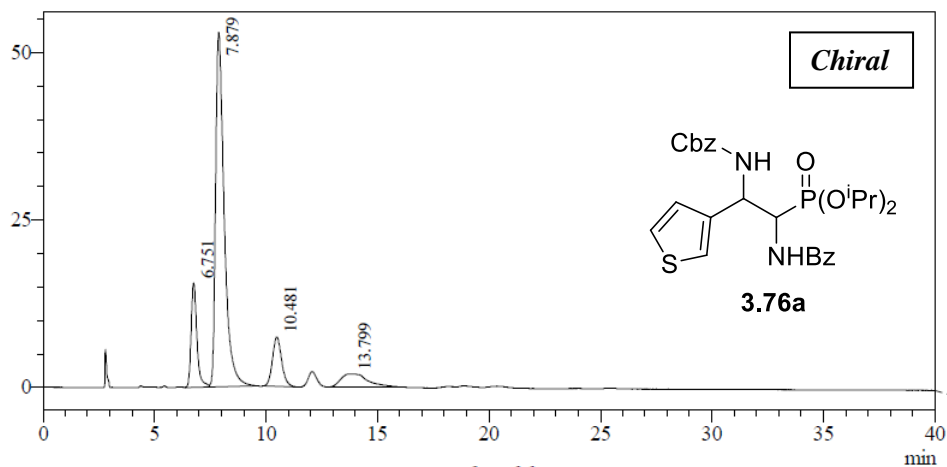
Column: Phenomenex Cellulose1
Hexanes:2-propanol 80:20, 0.75 mL/min



PeakTable

PDA Ch1 254nm 4mm

Peak#	Ret. Time	Area	Height	Area %
1	6.813	447588	29926	45.509
2	8.022	447931	16349	45.544
3	10.606	42267	1692	4.298
4	13.757	45732	638	4.650
Total		983519	48605	100.000

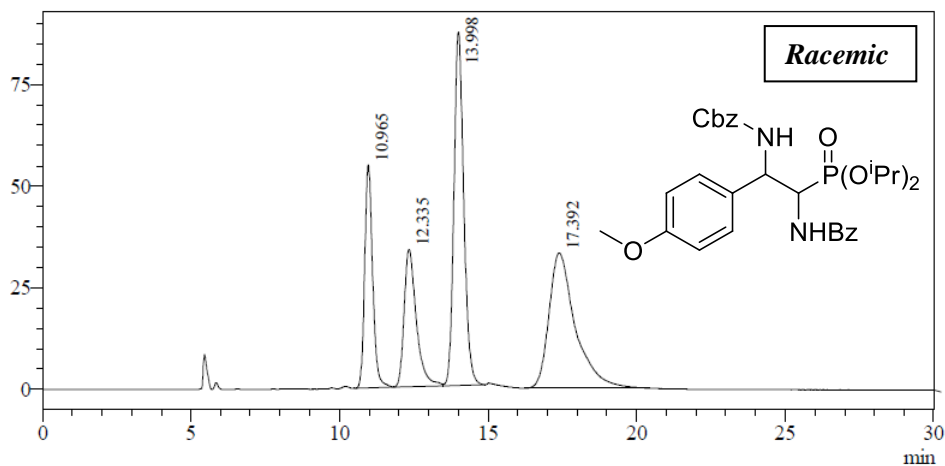


PeakTable

PDA Ch1 254nm 4mm

Peak#	Ret. Time	Area	Height	Area %
1	6.751	278534	15619	13.468
2	7.879	1416259	52962	68.483
3	10.481	212755	7428	10.288
4	13.799	160504	1960	7.761
Total		2068052	77970	100.000

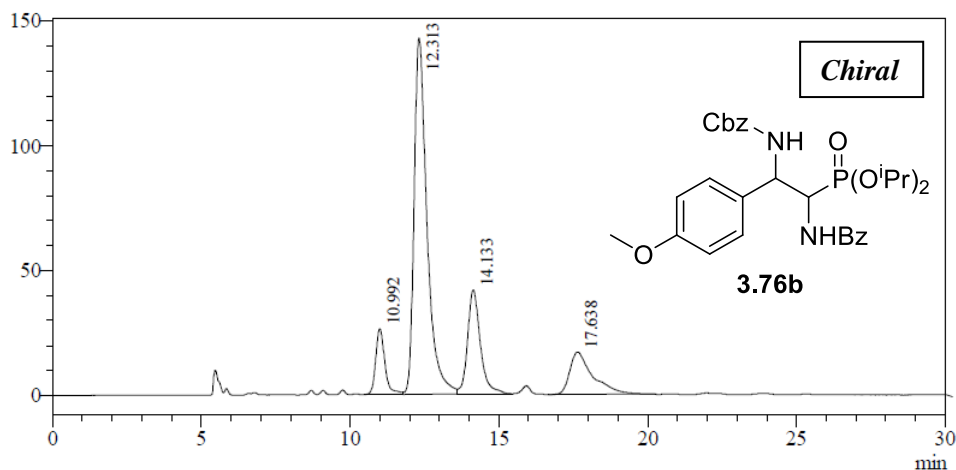
Column: Phenomenex Cellulose1
Hexanes:2-propanol 85:15, 0.5 mL/min



PeakTable

PDA Ch1 240nm 4nm

Peak#	Ret. Time	Area	Height	Area %
1	10.965	1019905	54898	16.875
2	12.335	973450	33812	16.107
3	13.998	1998607	86878	33.069
4	17.392	2051846	33242	33.950
Total		6043808	208830	100.000

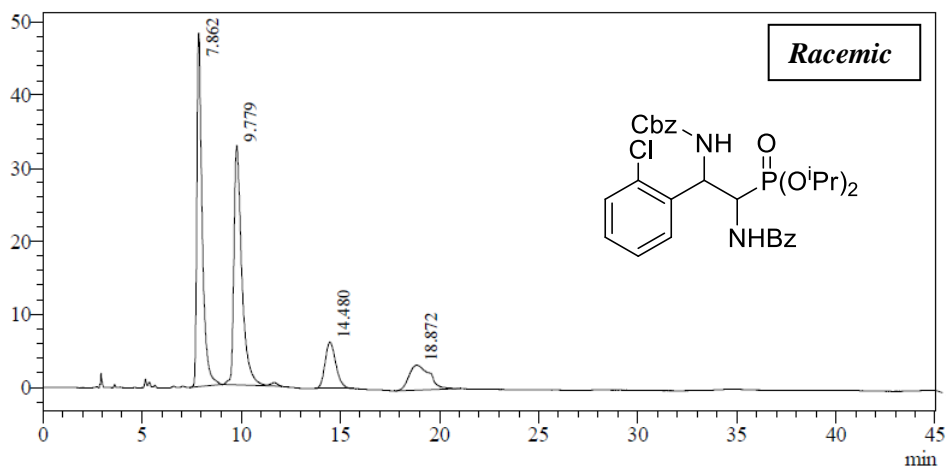


PeakTable

PDA Ch1 240nm 4nm

Peak#	Ret. Time	Area	Height	Area %
1	10.992	560053	26205	7.982
2	12.313	4296949	142621	61.241
3	14.133	1238550	41621	17.652
4	17.638	920942	17034	13.125
Total		7016494	227481	100.000

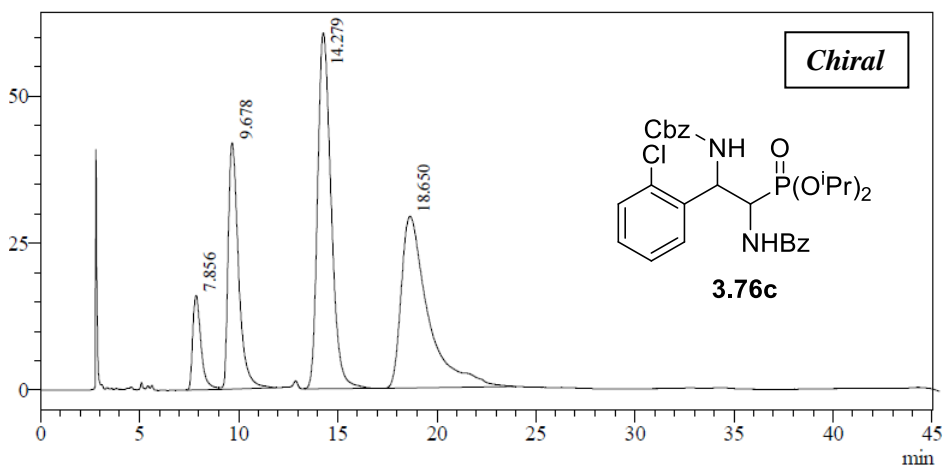
Column: Phenomenex Cellulose1
Hexanes:2-propanol 95:05, 1.0 mL/min



PeakTable

PDA Ch2 240nm 4mm

Peak#	Ret. Time	Area	Height	Area %
1	7.862	922912	48416	39.633
2	9.779	913461	32763	39.227
3	14.480	243687	6362	10.465
4	18.872	248612	3416	10.676
Total		2328671	90957	100.000

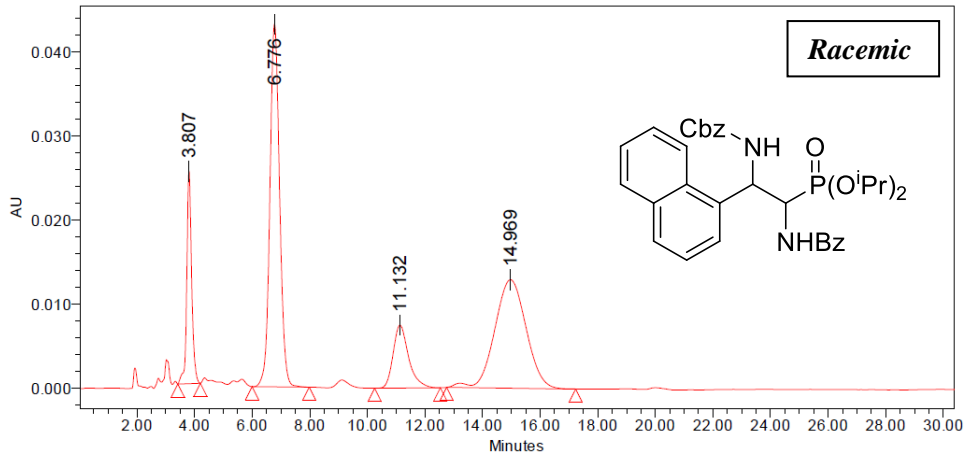


PeakTable

PDA Ch2 240nm 4mm

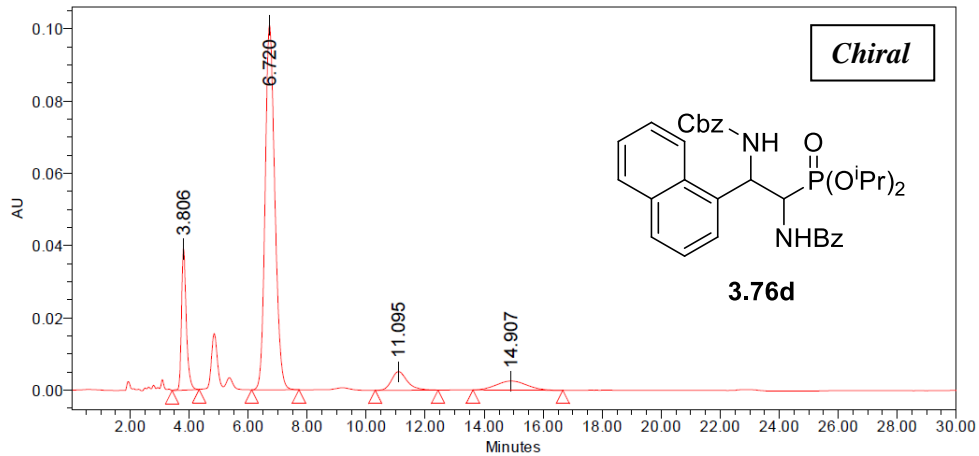
Peak#	Ret. Time	Area	Height	Area %
1	7.856	467844	16075	6.150
2	9.678	1520850	41879	19.991
3	14.279	2857739	60468	37.564
4	18.650	2761248	29194	36.296
Total		7607680	147616	100.000

Column: Chiralpak AD-H
Hexane:2-propanol 95:05, 1.0 mL/min



Peak Name:

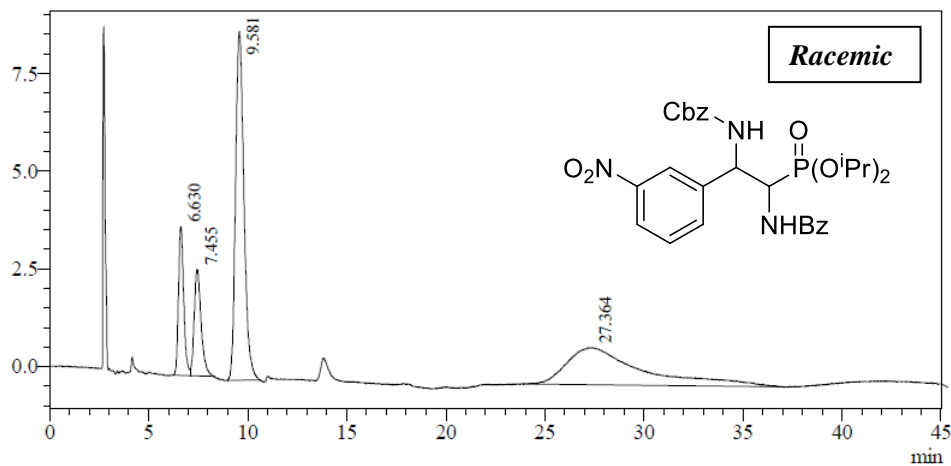
	Injection	RT	Area	% Area	Height
1	1	14.969	974721	38.07	12887
2	1	11.132	278957	10.90	7478
3	1	6.776	1008021	39.37	43121
4	1	3.807	298470	11.66	25376



Peak Name:

	Injection	RT	Area	% Area	Height
1	1	14.907	180196	5.78	2517
2	1	11.095	190007	6.10	5165
3	1	6.720	2301067	73.84	100973
4	1	3.806	445213	14.29	39322

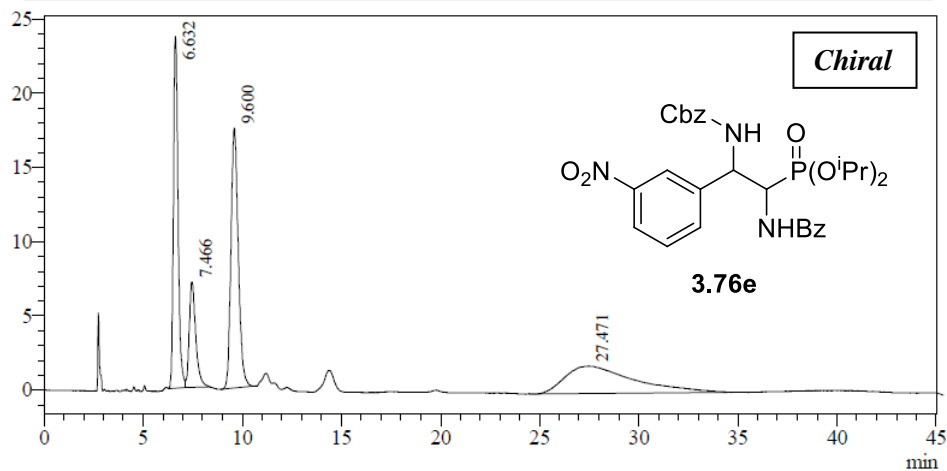
Column: Phenomenex Cellulose1
Hexanes:2-propanol 90:10, 1.0 mL/min



PeakTable

PDA Ch1 254nm 4mm

Peak#	Ret. Time	Area	Height	Area %
1	6.630	70922	3813	10.876
2	7.455	66484	2728	10.195
3	9.581	261466	8929	40.096
4	27.364	253223	957	38.832
Total		652095	16427	100.000

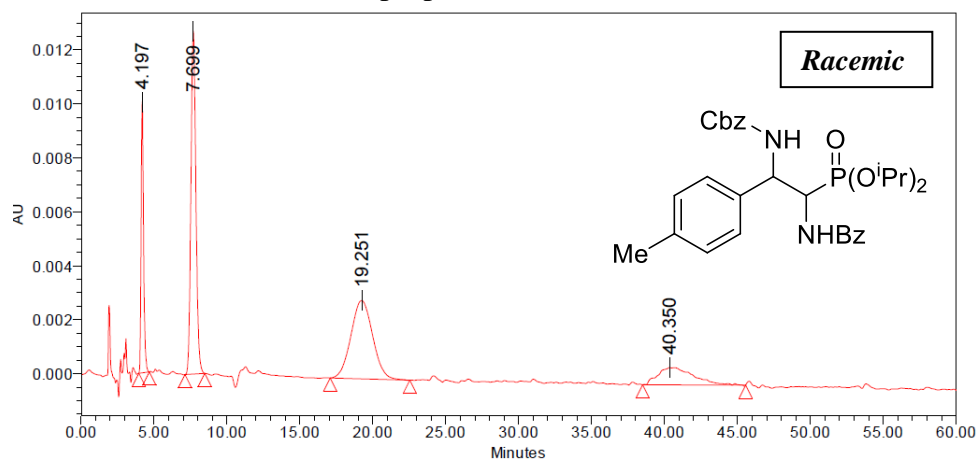


PeakTable

PDA Ch1 254nm 4mm

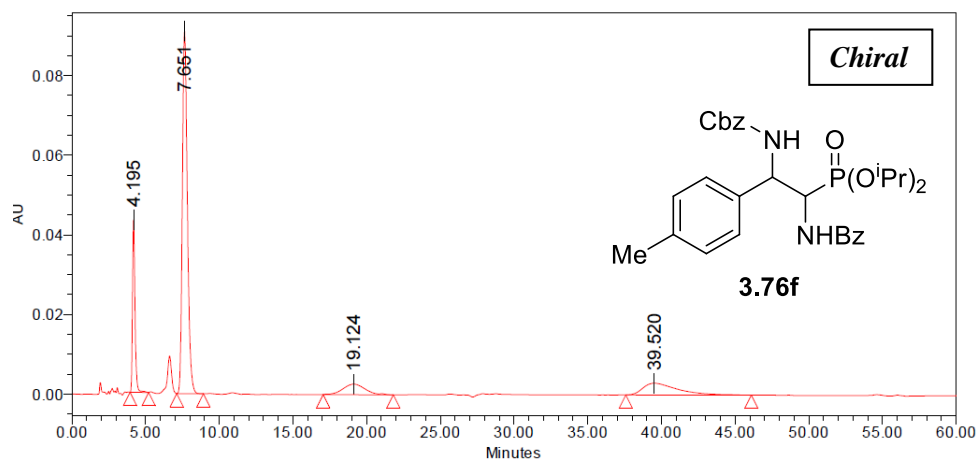
Peak#	Ret. Time	Area	Height	Area %
1	6.632	390934	23712	26.981
2	7.466	161580	7122	11.152
3	9.600	445915	17536	30.776
4	27.471	450470	1870	31.091
Total		1448898	50240	100.000

Column: Chiralpak AD-H
Hexane:2-propanol 95:05, 1.0 mL/min



Peak Name:

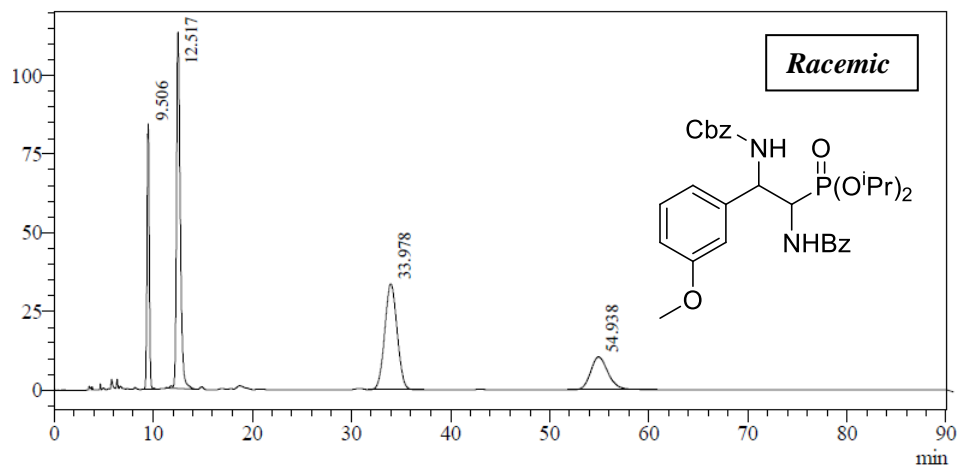
	Injection	RT	Area	% Area	Height
1	1	40.350	110011	13.27	642
2	1	19.251	301120	36.32	2904
3	1	7.699	299535	36.13	12708
4	1	4.197	118381	14.28	10047



Peak Name:

	Injection	RT	Area	% Area	Height
1	1	39.520	487002	14.16	2965
2	1	19.124	279027	8.11	2660
3	1	7.651	2163906	62.90	91154
4	1	4.195	510124	14.83	43488

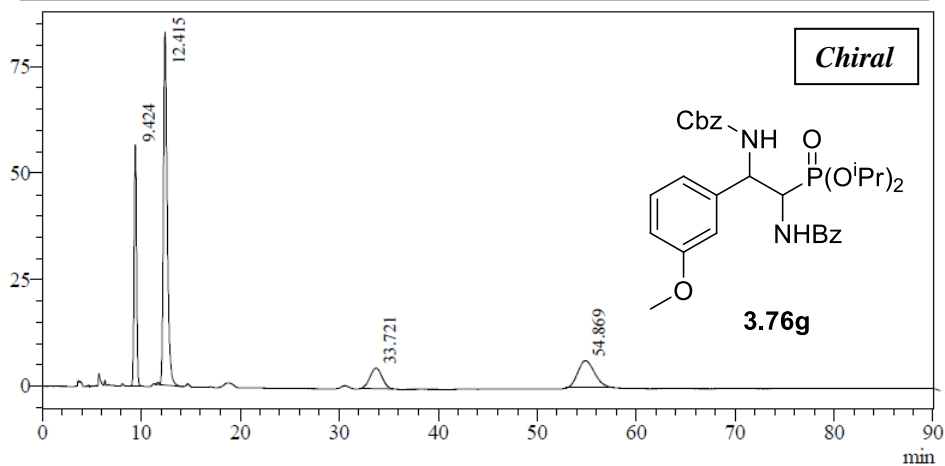
Column: Phenomenex Cellulose1
Hexanes:2-propanol 85:15, 1.0 mL/min



PeakTable

PDA Ch1 254nm 4mm

Peak#	Ret. Time	Area	Height	Area %
1	9.506	1311891	84301	15.534
2	12.517	2925283	113197	34.638
3	33.978	2922691	33680	34.607
4	54.938	1285494	10439	15.221
Total		8445359	241617	100.000



PeakTable

PDA Ch1 254nm 4mm

Peak#	Ret. Time	Area	Height	Area %
1	9.424	958626	56548	22.179
2	12.415	2194209	82747	50.765
3	33.721	407892	4828	9.437
4	54.869	761530	6412	17.619
Total		4322257	150535	100.000

